Bis(phosphinimino)amide supported monomeric heteroleptic boron complexes: Synthetic, reactivity and structural studies

A thesis submitted for the partial fulfilment of

the degree of Doctor of Philosophy

by

Kuldeep Jaiswal

Department of Chemical Sciences

Indian Institute of Science Education and Research (IISER) Mohali

Sector 81, Knowledge City, S. A. S. Nagar, Manauli PO, Mohali, 140306. Punjab, India.

February 2016

Dedicated to my family

for their love and affection

DECLARATION

The work presented in this thesis titled ***"Bis*(phosphinimino)amide supported monomeric heteroleptic boron complexes: Synthetic, reactivity and structural studies"** has been carried out by me under the supervision of **Dr. Sanjay Singh** in the Department of Chemical Sciences, Indian Institute of Science Education and Research (IISER) Mohali, Mohali.

This work has not been submitted in part or full for a degree, diploma or a fellowship to any other university or institute.

Whenever contributions of others are involved, every effort is made to indicate this clearly with due acknowledgements of collaborative work and discussions. This thesis is a bonafide record of original work done by me and all sources listed within have been detailed in the bibliography.

Kuldeep Jaiswal

Date:

Place:

In my capacity as the supervisor of the candidate's thesis work, I certify that the above statements by the candidate are true to the best of my knowledge.

Dr. Sanjay Singh

Associate Professor

Department of Chemical Sciences

Indian Institute of Science Education and Research Mohali

Date:

Place:

Acknowledgements

Foremost, from the innermost core of my heart I express my profound sense of reverence, obligations, respect and honour to Dr. Sanjay Singh, Assistant Professor, Department of Chemical Sciences & Chairman of my Advisory Committee for his inspiration, benign cooperation, industrious guidance, impeccable supervision, timely criticism and benevolent help during my entire period of PhD. He helped me in many ways, not only in professional front but also in personal life. He gave me so much freedom to think and I learnt many things from our friendly conversations. I wish to express my sincere thanks to Prof. R. Kapoor and Dr. A. R. Choudhury, Department of Chemical Sciences, members of my Advisory Committee for their valuable and sincere advice during the course of present investigation. I acknowledge special thanks to Prof. N. Sathyamurthy, Director IISER Mohali for providing well equipped platform with all amenities. I sincerely thank Prof. K. S. Viswanathan, Head of the Department, to provide all requisites in the Department. I also thank my family members for the moral support and the care they have shown to me.

I am thankful for pleasant company, friendly counselling, cooperation, practical help and patronage of my labmates Dr. Rishu, Dr. Billa Prasantha, Dr. Nagarjuna, Mr. Deependra Bawari, Mr. G. Sai, Kumar Mr. V. R. Sabari, Mr. Akhil Rag. I would like to thank the former labmates Mr. Shalender Jain and Mr. Aditya Verma. I would like to thank the former and present Dean(s), IISER Mohali, for providing best research facilities and atmosphere. I am thankful to all the faculty members of IISER Mohali for their help, cooperation and encouragement at various stages.

I also thank all the non-teaching staff of the IISER Mohali for their assistance on various occasions. I specially acknowledge Triveni Sankar, Balbir, Bahdur, Managat, Satwinder for their valuable support given to me all the time. I thank Dr. Billa Prashanth, Dr. Gurpreet Kaur and Mr. H. R. Yadav for their valuable suggestions in handling XRD

instrument. I would like to acknowledge IISER Mohali for providing the basic requirements like Single Crystal X-ray Diffraction Facility, NMR, HRMS, IR, and UGC & MHRD for the financial support.

My special thanks to my colleagues Vijay Gupta, Ashwani Bhardwaj, Pallavi Sharma, Nagesh Kadam, Vina Tikiyani, Nayyar, Rajkumar, C. K. Reddy, Ramarao Parella, Vinod, Manisha Wadhwa, Harpreet Singh, Satnam, Navdeep Gogna, Swagtam Nayak, Rajneesh Perhate, Satyam Srivastva, Shradha Gandhi and Ravinder Gulia.

Here I would like to take this opportunity to thank all my teachers starting from my first standard to M.Sc. especially Mrs. Rajni gupta (B.Sc.) for intuiting me to synchronize my inclination towards chemistry. It was that moment where I got the initial excitement to learn chemistry and eventually paved the way to come this far. Sometimes, remembering old days with my B.Sc. and M.Sc. beloved friends Naveen Malik, Sandeep Kumar, Vinod Khatri, Manjeet Saini, Mayank Malhotra, Rajeev and Sunil Chahal bring oodling of laugh and nostalgia. Thank to all my School friends who made my life joyful and colorful directly or apparently. This happy occasion entails to remember my childhood friends Sunil, Ravinder, Yogender Antil, Nitin Antil, Kuldeep Antil, Pawan Kaushik, Aanand Bhardwaj and Kuldeep Antil.

I thank my M.Sc. friend Sonu Saini, Sitaram Verma, Sandeep Kuwar, Satish Kadyan, Khemlata Seemar, Swati Munjal, Savita Sharma, Laxmi Yadav, Poonam Sharma, Swetha Bansal and other friends. I thank all of them for their sweet friendship.

At last I don't have words to express gratitude for those who support always me in my triumph and fiasco including Naveen, Sandeep, Vinod, Manjeet, Ashwani, Pallavi and Neeru Mittal. They always stood behind me in each and every tough moment irrespective of bothering anything. I can never forget their exorbitant love and affection; they will always dwell in the memory for the rest of my life. From inner core of my heart I pay my eventual acknowledgment to Dr. Pratima Panday, Dr. Yogesh Dahiya, Dr. Sonia Nain, Dr. Rajender Malik, Dr. Sumit Malik, Dr. Suman Lata and Dr. Hari Om for being good friends of mine. A special thank to my wonderful gifted sisters Sunita, Sabita and Usha. I

am always part of their prayers and you will always be in my thoughts too Sister. Finally, I would like to acknowledge my brother in law Mr. Ashok Kumar and my nephew Aman Singh and niece Amrita Singh.

It has been a privileged for me to work in IISER Mohali. It has provided me the best and world class amenities with well equipped facilities in a peaceful environment to achieve coveted degree of the paramountcy. I am going to miss this beautiful place; it will always be in my memories.

I thank my near and dear ones whom I haven't acknowledged here for their direct or indirect help. This closure of acknowledgement culminates with a gesture of gratitude to my dear parents whose love and support has encouraged me to pursue this direction.

Kuldeep Jaiswal

Synopsis of

***Bis*(phosphinimino)amide supported monomeric heteroleptic boron complexes: Synthetic, reactivity and structural studies**

1. Introduction

[N,N']-bidentate monoanionic ligands such as *β*-diketiminato,[1] *bis*(phosphinimino)methanide[2] and acyclic phosphazene[3] represent important classes of ligands having various interesting structural and physical properties. These ligands are capable of forming stable six-membered metallacycles/chelates with various metal ions. Obviously, the robustness of these metallacycles depends not only on the steric bulk but also on the electronic features of the ligand. The latter feature is reflected in the ligand due to the presence of C/N, C/P/N and P/N atoms in their backbone. We were stuck by the close resemblance, in both steric demand and denticity, among the aryl substituted acyclic phosphazene, *β*-diketiminato and *bis*(phosphinimino)methanide. Metal complexes of these ligands have proved to be of great utility in polymerization,[4] catalysis[4] or synthetic low-coordinate metal environments.[5]

Use of monoanionic sterically bulky P/N ligands with N_3P_2 backbones was considered to be ideal for our purpose and will be the central theme of the present work to elaborate the basic chemistry of group 13 halide, hydride and methyl derivatives. The longer P–N bond compared to the C–N bond is supposed to provide planar and flexible chelates, better donor ability of this ligand compared to the C/N based ligand attracted our attention.

A literature survey revealed that there is potential scope for the development of heteroleptic complexes of group 13 elements and further development of their reaction chemistry. This is particularly true in the case of *bis*(phosphinimino)amide based complexes of group 13 and especially for boron complexes, a very limited number of such complexes are known with this ligand. The complexes of group 13 elements with *bis*(phosphinimino)amide have been largely of the type; $N(PCl_2NMe_2)_2BX_2$ (X = Cl, F, OSO_2CF_3)[6] complexes of B, three complexes of Al; $[N(PCl_2NMe_2)_2AlMeX$; X = Cl, $O{-}C_6H_2$-2,4,6-tBu$_3]$[7] & $[N(PPh_2NSiMe_3)_2AlMe_2]$[8], no complex of Ga and only one complex

of In; $[N(PPh_2NSiMe_3)_2InMe_2]$[8] were reported prior to this work. The importance of such complexes has been demonstrated in the synthesis of several novel compounds such as borondihydride, cationic boron, thioxo– and selenoxo–borane complexes.

2. Objective(s) and scope

Utilization of steric and electronic properties of the ligand to stabilize metal ions to form stable complexes to perform further reaction chemistry on these complexes have been the interest of the present work.

Owing to less development in the area of cationic boron complexes and complexes of boron with chalcogens, the central theme of our work is to explore synthetic methods to prepare such derivatives. The P=N moieties have strong donor capability as compared to C=N moieties. The advantage of facile donation of electrons, to the central atom, by P=N moieties made us interested to work with a *bis*(phosphinimino)amide ligands with N_3P_2 backbones. Donor property of these ligands have been compared with the known systems with the (C_3N_2) backbone of *β*-diketiminato and (CP_2N_2) of *bis*(phosphinimino)methanide ligands. Selection of central atom and metal ions and synthesis of their complexes with the chosen ligands were undertaken with the following objectives:

(i) Stable and soluble heteroleptic complexes of group 13 element to explore their reaction chemistry.

(ii) Synthesis of thioxo– and selenoxo–borane complexes *via* reaction of borondihydride complex as a precursor with heavier chalcogens (S or Se).

(iii) Application of borondihydride complex for the synthesis of stable three coordinated cationic borenium complexes.

3. Description of the research work

3.1. Synthesis of ligands with N_3P_2 backbone for the preparation of six membered N_3P_2M metallacycles:

In the present research work, Staudinger reaction on tetraphenyldiphosphazane $(Ph_2P)_2NH$ with mesitylazide (2,4,6-$Me_3C_6H_2N_3$) or 2,6-diisopropylphenylazide (2,6-*i*$Pr_2C_6H_3N_3$) evolved nitrogen and gave the compounds, [(2,4,6-$Me_3C_6H_2$)-N-P(Ph_2)-N=P(Ph_2)NH-(2,4,6-$Me_3C_6H_2$)] (**L_1H**) and [(2,6-*i*$Pr_2C_6H_3$)-N-P(Ph_2)-N=P(Ph_2)NH-(2,6-*i*$Pr_2C_6H_3$)] (**L_2H**) (Scheme 1). Compounds **L_1**H and **L_2**H have been used in their monoanionic form as [N,N′] bidentate *bis*(phosphinimino)amide ligands having aryl groups at the terminal nitrogen atoms.

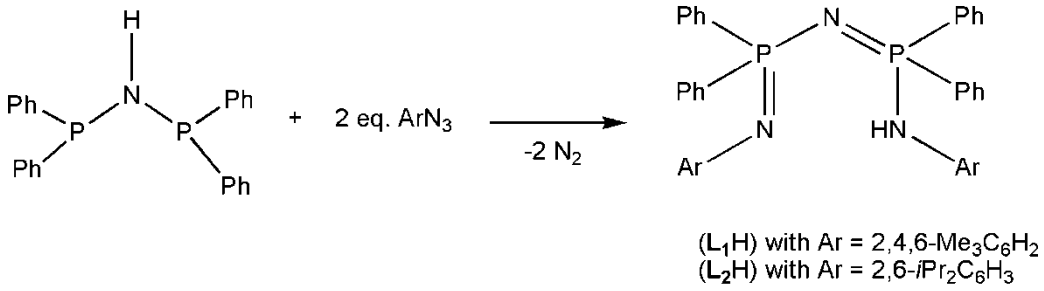

Scheme 1. *Synthesis of bis(phosphinimino)amine ligands [(2,4,6-$Me_3C_6H_2$)-N-P(Ph_2)-N=P(Ph_2)NH-(2,4,6-$Me_3C_6H_2$)] (**L_1H**) and [(2,6-i$Pr_2C_6H_3$)-N-P(Ph_2)-N=P(Ph_2)NH-(2,6-i$Pr_2C_6H_3$)] (**L_2H**).*

The ligands, **L_1**H and **L_2**H and their lithium derivatives have been used for the synthesis of various group 13 element complexes in the present research work.

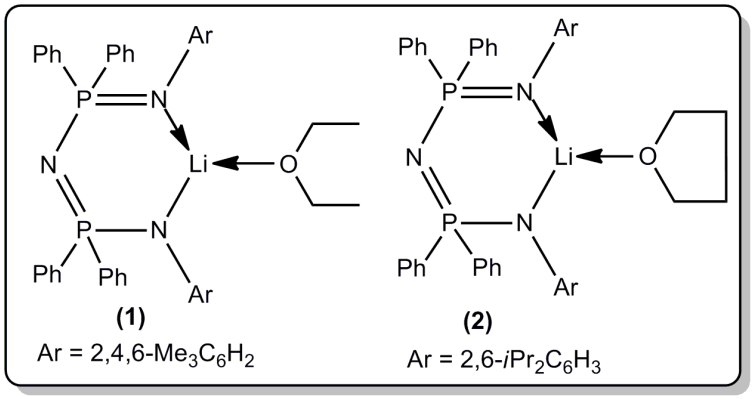

Chart 1. *Lithium derivatives **L_1**Li·OEt_2 (**1**) and **L_2**Li·THF (**2**) of bis(phosphinimino)amines.*

The lithium derivatives of above ligands (Chart 1), have been prepared by deprotonation using *n*BuLi in coordinating solvent (Et_2O for **1** and THF for **2**). These lithium derivates have further been used to prepare metal complexes under salt metathesis.

3.2. Synthesis of monomeric heteroleptic group 13 complexes:

In this section, the syntheses of various group 13 heteroleptic complexes have been shown. These complexes are supported by *bis*(phosphinimino)amide ligands and have been organized in the following subsections

(i) Synthesis of six membered N_3P_2M chelates of group 13 dihalides.

(ii) Preparation of aluminumdimethyl, aluminumdihydride and borondihydride complexes.

(iii) Nucleophilic substitution reactions on borondihydride complexes.

3.2.1. Synthesis of six membered N_3P_2M chelates of group 13 dihalides:

The reaction of $\mathbf{L_1}Li{\cdot}OEt_2$ (**1**) with MCl_3 leads to the formation of $\mathbf{L_1}MX_2$ (M = B, X = F (**3**); M = Al, X = Cl (**4**); M = Ga, X = Cl (**5**); M = In, X = Br (**6**)) with the elimination of LiX (Scheme 2). Complexes **3-6** have been characterized thoroughly by mass spectrometry, single crystal X-ray diffraction technique and heteronuclear NMR (^1H, ^{13}C, $^{31}P\{^1H\}$, ^{19}F and ^{11}B as applicable).

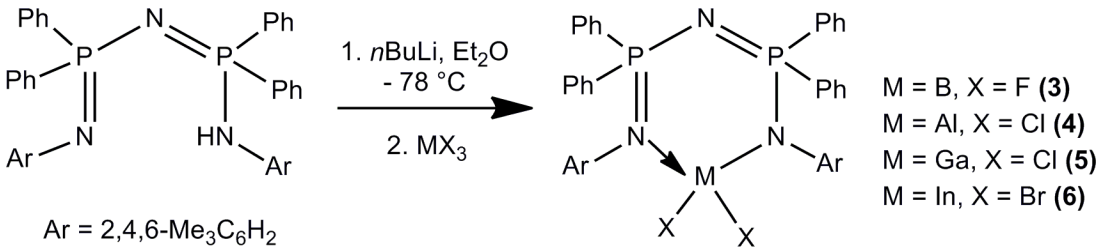

Scheme 2. *Synthesis of dihalo derivatives **3-6** of group 13 elements.*

Single crystal X-ray structure of compounds **3** and **6** showed that metal centres are present in a distorted tetrahedral geometry

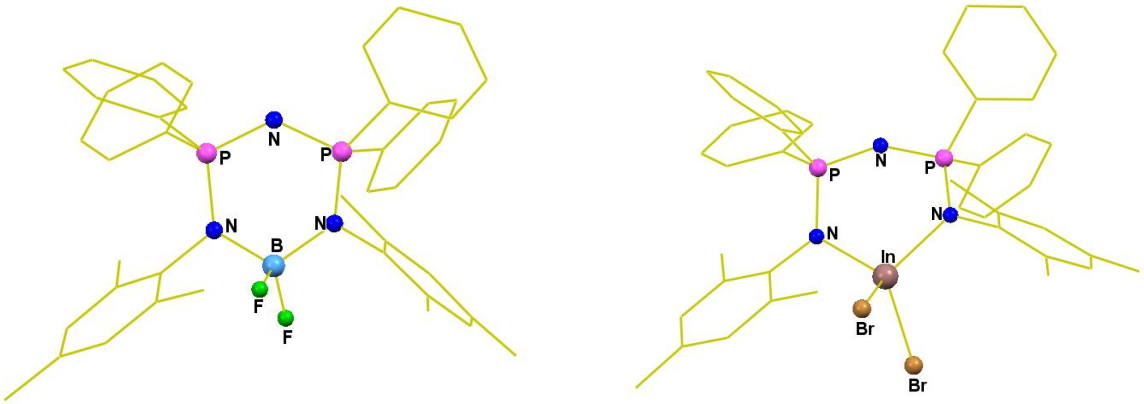

(3) **(6)**

***Figure 1**. Solid state structures of L_1BF_2 (3) and L_1InBr_2 (6).*

After successful isolation of hetroleptic group 13 dihalide complexes we were also interested in the synthesis of chloroborane species. Therefore, the reaction of $\mathbf{L_1}$H and $\mathbf{L_2}$H with $BH_2Cl{\cdot}SMe_2$ was undertaken that gave $\mathbf{L_1}$BHCl **(7)** and $\mathbf{L_2}$BHCl **(8)** (Scheme 3) accompanied by evolution of H_2 at elevated temperature.

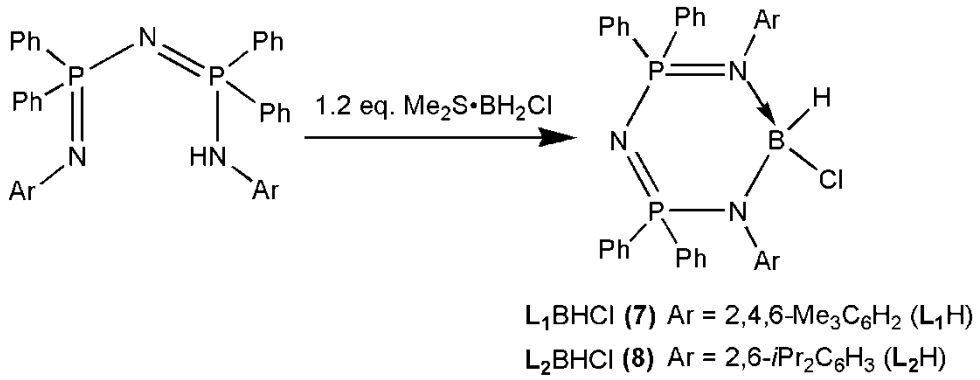

***Scheme 3.** Synthesis of heteroleptic chloroborane complexes* $\mathbf{L_1}$BHCl **(7)** and $\mathbf{L_2}$BHCl **(8)**.

3.2.2. Preparation of aluminumdimethyl, aluminumdihydride and borondihydride :

Reaction of $\mathbf{L_1}$H with equivalent amount of $AlMe_3$, $AlH_3{\cdot}NMe_2Et$ and $BH_3{\cdot}SMe_2$ gave respectively, $\mathbf{L_1}AlMe_2$ **(9)**, $\mathbf{L_1}AlH_2$ **(10)** and $\mathbf{L_1}BH_2$ **(11)** complexes with the evolution of methane and hydrogen gas (Scheme 4).

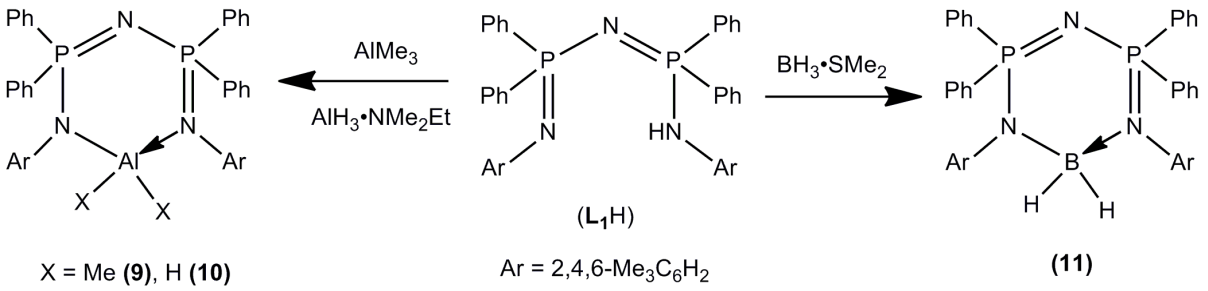

Scheme 4. *Synthesis of aluminumdimethyl* $\boldsymbol{L_1AlMe_2}$ ***(9)*** *and aluminumdihydride* $\boldsymbol{L_1AlH_2}$ ***(10)*** *derivatives and borondihydride complex* $\boldsymbol{L_1BH_2}$ ***(11)***.

These compounds have been characterized thoroughly by multinuclear NMR, IR and HRMS. Spectroscopic formulation of these compounds were consistent with the structure obtained from single crystal X-ray characterization.

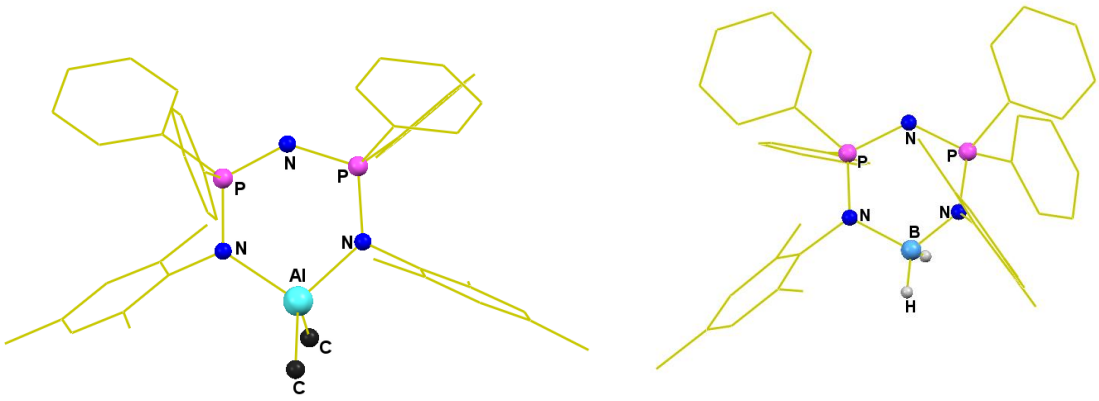

(9) **(11)**

Figure 2*. Crystal structures of* $\boldsymbol{L_1AlMe_2}$ ***(9)*** *and* $\boldsymbol{L_1BH_2}$ ***(11)***.

3.2.3. Nucleophilic substitution reactions on a borondihydride complex:

Nucleophilic substitution reactions were performed on the borondihydride complex $\mathbf{L_1BH_2}$ **(11)** to isolate the borondichloride complex $\mathbf{L_1BCl_2}$ **(12)**, the hydridebromide complex $\mathbf{L_1BHBr}$ **(13)**, the hydrideiodide complex $\mathbf{L_1BHI}$ **(14)**, and the hydride triflate complex $\mathbf{L_1BHOSO_2CF_3}$ **(15)** of boron (Scheme 5). Compounds **12-15** thus prepared have been characterized thoroughly by multinuclear NMR, IR and HRMS. Except in the case of complex **12**, the di-substituion of hydrides of complex **11** was not achieved, even with the use of excess reagents.

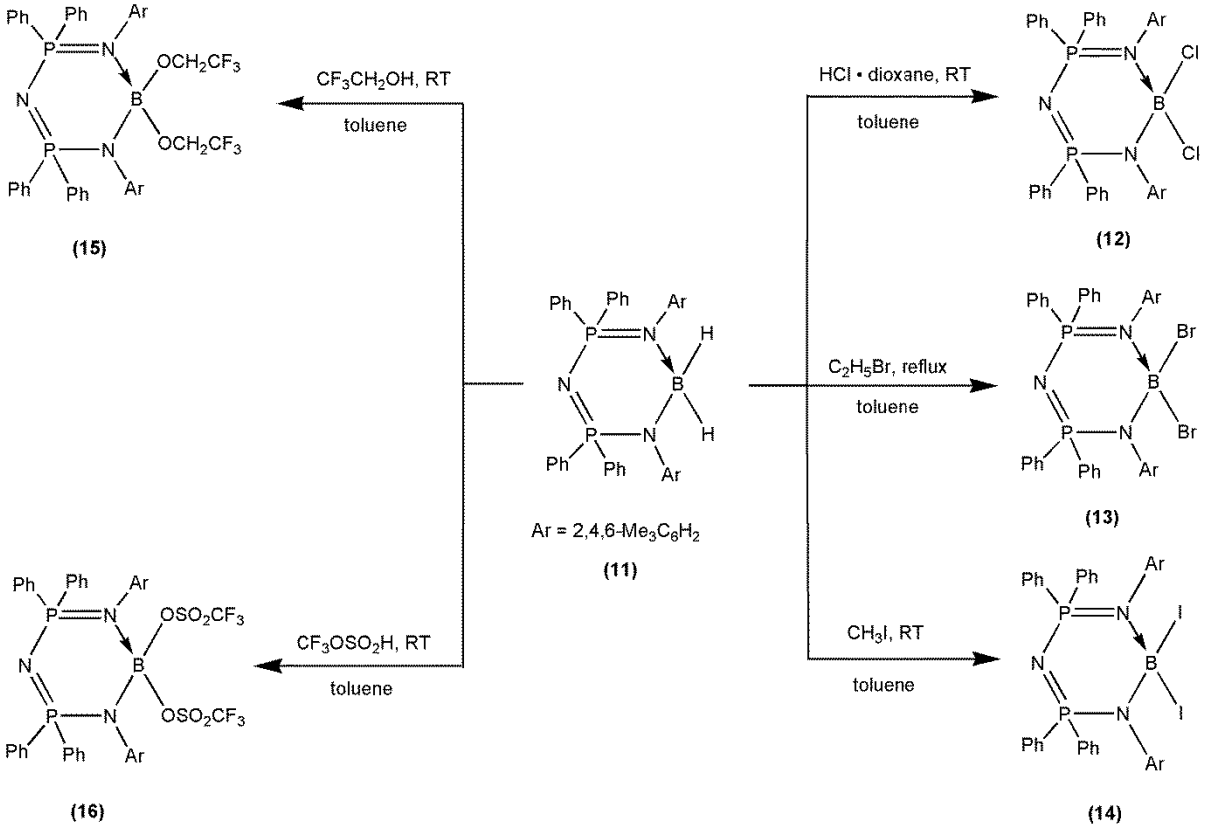

Scheme 5. *Nucleophilic substitution reactions on borondihydride complex* ***L₁BH₂ (11)****.*

3.3. Synthesis of thioxo– and selenoxo–boranes:

Treatment of $\mathbf{L_1}BH_2$ **(11)** with two equivalents of sulfur and selenium gave the thioxo– **(16)** and selenoxo–borane **(17)** complexes with evolution of H_2S and H_2Se gas, respectively (Scheme 6).

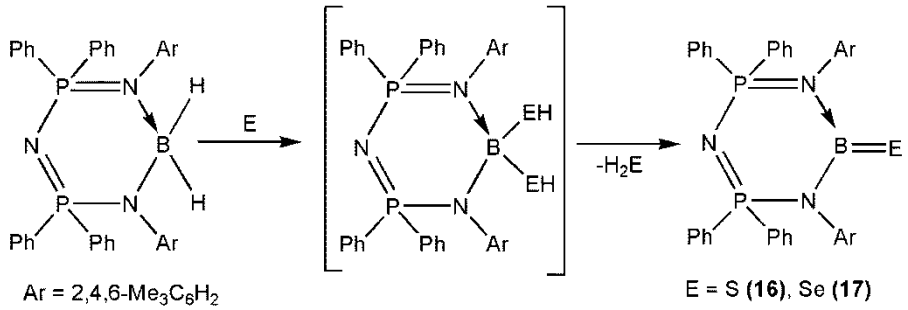

Scheme 6. *Synthesis of thioxoborane* ***L₁B=S (16)*** *and selenoxoborane* ***L₁B=Se (17)****.*

Solid state structures of compounds **16** and **17** have been elucidated by single crystal X-ray diffraction technique that revealed three coordinated boron atoms containing two N and S (or

Se) in a terminal double bonded B=S(Se) fashion. Formation of compounds **16** and **17** was followed by multinuclear NMR including ^{11}B NMR that showed very broad signals typical for a three coordinated boron centers.

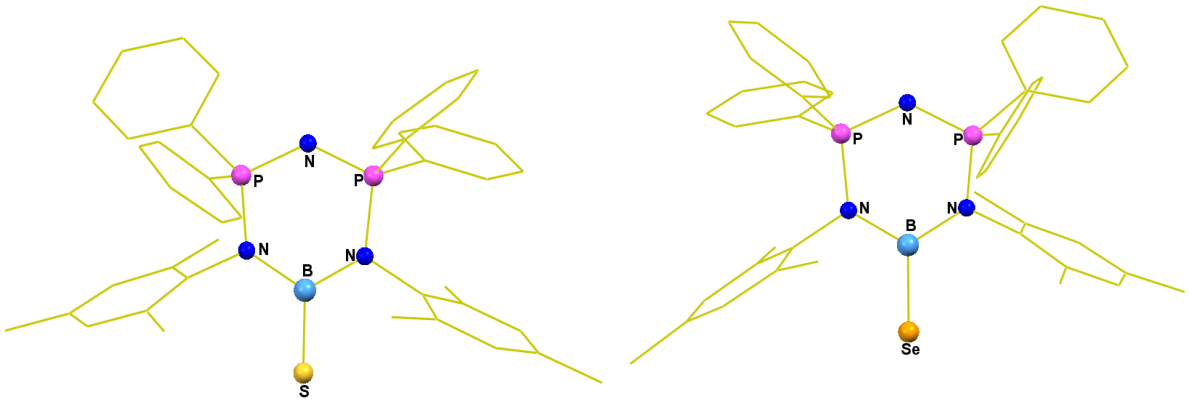

(16) **(17)**

***Figure 3**. Crystal structures of **L**$_1$B=S **(16)** and **L**$_1$B=Se **(17)**.*

The electronic structure of compound **16** was also investigated by geometry optimization that reproduced the structure obtained from X– ray method. The Kohn-Sham (KS) orbitals clearly show that the HOMO corresponds to the sulfur lone pair and HOMO-1 corresponds to the B-S π bond (Figure. 4).

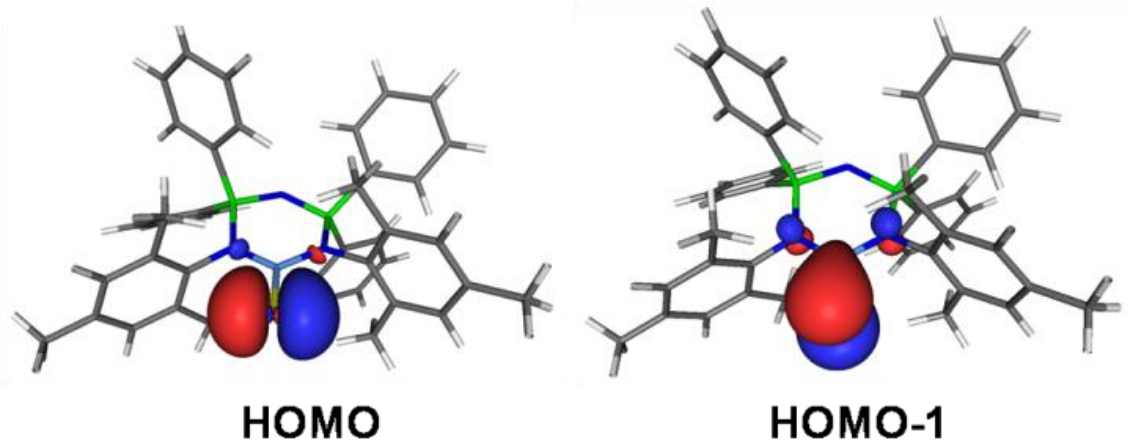

***Figure 4.** Frontier Kohn-Sham orbitals on the B=S unit of compound **L**$_1$B=S **(16)**.*

3.4. Cationic boron complexes:

Neutral three coordinated boron species are common Lewis acids and have been useful in many aspects of synthetic organic chemistry. Anionic complexes such as MBH_4 (M = Li, Na or K) are frequently used as reducing agents, and more recently their involvement in the synthesis of frustrated Lewis pairs have been explored. In contrast to the neutral and anionic species the cationic complexes of boron are less explored. In the literature the cationic species of boron have been classified, on the basis of coordination number of boron center, as borinium, borenium and boronium cation for two, three and four coordinate boron centers, respectively (Chart 2).

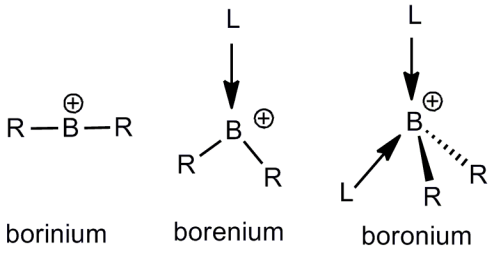

Chart 2. *Classification of boron cations.*

A few known examples related to borenium cations have been shown in (Chart 3).

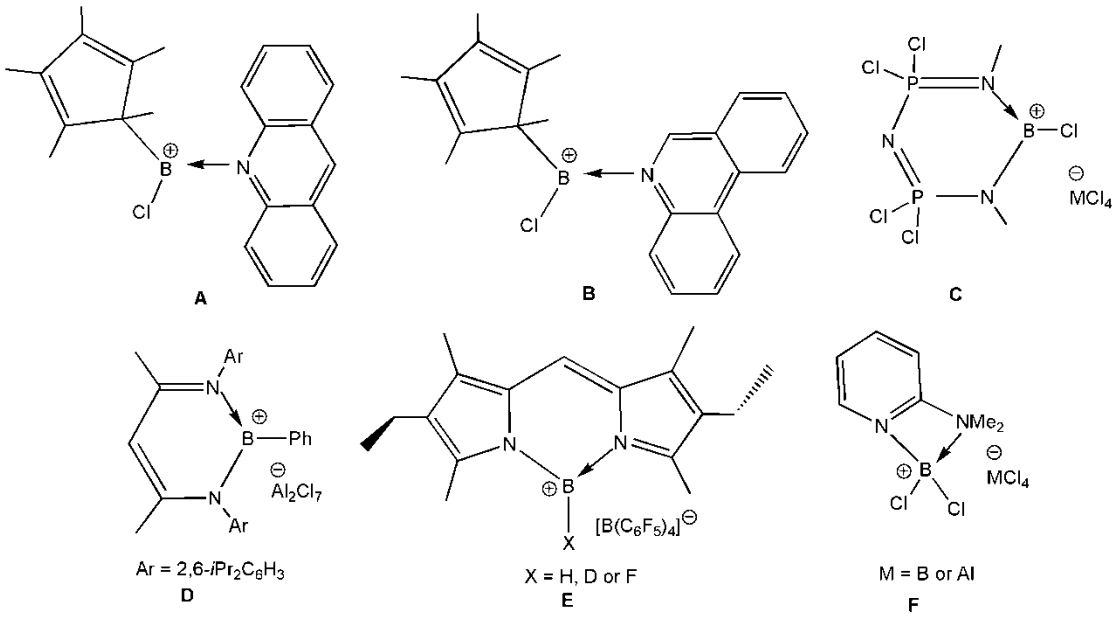

Chart 3. *Known examples of borenium cations.*

3.4.1. Synthesis of borenium complexes:

In this section, the synthesis of various boron cationic complexes has been shown. These complexes have been supported by *bis*(phosphinimino)amide ligands and have been organized in the following subsections

(i) Synthesis of chloro– and hydro–borenium complexes.

(ii) Synthesis of a boronium complex.

The reaction of borondihydride species $\mathbf{L_1}BH_2$ **(11)** with either 3 equivalents of $BH_2Cl{\cdot}SMe_2$ or one equivalent of BCl_3 affords the first hydroborenium species $[\mathbf{L_1}BH]^+[HBCl_3]^-$ **(18)** (Scheme 7) without the need for a weakly coordinating anion. Compound **18** can also be prepared by reacting $\mathbf{L_1}H$ with three equivalents of $BH_2Cl{\cdot}SMe_2$ at reflux temperature (Scheme 7).

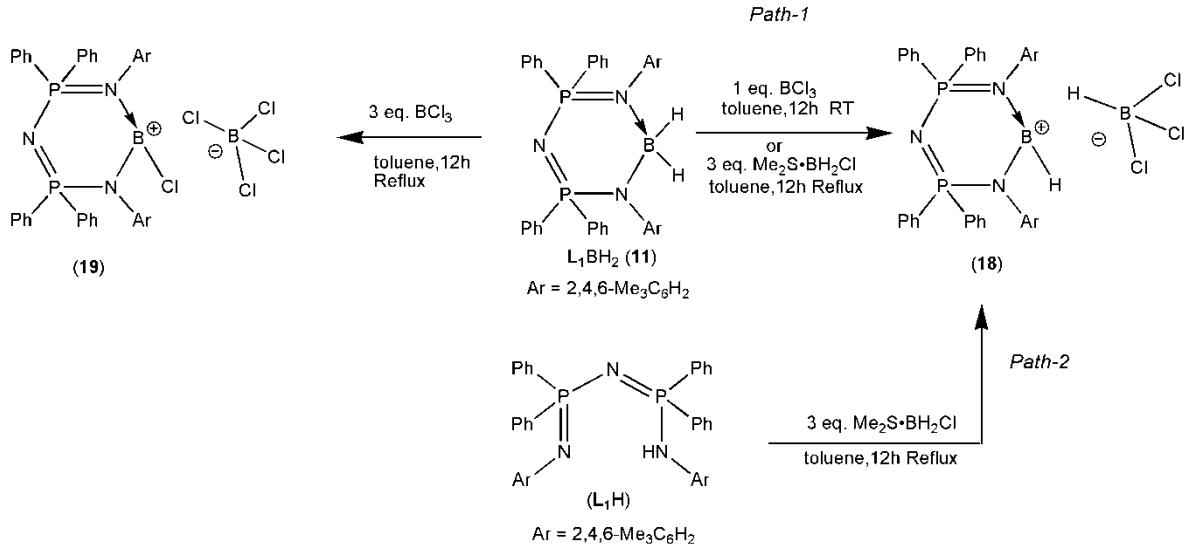

Scheme 7. *Synthesis of cationic boron complexes* $[\mathbf{L_1}BH]^+[HBCl_3]^-$ ***(18)*** *and* $[\mathbf{L_1}BCl]^+[BCl_4]^-$ ***(19)***.

Reaction of **11** with 3 equivalents of BCl_3 under reflux conditions produced a chloroborenium cation *via* exchange hydride and chloride exchange followed by abstraction of chloride to afford $[\mathbf{L_1}BCl]^+[BCl_4]^-$ **(19)** (Scheme 7).

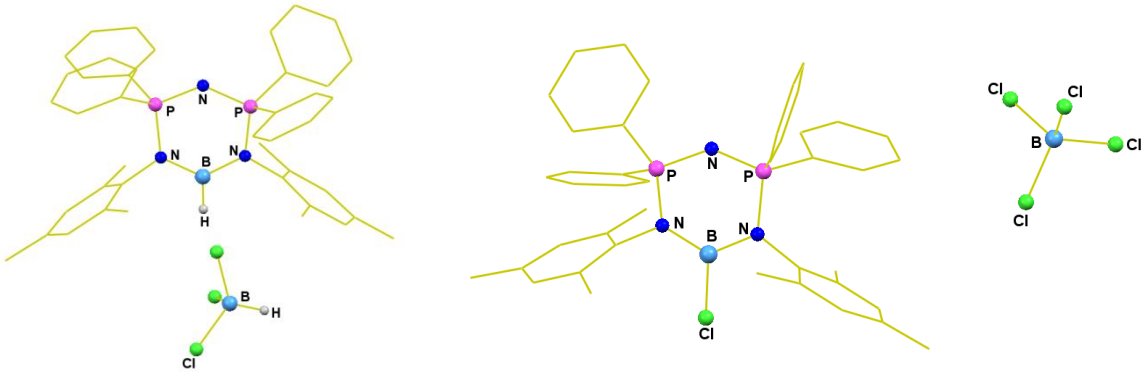

(18) **(19)**

Figure 5*. Solid state structures of* $[\mathbf{L_1}BH]^+[HBCl_3]^-$ ***(18)*** *and* $[\mathbf{L_1}BCl]^+[BCl_4]^-$ ***(19)***.

Another type of boron cation was synthesize by treating $\mathbf{L_1}BH_2$ **(11)** with one equivalent of $B(C_6F_5)_3$ and $[Ph_3C][B(C_6F_5)_4]$ that leads to hydride abstraction to give the products $[\mathbf{L_1}BH]^+[HB(C_6F_5)_3]^-$ **(20)** and $[\mathbf{L_1}BH]^+[B(C_6F_5)_4]^-$ **(21)**, respectively (Scheme 8).

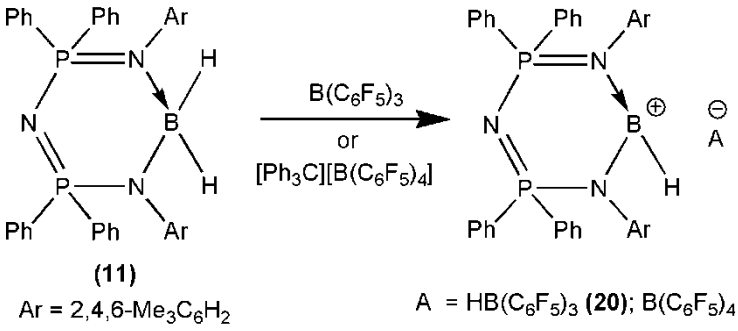

Scheme 8. *Synthesis of hydroborenium species* $[\mathbf{L_1}BH]^+[HB(C_6F_5)_3]^-$ ***(20)*** *and* $[\mathbf{L_1}BH]^+[B(C_6F_5)_4]^-$ ***(21)***.

3.4.2. Synthesis of a boronium complex:

Addition of 1 equivalent of DMAP (4-dimethylaminopyridine) to a solution of borenium cation $[\mathbf{L_1}BH]^+[B(C_6F_5)_4]^-$ (**21**) leads to the DMAP adduct of it in the form of a boronium complex, $[\mathbf{L_1}BH{\cdot}DMAP]^+[B(C_6F_5)_4]^-$ **(22)** (Scheme 9). Compound **22** was characterized by multinuclear NMR, IR and HRMS.

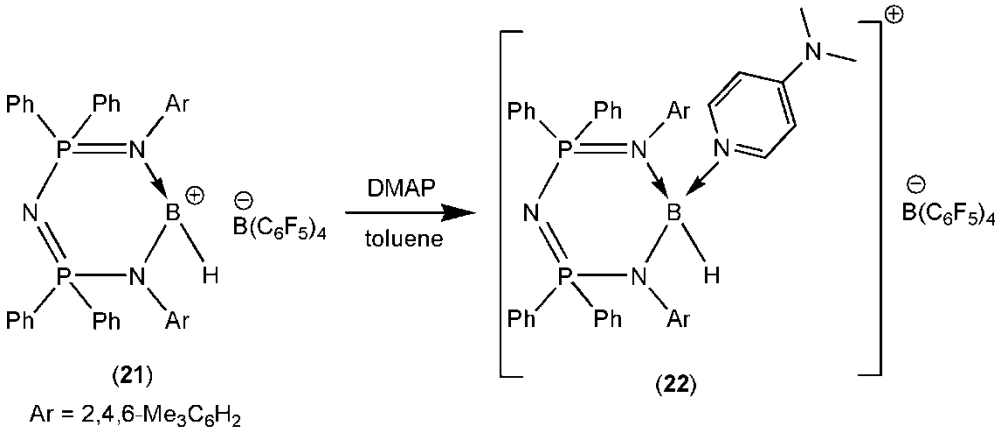

Scheme 9. *Synthesis of hydroboronium complex [**L₁**BH·DMAP]⁺[B(C₆F₅)₄]⁻(**22**).*

4. Conclusions/Summary of the work

A variety of halide, hydride and methyl derivatives of group 13 (mostly B and Al) have been isolated using a rational approach that relies on designing an appropriate sterically and electronically robust ligand based on *bis*(phosphinimino)amide with N_3P_2 skeletons. The work proved the capability of *bis*(phosphinimino)amide ligands to offer firm support in the form of kinetic and thermodynamic stability to the group 13 halides and hydrides. The borondihydride species mentioned in this work could be used as a candidates to explore the chemistry of double bonded chalcogen derivatives and various cationic borane complexes. In summary, the present work shows the synthesis of several novel compounds including borondihydride species, its thioxo– and selenoxo–boron and cationic boron derivatives.

5. References

1. Bourget-Merle, L.; Lappert, M. F.; Severn, J. R. *Chem. Rev.*, **2002,** *102*, 3031-3065.

2. Panda, T. K.; Roesky, P. W. *Chem. Soc. Rev.*, **2009,** *38*, 2782-2804.

3. Neilson, R.H.; Wisian-Neilson, P. *Chem. Rev.*, **1988,** *88*, 541-562.

4. Rong, W.; Liu, D.; Zuo, H,; Pan, Y,; Jian, Z,; Li, S,; Cui, D. *Organometallics*, **2013,** *32*, 1166-1175.

5. Cui, C.; Roesky, H. W.; Schmidt, H.-G.; Noltemeyer, M.; Hao, H.; Cimpoesu, F. *Angew. Chem., Int. Ed*., **2000**, *39*, 4274-4276.

6. Gates, D. P.; McWilliams, A. R.; Ziembinski, R.; liable-Sands,L. M. ; Guzei, I. A.; Yap, G. P. A.; Rheingold, A. L.; Mannrers, I. *Chem.-Eur. J.*, **1998**, *4*, 1489-1503.

7. Rivard, E.; Ragogna, P. J.; McWilliams, A. R.; Lough, A. J.; Manners, I. *Inorg. Chem*., **2005**, *44*, 6789-6798. (b) A. McWilliams, R.; Rivard, E.; Lough, A. J.; Manners, I. *Chem Commun.*, **2002,** 1102-1103.

8. Hasselbring, R.; Roesky, H. W.; Heine, A.; Stalke, D.; Sheldrick, G. M. *Z. Naturforsch*., **1994**, *48b*, 43-49.

Contents

Abbreviations

δ	Chemical shift
λ	Wavelength
$\tilde{\nu}$	Wave number
Ar	Aryl
av	Average
br	Broad
C	Celsius
calcd.	Calculated
Cp	Cyclopentadienyl
Cp*	Pentamethylcyclopetadienyl
Cy	Cyclohexyl
d	Doublet
dd	Doublet of doublet
DCM	Dichloromethane
decomp.	Decomposition
EI	Electron impact ionization
Et	Ethyl
Et_2O	Diethyl ether
eqv.	Equivalents
eV	Electron volt
G	Grams
Hz	Hertz
h	Hours
*i*Pr	*i*so-propyl
IR	Infrared
J	Coupling constant
K	Kelvin
L	Ligand
M	Metal
m	Multiplet

m/z	Mass/Charge
M.p.	Melting point
M^+	Molecular ion
Me	Methyl
Mes	Mesityl
min.	Minutes
MS	Mass spectrometry, mass spectra
NMR	Nuclear magnetic resonance
ppm	Parts per million
Q	Quartet
R, R’, R’’	Organic substituents
S	Singlet
Sept	Septet
sh	Shoulder or hump
st	Strong
T	Triplet
THF	Tetrahydrofuran
TMS	Tetramethylsilane
Tbp	Trigonal bipyramidal
V	Volume
W	Weak
Z	Number of molecules in the unit cell
DMAP	4-Dimethylaminopyridine

Bis(phosphinimino)amide Supported Hydride, Halide and Methyl Complexes of Group 13 Elements

Chapter 1

Abstract: The reaction of tetraphenyldiphosphazane $(Ph_2P)_2NH$ with mesitylazide 2,4,6-$Me_3C_6H_2N_3$ and a bulky azide 2,6-*i*$Pr_2C_6H_3N_3$ affords new [N,N'] chelating ligands, [HN(Ph_2PN(2,4,6-$Me_3C_6H_2$))$_2$] (**L_1**H) and [HN(Ph_2PN(2,6-*i*$Pr_2C_6H_3$))$_2$] (**L_2**H), respectively. The ligands can be easily deprotonated using *n*BuLi or Li[N($SiMe_3$)$_2$] in Et_2O to yield [{N(Ph_2PN(2,4,6-$Me_3C_6H_2$))$_2$}Li·OEt_2] **L_1**Li·OEt_2 (**1.1**) and [{N(Ph_2PN(2,6-*i*$Pr_2C_6H_3$))$_2$}Li·OEt_2] **L_2**Li·OEt_2 (**1.2**), respectively. The reactions of **1.1** with the trihalides, MX_3 of group 13 elements afford the corresponding dihalide complexes, [{N(Ph_2PN(2,4,6-$Me_3C_6H_2$))$_2$}MX_2] **L_1**MX_2 (M = B, X = F (**1.3**); M = Al, X = Cl (**1.4**); M = Ga, X = Cl (**1.5**); M = In, X = Br (**1.6**). The reactions of **L_1**H and **L_2**H with $BH_2Cl·SMe_2$ give the corresponding mononuclear complexes [{N(Ph_2PN(2,4,6-$Me_3C_6H_2$))$_2$}BHCl] **L_1**BHCl (**1.7**) and [{N(Ph_2PN(2,6-*i*$Pr_2C_6H_3$))$_2$}BHCl] **L_2**BHCl (**1.8**), respectively; rare examples of monochloroborane complexes. Similarly, the reactions of **L_1**H with $AlMe_3$, $AlH_3·NMe_2Et$ and $BH_3·SMe_2$ respectively, gives the corresponding mononuclear complexes [{N(Ph_2PN(2,4,6-$Me_3C_6H_2$))$_2$}$AlMe_2$] **L_1**$AlMe_2$ (**1.9**), [{N(Ph_2PN(2,4,6-$Me_3C_6H_2$))$_2$}AlH_2] **L_1**AlH_2 (**1.10**), and a rare borondihydride [{N(Ph_2PN(2,4,6-$Me_3C_6H_2$))$_2$}BH_2] **L_1**BH_2 (**1.11**). All the complexes reported in this chapter have been isolated in good yields and would serve as useful synthons to elaborate their reaction chemistry. Solid state structures of **L_1**H, **L_2**H and compounds **1.1-1.7**, **1.9-1.11** have been investigated by single crystal X-ray structural analysis.

Jaiswal, K.; Prashanth, B.; Bawari, D.; Singh, S. *Eur. J. Inorg. Chem*. 2015, 2565.

1.1 Introduction

Incorporation of main group elements within the ligand frameworks have far flung interest for inorganic chemists to afford interesting complexes of elements across the periodic table from the view point of unusual bonding, structural arrangement, novel reactivity and variety of stable coordination numbers and oxidation states.[1] These complexes have been commonly achieved by the use of [N,N']-bidentate monoanionic ligands that can strongly chelate these metal ions. Robustness of such systems can depend on the size of the chelate ring in addition to the effect of the steric and electronic factors of the supporting ligand. These chelates have largely been of two types: (i) the ones with the metal ion residing in a four membered heteroatom ring[2] and (ii) the other type where the metal ion is a part of a six membered heteroatom ring.[1,3] The former type of chelate skeleton is limited to NXNM rings (X = B, C, N, P, or S) (Chart 1)[2] and the latter type is mainly dominated by β-diketiminates (C_3N_2M),[1c] bis(phosphinimino)methanide (CN_2P_2M)[1d,e,3a,b] and bis(phosphinimino)amides (N_3P_2M) (Chart 2).[1a,b]

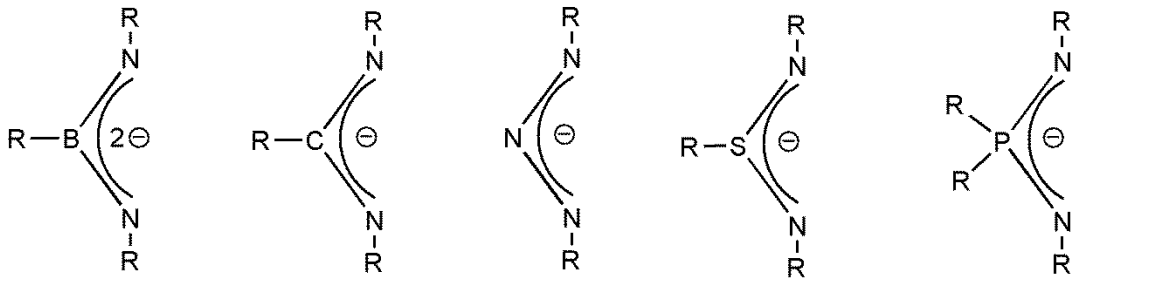

Chart 1. Popular four membered chelating ligands.

In the context of six membered chelate rings,[4] the β-diketiminato ligands have dominated the literature in which these ligands have been used for the stabilization of unusual low-coordinate/low valent metal environments,[5] polymerization catalysts[6] etc. The imino group (-C=NR) is isoelectronic to the oxo group (-C=O) and is able to donate a lone pair of

electrons to interact with the metal ions. The R-groups on the 'N' provide the necessary steric bulk to control the metal nuclearity and coordination number in addition to stabilizing the metal centre in an appropriate oxidation state. A variety of imino analogues of *p*-block elements of groups 14, 15 and 16 have been utilized as ligands in coordination chemistry. After the imino groups (–C=NR), the incorporation of aza-phosphorus (-(R_2)P=NR) group in ligand backbones has gained more attention in coordination chemistry and has found large applications in homogeneous catalysis.[1b] Incorporation of phosphorus in the ligand backbone offers a great advantage over carbon in the sense that phosphorus can exhibit a rich substitutional chemistry and a range of geometrical environments making it more versatile in nature.

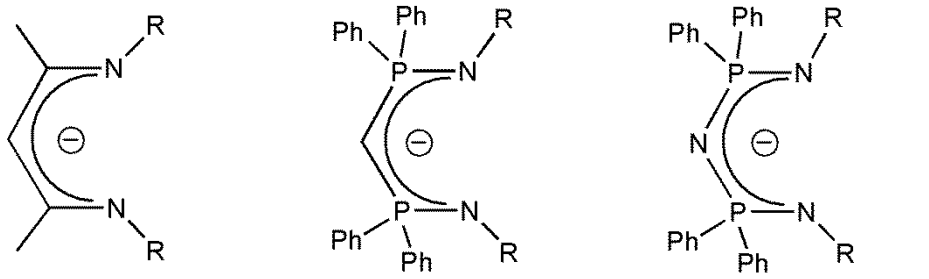

Chart 2. Popular six membered chelating ligands.

Another advantage of P–N based ligands over the C–N based ligands is the easy assessment of the reaction progress by ^{31}P NMR due to the appreciable sensitivity of the ^{31}P nucleus and a large chemical shift range. After β-diketiminates ligands, bis(phosphinimino)methanides (Chart 2) became more popular due to the above mentioned features. Bis(phosphinimino)methanides can act as monoanionic[3a] as well as dianionic[3b] ligand systems to form six membered chelates or carbene type bond formation, respectively. A literature survey revealed that bis(phosphinimino)methanide ligands have been used for the synthesis of a large number of main group,[1d] transition metal, and lanthanide complexes[1e,3a,b]

as well as, having been used for the activation of small molecules,[7a] homogeneous catalysis[7b,c] and organic synthesis.[7b]

Another type of ligand similar to bis(phosphinimino)methanides are bis(phosphinimino)amides (Chart 2) which have gained a lot of attention but usage of these ligands has largely been limited to the transition metals,[1a,b] complexes of *s*-block[1a,b] and lanthanides.[8] Bis(phosphinimino)amide ligands contain a common unit $[NR=P(R_2)]_2N$ similar to iminophosphorane ligand. Replacement of an R group in iminophosphorane **A** (Chart 3) at phosphorus with an imino function (=NR) leads to the formation of monoanionic, dianionic and trianionic systems (**B**, **C** and **D**, Chart 3), respectively. Neutral aza phosphazenes $[–(R_2)P=N-]_n$ are isoelectronic to silioxanes $[–(R_2)Si–O–]_n$ and exist as polymeric or cyclic compounds such as cyclotriphospatrizene **E** (Chart 3) commonly known as cyclophosphazenes. Chemistry of cyclophosphazenes mainly revolves around two themes: Nucleophilic substitution reactions of halogenocyclophosphazenes and ring-opening polymerization of $N_3P_3Cl_6$ to the linear polydichlorophosphazene.[1f]

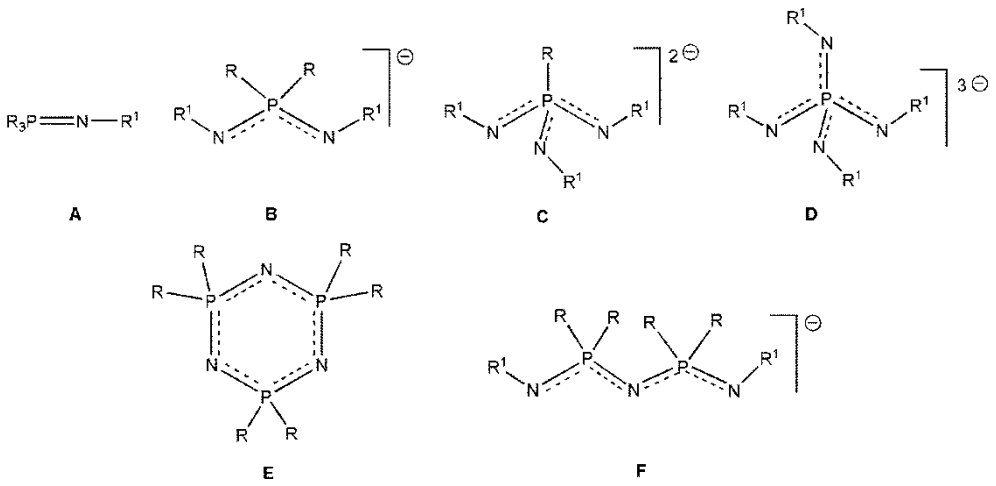

Chart 3. Various forms of iminophosphorane compounds.

Another class of P/N ligands are the monoanionic diiminodiphosphazenates **F** (Chart 3) which contain terminal imino and bridged aza groups. A literature survey reveals that acyclic phosphazenes with chlorine substituted P atoms have been used to prepare metal

complexes[9,10] but their reaction chemistry could be hampered due to the possibility of chlorine or other similar reactive groups participating in other side reaction in the main course of reaction. In order to be used as innocent ligand, bis(phosphinimino)amides frameworks should have nonreactive groups on the P as well as on the N atoms. Various reports on bis(phosphinimino)amides with dimethylamine substituted P and trimethylsilane substituted N may overcome some of these challenges nevertheless,[11] the presence of relatively bulky and non-reactive, preferably C based aryl substituents on P and N atoms of bis(phosphinimino)amide can be considered as ideal candidates in this regard.[8,12]

Surprisingly, prior to this work the structurally characterized neutral complexes of bis(phosphinimino)amide with group 13 elements comprised only $[(N(PCl_2NMe_2)_2)BX_2]$ (X = Cl, F, OSO_2CF_3)[10a] complexes of B, three complexes of Al; $[(N(PCl_2NMe_2)_2)AlMeX]$; X = Cl, $O{-}C_6H_2$-2,4,6-*t*Bu_3][9] & $[(N(PPh_2NSiMe_3)_2)AlMe_2]$,[11b] no complex of Ga and only one complex of In; $[(N(PPh_2NSiMe_3)_2)InMe_2]$.[11b] The *bis*(phosphinimino)amide ligand $[N(Me_2PNSiMe_3)_2]H$ with one equivalent of NaH and KH in toluene at reflux gave the corresponding alkali metal salt $[Na_2\{N(Me_2PNSiMe_3)_2\}_2]$ and $[KN(Me_2PNSiMe_3)_2]_{\infty}$.[11b] The corresponding lithium derivative, $[Li_2\{N(Ph_2PNSiMe_3)_2\}_2]$[11a] was prepared by the reaction of $[N(Ph_2PNSiMe_3)_2]H$ with one equivalent of *n*BuLi. The sodium complex $[Na_2\{N((Me_2N)_2PNSiMe_3)_2\}_2]$ and lithium complex $[Li_2\{N(Ph_2PNSiMe_3)_2\}_2]$ are dimeric in the solid state,[11a] whereas the potassium complex exists as a polymer in the solid state, involving imino-N of dimethylamino side groups as well as aza-N in metal coordination.[11b] Calcium $[Ca\{N((Me_2N)_2PNSiMe_3)_2\}_2]$ and barium derivatives $[Ba\{N((Me_2N)_2PNSiMe_3)_2\}_2]$ were synthesised by the reaction of $[N(Me_2PNSiMe_3)_2]H$ with $[M(N(SiMe_3)_2)_2]$ (M = Ca, Ba) where distorted octahedral coordination spheres, effectively shielded by two bulky tridentate ligands, were observed.[11b,d]

In fact, as mentioned above, only two compounds $[N(PPh_2NSiMe_3)_2AlMe_2]$ and $[N(PPh_2NSiMe_3)_2InMe_2]$ representing structurally characterized examples from group 13 based on aryl substituted P atoms in bis(phosphinimino)amide ligand[11b] were prepared by Roesky and co-workers by the reaction of neutral *bis*(phosphinimino)amide ligand with one equivalent of MMe_3 (M = Al, Ga, In). The solid state structures of these complexes showed a monomeric N_3P_2M chelate so that the overall result is a six-membered ring system in a twist-boat conformation.

The work described in this thesis focuses on monoanionic bis(phosphinimino)amides ligands of the form **F** (Chart 3). The advantage of bis(phosphinimino)amides ligands is their facile synthesis which further allows for an easy modification of their steric and electronic properties through variation of the substituents on the nitrogen atoms.

The *bis*(phosphinimino)amides can be synthesized by two main routes: (i) reaction of trihalophosphorane with excess ammonia followed by deprotonation and silylation (*path a*).[14] (ii) By the reaction of tetraphenyldiphosphazane $[NH(PPh_2)_2]$ with organic azides under elevated temperatures (*path b*)[8] (Chart 4).

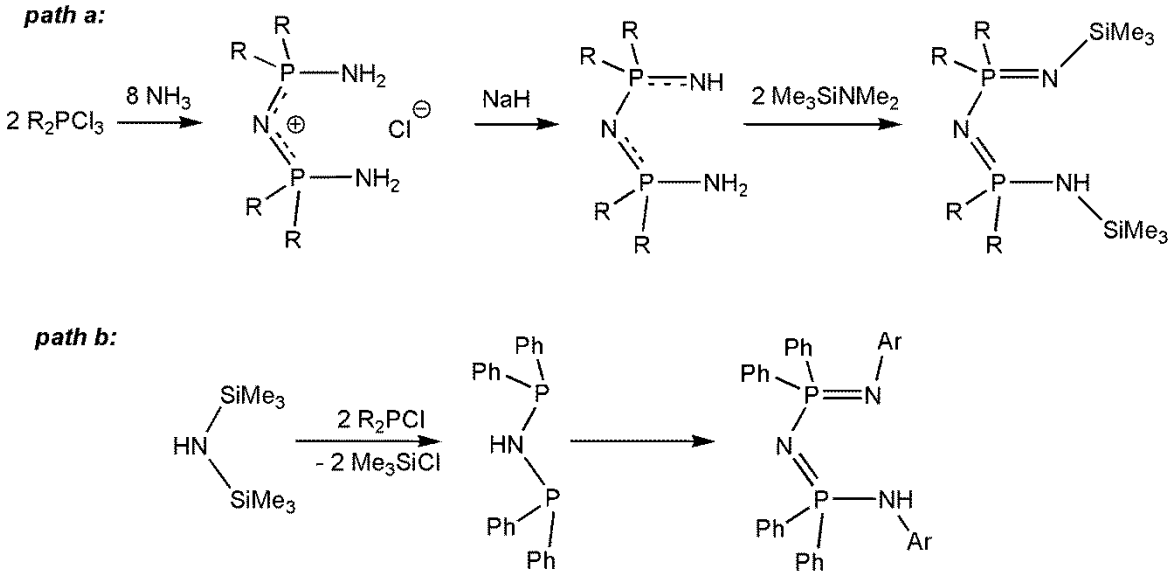

Chart 4. Synthetic routes to bis(phosphinimino)amide ligand.

In view of the scarcity of structurally characterized neutral complexes of group 13 elements with bis(phosphinimino)amides, the essence of the present work is to synthesize novel group 13 metal complexes with aryl substituted P and N atoms of bis(phosphinimino)amide ligand. Consequently, we report, in this chapter of the thesis, on the synthesis, characterization and structure of the [N,N'] donor ligand [HN(Ph_2PN(2,4,6-$Me_3C_6H_2$))$_2$] (**L_1**H) and its mononuclear complexes with group 13 elements.

1.2 Results and Discussion

The ligand [HN(Ph_2P(2,4,6-Me_3C6H_2))$_2$] (**L_1**H) was synthesized from the reaction of tetraphenyldiphosphazane $(Ph_2P)_2NH$[15] with mesitylazide[16] in toluene, and purified by recrystallization from toluene (Scheme 1). The ^{1}H NMR spectrum of **L_1**H showed two singlets at 1.86 and 2.03 ppm corresponding to the *o*- and *p*-Me of the mesityl group. The aromatic meta-hydrogen of the mesityl group appeared as a singlet at 6.53 ppm and the remaining aromatic hydrogens appeared as a multiplet between 7.59–7.54 and 7.22–7.10 ppm. The signal for NH was not detected in its ^{1}H NMR spectrum. The ^{13}C NMR spectrum of **L_1**H showed the expected P-C couplings and the number of signals in ^{13}C NMR were also consistent with its composition. The ^{31}P{^{1}H} NMR of **L_1**H showed a single resonance at 2.35 ppm which is considerably up-field shifted compared to $(Ph_2P)_2NH$ (42.54 ppm).

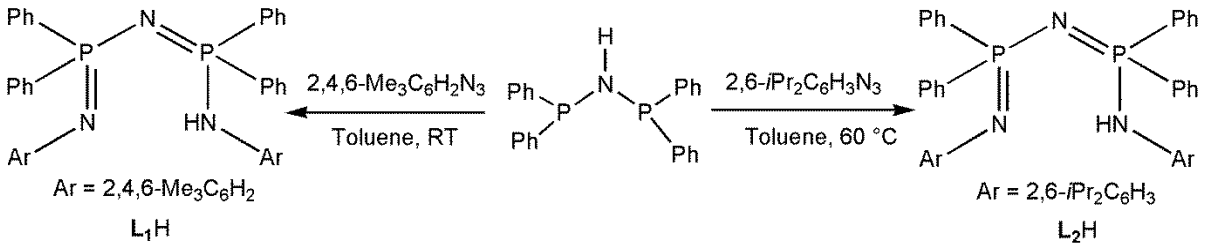

Scheme 1. Synthesis of bis(phosphinimino)amine (**L_1**H and **L_2**H).

The sharp absorption band around 3313 cm^{-1} in the IR spectrum of **L_1**H can be attributed to the N–H stretching frequency. The mass spectrum of **L_1**H showed the base peak at *m/z* = 652.3016 that is also the molecular ion peak $[M+H]^+$. The ligand [HN(Ph_2P(2,6-*i*$Pr_2C_6H_3$))$_2$]

(**L$_2$**H) was synthesized following the literature procedure by reacting tetraphenyldiphosphazane $(Ph_2P)_2NH$[15] with 2,6-diisopropylphenylazide[17] in toluene (Scheme 1). The spectroscopic characterization of ligand **L$_2$**H was consistent with the reported data.[8a] Single crystals of **L$_1$**H and **L$_2$**H suitable for X-ray structural analysis were grown from toluene solution at 4 °C. The ligands **L$_1$**H and **L$_2$**H crystallize in the monoclinic system with *C*2/*c* and triclinic system with *P*ī space group (Table 1, Figure 1), respectively.

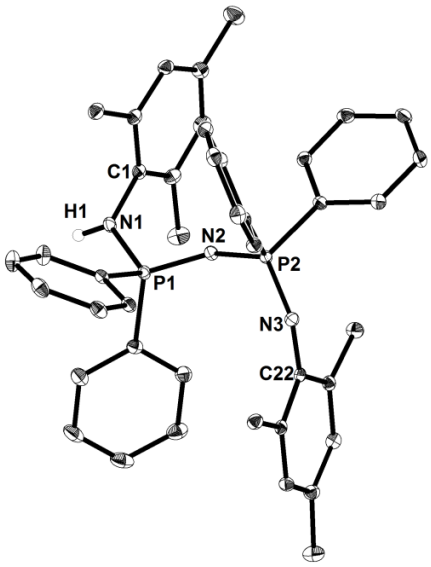

Figure 1. Solid state structure of the ligand (**L$_1$**H). All hydrogen atoms except the one on N(1) have been omitted for clarity. Thermal ellipsoids have been drawn at 30% probability. Selected bond lengths [Å] and bond angles [°]: N(1)–P(1) 1.652(2), N(2)–P(1) 1.560(2), N(2)–P(2) 1.612(2), N(3)–P(2) 1.563(2); P(1)–N(1)–H(1) 118.90(2), P(1)–N(2)–P(2) 140.20(1), N(1)–P(1)–N(2) 108.58(2), N(2)–P(2)–N(3) 120.73(2).

The P_2N_3 backbone of **L$_1$**H adopts a *zig-zag* arrangement with the P(1)–N(2)–P(2) core in a bent geometry with an angle of 140.20(1)° and the terminal nitrogen atoms have the mesityl substituents oriented in mutually transoid arrangement, whereas in ligand **L$_2$**H, the P_2N_3 backbone adopts a regular arrangement with the P(1)–N(2)–P(2) core in a bent geometry with an angle of 134.96(1)° and the terminal nitrogen atoms have the 2,6-

diisopropylphenyl substituents oriented in mutually *cisoid* arrangement The two phenyl groups in $\mathbf{L_1}$H on each phosphorus atom are arranged above and below the P–N–P plane, whereas in $\mathbf{L_2}$H two phenyl groups on each phosphorus atom are arranged above the P–N–P plane.

The N(3)-P(2) and N(2)-P(1) bonds of $\mathbf{L_1}$H (1.563(2) and 1.560(2) Å) are shorter due to the double bond character as compared to the N(2)–P(2) and N(1)–P(1) distances {1.612(2) and 1.652(2) Å} that are expected to exhibit single P-N bonds. The bond angles of N(1)–P(1)–N(2) and N(2)–P(2)–N(3) respectively, are 108.58(2)° and 120.73(2)°. The N(2)-P(2) and N(2)-P(1) bonds for $\mathbf{L_2}$H (1.579(6) and 1.582(3) Å) are shorter due to double bond character as compared to N(3)–P(2) and N(1)–P(1) distances {1.611(3) and 1.617(3) Å} that are expected to exhibit single P-N bonds. The bond angles of N(1)–P(1)–N(2) and N(2)–P(2)–N(3) respectively, are 111.47(1)° and 112.37(1)°.

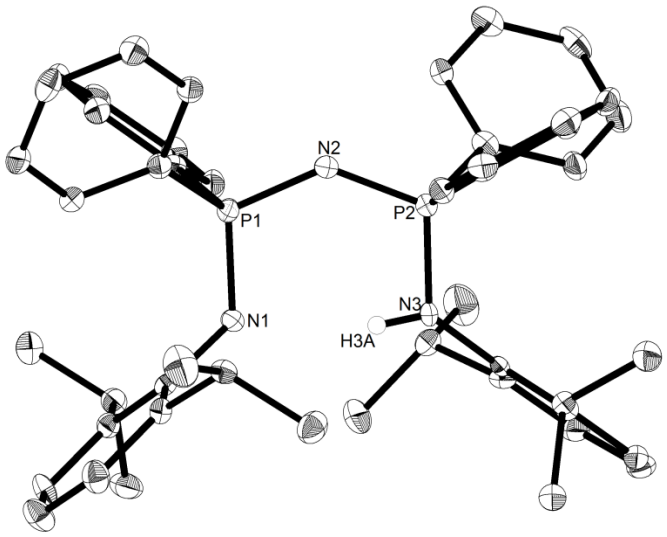

Figure 2: Single crystal structure of ligand ($\mathbf{L_2}$H). All hydrogen atoms, except that on N(3), have been omitted for clarity. Thermal ellipsoids have been drawn at 30% probability. Selected bond lengths [Å] and bond angles [°]: N(1)–P(1) 1.617(3), N(2)–P(1) 1.582(3), N(2)–P(2) 1.579(6), N(3)–P(2) 1.611(3), N(1)–P(1)–N(2) 111.47(1), P(1)–N(2)–P(2) 134.96(1), N(2)–P(2)–N(3) 112.37(1).

Treatment of the ligands $\mathbf{L_1}$H and $\mathbf{L_2}$H with $LiN(SiMe_3)_2$ or *n*BuLi in Et_2O forms [$\mathbf{L_1}$Li·OEt_2] (**1.1**) and [$\mathbf{L_2}$Li·OEt_2] (**1.2**) (Scheme 2), respectively. Compounds **1.1** and **1.2** are white crystalline solids that are highly sensitive to moisture. Compounds **1.1** and **1.2** were characterized by ^{1}H, ^{13}C, ^{31}P{^{1}H} and ^{7}Li NMR spectroscopy and their solid state structures were elucidated by single crystal X-ray structural analyses.

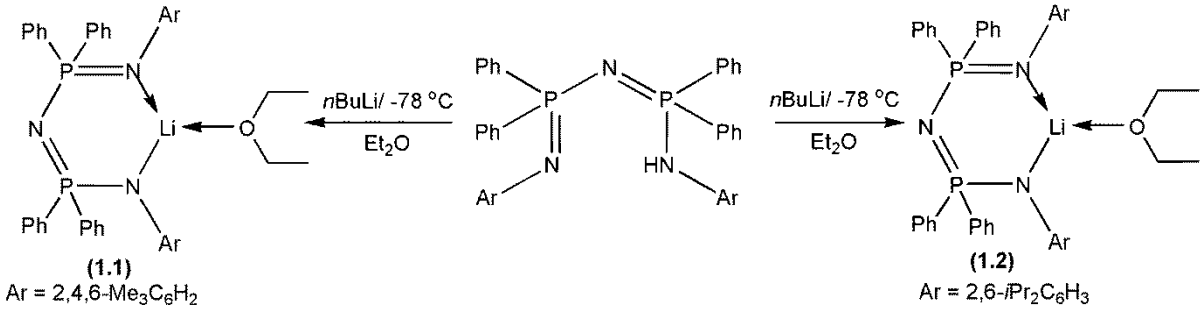

Scheme 2. Synthesis of the lithium derivatives [$\mathbf{L_1}$Li·OEt_2] (**1.1**) and [$\mathbf{L_2}$Li·OEt_2] (**1.2**) of bis(phosphinimino)amines $\mathbf{L_1}$H and $\mathbf{L_2}$H.

The ^{1}H NMR spectra of compounds **1.1** and **1.2** showed that the lithium atom was coordinated with a molecule of Et_2O for **1.1** (a triplet at 0.67 ppm and a quartet at 2.79 ppm) and for **1.2** (a triplet at 0.46 ppm and a quartet at 2.81 ppm), respectively. The ^{1}H NMR spectrum of $\mathbf{L_1}$H (**1.1**) showed two overlapped singlets at 2.21 and 2.23 ppm corresponding to the *o*- and *p*-Me of the mesityl group. Other features in the ^{1}H NMR spectrum of **1.1** were consistent with the ligand skeleton. The ^{31}P{^{1}H} NMR spectrum of **1.1** (1.75 ppm) showed a signal that is slightly upfield shifted as compared to its precursor $\mathbf{L_1}$H (2.35 ppm). The ^{7}Li NMR of **1.1** showed a signal at 1.23 ppm. The ^{1}H NMR spectrum of $\mathbf{L_2}$H (**1.2**) showed a doublet at 1.03 ppm corresponding to the $CH(CH_3)_2$ of 2,6-diisopropylphenyl group. Other features in the ^{1}H NMR spectrum of **1.2** were consistent with the ligand skeleton. The ^{31}P{^{1}H} NMR spectrum of **1.2** showed a signal (2.81 ppm) that is slightly upfield shifted as compared to its precursor $\mathbf{L_2}$H (6.5 ppm). The ^{7}Li NMR of **1.2** showed a signal at 1.06 ppm.

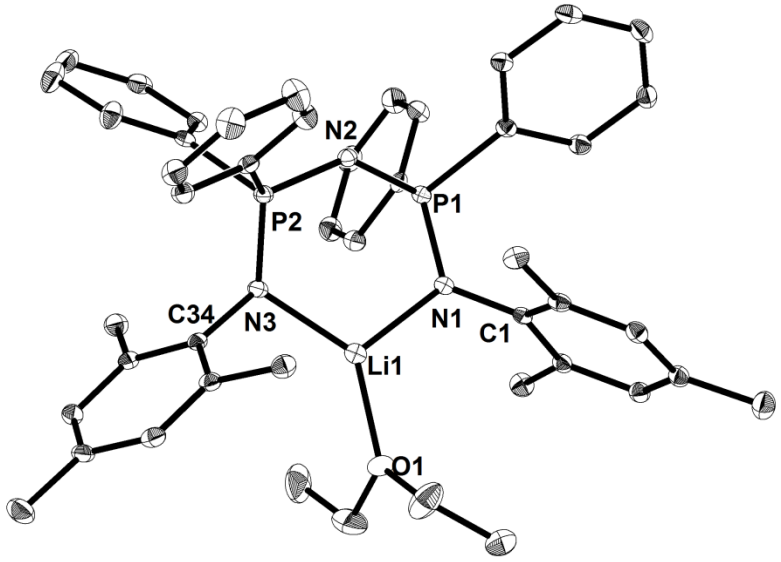

Figure 3. Solid state structure of compound **1.1**. All hydrogen atoms have been deleted for clarity. Thermal ellipsoids have been drawn at 30% probability. Selected bond lengths [Å] and bond angles [°]: Li(1)–N(1) 1.921(1), Li(1)–N(3) 1.964(2), Li(1)–O(1) 1.918(2), N(1)–P(1) 1.588(2), N(2)–P(1) 1.591(2), N(2)–P(2) 1.590(2), N(3)–P(2) 1.593(2), P(1)–N(2)–P(2) 132.78(2), P(1)–N(1)–Li(1) 115.41(2), N(3)–Li(1)–N(1) 110.35(1), P(2)–N(3)–Li(1) 120.65(2), O(1)–Li(1)–N(1) 115.56(2), O(1)–Li(1)–N(3) 134.02(1).

Crystals suitable for single crystal X-ray analysis of compound **1.1** were grown from Et_2O at 4 °C. Compound **1.1** crystallized in monoclinic system with space group $P2_1/n$ (Table 2, Figure 3). The solid state structure of compound **1.1** confirmed Et_2O coordination to the lithium centre in a three coordinated environment. The N_3P_2Li six-membered ring is highly puckered, almost in a form of a boat with P(1) and N(3) forming bow and stern of it and other atoms of this six membered chelate N(1), N(2), P(2) and Li(1) are nearly planar. The average P–N distance in the N_3P_2 backbone of the ligand in **1.1** is 1.590 Å. The Li–N bond distances (1.964(1) and 1.921(1) Å), the Li(1)–O(1) bond length (1.918(2) Å) and N(3)–Li(1)–N(1) bond angle (110.35(1)°) in **1.1** are comparable to that seen in three coordinate Li bound to Et_2O and amide nitrogens in $[HC\{Ph_2PN(2,4,6\text{-}Me_3C_6H_2)\}_2Li{\cdot}OEt_2]$.[18a]

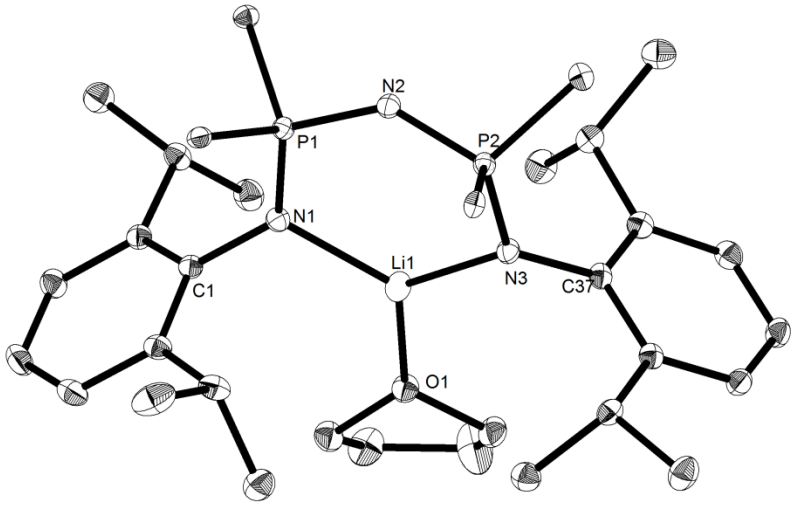

Figure 4: Single crystal X-ray structure of compound **1.2**. All hydrogen atoms and two phenyl rings on phosphorus have been omitted for clarity. Thermal ellipsoids have been drawn at 30% probability. Selected bond lengths [Å] and bond angles [°]: Li(1)–N(1) 1.951(1), Li(1)–N(3)1.988(2), Li(1)–O(1) 1.934(0), N(1)–P(1) 1.599(1), N(2)–P(1) 1.585(2), N(2)–P(2) 1.593(1), N(3)–P(2) 1.596(1), P(1)–N(2)–P(2) 137.7(1), Li(1)–N(1)–P(1) 116.74(2), N(3)–Li(1)–N(1) 115.77(1), Li(1)–N(3)–P(2) 113.18(1), O(1)–Li(1)–N(1) 121.26(2), O(1)–Li(1)–N(3) 122.79(2).

Crystals suitable for single crystal X-ray analysis of compound **1.2** were grown from THF at 4 °C. Compound **1.2** crystallized in a monoclinic system with space group $P2_1/n$ (Table 2, Figure 4). The solid state structure of compound **1.2** showed THF coordination to the lithium centre in a three coordinated environment. The N_3P_2Li six-membered ring is highly puckered, almost in a form of a boat with P(1) and N(3) forming bow and stern of it and other atoms of this six membered chelate N(1), N(2), P(2) and Li(1) are nearly planar. The average P–N distance in the N_3P_2 backbone of **1.2** is 1.590 Å. The Li–N bond distances (1.951(1) and 1.988(2) Å) in **1.2** are comparable to the β-diketiminate lithium complex [HC{$CH_3CN(2,6\text{-}i Pr_2C_6H_3)$}$_2$Li·THF] (1.958 Å).[18b] The Li–O bond distances (1.934(0) Å) in **1.2** are longer than that in β-diketiminate lithium complex, [HC{CH_3CN(2,6-

i$Pr_2C_6H_3$)}$_2$Li·THF] (1.790 Å), and showed that weak coordination of oxygen to lithium in **1.2** as compared to the later complex. The N(1)-Li(1)-N(3) bond angle **1.2** is (115.77(1)°) is wider than that in [HC{CH_3CN(2,6-*i*$Pr_2C_6H_3$)}$_2$Li·THF] (95.5).[18b]

As shown in Scheme 3, a borondifluoride complex $\mathbf{L_1}BF_2$ (**1.3**) was prepared by the reaction of BF_3 with *in situ* generated lithium derivative of the bis(phosphinimino)amide ligand.

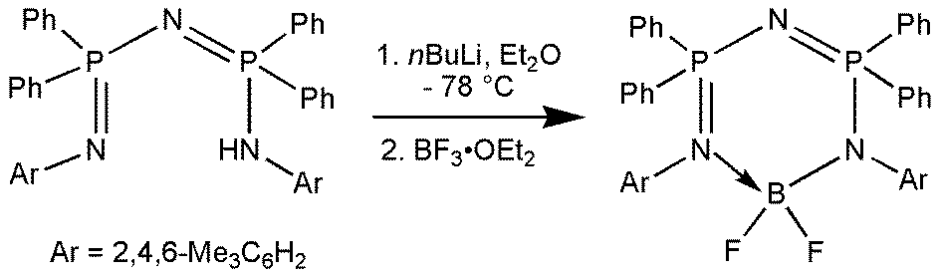

Scheme 3. Synthesis of borondifluoride complex $\mathbf{L_1}BF_2$ (**1.3**) with bis(phosphinimino)amide.

Compound **1.3** was characterized by ^{1}H, ^{13}C, ^{31}P{^{1}H},^{19}F and ^{11}B NMR spectroscopy and its solid state structure was elucidated by single crystal X-ray structural analysis. The ^{1}H NMR spectrum of **1.3** showed two singlets at 2.0 and 2.21 ppm corresponding to the *o*- and *p*-Me of the mesityl group. Other features in the ^{1}H NMR spectrum of **1.3** were consistent with the ligand skeleton. The ^{31}P{^{1}H} NMR of **1.3** showed a single resonance at 23.43 ppm which is considerably down-field shifted compared to **1.1** (1.75 ppm) and $\mathbf{L_1}$H (2.35 ppm). The ^{19}F NMR spectrum of complex **1.3** showed an expected quartet (-132.6 ppm) due to B–F coupling ($^1J_{B\text{-}F}$ = 35.4 Hz) and the ^{11}B NMR also exhibits a triplet (2 ppm) due to this B-F coupling. Each signal of this triplet carried features resulting a triplet of a triplets (tt) (Figure 5.) due to coupling with two P atoms of the ligand backbone ($^2J_{B\text{-}P} \approx 9$ Hz). The HRMS investigations under +ve ion mode of **1.3** revealed the signal at *m/z* = 700.2974 (calculated *m/z* = 700.3000) for $[M]^+$ and *m/z* = 680.2986 (calculated *m/z* = 680.2938) as the base peak corresponding to the $[M - F - H]^+$.

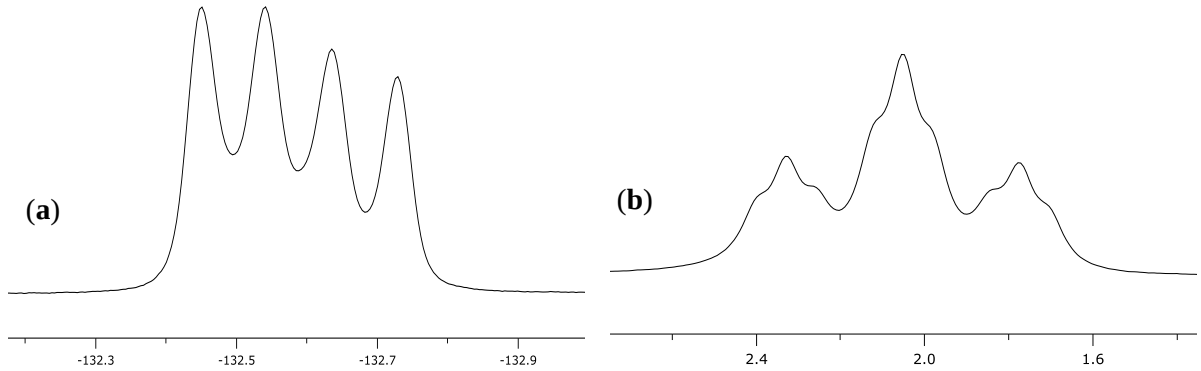

Figure 5. (**a**) ^{19}F NMR spectrum of compound **1.3** showing B-F coupling for BF_2. (**b**) ^{11}B NMR spectrum of compound **1.3** showing B-F coupling for BF_2 fragment.

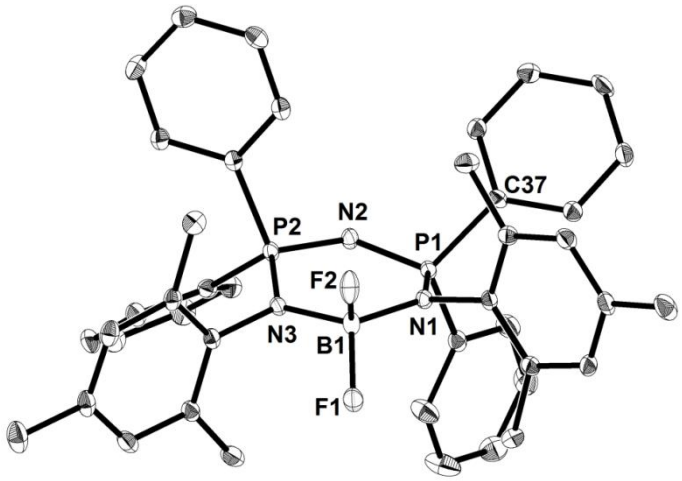

Figure 6. Solid state structure of compound $\mathbf{L_1}BF_2$ (**1.3**). All hydrogen atoms have been deleted for clarity. Thermal ellipsoids have been drawn at 30% probability. Selected bond lengths [Å] and bond angles [°]: B(1)–N(1) 1.565(4), B(1)–N(3) 1.571(4), B(1)–F(1) 1.395(3), B(1)–F(2) 1.398(4), P(1)–N(1) 1.634(2), P(2)–N(3) 1.635(2), P(1)–N(2) 1.589(3), P(2)–N(2) 1.581(3); N(1)–B(1)–N(3) 114.12(2), F(1)–B(1)–F(2) 107.03(2), P(1)–N(1)–B(1) 125.21(2), P(2)–N(3)–B(1) 125.73(2), P(1)–N(2)–P(2) 128.63(1), F(2)–B(1)–N(1) 108.23(2), F(2)–B(1)–N(3) 109.65(2), F(1)–B(1)–N(1) 109.86(2), F(1)–B(1)–N(3) 107.72(2), N(2)–P(2)–N(3) 110.47(1), N(2)–P(1)–N(1) 110.42(1).

Compound **1.3** crystallizes in the monoclinic system with space group $P2_1/c$ with 1 molecule in the asymmetric unit (Table 3, Figure 6). The molecular unit of complex **1.3**

showed a distorted tetrahedral geometry around boron. The B-F bond length of 1.395(3) and 1.398(4) Å in complex **1.3** (Figure 6) is comparable to the β-diketiminate borondifluoride complex, [HC{*t*BuCN(2,6-*i*Pr$_2$C$_6$H$_3$)}$_2$BF$_2$] (1.564 and 1.560 Å). The F(1)-B(1)-F(2) bond angle (107.03(2)°) in compound **1.3** also compares well with 108.73° seen in [HC{*t*BuCN(2,6-*i*Pr$_2$C$_6$H$_3$)}$_2$BF$_2$][19] and the N(1)-B(1)-N(3) bond angle in **1.3** (114.12(2)°) is slightly wider than that in [HC{*t*BuCN(2,6-*i*Pr$_2$C$_6$H$_3$)}$_2$BF$_2$] (110.66°).[19]

The heteroleptic dichloride of aluminium **L$_1$**AlCl$_2$ (**1.4**) and gallium **L$_1$**GaCl$_2$ (**1.5**) supported by bis(phosphinoimine)amide have been prepared by the reaction of appropriate metal halides, MCl$_3$ with *in situ* generated lithium derivative of the ligand (Scheme 4). These complexes have been characterized by ^{1}H and other heteronuclear ^{13}C, and ^{31}P{^{1}H} NMR spectroscopy. The ^{31}P{^{1}H} NMR spectra of the reactions between *in situ* generated **1.1** and MCl$_3$, have been very useful in preliminary investigations that showed a single resonance in each case {(23.7 ppm for **1.4** (M = Al, X = Cl); 24 ppm and for **1.5** (M = Ga, X = Cl)} that was different from **1.1** (1.75 ppm). The ^{1}H NMR spectrum of **1.4** and **1.5** each showed two singlets at 2.02 and 2.18 and 2.05 and 2.17 ppm, respectively corresponding to the *o*- and *p*-Me of the mesityl group. Other features in the ^{1}H NMR spectrum of **1.4** and **1.5** were consistent with the ligand skeleton.

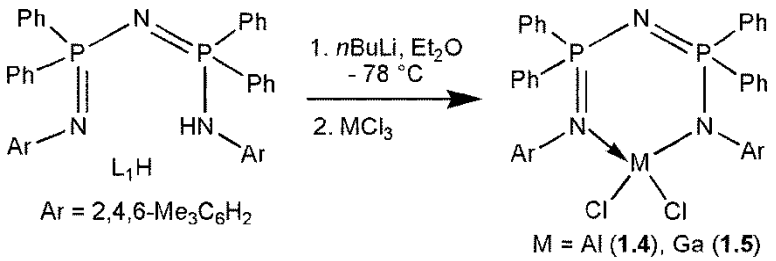

Scheme 4. Synthesis of aluminumdichloride **L$_1$**AlCl$_2$ (**1.4**) and galliumdichloride **L$_1$**GaCl$_2$ (**1.5**) complexes with bis(phosphinimino)amide.

The HRMS investigations under +ve ion mode of **1.4** and **1.5** revealed the signal at *m/z* = 712.2332 (calculated *m/z* = 712.2358) for **1.4** [M - Cl - H]$^+$ and *m/z* = 756.1733

(calculated *m/z* = 756.1798) as the base peak corresponding to the $[M - Cl - H]^+$ for **1.5**. Complexes **1.4** and **1.5** were subsequently characterized by single crystal X-ray structures.

Compounds **1.4** and **1.5** crystallize in the monoclinic system with space group $P2_1/c$ with 1 molecule in the asymmetric unit (Table 3 and 4). The molecular unit of complexes **1.4** and **1.5** showed a distorted tetrahedral geometry around the metal centers.

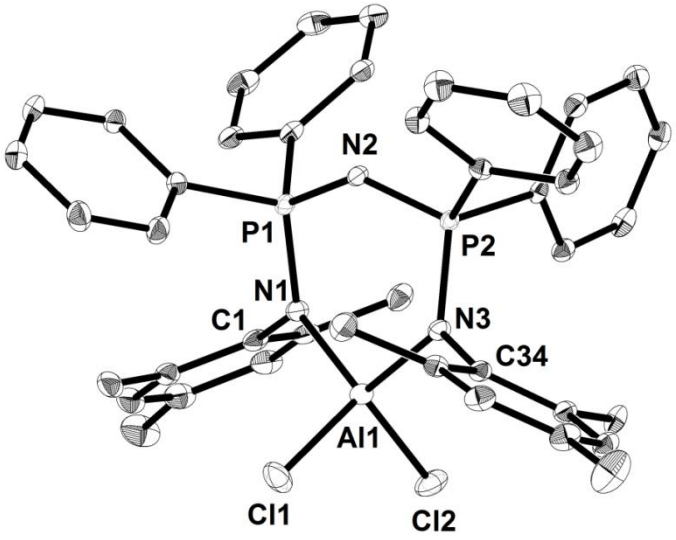

Figure 7. Solid state structure of compound $\mathbf{L_1}AlCl_2$ (**1.4**). All hydrogen atoms have been deleted for clarity. Thermal ellipsoids have been drawn at 30% probability. Selected bond lengths [Å] and bond angles [°]: N(2)–P(1) 1.592(2), N(2)–P(2) 1.582(2), Al(1)–N(1) 1.869(3), Al(1)–N(3) 1.880(3), N(1)–P(1) 1.646(2), N(3)–P(2) 1.649(3), Al(1)–Cl(1) 2.151(2), Al(1)–Cl(2) 2.138(2); P(2)–N(2)–P(1) 132.32(2), P(1)–N(1)–Al(1) 119.68(1), P(2)–N(3)–Al(1) 122.83(1), N(1)–Al(1)–N(3) 108.08(2), N(1)–Al(1)–Cl(1) 112.76(9), N(3)–Al(1)–Cl(1) 107.68(9), Cl(2)Al(1)–Cl(1) 106.57(6), N(2)–P(1)–N(1) 111.44(13), N(2)–P(2)–N(3) 111.18(1).

The Al-Cl bond length of 2.151(2) and 2.138(2) Å in complex **1.4** (Figure 7) is comparable to that in $[HC\{MeCN(2,6\text{-}iPr_2C_6H_3)\}_2AlCl_2]$ (2.134 and 2.118 Å)[20] and $[HC\{Ph_2PN(2,4,6\text{-}Me_3C_6H_2)\}_2AlCl_2]$ (2.160 and 2.137 Å).[18a] The Cl(1)-Al(1)-Cl(2) bond angle (106.57(6)°) in compound **1.4** compares well with 108.02° seen in [HC{MeCN(2,6-

*i*Pr$_2$C$_6$H$_3$)}$_2$AlCl$_2$][20] and [HC{Ph$_2$PN(2,4,6-Me$_3$C$_6$H$_2$)}$_2$AlCl$_2$] (106.46°).[18a] The N(1)-Al(1)-N(3) bond angle in **5** (108.08(2)°) is wider than that in [HC{MeCN(2,6-*i*Pr$_2$C$_6$H$_3$)}$_2$AlCl$_2$][20] (99.36°) but narrower than that in [HC{Ph$_2$PN(2,4,6-Me$_3$C$_6$H$_2$)}$_2$AlCl$_2$] (113.01°).[18a]

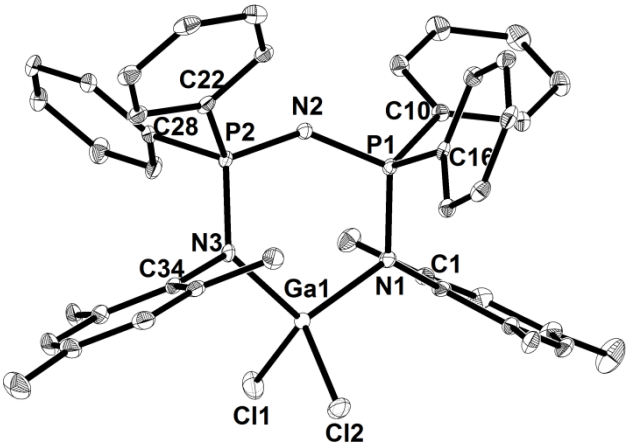

Figure 8. Molecular structure of compound **L$_1$**GaCl$_2$ (**1.5**). All hydrogen atoms have been deleted for clarity. Thermal ellipsoids have been drawn at 30% probability. Selected bond lengths [Å] and bond angles [°]: N(1)–P(1) 1.640(3), N(3)–P(2) 1.645(4), N(2)–P(1) 1.587(3), N(2)–P(2) 1.584(3), Ga(1)–N(1) 1.917(3), Ga(1)–N(3) 1.924(3), Ga(1)–Cl(1) 2.172(1), Ga(1)–Cl(2) 2.193(1); P(1)–N(1)–Ga(1) 117.85(2), P(2)–N(2)–P(1) 134.1(2), P(2)–N(3)–Ga(1) 121.19(2), N(2)–P(2)–N(3) 111.23(2), N(1)–Ga(1)–N(3) 108.96(1), N(1)–Ga(1)–Cl(1) 108.31(1), N(1)–Ga(1)–Cl(2) 112.47(1), N(3)–Ga(1)–Cl(1) 113.31(1), N(3)–Ga(1)–Cl(2) 107.50(1), Cl(1)–Ga(1)–Cl(2) 106.35(6).

Compound **1.5** is the first example of a structurally characterized gallium(III) complex with a bis(phosphinimino)amide ligand (Figure 8). The Ga-Cl bond length of 2.172(1) and 2.193(1) Å in complex **1.5** are comparable to the corresponding bonds in [HC{MeCN(2,6-*i*Pr$_2$C$_6$H$_3$)}$_2$GaCl$_2$] (2.228 and 2.218 Å)[20] and [HC{Ph$_2$PN(2,4,6-Me$_3$C$_6$H$_2$)}$_2$GaCl$_2$] (2.199 and 2.169 Å).[18a] The Cl(1)-Ga(1)-Cl(2) bond angle (106.35(6)°) in compound **1.5** compares well with similar angle (105.91°) seen in [HC{Ph$_2$PN(2,4,6-Me$_3$C$_6$H$_2$)}$_2$GaCl$_2$][18a] and is slightly narrower than that in [HC{MeCN(2,6-*i*Pr$_2$C$_6$H$_3$)}$_2$GaCl$_2$] (110.20°).[20] The N(1)-Ga(1)-N(3) bond angle in **1.5** (108.96(1)°) is wider

than that in [HC{MeCN(2,6-*i*Pr$_2$C$_6$H$_3$)}$_2$GaCl$_2$] (100.2°) but narrower than that in [HC{Ph$_2$PN(2,4,6-Me$_3$C$_6$H$_2$)}$_2$GaCl$_2$] (111.21°).[20]

The indiumdibromide complex of bis(phosphinoimine)amide **L$_1$**InBr$_2$ (**1.6**) was prepared by the reaction of InBr$_3$ with the *in situ* generated lithium derivative of the ligand (Scheme 5).

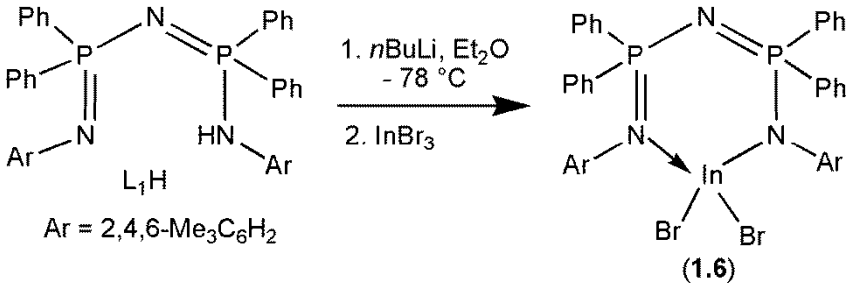

Scheme 5. Synthesis of indiumdibromide complex **L$_1$**InBr$_2$ (**1.6**) with bis(phosphinimino)amide.

Compound **1.6** was characterized by ^{1}H, ^{13}C and ^{31}P{^{1}H} NMR spectroscopy and its solid state structure was elucidated by single crystal X-ray structural analysis. The ^{1}H NMR spectrum of **1.6** showed two singlets at 2.08 and 2.17 ppm corresponding to the *o*- and *p*-Me of the mesityl group. Other features in the ^{1}H NMR spectrum of **1.6** were consistent with the ligand skeleton. The ^{31}P{^{1}H} NMR of **1.6** showed a single resonance at 21.0 ppm which is considerably down-field shifted compared to **1.1** (1.75 ppm) and **L$_1$**H (2.35 ppm). The HRMS investigations under +ve ion mode of **1.6** revealed the signal at *m/z* = 925.0316 (calculated *m/z* = 925.0244) as the base peak corresponding to the [M - H]$^+$.

Compound **1.6** crystallizes in tetragonal system with space group *I*-4$_2$*d*. Complex **1.6** is the first example of a structurally characterized indium(III)dihalide complex with a bis(phosphinimino)amide ligand (Figure 9, Table 4). The central indium atom is chelated in a puckered N$_3$P$_2$In six membered ring with the bromine atoms oriented above and below this plane leaving In center in a distorted tetrahedral arrangement. The In-Br bond lengths of

2.507(1) Å can be compared with the corresponding distances in [N{($CH_2CH_2NEt_2$)$_2$}$InBr_2$] (2.522(13).[21] The Br(1)–In(1)–Br(1') bond angle of 103.78(1) in compound **1.6** is narrower than that in [N{($CH_2CH_2NEt_2$)$_2$}$InBr_2$] (111.13(6)°).[21] The In-N bond distances in compound **1.6** are 2.113(2) Å.

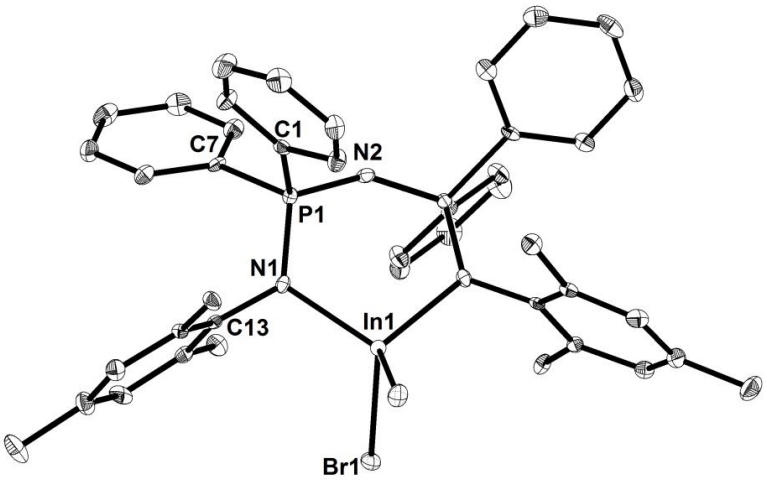

Figure 9. Solid state structure of compound **1.6**. All hydrogen atoms have been deleted for clarity. Thermal ellipsoids have been drawn at 30% probability. Selected bond lengths [Å] and bond angles [°]: In(1)–N(1) 2.113(2), In(1)–Br(1) 2.507(1), P(1)–N(1) 1.641(2), P(1)–N(2) 1.5677(12); N(1)–In(1)–N(1') 104.95(2), Br(1)–In(1)–Br(1') 103.78(1), P(1)–N(1)–In(1) 119.47(1), P(1)–N(2)–P(1') 146.65(2), N(1)–In(1)–Br(1) 111.55(6), N(2)–P(1)–N(1) 110.99(9).

Reaction of $\mathbf{L_1}$H (**L** = [N{$Ph_2PN(2,4,6\text{-}Me_3C_6H_2)$}$_2$]$^-$) with 1.2 equivalent of $BH_2Cl{\cdot}SMe_2$ in toluene at 80 ^oC (Scheme 6) results in the formation of chloroborane complex $\mathbf{L_1}$BHCl (**1.7)**. To the best of our knowledge compound **1.7** is the first example of structurally characterized monomeric chloroborane complex. The only other chlorobarane molecule reported in the literature is β-diketiminato supported [HC{CMeN(2,6-$Me_2C_6H_3$)$_2$}]BHCl characterized only by spectroscopic and spectrometric techniques[22] and lacks the structural investigation by X-ray technique.

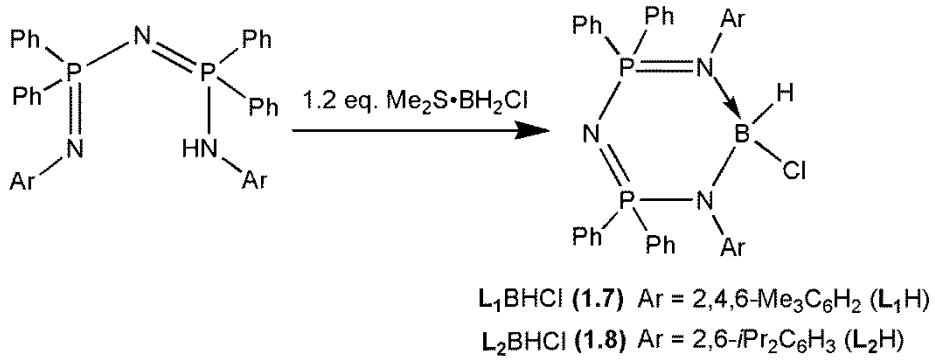

Scheme 6. Synthesis of heteroleptic chloroborane complexes $\mathbf{L_1}$BHCl (**1.7**) and $\mathbf{L_2}$BHCl (**1.8**).

Compound **1.7** was characterized by spectroscopic, spectrometric, and single crystal X-ray techniques. The IR spectrum of **1.7** showed the B–*H* stretch at 2464 cm^{-1}. The HRMS investigations under +ve ion mode of **1.7** revealed the signal at *m/z* = 662.3130 (calculated *m/z* = 662.3111) that corresponds to the loss of Cl^- from the $[M + H]^+$. The ^1H NMR spectrum of **1.7** showed two singlets at 1.70 and 2.32 ppm corresponding to the *o*- and *p*-Me of the mesityl group. In the ^1H NMR spectrum of complex **1.7,** the B*H* resonance appeared as a broad signal around 4.29 ppm and other signals were consistent with the ligand framework in the complex. A downfield shift in the $^{31}P\{^1H\}$ NMR spectrum of **1.7** (22.5 ppm) was observed when compared to ligand $\mathbf{L_1}$H (2.35 ppm). The ^{11}B NMR spectrum of **1.7** showed a sharp singlet at 7.06 ppm. Single crystals of **1.7** suitable for X-ray structural analysis were grown from toluene. Compound **1.7** crystallizes in the orthorhombic crystal system with $P2_12_12_1$ space group (Figure 10, Table 5). The coordination environment around boron is distorted tetrahedral. The central N_3P_2B ring in **1.7** slightly deviates from planarity. The B-H bond length in **1.7** (1.112(2) Å) is slightly shorter than the B-H distance reported in $\mathbf{L_1}BH_2$ (**1.11**) (1.116 Å) (vida infra). The B-N distances in **1.7** (1.537(3) and 1.559(3) Å) are slightly shorter than **1.11** (1.588(5) and 1.615(5) Å) (*vide infra*). The N(1)-B(1)-N(3) bond angle in **1.7** (114.38(2)°) is wider than the N-B-N bond angle in **1.11** (110.60(2)°) (*vida infra*).

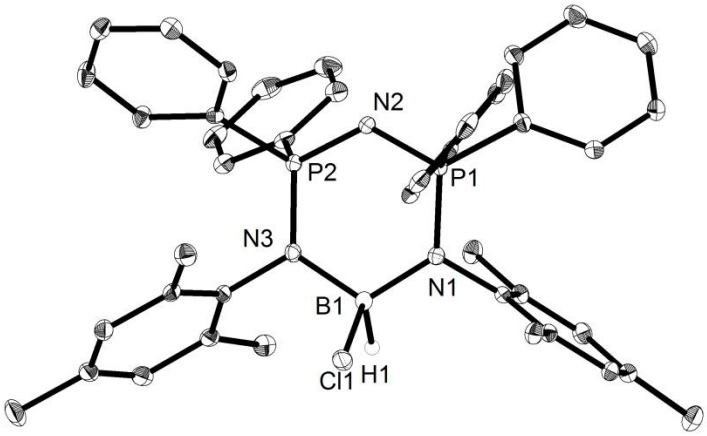

Figure 10. Solid state structure of complex $\mathbf{L_1}$BHCl **(1.7)**. All hydrogen atoms except on boron have been deleted for clarity. Thermal ellipsoids have been drawn at 50% probability. Selected bond lengths (Å) and bond angles (°): B(1)–H(1) 1.112(2), B(1)–Cl(1) 1.981(2), B(1)–N(1) 1.537(3), B(1)–N(3) 1.559(3), N(1)–P(1) 1.644(2), N(2)–P(1) 1.590(2), N(2)–P(2) 1.587(2), N(3)–P(2) 1.641(2), N(1)–B(1)–N(3) 114.38(2), N(1)–B(1)–Cl(1) 111.47(2), N(3)–B(1)–Cl(1) 105.96(1), H(1)–B(1)–Cl(1) 98.84(9).

In a similar manner, reaction of $\mathbf{L_2}$H ($\mathbf{L_2}$ = $[N\{Ph_2PN(2,6\text{-}i Pr_2C_6H_2)\}_2]^-$) with 1.2 equivalent of $BH_2Cl{\cdot}SMe_2$ in toluene at 110 ^oC (Scheme 6) results in the formation of chloroborane complex $\mathbf{L_2}$BHCl (**1.8)**. Compound **1.8** was characterized by spectroscopic and spectrometric techniques. The IR spectrum of **1.8** showed the B–*H* stretch at 2463 cm^{-1}. The HRMS investigations under +ve ion mode of **1.8** revealed the signal at *m/z* = 746.3942 (calculated *m/z* = 746.3972) that corresponds to the loss of Cl^- from the $[M + H]^+$. The ^1H NMR spectrum of **1.8** showed two doublets at 0.37 and 0.99 ppm corresponding to the $CH(CH_3)_2$ of the 2,6-diisopropylphenyl group. In the ^1H NMR spectrum of complex **1.8,** the B*H* resonance appeared as a broad signal around 4.68 ppm and other signals were consistent with the ligand framework in the complex. A downfield shift in the $^{31}P\{^1H\}$ NMR spectrum of **1.8** (25.22 ppm) was observed when compared to ligand $\mathbf{L_2}$H (6.5 ppm). The ^{11}B NMR spectrum of **1.8** showed a sharp doublet (3.27 ppm) due to B–H coupling ($^1J_{B\text{-}H}$ = 163.8 Hz).

Compound $\mathbf{L_1}AlMe_2$ (**1.9**) was prepared by reacting $AlMe_3$ with $\mathbf{L_1}H$ in Et_2O at -30 °C (Scheme 7). The ^1H NMR spectrum of **1.9** showed two singlets at 1.90 and 2.22 ppm corresponding to the *o*- and *p*-Me of the mesityl group. The Al*Me* protons resonated at -1.0 ppm in the ^1H NMR spectrum of **1.9**, the corresponding carbon is seen at -6.12 ppm in its ^{13}C NMR spectrum and the $^{31}P\{^1H\}$ NMR spectrum of **1.9** revealed the backbone phosphorus to appear at 18.9 ppm which is considerably downfield shifted as compared to $\mathbf{L_1}H$ (2.35 ppm). The signal at *m/z* = 692.2852 in the mass spectrum of **1.9** is due to $[M]^+$ which is also the base peak.

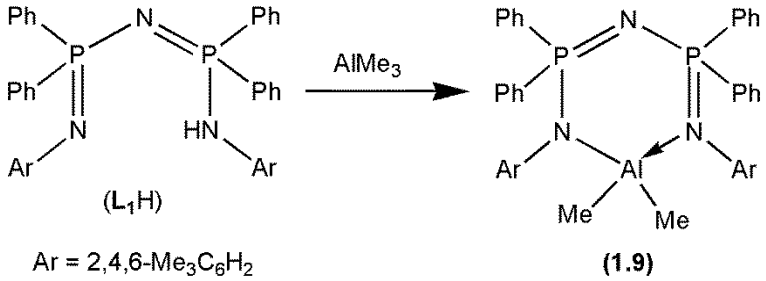

Scheme 7. Synthesis of aluminumdimethyl complex $\mathbf{L_1}AlMe_2$ **(1.9).**

Compound **1.9** crystallizes in the monoclinic system (space group $P2_1/c$) (Table 5, Figure 11). The chelated Al atom in the complex is four coordinated with distorted tetrahedral environment around it. The ligand skeleton in the six membered chelate is puckered with the Me substituents oriented above and below this chelate and pointing away from this. The C(43)–Al(1)–C(44) angle in **1.9** is 108.90(2)°. The N(1)–Al(1)–N(3) bond angle in **1.9** is 103.54(2)°. The Al-Me bond lengths of 1.984(3) and 1.966(3) Å in complex **1.9** are comparable to the corresponding bond lengths in $[N(Ph_2PNSiMe_3)_2AlMe_2]$ (1.971(2) and 1.988(2) Å),[11b] β-diketiminate aluminumdimethyl complex $[HC\{MeCN(2,6\text{-}iPr_2C_6H_3)\}_2AlMe_2]$ (1.963 and 1.971 Å)[23] and bis(phosphinimino)methanide aluminumdimethyl complex $[HC\{Ph_2PN(SiMe_3)\}_2AlMe_2]$ (1.984 and 1.986 Å).[24] While Me(1)-Al(1)-Me(2) bond angle (108.90(2)°) in compound **1.9** is narrower than that seen in $[N(Ph_2PNSiMe_3)_2AlMe_2]$ (115.11(12)°),[11b] $[HC\{MeCN(2,6\text{-}iPr_2C_6H_3)\}_2AlMe_2]$ (117.39°)[23]

and [HC{$Ph_2PN(SiMe_3)$}$_2AlMe_2$] (111.5°).[24] The N(1)-Al(1)-N(3) bond angle in **1.9** (103.54(2)°) is wider than that in [HC{MeCN(2,6-*i*$Pr_2C_6H_3$)}$_2AlMe_2$] (96.17°)[23] but narrower than that in [N($Ph_2PNSiMe_3$)$_2AlMe_2$] (108.92(7)°)[11b] and [HC{$Ph_2PN(SiMe_3)$}$_2AlMe_2$] (111.5(1)°).[24]

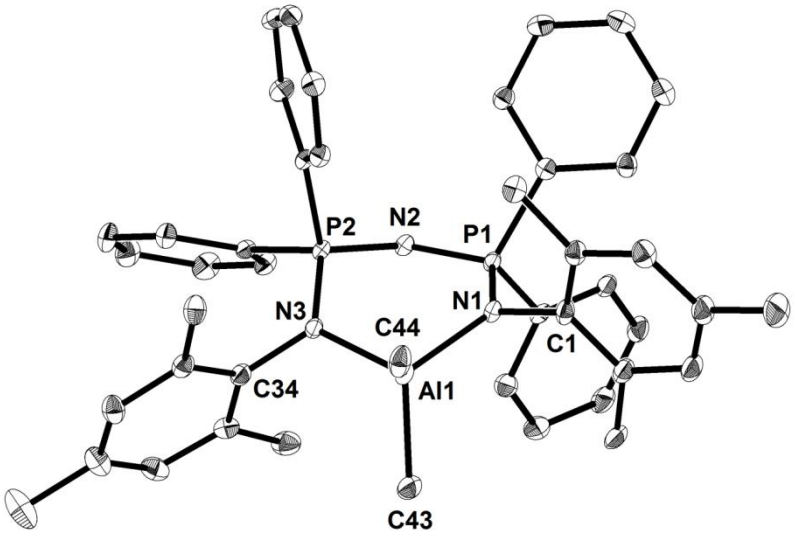

Figure 11. Solid state structure of compound **L_1**$AlMe_2$ (**1.9**). All hydrogen atoms have been deleted for clarity. Thermal ellipsoids have been drawn at 30% probability. Selected bond lengths [Å] and bond angles [°]: Al(1)–C(44) 1.984(3), Al(1)–C(43) 1.966(3), N(2)–P(2) 1.590(2), N(2)–P(1) 1.585(2), Al(1)–N(1) 1.936(2), N(1)–P(1) 1.632(2), Al(1)–N(3) 1.923(2), N(3)–P(2) 1.627(2); N(1)–Al(1)–N(3) 103.54(2), P(1)–N(1)–Al(1) 124.89(12), P(2)–N(3)–Al(1) 121.89(11), C(43)–Al(1)–C(44) 108.90(2).

Similarly, when the ligand **L_1**H was reacted with AlH_3·NMe_2Et and BH_3·SMe_2 in toluene formed the corresponding complexes [{N($Ph_2PN(2,4,6\text{-}Me_3C_6H_2)$)$_2$}$AlH_2$] (**1.10**) and [{N($Ph_2PN(2,4,6\text{-}Me_3C_6H_2)$)$_2$}$BH_2$] **(1.11)** (Scheme 8) were formed. Complex **1.11** is a rare example of borondihydride complex where a dihydroboronium species is chelated with a cyclic monoanionic ligand.[13a] To our surprise, even the much celebrated β-diketiminato ligands have no borondihydride complex known.[22] Encapsulation of BH_2 unit in the ligand

backbone in complex **1.11** was possible due to the absence of any reactive H on the ligand backbone that excludes any hydrogen migration[22] or insertion of ligand atoms in the B-H bonds.[13b,c] Complexes **1.10** and **1.11** were characterized by ^{1}H NMR spectroscopy that showed the Al*H* and B*H* to appear as broad signals around 3.97 and 3.23 ppm, respectively. A slightly upfieid shift in the ^{31}P{^{1}H} NMR spectrum of **1.10** (18.8 ppm) was observed comparable to that of **1.9** (18.9 ppm) whereas, a slightly downfield shift in the ^{31}P{^{1}H} NMR spectrum of **1.11** (19.2 ppm) was observed comparable to that of **1.9** (18.9 ppm). The ^{11}B NMR spectrum of **1.11** showed a sharp signal at -5.2 ppm that is typical of boron in a tetrahedral environment. The IR spectrum of **1.10** and **1.11** showed symmetric and asymmetric stretch corresponding to Al–*H* and B−*H* stretches at 1820, 1757 and 2296, 2294 cm^{-1}, respectively. The mass spectra of **1.10** and **1.11** showed the base peak at *m/z* = 678.2725 and 665.2986 corresponding to $[M - H]^{+}$ and $[M + H]^{+}$, respectively.

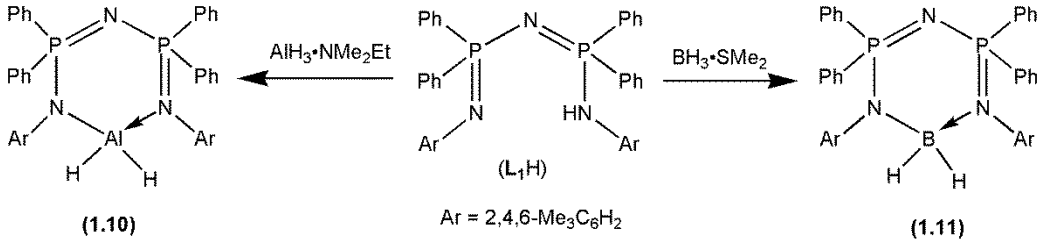

Scheme 8. Synthesis of aluminumdihydride $\mathbf{L_1}AlH_2$ **(1.10)** and borondihydride $\mathbf{L_1}BH_2$ **(1.11)** complexes with bis(phosphinimino)amide.

Compound **1.10** crystallizes in a monoclinic system (space group $P2_1/n$) and **1.11** crystallizes in triclinic system (space group $P\bar{1}$) (Table 6, Figure **12** and **13**). The chelated atom in both the complexes are four coordinated with distorted tetrahedral environment around them. The ligand skeleton in the six membered chelate is puckered with the H substituents oriented above and below this chelate and pointing away from this. The H(1A)–Al(1)–H(1B) and H(1A)–B(1)–H(1B) angle in **1.10** and **1.11**, respectively, are 115.88(1) and

111.58(2)°. The N(1)–Al(1)–N(3) and N(1)–B(1)–N(3) bond angles in **1.10** and **1.11**, respectively, are 105.28(1) and 110.60(2)°.

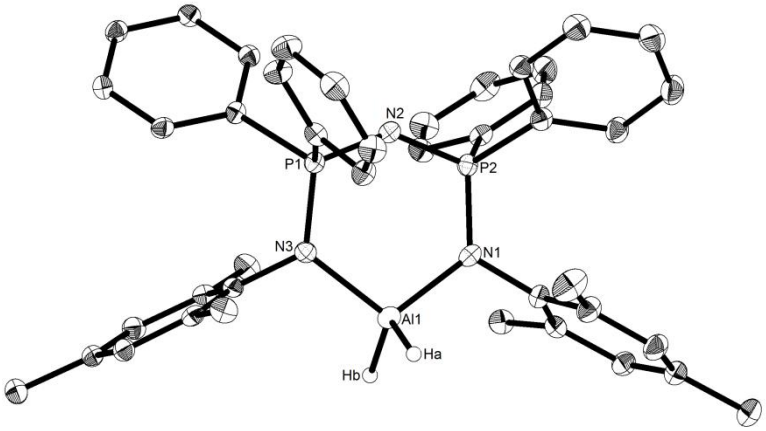

Figure 12. Single crystal structure of compound $\mathbf{L_1}AlH_2$ (**1.10**). All hydrogen atoms have been omitted except those on Al for clarity. Thermal ellipsoids have been drawn at 30% probability. Selected bond lengths [Å] and bond angles [°] H(a)–Al(1) 1.617(6), H(b)–Al(1) 1.617(6), N(2)–P(2) 1.574(6), N(2)–P(1) 1.578(5), N(1)– Al(1) 1.901(4), N(3)–Al(1) 1.900(5), N(3)–P(1) 1.630(1), P(2)–N(1)–Al(1) 126.01(1), P(1)–N(2)–P(2) 137.5(1), P(1)–N(3)–Al(1) 122.63(1), H(a)–Al(1)–H(b) 115.88(1), N(3)–Al(1)–N(1) 105.28(1).

The B-H bond lengths in complex $\mathbf{L_1}BH_2$ (**1.11**), 1.116(3) and 1.148(3) Å are comparable to that in $[ClC\{Ph_2PN(2,4,6\text{-}Me_3C_6H_2)\}_2BH_2]$ (1.12(5) and 1.13(2) Å) and the H(1A)-B(1)-H(1B) bond angle of 111.58(2)° is in agreement with the corresponding angle in $[ClC\{Ph_2PN(2,4,6\text{-}Me_3C_6H_2)\}_2BH_2]$ (113.93°).[13a] The B-N distances in **1.11** (1.588(5) and 1.615(5) Å) and N(1)-B(1)-N(3) bond angle (110.60(2)°) compare well with the respective metric parameters in $[ClC\{Ph_2PN(2,4,6\text{-}Me_3C_6H_2)\}_2BH_2]$ (1.585(3), 1.596(3) Å and 110.59(15)°).[13a]

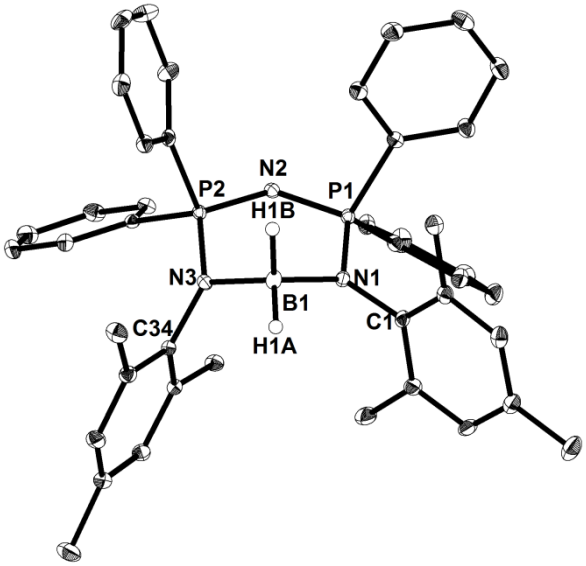

Figure 13. Solid state structure of compound $\mathbf{L_1}BH_2$ (**1.11**). All hydrogen atoms and THF molecule present in the crystal lattice have been deleted for clarity. Thermal ellipsoids have been drawn at 30% probability. Selected bond lengths [Å] and bond angles [°]: B(1)–N(1) 1.588(5), B(1)–N(3) 1.615(5), B(1)–H(1A) 1.116(3), B(1)–H(1B) 1.148(3), N(1)–P(1) 1.623(4), N(3)–P(2) 1.631(4), N(2)–P(1) 1.593(3), N(2)–P(2) 1.594(4); N(1)–B(1)–N(3) 110.60(2), H(1A)–B(1)–H(1B) 111.58(2), P(1)–N(1)–B(1) 110.04(2), P(2)–N(3)–B(1) 116.71(2), P(1)–N(2)–P(2) 126.59(2).

Reaction of $\mathbf{L_1}BH_2$ (**1.11**) ($\mathbf{L_1}$ = $[N\{Ph_2PN(2,4,6\text{-}Me_3C_6H_2)\}_2]^-$) with 2.2 equivalent of HCl·dioxane in toluene at 80 ^oC (Scheme 9) results in the formation of a mixture of products (dichloroborane complex $\mathbf{L_1}BCl_2$ (**1.12**) and $[\mathbf{L_1}BCl]^+[BCl_4]^-$). The ^1H NMR spectrum of **1.12** showed singlets 1.68 and 2.30 ppm corresponding to the *o*- and *p*-Me of the mesityl group. These major signals were overlapped with a minor impurity of side product $[[\mathbf{L_1}BCl]^+[BCl_4]^-$ **(3.2)** ; synthesis and characterization of this product to be discussed in detail in (Chapter 3).The $^{31}P\{^1H\}$ NMR spectrum of **1.12** revealed the backbone phosphorus to appear at 26.1 ppm which is considerably downfield shifted as compared to $\mathbf{L_1}H$ or its starting material **1.11** (*vide supra*), the minor impurity was seen at 26.3 ppm. The signal at *m/z* = 696.2674 in the mass spectrum of **1.12** was due to $[M - Cl]^+$ which was also the base

peak. The signal could be due to the minor product. Attempts made to separate **1.12** from **3.2** was not successful due to their similar solubility behaviour.

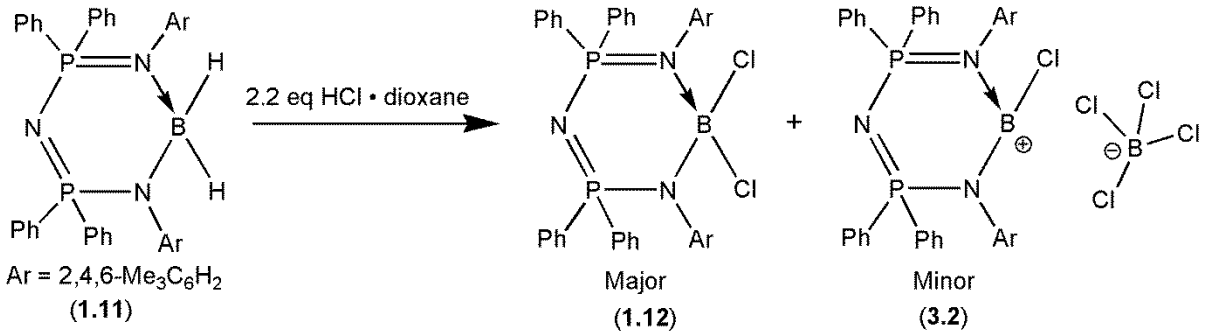

Scheme 9. Synthesis of dichloroborane $\mathbf{L_1}BCl_2$ **(1.12)** complex of bis(phosphinimino)amide.

Similarly, when $\mathbf{L_1}BH_2$ (**1.11**) was reacted with excess (10 equivalent) of C_2H_5Br and CH_3I in toluene at 110 °C and at room temperature, formed the corresponding complexes [{N($Ph_2PN(2,4,6\text{-}Me_3C_6H_2)$)$_2$}BHBr] (**1.13**) and [{N($Ph_2PN(2,4,6\text{-}Me_3C_6H_2)$)$_2$}BHI] **(1.14)**, respectively (Scheme 10) were formed. Complexes **1.13** and **1.14** were characterized by ^{1}H NMR spectroscopy that showed the B*H* to appear as a broad signal around 4.10 and 4.25 ppm, respectively. A slightly downfield shift in the $^{31}P\{^1H\}$ NMR spectrum of **1.13** (22.47 ppm) and **1.11** (22.56 ppm) were observed, comparable to that of **1.11** (19.2 ppm).

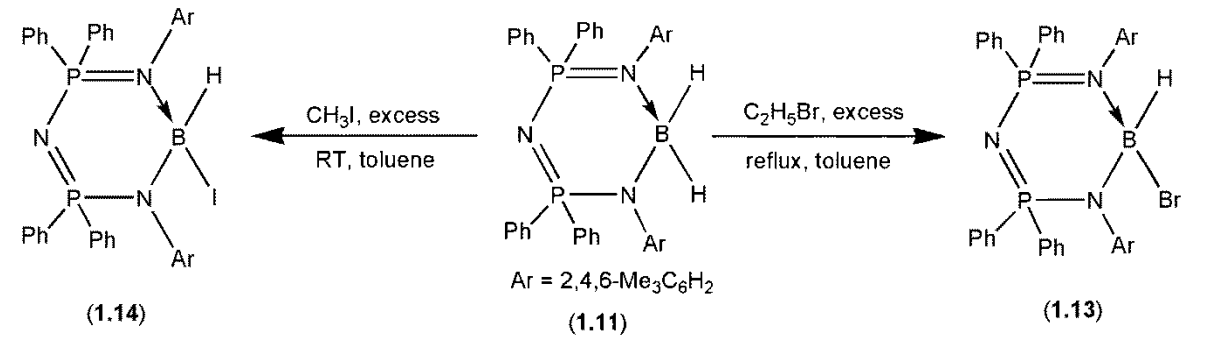

Scheme 10. Synthesis of bromoborane $\mathbf{L_1}BHBr$ (**1.13**) and iodoborane $\mathbf{L_1}BHI$ **(1.13)** complexes of bis(phosphinimino)amide.

The ^{11}B NMR spectrum of **1.13** showed a broad signal at 0.65 ppm that is typical of boron in a tetrahedral environment however, no signal for **1.14** was detected in its ^{11}B NMR. The IR spectrum of **1.13** and **1.14** showed B−H stretches at 2542 and 2548 cm^{-1}, respectively.

The mass spectrum of **1.13** and **1.14** showed the base peak at *m/z* = 662.3015 and 662.3052 corresponding to $[M - Br]^+$ and $[M - I]^+$, respectively.

Following the same strategy, reaction of $\mathbf{L_1}BH_2$ (**1.11**) (L = $[N\{Ph_2PN(2,4,6\text{-}Me_3C_6H_2)\}_2]^-$) with 2.0 equivalent of TfOH in toluene at room temperature (Scheme 11) resulted in the formation of complex $\mathbf{L_1}$BHOTf (**1.15**). The ^{1}H NMR spectrum of **1.15**

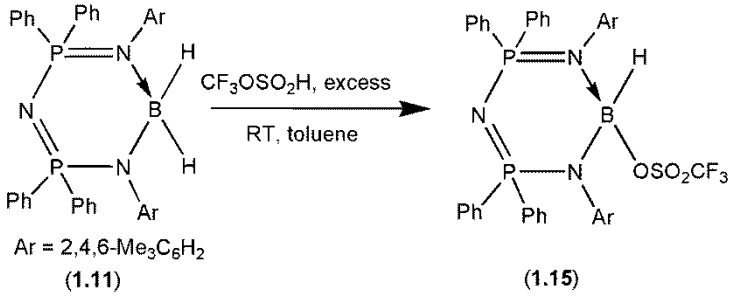

Scheme 11. Synthesis of triflicborane **(1.15)** complex of bis(phosphinimino)amide.

showed two singlets at 1.72 and 2.32 ppm corresponding to the *o*- and *p*-Me of the mesityl group and the B*H* appeared as a broad signal around 4.33 ppm, respectively. The $^{31}P\{^1H\}$ NMR spectrum of **1.15** revealed the backbone phosphorus to appear at 22.76 ppm which is considerably downfield shifted as compared to $\mathbf{L_1}$H or its starting material **1.11** (*vide supra*) however, no ^{11}B signal for **1.15** was detected in its ^{11}B NMR spectrum. The signal at *m/z* = 662.3012 in the mass spectrum of **1.15** was due to $[M - OTf]^+$ which was also the base peak.

1.3 Conclusions

In conclusion, we have reported on the syntheses, spectroscopic and structural investigations of group 13 complexes of a new ligand, $[N(Ph_2PN(2,4,6\text{-}Me_3C_6H_2))_2]^-$ that offers monoanionic chelate binding to the metal ions. The unique feature of this ligand is that it carries non-reactive phenyl substituents on P and mesityl substituent on terminal N atoms of the ligand backbone. This property in combination with good donor characteristics of the ligand has been realized in the synthesis of stable borondihydride, aluminumdihydride and aluminumdimethyl complexes. Additionally, monochloroborane complexes, dihalo complexes of B(III), Al(III), Ga(III) and In(III) have also been reported in this chapter that

adopt a distorted tetrahedral arrangement. Further, we explored the reaction chemistry of a borondihydride complex in the synthesis of a variety of neutral and cationic complexes. In this chapter we described on mono substituted bromo, iodo and triflate complexes derived from substituted borondihydride complex. Further reaction chemistry of borondihydride complex has been discussed in Chapters 2 and 3.

1.4 Experimental Section

1.4.1 General procedure

All syntheses were carried out under an inert atmosphere of dinitrogen in oven dried glassware using standard Schlenk techniques[25] or a glovebox where O_2 and H_2O levels were maintained usually below 0.1 ppm. All the glassware was dried at 150 °C in an oven for at least 12 h and assembled hot and cooled *in vacuo* prior to use. Solvents were purified by MBRAUN solvent purification system MB SPS-800. THF was dried over (Na/benzophenone ketyl) and distilled under nitrogen and degassed prior to use. For NMR, $CDCl_3$ was dried over 4 Å molecular sieves whereas C_6D_6 was dried over Na.

1.4.2 Starting materials

All chemicals used in this work were purchased from commercial sources and were used without further purification. The starting materials $HN(PPh_2)_2$,[15] 2,4,6-$Me_3C_6H_2N_3$[16] and 2,6-*i*$Pr_2C_6H_3N_3$[17] were synthesized as per the procedure mentioned in the literature.

1.4.3 Physical measurements

The ^1H, ^{13}C, $^{31}P\{^1H\}$ and ^{11}B NMR spectra were recorded with a Bruker 400 MHz spectrometer with TMS, H_3PO_4 (85 %) , $CFCl_3$, LiCl and $BF_3{\cdot}OEt_2$ respectively, as external references and chemical shifts were reported in ppm. Down-field shifts relative to the reference were quoted positive while the up-field shifts were assigned negative values. High resolution mass spectra were recorded on a Waters SYNAPT G2−S instrument. IR spectra of

the complexes were recorded in the range 4000–400 cm^{-1} using a Perkin Elmer Lambda 35-spectrophotometer. The C-H stretch of aromatic moiety of the complexes is over shadowed (2800-3000 cm^{-1}) by Nujol absorption and hence not included in the list of bands in the experimental section. The absorptions of the characteristic functional groups were only assigned and other absorptions (moderate to very strong) were only listed. Melting points were obtained in sealed capillaries on a Büchi B–540 melting point instrument.

Single crystal X-ray diffraction data for **L_1H, 1.1, 1.3-1.8** and **1.11** were collected on a Bruker AXS KAPPA APEX-II CCD diffractometer (Monochromatic MoKα radiation) equipped with Oxford cryosystem 700 plus at 100 K. Data collection and unit cell refinement for the data sets were done using the Bruker APPEX-II suite, data reduction and integration were performed using SAINTV 7.685A (Bruker AXS, 2009) and absorption corrections and scaling were done using SADABSV2008/1 (Bruker AXS, 2009). Single crystal X-ray diffraction data for **L_2H, 1.2** and **1.10** were collected using a Rigaku XtaLAB mini diffractometer equipped with Mercury375M CCD detector. The data were collected with graphite monochromatic MoKα radiation (λ = 0.71073 Å) at 100.0(2) K using scans. During the data collection, the detector distance was maintained at 50 mm (constant) and the detector was placed at 2θ = 29.85° (fixed) for all the data sets. The data collection and data reduction were done using Crystal Clear suite.[26] The crystal structures were solved by using either OLEX2[27] or WINGX package using SHELXS-97 and the structure were refined using SHELXL-97 2008.[28] All non hydrogen atoms were refined anisotropically. Hydrogen atom were fixed at geometrically calculated positions and were refined by using the riding model except for the hydrides in complexes **1.7**, **1.10** and **1.11**. Half a molecule of disordered Et_2O molecule found in the asymmetric unit of **1.4-1.6** and **1.9** could not be treated using standard commands available in SHELXL. The squeeze method was used to remove the contribution

of this disordered molecule from the original *hkl* file. The resulting squeezed *hkl* file was used for further refinement.

1.4.4 Synthetic procedures

Synthesis of [HN($Ph_2PN(2,4,6\text{-}Me_3C_6H_2)$)$_2$] ($L_1$H): Tetraphenyldiphosphazane ($(Ph_2P)_2NH$)(12.7 g, 33.0 mmol) was dissolved in dry toluene (150 mL), and a solution of mesityl azide (10.63 g, 66.0 mmol) in toluene (40 mL) was added drop-wise. Rapid evolution of nitrogen gas was observed and stirring was continued for overnight. Concentration of the solution to half volume and storage at 0 ºC for one day afforded crystalline solid that was collected by filtration and washed with hexane. X-ray quality crystals were grown from a toluene solution at 4 ºC. Yield: (14 g , 65%). M.p. 187-190 ºC. IR (ν cm^{-1}, KBr): 3313, 3059, 2959, 2913, 1604, 1477, 1431, 1346, 1259, 1218, 1109, 1036, 922, 854, 695, 532. ^{1}H NMR (400 MHz, $CDCl_3$, δ ppm): 1.86 (s, *o*-CH_3, 12 H), 2.03 (s, *p*-CH_3, 6 H), 6.53 (s, 2,4,6-$Me_3C_6H_2$, 4 H), 7.22-7.10 (m, Ph, 12 H), 7.59-7.54 (m, Ph, 8 H), (the N*H* signal did not appear). ^{13}C NMR (100 MHz, $CDCl_3$, δ ppm): 20.6 (s, *p*-*C*H_3), 21.0 (s, *o*-*C*H_3), 127.6 (d, $J_{C\text{-}P}$ = 13.4 Hz, aromatic), 128.8 (s, aromatic), 130.3 (s, aromatic), 130.7 (s, aromatic), 131.6 (d, $J_{C\text{-}P}$ = 10.6 Hz, aromatic), 134.4 (d, $J_{C\text{-}P}$ = 6.2 Hz, aromatic), 136.5 (dd, $J_{C\text{-}P}$ = 131 Hz & 4.4 Hz, aromatic), 140.3 (s, aromatic). ^{31}P{^{1}H} NMR (162 MHz, $CDCl_3$, δ ppm): 2.35. Mass spectrum (+ve ion, EI), *m/z* = calculated (found): 652.3010 (652.3016) $[M+H]^+$.

Synthesis of [{N($Ph_2PN(2,4,6\text{-}Me_3C_6H_2)$)$_2$}Li·$OEt_2$] (1.1): To a solution of $\mathbf{L_1}$H (0.65 g, 1.0 mmol) in Et_2O (15 mL) at -78 °C was added a solution of $LiN(SiMe_3)_2$ (0.18 g, 1.1 mmol) or *n*BuLi (1.6 M in hexane, 0.7 mL, 1.1 mmol) in Et_2O (5 mL) dropwise. The mixture was warmed to room temperature and a clear solution was obtained that was stirred for another 2 h. Concentration of the solution to 5 mL and storage at -10 °C, gave colourless block shaped crystal after 3 days. Yield: (0.62 g, 85%). M.p. 196 ºC. IR (ν cm^{-1}, Nujol): 1306, 1260, 1096, 1020, 799, 528. ^{1}H NMR (400 MHz, C_6D_6, δ ppm): 0.67 (t, $^3J_{H\text{-}H}$ = 7.0 Hz, OCH_2CH_3, 6 H).

2.21 & 2.23 (two overlapped singlet, *o*- & *p*-CH_3, 18 H), 2.79 (q, $^3J_{H\text{-}H}$ = 7.0 Hz, OCH_2CH$_3$, 4 H), 6.84 (s, 2,4,6-Me$_3$C$_6H_2$, 4 H), 7.03 (m, Ph, 12 H), 7.93-7.89 (m, Ph, 8 H). ^{13}C NMR (100 MHz, C_6D_6, δ ppm): 14.0 (s, OCH$_2$*C*H$_3$), 20.6 (s, *p*-*C*H$_3$), 21.1 (s, *o*-*C*H$_3$), 64.7 (s, O*C*H$_2$CH$_3$), 127.3 (d, $J_{C\text{-}P}$ = 12.5 Hz, aromatic), 128.4 (b, aromatic), 128.9 (s, aromatic), 129.2 (s, aromatic), 131.3 (d, $J_{C\text{-}P}$ = 10 Hz, aromatic), 133.9 (d, $J_{C\text{-}P}$ = 6.7 Hz, aromatic), 139.3 (dd, $J_{C\text{-}P}$ = 118 & 4.6 Hz, aromatic), 146.1 (b, aromatic). ^{31}P{^{1}H} NMR (162 MHz, C_6D_6, δ ppm): 1.75. ^{7}Li NMR (155 MHz, C_6D_6, δ ppm): 1.23.

Synthesis of [{N(Ph$_2$PN(2,6-*i*Pr$_2$C$_6$H$_3$))$_2$}Li·OEt$_2$] (1.2): To a solution of **L$_2$**H (1.1 g, 1.5 mmol) in Et$_2$O was added *n*BuLi (1.6 M in hexane, 1 mL, 1.6 mmol) at -78 °C drop by drop. The mixture was warmed to room temperature and a clear solution was obtained that was stirred for another 2 h. The solvent was evaporated under vaccum and crystal grown from THF at 4 °C. Yield: (0.98 mg, 80%) M.p: 214-216 ºC. IR (ν cm^{-1}, Nujol): 1967, 1905, 1815, 1767, 1587, 1446 1112, 912, 774 717, 665, 562. ^{1}H NMR (400 MHz, C_6D_6, δ ppm): 0.46 (t, $^3J_{H\text{-}H}$ = 6.8 Hz, OCH$_2$C*H*$_3$, 6 H), 1.03 (d, $^3J_{H\text{-}H}$ = 6.0 Hz, CH(C*H*$_3$)$_2$, 24 H), 2.81 (q, $^3J_{H\text{-}H}$ = 6.8 Hz, OC*H*$_2$CH$_3$, 4 H), 3.92 (sept, $^3J_{H\text{-}H}$ = 6.8 Hz, C*H*(CH$_3$)$_2$, 4H), 7.10-7.0 (m, Ar, 18 H), 7.70-7.66 (m, Ar, 8 H). ^{13}C NMR (100 MHz, C_6D_6, δ ppm): 12.4 (s, CH(*C*H$_3$)$_2$), 24.0 (s, OCH$_2$*C*H$_3$), 28.1 (s, *C*H(CH$_3$)$_2$), 61.4 (s, O*C*H$_2$CH$_3$), 121.4 (d, $J_{C\text{-}P}$ = 3.0 Hz, aromatic), 123.5 (d, $J_{C\text{-}P}$ = 2.3 Hz, aromatic), 127.3 (d, $J_{C\text{-}P}$ = 12.3 Hz, aromatic), 129.3 (s, aromatic), 131.3 (d, $J_{C\text{-}P}$ = 9.7 Hz, aromatic), 138.4 (dd, $J_{C\text{-}P}$ = 117.3 & 4.1 Hz, aromatic), 144.4 (d, $J_{C\text{-}P}$ = 6.6 Hz, aromatic), 146.1 (d, $J_{C\text{-}P}$ = 6.6 Hz, aromatic). ^{31}P{^{1}H} NMR (162 MHz, C_6D_6, δ ppm): 2.81. ^{7}Li NMR (155 MHz, C_6D_6, δ ppm): 1.06.

Synthesis of [{N(Ph$_2$PN(2,4,6-Me$_3$C$_6$H$_2$))$_2$}BF$_2$] (1.3): To a solution of **L$_1$**H (0.65 g, 1.0 mmol) in Et$_2$O (50 mL) was added *n*BuLi (1.6 M in hexane, 0.7 mL,1.1 mmol) drop-wise at -78 °C. A clear solution was obtained when the mixture was brought to room temperature and further stirring for 3 h at room temperature. This reaction mixture was then added at -78 °C to

a solution of $BF_3{\cdot}Et_2O$ (0.14 mL, d = 1.15 g/mL) drop-wise at -78 °C and was allowed to come to room temperature and stirred for another 6 hours. The precipitate formed was filtered off and the filtrated was reduced in volume to half. Colorless crystals of **1.3** were obtained at 4 °C in 2 days. Yield: (0.36 g, 53%). M.p. 233-236 ºC. IR (ν cm^{-1}, Nujol): 1588, 1461, 1374, 1246, 1216, 1200, 1112, 1077, 1037, 997, 959, 917, 880, 694. ^{1}H NMR (400 MHz, $CDCl_3$, δ ppm): 2.0 (s, *o*-CH_3, 12 H), 2.21 (s, *p*-CH_3, 6 H), 6.71 (s, 2,4,6-$Me_3C_6H_2$, 4 H), 7.34-7.29 (m, Ph, 8 H), 7.49-7.46 (m, Ph, 4 H), 7.74-7.69 (m, Ph, 8 H), ^{13}C NMR (100 MHz, $CDCl_3$, δ ppm): 20.4 (s, *o*-CH_3), 20.8 (s, *p*-CH_3), 127.7 (d, $J_{C\text{-}P}$ = 13.5 Hz, aromatic), 129.4 (s, aromatic), 131.4 (s, aromatic), 132.5 (d, $J_{C\text{-}P}$ = 10.9 Hz, aromatic), 132.7 (dd, $J_{C\text{-}P}$ = 124 & 2.9 Hz, aromatic), 135.1 (s, aromatic), 135.5 (b, aromatic), 139.7 (b, aromatic). ^{31}P{^{1}H} NMR (162 MHz, $CDCl_3$, δ ppm): 23.43 (broad). ^{19}F NMR (376.5 MHz, $CDCl_3$, δ ppm): –132.6 (q, $^1J_{F\text{-}B}$ = 35.4 Hz). ^{11}B NMR (128.4 MHz, $CDCl_3$, δ ppm): 2 (tt, $^1J_{B\text{-}F}$ = 35.4 & $^2J_{B\text{-}P} \approx$ 9 Hz). Mass spectrum (+ve ion, EI), *m/z* = calculated (found): 700.3000 (700.2974) $[M]^+$, 680.2938 (680.2986) $[M\text{-}F\text{-}H]^+$.

Synthesis of [{N(Ph$_2$PN(2,4,6-Me$_3$C$_6$H$_2$))$_2$}AlCl$_2$] (1.4): To a solution of **L$_1$**H (0.65 g, 1.0 mmol) in Et_2O (50 mL) was added *n*BuLi (1.6 M in hexane, 0.7 mL,1.1 mmol) drop-wise at -78 °C. A clear solution was obtained when the mixture was brought to room temperature and further stirring for 3 h at room temperature. This reaction mixture was then added at -78 °C to a solution of $AlCl_3$ in 10 ml diethyl ether (0.13 g, 1.0 mmol) drop-wise and was allowed to come to room temperature and stirred for another 8 hours. The precipitate formed was filtered off and the filtrated was reduced in volume to half. Colorless crystals of **1.4** were obtained at 4 °C in 2 days. Yield: (0.45 g, 60 %). M.p. 298-302 ºC. IR (ν cm^{-1}, Nujol): 1590, 1464, 1377, 1260, 1107, 1027, 975, 854, 798, 698, 586, 531. ^{1}H NMR (400 MHz, $CDCl_3$, δ ppm): 2.02 (s, *o*-CH_3, 12 H), 2.18 (s, *p*-CH_3, 6 H), 6.67 (s, 2,4,6-$Me_3C_6H_2$, 4 H), 7.29-7.24 (m, Ph, 8 H), 7.48-7.44 (m, Ph, 4 H), 7.58-7.52 (m, Ph, 8 H), half a molecule of OEt_2 was also observed

{1.22 (t, $^{3}J_{H\text{-}H}$ = 7.0 Hz, $OCH_2C\mathit{H}_3$), 3.49 (q, $^{3}J_{H\text{-}H}$ = 7.0 Hz, $OC\mathit{H}_2CH_3$)}, this is also consistent with the X-ray structure. ^{13}C NMR (100 MHz, $CDCl_3$, δ ppm): 15.3 (s, $OCH_2\mathit{C}H_3$), 20.7 (s, *p*-$\mathit{C}H_3$), 21.2 (s, *o*-$\mathit{C}H_3$), 65.9 (s, OCH_2CH_3), 127.7 (d, $J_{C\text{-}P}$ = 13.6 Hz, aromatic), 129.9 (s, aromatic), 131.3 (d, $J_{C\text{-}P}$ = 3.7 Hz, aromatic), 131.6 (s, aromatic), 132.5 (m, aromatic), 135.1 (b, aromatic), 135.3 (b, aromatic) 138.4 (b, aromatic). ^{31}P{^{1}H} NMR (162 MHz, $CDCl_3$, δ ppm): 23.7. Mass spectrum (+ve ion, EI), *m/z* = calculated (found): 712.2358 (712.2322) $[M - Cl - H]^+$.

Synthesis of [{N(Ph$_2$PN(2,4,6-Me$_3$C$_6$H$_2$))$_2$}GaCl$_2$] (1.5): To a solution of **L$_1$**H (0.65 g, 1.0 mmol) in Et_2O (50 mL) was added *n*BuLi (1.6 M in hexane, 0.7 mL,1.1 mmol) drop-wise at -78 °C. A clear solution was obtained when the mixture was brought to room temperature and further stirring for 3 hours at room temperature. This reaction mixture was then added at -78 °C to a solution of $GaCl_3$ in 10 mL diethyl ether (0.18 g, 1.0 mmol) drop-wise and was allowed to come to room temperature and stirred for another 8 h. The precipitate formed was filtered off and the filtrated was reduced in volume to half. Colorless crystals of **1.5** were obtained from Et_2O at 4 °C in 3 days. Yield: (0.48 g, 60%). M.p. 238-240 ºC. IR (ν cm^{-1}, Nujol): 1458, 1376, 1260, 1149, 1105, 1024, 852, 802, 583, 526. ^{1}H NMR (400 MHz, $CDCl_3$, δ ppm): 2.05 (s, *o*-CH_3, 12 H), 2.17 (s, *p*-CH_3, 6 H), 6.66 (s, 2,4,6-$Me_3C_6\mathit{H}_2$, 4 H), 7.29-7.24 (m, Ph, 8 H), 7.47-7.43 (m, Ph, 4 H), 7.59-7.54 (m, Ph, 8 H), half a molecule of OEt_2 was also observed {1.22 (t, $^{3}J_{H\text{-}H}$ = 7.0 Hz, $OCH_2C\mathit{H}_3$), 3.49 (q, $^{3}J_{H\text{-}H}$ = 7.0 Hz, $OC\mathit{H}_2CH_3$)}, this is also consistent with the X-ray structure. ^{13}C NMR (100 MHz, $CDCl_3$, δ ppm): 15.3 (s, $OCH_2\mathit{C}H_3$), 20.7 (s, *p*-$\mathit{C}H_3$), 21.1 (s, *o*-$\mathit{C}H_3$), 65.9 (s, OCH_2CH_3), 127.7 (d, $J_{C\text{-}P}$ = 13.7 Hz, aromatic), 129.7 (s, aromatic), 131.7 (s, aromatic), 131.9 (dd, $J_{C\text{-}P}$ = 124 & 3.8 Hz, aromatic), 132.3 (d, $J_{C\text{-}P}$ = 11 Hz, aromatic), 135.1 (b, aromatic), 136.1 (b, aromatic), 138.3 (b, aromatic). ^{31}P{^{1}H} NMR (162 MHz, $CDCl_3$, δ ppm): 24. Mass spectrum (+ve ion, EI), *m/z* = calculated (found): 792.1565 (792.1526) $[M]^+$, 756.1798 (756.1773) $[M - Cl - H]^+$.

Synthesis of [{N(Ph$_2$PN(2,4,6-Me$_3$C$_6$H$_2$))$_2$}InBr$_2$] (1.6): To a solution of **L$_1$**H (0.65 g, 1.0 mmol) in Et$_2$O (50 mL) was added *n*BuLi (1.6 M in hexane, 0.7 mL, 1.1 mmol) drop-wise at -78 °C. A clear solution was obtained when the mixture was brought to room temperature and further stirring for 3 h at room temperature. This reaction mixture was then added at -78 °C to a solution of $InBr_3$ in 10 ml diethyl ether (0.36 g, 1.0 mmol) drop-wise and was allowed to come to room temperature and stirred for another 8 h. The precipitate formed was filtered off and the filtrated was reduced in volume to half. Colorless crystals of **1.6** were obtained from the concentrated mother liquor at room temperature in 5 days. Yield: (0.55 g, 60%). M.p. 266-268 ºC. IR (ν cm^{-1}, Nujol): 1590, 1331, 1256, 1101, 1022, 794, 566. ^{1}H NMR (400 MHz, $CDCl_3$, δ ppm): 2.08 (s, *o*-C*H*$_3$, 12 H), 2.17 (s, *p*-C*H*$_3$, 6 H), 6.68 (s, 2,4,6-Me$_3$C$_6$*H*$_2$, 4 H), 7.26-7.21 (m, Ph, 8 H), 7.44-7.40 (m, Ph, 4 H), 7.55-7.50 (m, Ph, 8 H), half a molecule of OEt_2 was also observed {1.22 (t, $^3J_{H\text{-}H}$ = 7.0 Hz, OCH$_2$C*H*$_3$), 3.49 (q, $^3J_{H\text{-}H}$ = 7.0 Hz, OC*H*$_2$CH$_3$)}, this is also consistent with the X-ray structure. ^{13}C NMR (100 MHz, $CDCl_3$, δ ppm): 15.3 (s, OCH$_2$*C*H$_3$), 20.8 (s, *p*-*C*H$_3$), 21.3 (s, *o*-*C*H$_3$), 65.9 (s, O*C*H$_2$CH$_3$), 127.8 (d, $J_{C\text{-}P}$ = 13.2 Hz, aromatic), 129.61 (s, aromatic), 131.49 (s, aromatic), 131.93 (d, $J_{C\text{-}P}$ = 10.5 Hz, aromatic), 132.3 (dd, 122 & 4.2 Hz, aromatic), 134.6 (d, $J_{C\text{-}P}$ = 3.1 Hz, aromatic), 137.3 (d, $J_{C\text{-}P}$ = 5.2 Hz, aromatic), 137.7 (d, $J_{C\text{-}P}$ = 6.4 Hz, aromatic). ^{31}P{^{1}H} NMR (162 MHz, $CDCl_3$, δ ppm): 21. Mass spectrum (+ve ion, EI), *m/z* = calculated (found): 925.0244 (925.0316) [M - H]$^+$.

Synthesis of [{(2,4,6-Me$_3$C$_6$H$_2$NPPh$_2$)$_2$N}BHCl] (1.7): To a solution of **L$_1$**H (2.60 g, 4.0 mmol) in toluene (120 mL) at room temperature was added $BH_2Cl{\cdot}Me_2S$ (0.48 mL, 10 M in Me_2S, 4.8 mmol). This reaction mixture was heated for 12 h at 80 °C. Evaporation of all volatiles under vacuum afforded a white solid. This was crystallized from toluene at room temperature. Yield: (2.23 g, 80 %). M.p. 253-255 ºC. IR (ν cm^{-1}, KBr): 2917, 2464 (B-H stretch), 1588, 1480, 1437, 1376, 1229, 1159, 1113, 1023, 985, 697. ^{1}H NMR (400 MHz,

$CDCl_3$, δ ppm): 1.70 (s, *o*-C*H*$_3$, 12 H), 2.32 (s, *p*-C*H*$_3$, 6 H), 4.29 (broad, B*H*), 6.88 (s, 2,4,6-$Me_3C_6H_2$, 4 H), 7.68-7.57 (m, Ph, 16 H), 7.86-7.83 (m, Ph, 4 H). ^{13}C NMR (100 MHz, $CDCl_3$, δ ppm): 19.2 (s, *o*-*C*H$_3$), 20.5 (s, *p*-*C*H$_3$), 125.4 (d, $J_{C\text{-}P}$ = 2.0 Hz, aromatic), 126.9 (d, $J_{C\text{-}P}$ = 2.0 Hz, aromatic), 129.3 (m not resolved, due to $J_{C\text{-}P}$ & $J_{C\text{-}B}$, aromatic), 130.5 (s, aromatic), 132.4 (m not resolved, due to $J_{C\text{-}P}$ & $J_{C\text{-}B}$, aromatic), 134.1 (s, aromatic), 134.9 (s, aromatic), 136.3 (s, aromatic), 138.9 (s, aromatic).^{31}P{^{1}H} NMR (162 MHz, $CDCl_3$, δ ppm): 22.5. ^{11}B NMR (128.4 MHz, $CDCl_3$, δ ppm): 7.01. Mass spectrum (+ve ion, EI), *m/z* = calculated (found): 663.3111 (661.3130) $[M + H - Cl]^+$.

Synthesis of [{N(Ph$_2$PN(2,6-*i*Pr$_2$C$_6$H$_3$))$_2$}BHCl] (1.8): To a solution of **L$_2$**H (2.94 g, 4.0 mmol) in toluene (120 mL) at room temperature was added $BH_2Cl{\cdot}Me_2S$ (0.48 mL, 10 M in Me_2S, 4.8 mmol). This reaction mixture was heated for 12 h at 110 °C gave a white precipitate. This solution was filtered to give a white solid. Yield: (2.46 g, 80 %). M.p. 272-274 ºC. IR (ν cm^{-1}, KBr): 2970, 2922, 2873, 2564, 2463 (B-H stretch), 1590, 1463, 1439, 1311, 1140, 1115, 1015, 934, 804, 775, 738, 694. ^{1}H NMR (400 MHz, $CDCl_3$, δ ppm): 0.37 (d, $^3J_{H\text{-}H}$ = 6.0 Hz, CH(C*H*$_3$)$_2$, 12 H), 0.99 (d, $^3J_{H\text{-}H}$ = 6.0 Hz, -CH(C*H*$_3$)$_2$, 12 H), 2.98 (sept, $^3J_{H\text{-}H}$ = 6.0 Hz, C*H*(CH$_3$)$_2$, 4 H), 4.68 (broad, B*H*), 7.14-7.12 (m, Ar, 4 H), 7.45-7.41 (m, Ar, 10 H), 7.56 (m, Ar, 8 H) 7.81-7.78 (m, Ar, 4 H). ^{13}C NMR (100 MHz, $CDCl_3$, δ ppm): 20.7 (s, -CH(*C*H$_3$)$_2$), 26.2 (s, CH(*C*H$_3$)$_2$), 29.6 (s, *C*H(CH$_3$)$_2$), 124.0 (s, aromatic), 125.1 (s, aromatic), 125.3 (s, aromatic), 129.2 (d, $J_{C\text{-}P}$ = 14.3, aromatic), 129.8 (s, aromatic), 132.8 (d, $J_{C\text{-}P}$ = 11.6, aromatic), 134.7 (s, aromatic) 146.7 (s, aromatic).^{31}P{^{1}H} NMR (162 MHz, $CDCl_3$, δ ppm): 25.22. ^{11}B NMR (128.4 MHz, $CDCl_3$, δ ppm): 3.27 (d, $J_{B\text{-}H}$ 163.8 Hz). Mass spectrum (+ve ion, EI), *m/z* = calculated (found): 779.3505 (779.3475) $[M - H]^+$ and 746.3972 (746.3942) $[M - Cl]^+$.

Synthesis of [{N(Ph$_2$PN(2,4,6-Me$_3$C$_6$H$_2$))$_2$}AlMe$_2$] (1.9): To a solution of **L$_1$**H (1.30 g, 2.0 mmol) in Et_2O (50 mL) was added $AlMe_3$ (1.1 mL, 2 M in toluene, 2.2 mmol) at -78 °C drop

by drop. After warming to room temperature the initial light turbidity disappeared to give a clear solution. Solvent was removed under vacuum to half of the initial volume and storage at 4 °C afforded colorless crystals of **1.9** in 3 days. Yield: (1.28 g, 90%). M.p. 236-239 ºC. IR (ν cm^{-1}, Nujol): 1592, 1437, 1242, 1197, 1144, 1114, 989, 853, 805, 747, 692, 653, 524. ^{1}H NMR (400 MHz, $CDCl_3$, δ ppm): –1.0 (s, Al*Me*, 6 H), 1.90 (s, *o*-CH_3, 12 H), 2.22 (s, *p*-CH_3, 6 H), 6.69 (s, 2,4,6-$Me_3C_6H_2$, 4 H), 7.29-7.24 (m, Ph, 8 H), 7.45-7.40 (m, Ph, 4 H), 7.61-7.56 (m, Ph, 8 H), half a molecule of OEt_2 was also observed {1.24 (t, $^{3}J_{H\text{-}H}$ = 7.0 Hz, OCH_2CH_3), 3.51 (q, $^{3}J_{H\text{-}H}$ = 7.0 Hz, OCH_2CH_3)}, this is also consistent with the X-ray structure. ^{13}C NMR (100 MHz, $CDCl_3$, δ ppm): –6.1 (s, Al*Me*), 15.3 (s, OCH_2CH_3), 20.6 (s, *o*-CH_3), 20.7 (s, *p*-CH_3), 65.9 (s, OCH_2CH_3), 127.5 (d, $J_{C\text{-}P}$ = 13.2 Hz, aromatic), 129.4 (s, aromatic), 130.8 (s, aromatic), 132.2 (d, $J_{C\text{-}P}$ = 10.5 Hz, aromatic), 133.6 (m, aromatic), 134.1 (dd, $J_{C\text{-}P}$ = 120 & 3.6 Hz, aromatic), 137.9 (b, aromatic). ^{31}P{^{1}H} NMR (162 MHz, $CDCl_3$, δ ppm): 18.9. Mass spectrum (+ve ion, EI), *m/z* = calculated (found): 692.2904 (692.2852) $[M]^+$.

Synthesis of [{N(Ph_2PN(2,4,6-$Me_3C_6H_2$))$_2$}AlH_2] (1.10): To a solution of $\mathbf{L_1}$H (2.60 g, 4.0 mmol) in toluene (60 mL) at 10 ºC was added AlH_3·NMe_2Et (8 mL, 0.5 M in toluene, 4 mmol). The initial turbid solution became clear after the reaction mixture was brought to room temperature and was further stirred for 24 h. Evaporation of all volatiles under vacuum afforded a pale yellow solid. This was crystallized from toluene at 4 ºC. Yield: (2.5 g, 92.2 %). M.p. 169-171 ºC. IR (ν cm^{-1}, KBr): 3060, 2914, 2854, 1820, 1757 (Al-H stretch), 1478, 1434, 1297, 1215, 1205, 1115, 996, 947, 850, 783, 694. ^{1}H NMR (400 MHz, $CDCl_3$, δ ppm): 2.05 (s, *o*-CH_3, 12 H), 2.25 (s, *p*-CH_3, 6 H), 3.97 (broad, Al*H*), 6.76 (s, 2,4,6-$Me_3C_6H_2$, 4 H), 7.34-7.28 (m, Ph, 8 H), 7.50-7.46 (m, Ph, 4 H), 7.67-7.62 (m, Ph, 8 H), ^{13}C NMR (100 MHz, $CDCl_3$, δ ppm): 20.5 (s, *o*-CH_3), 20.8 (s, *p*-CH_3), 127.7 (m not resolved, due to $J_{C\text{-}P}$ & $J_{C\text{-}B}$, aromatic), 129.7 (s, aromatic), 131.1 (s, aromatic), 132.0 (m not resolved, due to $J_{C\text{-}P}$ & $J_{C\text{-}B}$, aromatic), 133.5 (dd, $J_{C\text{-}P}$ = 121 & 3.6 Hz, aromatic), 134.3 (b, aromatic), 136.8 (b, aromatic),

138.1 (b, aromatic). $^{31}P\{^{1}H\}$ NMR (162 MHz, $CDCl_3$, δ ppm): 18.78. Mass spectrum (+ve ion, EI), *m/z* = calculated (found): 678.2748 (678.2725) $[M - H]^+$.

Synthesis of [{N(Ph$_2$PN(2,4,6-Me$_3$C$_6$H$_2$))$_2$}BH$_2$] (1.11): To a solution of **L$_1$**H (2.60 g, 4.0 mmol) in toluene (50 mL) at - 40 °C was added $BH_3{\cdot}Me_2S$ (0.4 mL, 10 M in Me_2S, 4 mmol). The initial turbid solution became clear after the reaction mixture was brought to room temperature and was further stirred for 24 h. Evaporation of all volatiles under vacuum afforded a white solid. This was crystallized from THF at -20 ºC. Yield: (2.55 g, 96.7 %). M.p. 222-225 ºC. IR (ν cm^{-1}, Nujol): 2296, 2294 (B-H stretch), 1587, 1373, 1303, 1105, 1057, 1022, 969, 947, 880, 637, 529. ^{1}H NMR (400 MHz, $CDCl_3$, δ ppm): 1.96 (s, *o*-C*H*$_3$, 12 H), 2.23 (s, *p*-C*H*$_3$, 6 H), 3.23 (broad, B*H*), 6.72 (s, 2,4,6-Me$_3$C$_6$*H*$_2$, 4 H), 7.38-7.34 (m, Ph, 8 H), 7.49-7.45 (m, Ph, 4 H), 7.85-7.80 (m, Ph, 8 H), ^{13}C NMR (100 MHz, $CDCl_3$, δ ppm): 20.2 (s, *o*-*C*H$_3$), 20.9 (s, *p*-*C*H$_3$), 127.8 (m not resolved, due to $J_{C\text{-}P}$ & $J_{C\text{-}B}$, aromatic), 129.3 (s, aromatic), 131.0 (s, aromatic), 132.0 (m not resolved, due to $J_{C\text{-}P}$ & $J_{C\text{-}B}$, aromatic), 134.0 (s, aromatic), 134.41 (dd, $J_{C\text{-}P}$ = 121 & 2.1 Hz, aromatic), 137.9 (b, aromatic), 140.7 (s, aromatic). $^{31}P\{^{1}H\}$ NMR (162 MHz, $CDCl_3$, δ ppm): 19.2. ^{11}B NMR (128.4 MHz, $CDCl_3$, δ ppm): –5.2. Mass spectrum (+ve ion, EI), *m/z* = calculated (found): 665.3267 (665.2986) $[M + H]^+$.

Synthesis of [{N(Ph$_2$PN(2,4,6-Me$_3$C$_6$H$_2$))$_2$}BCl$_2$] (1.12): To a solution of **L$_1$**BH$_2$ (**1.11**) (1.33 g, 2.0 mmol) in toluene (40 mL) at room temperature was added HCl·dioxane (1.1 mL, 4 M in dioxane, 4.4 mmol). The reaction mixture was further stirred for 2 h. This reaction mixture was heated for 12 h at 80 °C. Evaporation of all volatiless under vacuum afforded a white solid gave a mixture of two products. The other product identified to be $[\mathbf{L_1}BCl]^+[BCl_4]^-$ is discussed in detail along with its exclusive synthesis, spectroscopic and structural characterization in chapter 3 compound **3.2**. Crude yield: (1.02 g, 70 %). M.p. 153-155 ºC. IR (ν cm^{-1}, KBr): 3063, 2970, 2925, 1483, 1438, 1371, 1277, 1116, 1019, 804, 693.

^{1}H NMR (400 MHz, $CDCl_3$, δ ppm): 1.68 (overlapped singlet, *o*-C*H*$_3$, 12 H), 2.30 (s, *p*-C*H*$_3$, 6 H), 6.87 (s, 2,4,6-$Me_3C_6H_2$, 4 H), 7.63-7.55 (m, Ph, 16 H), 7.84-7.80 (m, Ph, 4 H). ^{13}C NMR (100 MHz, $CDCl_3$, δ ppm): 19.2 (s, *o*-*C*H$_3$), 21.0 (s, *p*-*C*H$_3$), 125.5 (d, $J_{C\text{-}P}$ = 2.2 Hz, aromatic), 126.7 (d, $J_{C\text{-}P}$ = 2.2 Hz, aromatic), 129.2 (m not resolved, due to $J_{C\text{-}P}$ & $J_{C\text{-}B}$, aromatic), 130.0 (s, aromatic), 131.0 (s, aromatic), 132.5 (m not resolved, due to $J_{C\text{-}P}$ & $J_{C\text{-}B}$, aromatic), 134.6 (s, aromatic), 137.4 (s, aromatic), 139.4 (s, aromatic).^{31}P{^{1}H} NMR (162 MHz, $CDCl_3$, δ ppm): 26.1. ^{11}B NMR (128.4 MHz, $CDCl_3$, ppm): δ 7.2. Mass spectrum (+ve ion, EI), *m/z* = calculated (found): 696.2643 (696.2674) $[M - Cl]^+$.

Synthesis of [{N(Ph$_2$PN(2,4,6-Me$_3$C$_6$H$_2$))$_2$}BHBr] (1.13): To a solution of **L$_1$**BH_2 (**1.11**) (1.33 g, 2.0 mmol) in toluene (40 mL) at room temperature was added C_2H_5Br (0.74 mL, 10 mmol). This reaction mixture was heated for 12 h at 110 °C to produce a white precipitate. Filteration and subsequently washing of this precipitate with hexane afforded a white solid. Yield: (1.19 g, 80 %). M.p. 218-221 ºC. IR (ν cm^{-1}, KBr): 3060, 2921, 2542 (B-H stretch), 1588, 1483, 1435, 1360, 1326, 1214, 1116, 1026, 727, 697. ^{1}H NMR (400 MHz, $CDCl_3$, δ ppm): 1.50 (s, *o*-C*H*$_3$, 12 H), 2.11 (s, *p*-C*H*$_3$, 6 H), 4.10 (broad, B*H*), 6.68 (s, 2,4,6-$Me_3C_6H_2$, 4 H), 7.48-7.39 (m, Ph, 16 H), 7.68-7.64 (m, Ph, 4 H). ^{13}C NMR (100 MHz, $CDCl_3$, δ ppm): 19.1 (s, *o*-*C*H$_3$), 20.8 (s, *p*-*C*H$_3$), 124.9 (d, $J_{C\text{-}P}$ = 1.8 Hz, aromatic), 126.2 (d, $J_{C\text{-}P}$ = 1.8 Hz, aromatic), 129.3 (m not resolved, due to $J_{C\text{-}P}$ & $J_{C\text{-}B}$, aromatic), 130.5 (s, aromatic), 132.3 (m not resolved, due to $J_{C\text{-}P}$ & $J_{C\text{-}B}$, aromatic), 134.0 (s, aromatic), 136.2 (s, aromatic), 138.8 (s, aromatic). ^{31}P{^{1}H} NMR (162 MHz, $CDCl_3$, δ ppm): 22.5. ^{11}B NMR (128.4 MHz, $CDCl_3$, ppm): δ 0.7. Mass spectrum (+ve ion, EI), *m/z* = calculated (found): 662.3032 (662.3015) $[M - Br]^+$.

Synthesis of [{N(Ph$_2$PN(2,4,6-Me$_3$C$_6$H$_2$))$_2$}BHI] (1.14): To a solution of **L$_1$**BH_2 (**1.11**) (1.326 g, 2.0 mmol) in toluene (40 mL) at room temperature was added CH_3I (0.6 mL, 10 mmol). The reaction mixture was further stirred for 12 h at room temperature gave a white

precipitate. Filtration and subsequently washing of this precipitate with hexane afforded a white solid. Yield: (1.26 g, 80 %). M.p. 263-265 ºC. IR (ν cm^{-1}, KBr): 3051, 2918, 2548 (B-H stretch), 1587, 1481, 1437, 1357, 1329, 1301, 1116, 730, 693. ^{1}H NMR (400 MHz, $CDCl_3$, δ ppm): 1.61 (s, *o*-CH_3, 12 H), 2.23 (s, *p*-CH_3, 6 H), 4.25 (broad, B*H*), 6.79 (s, 2,4,6-$Me_3C_6H_2$, 4 H), 7.59-7.50 (m, Ph, 16 H), 7.79-7.75 (m, Ph, 4 H). ^{13}C NMR (100 MHz, $CDCl_3$, δ ppm): 19.2 (s, *o*-*C*H_3), 20.9 (s, *p*-*C*H_3), 125.0 (d, $J_{C\text{-}P}$ = 1.5 Hz, aromatic), 126.3 (d, $J_{C\text{-}P}$ = 1.5 Hz, aromatic), 129.4 (m not resolved, due to $J_{C\text{-}P}$ & $J_{C\text{-}B}$, aromatic), 130.6 (s, aromatic), 132.4 (m not resolved, due to $J_{C\text{-}P}$ & $J_{C\text{-}B}$, aromatic), 134.1 (s, aromatic), 134.9 (s, aromatic), 136.3 (s, aromatic), 138.9 (s, aromatic).^{31}P{^{1}H} NMR (162 MHz, $CDCl_3$, δ ppm): 22.6. Mass spectrum (+ve ion, EI), *m/z* = calculated (found): 662.3032 (662.3052) $[M - I]^+$.

Synthesis of [{N(Ph$_2$PN(2,4,6-Me$_3$C$_6$H$_2$))$_2$}BH(OTf)] (1.15): To a solution of **L$_1$**BH_2 (**1.11**) (1.326 g, 2.0 mmol) in toluene (40 mL) at room temperature was added TfOH (0.18 mL, 2 mmol). The reaction mixture was further stirred for 3 h at room temperature gave viscous liquid. Evaporation of all volatiless under vacuum and subsequently washing with hexane afforded a white semisolid. Yield: (1.2 g, 75 %). IR (ν cm^{-1}, nujol): 3067, 2959, 2862, 2553, (B-H stretch), 1609, 1587, 1483, 1440, 1404, 1329, 1197, 1025, 913, 733, 688. ^{1}H NMR (400 MHz, $CDCl_3$, δ ppm): 1.72 (s, *o*-CH_3, 12 H), 2.32 (s, *p*-CH_3, 6 H), 4.33 (broad, B*H*), 6.9 (s, 2,4,6-$Me_3C_6H_2$, 4 H), 7.7-7.56 (m, Ph, 16 H), 7.83-7.8 (m, Ph, 4 H). ^{13}C NMR (100 MHz, $CDCl_3$, δ ppm): 19.1 (s, *o*-*C*H_3), 20.8 (s, *p*-*C*H_3), 119.1 (q, $J_{C\text{-}F}$ = 318 Hz, *CF$_3$*), 125.2 (d, $J_{C\text{-}P}$ = 2.0 Hz, aromatic), 126.4 (d, $J_{C\text{-}P}$ = 2.0 Hz, aromatic), 129.3 (m not resolved, due to $J_{C\text{-}P}$ & $J_{C\text{-}B}$, aromatic), 130.6 (s, aromatic), 132.5 (m not resolved, due to $J_{C\text{-}P}$ & $J_{C\text{-}B}$, aromatic), 134.2 (s, aromatic), 134.8 (s, aromatic), 136.4 (s, aromatic), 139.0 (s, aromatic). ^{19}F NMR (376 MHz, $CDCl_3$, δ ppm): –77.79 (s, 3F, -CF_3). ^{31}P{^{1}H} NMR (162 MHz, $CDCl_3$, δ ppm): 22.7. Mass spectrum (+ve ion, EI), *m/z* = calculated (found): 662.3032 (662.3012) [M – OTf]$^+$.

1.5 Crystallographic Data

Table 1. Crystal data and structure refinement details for compounds L_1H and L_2H.

Compound	**L_1H**	**L_2H**
Empirical Formula	$C_{42}H_{43}N_3P_2$	$C_{48}H_{54}N_3P_2$
Formula mass	651.7	734.88
T (K)	100 (2)	100 (2)
Crystal system	monoclinic	Triclinic
Space Group	*C2/c*	*P*ī
a (Å)	34.3934 (2)	9.0338(2)
b (Å)	9.5807 (6)	10.6913(2)
c (Å)	20.9481 (1)	22.207(3)
α (°)	90	92.389(6)
β (°)	90.553 (3)	99.361(4)
γ (°)	90	104.789(7)
V (Å)	6902.35 (8)	2038.4(6)
Z	8	2
D_{calc} (g cm^{-3})	1.25	1.197
M (MoKα) (mm^{-1})	0.161	0.144
F (000)	2768	786
θ range (°)	2.2–25.0	0.8-25.4
Index range	$-40 \leq h \leq 34$	$-10 \leq h \leq 10$
	$-11 \leq k \leq 11$	$-12 \leq k \leq 9$
	$-24 \leq l \leq 24$	$-26 \leq l \leq 26$
Reflections collected	20792	7463
Independent reflections	6094	4104
Data/restraints/parameters	6094/0/434	4104/0/499
R1, wR2 [$I > 2\sigma(I)$][a]	0.037, 0.083	0.0780, 0.1598
R1, wR2 (all data) [a]	0.052, 0.090	0.1211, 0.1956
GOF	1.025	1.139
$\Delta\rho_{max, min}$/ e $Å^{-3}$	0.313, -0.349	0.381, -0.460

[a] $R1 = \Sigma||Fo| - |Fc||/\Sigma|Fo|$. $wR2 = [\Sigma w(|Fo^2| - |Fc^2|)^2/\Sigma w|Fo^2|^2]^{1/2}$

Table 2. Crystal data and structure refinement details for compounds 1.1 and 1.2.

Compound	**1.1**	**1.2**
Empirical Formula	$C_{46}H_{52}N_3P_2O_1Li_1$	$C_{52}H_{62}N_3P_2O_1Li_1$
Formula mass	731.8	813.93
T (K)	100 (2)	100 (2)
Crystal system	Monoclinic	monoclinic
Space Group	$P2_1/n$	$P2_1/n$
a (Å)	11.3598 (3)	10.6944
b (Å)	22.6450 (5)	22.7223(2)
c (Å)	15.6810 (3)	18.6697(1)
α (°)	90	90
β (°)	93.225(1)	91.515(4)
γ (°)	90	90
V (Å)	4027.4 (2)	4355.2(5)
Z	4	4
D_{calc} (g cm^{-3})	1.21	1.192
M (MoKα) (mm^{-1})	0.146	0.137
F (000)	1560	1744
θ range (°)	1.6–25	1.0-25.4
Index range	$-13 \leq h \leq 13$	$-12 \leq h \leq 12$
	$-26 \leq k \leq 25$	$-27 \leq k \leq 27$
	$-18 \leq l \leq 14$	$-22 \leq l \leq 22$
Reflections collected	23430	8284
Independent reflections	7188	7064
Data/restraints/parameters	7188/0/486	7064/0/540
R1, wR2 [$I > 2\sigma(I)$][a]	0.047, 0.114	0.0478, 0.1120
R1, wR2 (all data) [a]	0.072, 0.132	0.0578, 0.1198
GOF	1.071	1.083
$\Delta\rho_{max, min}$/ e $Å^{-3}$	0.576, -0.386	0.314, -0.333

[a] $R1 = \Sigma||Fo| - |Fc||/\Sigma|Fo|$. $wR2 = [\Sigma w(|Fo^2| - |Fc^2|)^2/\Sigma w|Fo^2|^2]^{1/2}$

Table 3. Crystal data and structure refinement details for compounds 1.3 and 1.4.

Compound	**1.3**	**1.4**
Empirical Formula	$C_{42}H_{42}B_1F_2N_3P_2$	$C_{42}H_{42}Al_1Cl_2N_3P_2$
Formula mass	699.6	748.6
T (K)	100 (2)	100 (2)
Crystal system	monoclinic	monoclinic
Space Group	$P2_1/c$	$P2_1/c$
a (Å)	12.8293(5)	12.9383(1)
b (Å)	17.3644(7)	13.3965(1)
c (Å)	16.3545(8)	24.2002(2)
α (°)	90	90
β (°)	96.254(3)	104.261(4)
γ (°)	90	90
V (Å)	3621.7(3)	4065.3(6)
Z	4	4
D_{calc} (g cm^{-3})	1.28	1.22
M (MoKα) (mm^{-1})	0.165	0.293
F (000)	1472	1568
θ range (°)	1.7-2.54	2.2–25.4
Index range	$-15 \leq h \leq 15$	$-15 \leq h \leq 15$
	$-20 \leq k \leq 18$	$-15 \leq k \leq 12$
	$-19 \leq l \leq 18$	$-28 \leq l \leq 28$
Reflections collected	23519	28365
Independent reflections	6631	7437
Data/restraints/parameters	6631/0/457	7437/0/457
R1, wR2 [$I > 2\sigma(I)$][a]	0.047, 0.106	0.040, 0.104
R1, wR2 (all data) [a]	0.076, 0.120	0.052, 0.115
GOF	1.005	1.094
$\Delta\rho_{max, min}$/ e $Å^{-3}$	0.420, -0.407	0.540, -0.428

[a] $R1 = \Sigma||Fo| - |Fc||/\Sigma|Fo|$. $wR2 = [\Sigma w(|Fo^2| - |Fc^2|)^2/\Sigma w|Fo^2|^2]^{1/2}$

Table 4. Crystal data and structure refinement details for compounds 1.5 and 1.6.

Compound	**1.5**	**1.6**
Empirical Formula	$C_{42}H_{42}Cl_2Ga_1N_3P_2$	$C_{42}H_{42}In_1Br_2N_3P_2$
Formula mass	791.4	925.4
T (K)	100 (2)	100 (2)
Crystal system	monoclinic	tetragonal
Space Group	$P2_1/c$	$I\text{-}4_2d$
a (Å)	12.9263(2)	28.5397(1)
b (Å)	13.3939(2)	28.5397(1)
c (Å)	24.1728(4)	10.5564(7)
α (°)	90	90
β (°)	104.200(7)	90
γ (°)	90	90
V (Å)	4057.2(1)	8598.8(8)
Z	4	8
D_{calc} (g cm^{-3})	1.35	1.43
M (MoKα) (mm^{-1})	0.925	2.514
F (000)	1640	3712
θ range (°)	2.2–25.0	1.4-25.3
Index range	$-15 \leq h \leq 14$	$-34 \leq h \leq 33$
	$-16 \leq k \leq 10$	$-33 \leq k \leq 34$
	$-29 \leq l \leq 28$	$-12 \leq l \leq 12$
Reflections collected	21901	24753
Independent reflections	7124	3939
Data/restraints/parameters	7124/0/457	3939/0/230
R1, wR2 [$I > 2\sigma(I)$][a]	0.041, 0.104	0.027, 0.071
R1, wR2 (all data) [a]	0.058, 0.159	0.029, 0.072
GOF	1.027	1.054
$\Delta\rho_{max, min}$/ e $Å^{-3}$	0.372, -0.557	0.267, -0.406

[a] $R1 = \Sigma||Fo| - |Fc||/\Sigma|Fo|$. $wR2 = [\Sigma w(|Fo^2| - |Fc^2|)^2/\Sigma w|Fo^2|^2]^{1/2}$

Table 5. Crystal data and structure refinement details for compounds 1.7 and 1.9.

Compound	**1.7**	**1.9**
Empirical Formula	$C_{42}H_{43}N_3P_2BCl$	$C_{44}H_{48}Al_1N_3P_2$
Formula mass	698.05	707.8
T (K)	100 (2)	100 (2)
Crystal system	Orthorhombic	monoclinic
Space Group	$P2_12_12_1$	$P2_1/c$
a (Å)	11.4021(1)	12.8957(2)
b (Å)	17.1329(2)	13.5065(2)
c (Å)	18.7089(2)	24.3740(4)
α (°)	90	90
β (°)	90	103.800(3)
γ (°)	90	90
V (Å)	3654.8(6)	4122.9(1)
Z	4	4
D_{calc} (g cm^{-3})	1.268	1.14
M (MoKα) (mm^{-1})	0.227	0.159
F (000)	1474	1504
θ range (°)	2.38–26.94	1.6-25.4
Index range	$-13 \leq h \leq 11$	$-15 \leq h \leq 15$
	$-20 \leq k \leq 20$	$-14 \leq k \leq 16$
	$-22 \leq l \leq 22$	$-27 \leq l \leq 29$
Reflections collected	22566	30465
Independent reflections	6690	7556
Data/restraints/parameters	6690/0/451	7556/0/459
R1, wR2 [$I > 2\sigma(I)$][a]	0.0322, 0.0746	0.045, 0.115
R1, wR2 (all data) [a]	0.0376, 0.777	0.060, 0.121
GOF	1.041	1.060
$\Delta\rho_{max, min}$/ e $Å^{-3}$	0.337, -0.302	0.407, -0.420

[a] $R1 = \Sigma||Fo| - |Fc||/\Sigma|Fo|$. $wR2 = [\Sigma w(|Fo^2| - |Fc^2|)^2/\Sigma w|Fo^2|^2]^{1/2}$

Table 6. Crystal data and structure refinement details for compounds 1.10 and 1.11.

Compound	**1.10**	**1.11**
Empirical Formula	$C_{42}H_{44}Al_1N_3P_2$	$C_{42}H_{44}B_1N_3P_2 \cdot THF$
Formula mass	679.77	733.6
T(K)	100(2)	100(2)
Crystal system	monoclinic	triclinic
Space Group	$P2_1/n$	$P\bar{1}$
a (Å)	14.050(2)	10.7108(7)
b (Å)	17.349(3)	13.7747(8)
c (Å)	15.439(3)	14.2804(8)
α (°)	90	85.004(4)
β (°)	96.119(1)	76.209(4)
γ (°)	90	80.07(4)
V (Å)	3741.8(1)	2013.2(2)
Z	4	2
D_{calc} (g cm^{-3})	1.21	1.21
M (MoKα) (mm^{-1})	0.173	0.147
F (000)	1441	780
θ range (°)	3.0-25.3	2.0-25.0
Index range	$-16 \leq h \leq 16$	$-12 \leq h \leq 12$
	$-20 \leq k \leq 20$	$-16 \leq k \leq 16$
	$-18 \leq l \leq 18$	$-16 \leq l \leq 16$
Reflections collected	33017	16804
Independent reflections	6821	7088
Data/restraints/parameters	6821/0/446	7088/0/492
R1, wR2 [$I > 2\sigma(I)$][a]	0.072, 0.1700	0.054, 0.150
R1, wR2 (all data) [a]	0.1048, 0.2051	0.076, 0.162
GOF	1.027	1.048
$\Delta\rho_{max, min}$/ e Å^{-3}	0.580, -0.550	0.990, -0.912

[a] $R1 = \Sigma||Fo| - |Fc||/\Sigma|Fo|$. $wR2 = [\Sigma w(|Fo^2| - |Fc^2|)^2/\Sigma w|Fo^2|^2]^{1/2}$

1.6 References

1. (a) Witt, M.; Roesky, H. W. *Chem. Rev*. **1994**, *94*, 1163. (b) Steiner, A.; Zacchini, S.; Richards, P. I. *Coord. Chem. Rev*. **2002**, *227*, 193. (c) Bourget-Merle, L.; Lappert, M. F.; Severn, J. R. *Chem. Rev*. **2004**, *102*, 3031. (d) Panda, T. K.; Roesky, P. W. *Chem. Soc. Rev*. **2009**, *38*, 2782. (e) Jones, N. D.; Cavell, R. G. *J. Organomet. Chem*. **2005**, *690*, 5485. (f) Chandrasekhar, V.; Thilagar, P.; Pandian, B. M. *Coord. Chem. Rev*. **2007**, *251*, 1045.
2. (a) Prashanth, B.; Singh, S. *Dalton Trans*. **2014**, *43*, 16880. (b) Fedorchuk, C.; Copsey, M.; Chivers, T. *Coord. Chem. Rev*. **2007**, *251*, 897. (c) Edelmann, F. T. *Coord. Chem. Rev*. **1994**, *137*, 403. (d) Hauber, S.-O.; Lissner, F.; Deacon, G. B.; Niemeyer, M. *Angew. Chem., Int. Ed*. **2005**, *44*, 5871. (e) Meinholz, M. M.; Pandey, S. K.; Deuerlein, S. M.; Stalke, D. *Dalton Trans*. **2011**, *40*, 1662. (f) Steiner, A.; Zacchini, S.; Richards, P. I. *Coord. Chem. Rev*. **2002**, *227*, 193.
3. (a) Roesky, P. W. *Z. Anorg. Allg.Chem*. **2006**, *632*, 1918. (b) Cavell, R. G.; Babu, R. P. K.; Aparna, K. *J. Organomet. Chem*. **2001**, *617*-618, 158.
4. Five membered chelates of monoanionic ligands are mostly known with aminotroponiminates, 1,4-diaza-1,3-butadiene, and bidentate ligands with PC^- and NC^- chelating atoms. Seven or higher membered chelates are rare and are formed by pincer type tridentate PCP^-, NCN^-, and CNN^- connectors. These systems are beyond the scope of present discussion and have not been included.
5. (a) Nagendran, S.; Roesky, H. W. *Organometallics* **2008**, *27*, 457. (b) Tsai, Y.-C. *Coord. Chem. Rev*. **2012**, *256*, 722.
6. (a) Dagorne, S.; Normand, M.; Kirillov, E.; Carpentier, J.-F. *Coord. Chem. Rev*. **2013**, *257*, 1869. (b) Bai, G.; Singh, S.; Roesky, H. W.; Noltemayer, M.; Schmidt, H. -G. *J. Am. Chem. Soc*. **2005**, *127*, 3449. (c) Chai, J.; V.; Jancik, Singh, S.; Zhu, H.; He, C.;

Roesky, H. W.; Schmidt, H.-G.; M. Noltemeyer, N. S. Hosmane, *J. Am. Chem. Soc*. **2005**, *127*, 7521-7528.

7. (a) Fryzuk, M. D. *Mod. Coord. Chem.* **2002** 187. (b) Gade, L. H. *J. Organomet. Chem*. **2002**, *661*, 85. (c) Kempe, R. *Eur. J. Inorg. Chem.* **2003,** 791.
8. (a) Rong, W.; Liu, D.; Zuo, H.; Pan, Y.; Jian, Z.; Li, S.; Cui, D. *Organometallics* **2013**, *32*, 1166. (b) Rong, W.; Cheng, J.; Mou, Z.; Xie, H.; Cui, D. *Organometallics* **2013**, *32*, 5523.
9. (a) Rivard, E.; Ragogna, P. J.; McWilliams, A. R.; Lough, A. J.; Manners, I. *Inorg. Chem*. **2005**, *44*, 6789. (b) McWilliams, A. R.; Rivard, E.; Lough, A. J.; Manners, I. *Chem. Commun.* **2002**, 1102.
10. (a) Gates, D. P.; McWilliams, A. R.; Ziembinski, R.; liable-Sands, L. M.; Guzei, I. A.; Yap, G. P. A.; Rheingold, A. L.; Manners, I. *Chem. Eur. J*. **1998**, *4*, 1489. (b) Gates, D. P.; Ziembinski, R.; Rheingold, A. L.; Haggerty, B. H.; Manners, I. *Angew. Chem., Int. Ed. Engl*. **1994**, *33*, 2277. (c) Gates, D. P.; L.-Sands, L. M.; Yap, G. P. A.; Rheingold, A. L.; Manners, I. *J. Am. Chem. Soc*. **1997**, *119*, 1125.
11. (a) Hasselbring, R.; Pandey, S. K.; Roesky, H. W.; Stalke, D.; Steiner, A. *J. Chem. Soc. Dalton Trans*. **1993**, 3447. (b) Hasselbring, R.; Roesky, H. W.; Heine, A.; Stalke, D.; Sheldrick, G. M. *Z. Naturforsch*. **1994**, *48b*, 43. (c) Paul, Y.; Pandey, S. K. *Phosphorus, Sulfur and Silicon* **2003**, *178*, 159. (d) Pandey, S. K.; Steiner, A.; Roesky, H. W.; Stalke, D. *Angew. Chem., Int. Ed. Engl*. **1993**, *32*, 596-598.
12. (a) Paul, Y.; Pandey, S. K. *J. Coord. Chem*. **2008**, *61*, 2655. (b) Paul, Y.; Magotra, S.; Pandey, S. K. *Synth. React. Inorg. Met.-Org. Nano-Met. Chem*. **2007**, *37*, 705. (c) Paul, Y.; Pandey, S. K. *Synth. React. Inorg. Met.-Org. Chem*. **2003**, *33*, 1515. (d) Braunstein, P.; Hasselbring, R.; Stalke, D. *New J. Chem*. **1996**, *20*, 337. (e) Hasselbring, R.; Braunstein, P. *Phosphorus, Sulfur and Silicon* **1994**, *93-94*, 423.

13. (a) Ho, S. Y.-F.; So, C.-W.; Saffon-Merceron, N.; Mezailles, N. *Chem. Commun.* **2015,** *51*, 2107. (b) Heuclin, H.; Ho, S. Y.-F.; Le Goff, X. F.; So, C.-W.; Mézailles, N. *J. Am. Chem. Soc.* **2013**, *135*, 8774. (c) Molitor, S.; Gessner, V. H. *Chem.-Eur. J.* **2013**, *19*, 11858.
14. Bezman, I. I.; Smalley, J. H. *Chem. Ind.* **1960,** 839. (b) Schmidpeter, A.; Weingand, C.; Hafner-Roll, E. *Z. Naturforsch.* **1969,** *B 24,* 799. (c) Pandey, S. K.; Roesky, H. W.; Stalke, D.; Steiner, A.; Schmidt, H.-G.; Noltemeyer, M. *Phosphorus Sulfur Silicon* **1993,** *84,* 231. (d) Pandey, S. K.; Hasselbring, R.; Steiner, A.; Stalke, D.; Roesky, H. W. *Polyhedron* **1993,** *12*, 2941.
15. Nöth, V. H.; Meinel, L. *Z. Anorg. Allg. Chem*. **1967**, *5-6*, 225.
16. Murata, S.; Abe, S.; Tomioka. H. *J. Org. Chem*. **1997**, *62*, 3055.
17. Liu, Q.; Tor, Y. *Org. Lett.* **2003,** *14*, 2571.
18. (a) Hill, M. S.; Hitchcock, P. B.; Karagonuni, S. M. A. *J. Organomet. Chem*. **2004**, *689*, 722. (b) Stender, M.; Wright, R. J.; Eichler, B. E.; Prust, J.; Olmstead, M. M.; Roesky, H. W.; Power, P. P. *J. Chem. Soc., Dalton Trans.* **2001**, 3465.
19. Aramaki, Y.; Omiya, H.; Yamashita, M.; Nakabayashi, K.; Ohkoshi, S.-I.; Nozaki, K. *J. Am. Chem. Soc*. **2012**, *134*, 19989
20. Stender, M.; Eichler, B. E.; Hardman, N. J.; Power, P. P.; *Inorg. Chem.* **2001**, *40*, 2794.
21. Sussek, H.; Stark, O.; Devi, A.; Pritzkow, H.; Fischer, R. A. *J. Organomet. Chem.* **2000**, *602*, 29.
22. Wang, H.; Zhang, J.; Hu, H.; Cui, C. *J. Am. Chem. Soc*. **2010**, *132*, 10998.
23. Radzewich, C. E.; Coles, M. P.; Jordan, R. F. *J. Am. Chem. Soc*. **1998**, *120*, 9384.
24. Aparna, K.; Mcdonald, R.; Ferguson, M.; Cavell, R. G. *Organometallics* **1999**, *18*, 4241.

25. Shriver, D. F.; Drezdon, M. A. The Manipulation of Air–Sensitive Compounds, 2nd Ed. McGraw–Hill, New York, USA, 1969.
26. CrystalClear 2.0, Rigaku Corporation, Tokyo, Japan.
27. Dolomanov, O. V.; Bourhis, L. J.; Gildea, R. J.; Howard, J. A. K.; Puschmann, H. *J. Appl. Cryst.* **2009**, *42*, 339.
28. SHELXS-97, Program for Structure Solution: Sheldrick, G. M. *Acta Crystallogr. Sect. A.* **2008**, *64*, 112.

Synthesis and Structural Studies of Novel Thioxo- and Selenoxo-borane Complexes

Chapter 2

Abstract: The unusual reactivity of a newly synthesized bis(phosphinimino)amide dihydroboron complex $\mathbf{L_1}BH_2$ ($\mathbf{L_1}$ = $[N(Ph_2PN(2,4,6\text{-}Me_3C_6H_2))_2]^-$) with elemental sulfur and selenium have been investigated. The reactions involve oxidative addition of S and Se into B-H bonds with subsequent release of H_2S (or H_2Se) from the intermediate species resulting in the formation of stable compounds with terminal boron-chalcogen double bonds $\mathbf{L_1}B{=}S$ **(2.1)** and $\mathbf{L_1}B{=}Se$ **(2.2)**. The electronic structures of **2.1** and **2.2** have been elucidated by multi-nuclear NMR and single crystal X-ray diffraction studies. Ab initio calculations on **2.1** are in excellent agreement with its experimental structure and clearly support the existence of boron-sulfur double bond.

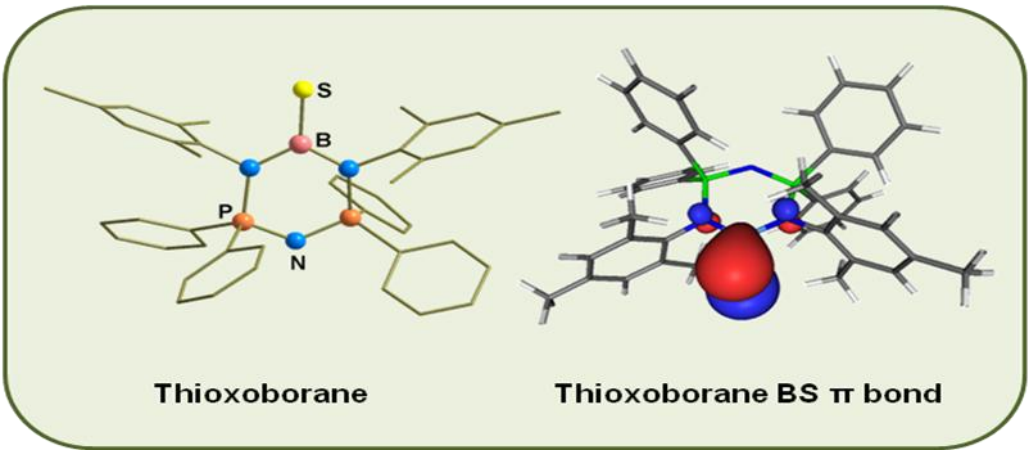

Jaiswal, K.; Prashanth, B.; Ravi, S.; Shamasunder, K. R.; Singh, S. *Dalton Trans*. 2015, 15779.

2.1 Introduction

In the present work, we were interested in utilizing a sterically demanding acyclic phosphazene ligand (**L_1**) [**L_1** = $\{N(Ph_2PN(2,4,6\text{-}Me_3C_6H_2))_2\}^-$] that offers a [N,N′] chelate to the main group metal ions. The primary aim was to incorporate main group elements with a double bond with chalcogens using this ligand. Generation of metal chalcogen double bonds has attracted the attention of inorganic chemists in the past two decades. Heavy analogues of group 14 elements with double bonded chalcogens are very well known.[1] In contrast, group 13 elements with double bonded chalcogens of the type (RM=E) [(M = B, Al) (E = O, S, Se and Te)] are barely known due to their high reactivity and unstable nature under normal conditions. A literature survey revealed that alumoxanes $(RAlO)_n$ for n > 1 can be obtained by controlled reaction of organoaluminum compounds with either water or water containing salt or $(Me_2SiO)_3$. In the field of aluminum chalcogen double bonded compounds Roesky and co-workers reported the first monoalumoxane $[CHC\{(Me)NCH_2CH_2NEt_2\}_2Al{=}O]$ stabilized by a Lewis acid, $[B(C_6F_5)_3]$.[2] Very recently Inoue and co-workers reported the first aluminum telluride **L**Al=Te (**L** = 1,3-(2,6-diisopropylphenyl)-imidazolin-2-imine) double bond stabilized by N-heterocyclic carbenes.[3]

The double bonded boron chalcogen species have been known for a long time and have been trapped, as the transient species Tbt-B=S (Tbt = 2,4,6-tris{bis(trimethylsilyl)methyl}phenyl), with 1,3-butadienes in [4+2]cycloaddition reactions (Scheme 1),[4] but due to the high reactivity of these species their isolation could not be achieved till 2010. In the last decade, isolation of a few stable compounds of the type RB=O gave a breakthrough in oxoborane chemistry (Chart 1).[5] This quest started with the synthesis of the first neutral oxoborane complex **I** (Chart 1) reported by Cowley and co-workers in 2005. This molecule was stabilized with a Lewis acid ($AlCl_3$) and was formed *via* controlled hydrolysis of $[(HC(CMe)_2(NC_6F_5)_2)BCl]^+$ $[AlCl_4]^-$. Successful isolation of this stable neutral

oxoborane and short B–O distance (1.304 Å) determined by X–ray, confirmed the presence of 'B=O'. In 2011, Cui and co-workers reported neutral as well as anionic oxoborane species **II** and **III** (Chart 1) stabilized by Lewis acid [$B(C_6F_5)_3$ and BCl_3] and N-heterocyclic carbenes (NHCs), respectively.[6]

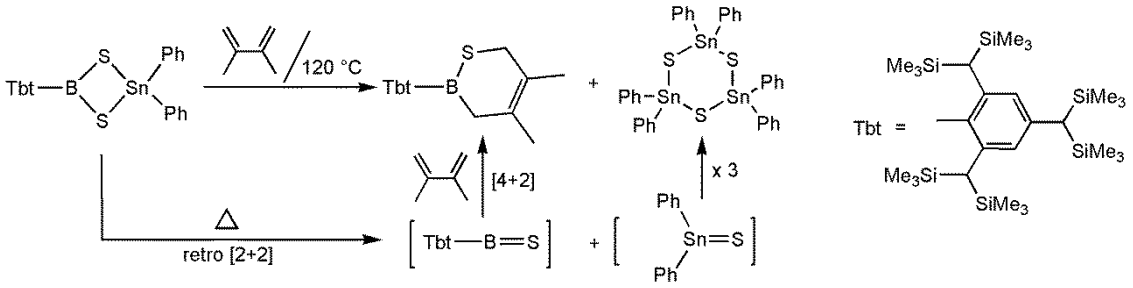

Scheme 1. Trapping experiments of thioxoborane (Tbt-B=S) with 1,3-butadine leading to [4+2] cycloaddition product.

Both of these (neutral as well as anionic oxoborane) species were prepared using borinic acid and were supported by β-dikitiminato ligands. In 2014, Kinjo and co-workers reported a 1,2,4,3-triazaborole based neutral oxoborane stabilized by a Lewis acid ($AlCl_3$) **IV** (Chart 1).[7] In 2010, Braunschweig and co-workers reported the first Lewis acid free boron-oxygen triply bonded compound, supported by late transition metal fragment $[(PCy_3)_2BrPt(B{\equiv}O)]$ **V** (Chart 1).[8] This compound was formed *via* liberation of trimethylsilylbromide from the boron-bromine oxidative addition product of dibromo(trimethylsiloxy)borane and $[Pt(PCy_3)_2]$.

Exploring this chemistry in 2010, Cui and co-workers produced the first isolable stable molecule of thioxo- and selenoxo-borane **VI** (Chart 1, Scheme 2).[9] Their approach relied on use of N-heterocyclic carbenes (NHCs) to isolate an expected B(I) species instead resulted in the isolation of a hydroborane complex. Further, oxidative insertion of S and Se into the B-H bond followed by 1,3-sigmatropic hydrogen migration to the ligand backbone resulted in the formation of stable thioxo- and selenoxo-borane compounds.

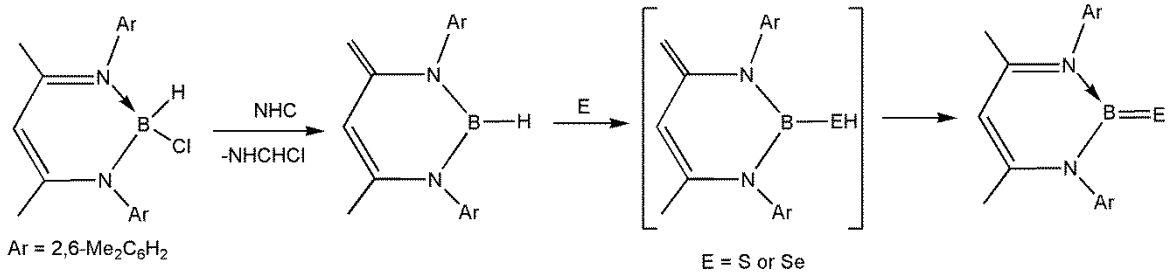

Scheme 2. Synthesis of the first stable thioxo- and selenoxo-borane compounds.

In a similar pattern, Inoue and co-workers (2014) reported a boron cation, containing a boron-sulfur double bond **VII** (Chart 1)[10] supported by a bulky *bis*(imidazolin-2-iminato) ligand, but the corresponding Se analogue has not yet been reported. Therefore, we believe that the notion to explore the synthesis and characterization of stable molecules of boron bonded with heavier chalcogens as thiol/selenol and doubly bonded derivatives (thioxo- and selenoxo-borane) is an important step towards the study of electronic structure, bonding, and chemical reactivity of these classes of compounds.

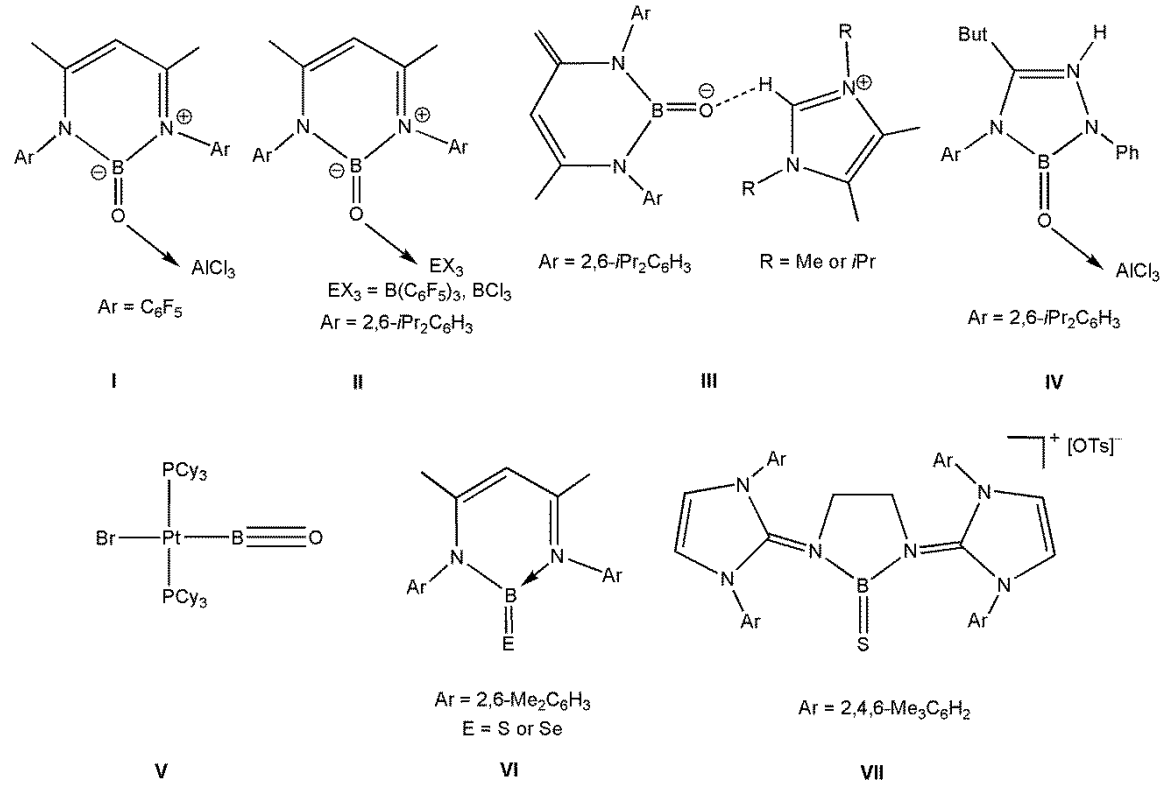

Chart 1. Structurally characterized compounds of boron containing double and triple bonds with chalcogens.

Lack of a suitable starting materials and a rational synthetic routes are major synthetic challenges in this area. The alkyl or aryl borinic (R_2BOH) and boronic ($RB(OH)_2$) acids[11] can be easily prepared and have been extensively used in organic synthesis as building blocks and as intermediates in Suzuki coupling.[12] In contrast to these borinic and boronic species the thio- and seleno-boric acid derivatives, R_2BEH and $RB(EH)_2$ have not been much explored (E = S, Se).[13-17] These heavy analogues of borinic and boronic acids are generally detected in the reactions of halogenoboranes with H_2E.[13] At high temperature thio derivatives led to elimination of hydrocarbons to generate diborylsulfanes (R_2BSBR_2) and further loss of H_2S led to borthiins $(RBS)_3$ and tri-organylboranes (Scheme 3).[13]

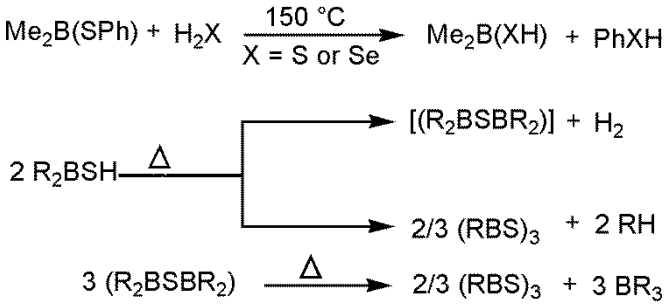

Scheme 3. Synthesis of diborylsulfanes and borthiins.

The Se analogues of these compounds are even rarer; the compounds $BX_{3-n}(SeH)_n$ (X = Cl, Br, I) have been studied by vibrational spectroscopy.[17] The oxidative addition of S and Se into the Al-H bonds in allanes has been established and it could be an alternative route to prepare the B-EH or $B(EH)_2$ derivatives (E = S, Se).[18] These thio- and seleno-boric acid derivatives can be considered as the important precursors in order to synthesize thioxo- and selenoxo-borane compounds.

Recently, we reported on the synthesis and characterization of a dihydroboron species, $\mathbf{L_1}BH_2$ (**1.11**) complexed with a bulky monoanionic bis(phosphinimino)amide ligand ($\mathbf{L_1}$ = $[N(Ph_2PN(2,4,6\text{-}Me_3C_6H_2))_2]^-$).[19] Selection of bis(phosphinimino)amide ligand was induced to mitigate the known facile tendency of H migration from/or to the boron atom in boranes.[9] However, this ligand was expected to behave innocently to support dithiol and

diselenol functionality *via* oxidative insertion of elemental S or Se on reacting with $\mathbf{L_1}BH_2$ (**1.11**). The efforts to prepare dithiol and diselenol derivatives led to the sequential insertion of S and Se into the B-H[9] bonds and subsequent elimination of H_2S and H_2Se gas to afford a facile synthesis of terminal 'B=S' and 'B=Se' moieties supported by bulky *bis*(phosphinimino)amides. The formation of these boron doubly bonded chalcogen species was confirmed by multinuclear NMR, IR, mass spectrometry and X-ray diffraction techniques.

2.2 Results and Discussion

The reaction of $\mathbf{L_1}BH_2$ (**1.11**) with two equivalents of elemental S or Se in toluene at room temperature and at 80 °C respectively, resulted in complete consumption of the chalcogen with concomitant evolution of H_2S and H_2Se leading to the formation of $\mathbf{L_1}B{=}S$ (**2.1**) and $\mathbf{L_1}B{=}Se$ (**2.2**) ($\mathbf{L_1}$ = $[N(Ph_2PN(2,4,6\text{-}Me_3C_6H_2))_2]^-$) (Scheme 4) in good yields. Confirmation of the identity of gases was done by passing into a solution of lead acetate/$CuSO_4$ (for H_2S) and water (for H_2Se to form colloidal Se). To rule out any H_2 evolution from the possible intermediate $\mathbf{L_1}B(SH)H$ species, leading to **2.1**, we performed a stoichiometric reaction between $\mathbf{L_1}BH_2$ (**1.11**) and S (1:1). To our surprise, as monitored by *in-situ* $^{31}P\{^1H\}$ NMR measurements, almost half of the starting material was consumed to form only **2.1** and the remaining half of $\mathbf{L_1}BH_2$ (**1.11**) was present unreacted. This not only supports the intramolecular evolution of H_2S but also suggests that the insertion of S in the B-H bond of $\mathbf{L_1}B(SH)H$ to be more facile than that in $\mathbf{L_1}BH_2$ (**1.11**) itself with concomitant release of H_2S to form **2.1**. The experimental behaviour of the Se analogue **2.2** was found to be similar to that of **2.1**.

Thus, this synthetic method represents an attainable and facile route for the preparation of novel compounds with boron chalcogen double bonds. The intermediate dithiol (or diselenol) species turned out to be kinetically labile leading to intramolecular H_2S or H_2Se evolution. This

is presumably due to the wider N-B-N bite angle offered by the chelating bis(phosphinimino)amide ligand thus, bringing the two B-SH bonds in a proximity close enough to eliminate H_2S or H_2Se (*vide infra*).

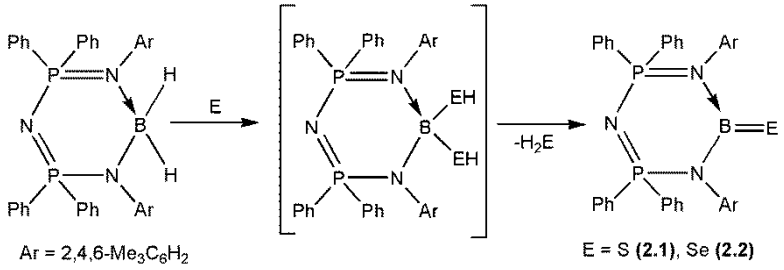

Scheme 4: Synthesis of thioxoborane, $\mathbf{L_1}$B=S (**2.1**) and selenoxoborane, $\mathbf{L_1}$B=Se (**2.2**).

Compounds **2.1** and **2.2** have been unambiguously characterized by means of spectroscopic, spectrometric, and crystallographic techniques. Both **2.1** and **2.2** are thermally quite stable and undergo decomposition with melting at 187 and 190 °C, respectively. The HRMS investigations of **2.1** revealed the $[M\text{-}H]^+$ at *m/z* = 693.2664 (calculated *m/z* = 693.2675), similarly a peak at *m/z* = 742.3522 (calculated *m/z* = 742.2201) in **2.2** was due to $[M^+]$. The IR spectrum of **2.1** showed a sharp band (1096 cm^{-1}) which can be assigned to the B=S fragment.[9] The corresponding stretching mode for **2.2** appeared at 1076 cm^{-1}.[9] The ^{1}H NMR resonance for *o*-CH_3 and *p*-CH_3 group on mesityl substituents of the ligand backbone for **2.1** (1.86 and 2.23 ppm) and for **2.2** (1.85 and 2.23 ppm) were in accordance with the ligand backbone and composition. No other appreciable signals were detected in the crude products which can be attributed to any residual/adventitious SH/SeH moiety. The $^{31}P\{^1H\}$ spectrum of **2.1** and **2.2** showed a sharp single resonance at 23.5 and 21.63 ppm respectively, which is downfield shifted as compared to its precursor **1.11** (19.2 ppm).[19] The ^{11}B NMR spectrum of **2.1** (and **2.2**) revealed a broad resonance at 41 ppm (and 45.2 ppm), suggesting a low local symmetry around the boron atom for three coordinated boron species.[9,10] This also excludes the possibility of any dimer formation (B_2S_2/B_2Se_2 core), due to [2+2] addition of the B=S/B=Se bonds in the solution state.

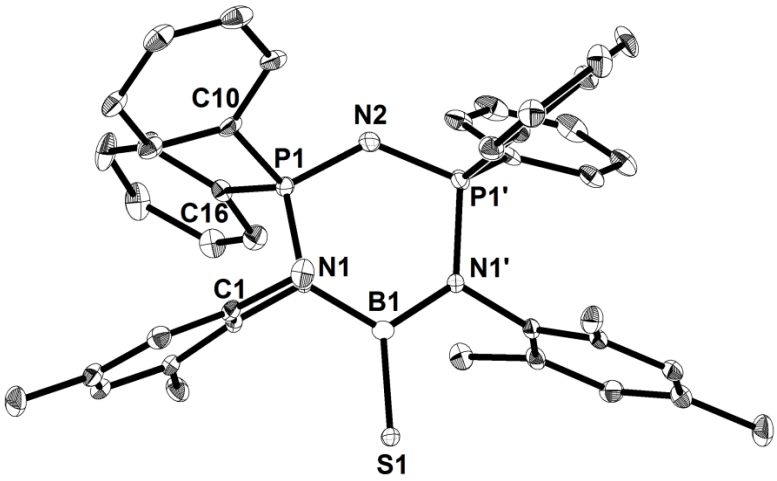

Figure 1. Solid state structure of $\mathbf{L_1}$B=S (**2.1**). All hydrogen atoms and THF molecule have been deleted for clarity. Thermal ellipsoids have been drawn at 30% probability. Selected bond lengths [Å] and bond angles [°]: B(1)–S(1) 1.752(5), B(1)–N(1) 1.494(5), N(1)–P(1) 1.661(3), N(2)–P(1) 1.575(3), C(1)–N(1) 1.471(5), P(1)–C(1) 1.817(5), P(1)–C(16) 1.805(4), N(1)–B(1)–N(1‘) 117.10(2), N(1)–B(1)–S(1) 121.45(1), N(2)–P(1)–N(1) 109.83(1), P(1)–N(2)–P(1‘) 128.77(5), C(1)–N(1)–P(1) 114.80(3), C(16)–P(1)–C(10) 109.05(2), N(1)–P(1)–C(10) 109.94(2), N(1)–P(1)–C(16) 110.25(2), N(2)–P(1)–C(10) 109.56(2), N(2)–C(16)–C(16) 108.16 (2).

Single crystals of **2.1** and **2.2** suitable for X-ray structural analysis were obtained, respectively, from their THF and toluene solutions. Compounds **2.1** and **2.2** were found to crystallize in the orthorhombic space group *Pnc*2 and the tetragonal space group $I4_1/a$, respectively. The X-ray crystal structures of **2.1** and **2.2** (shown in Figures. **1** and **2**) are in agreement with spectroscopic and HRMS characterizations. Both the molecules possess boron atoms in a three coordinated arrangement of a puckered N_3P_2B six-membered ring. Two terminal N atoms of the ligand and the doubly bonded terminal S (or Se) atom form the requisite bonds with the B atom. The two terminal N atoms and S (or Se) atom in compound **2.1** (and **2.2**) are bonded to the B atom in a trigonal planar arrangement (sum of angles at B was found to be 360°). The mesityl substituents on these terminal N atoms are oriented

perpendicular to the N-B(S, Se)-N plane and provide necessary steric protection. The phenyl rings on the remote P atom of the ligand backbone are arranged above and below the P-N-P plane. The two phenyl rings attached to a P atom are approximately transverse to each other, with a dihedral angle of 65° between the two phenyl planes. On each P atom, one of the phenyl groups is in the same plane as the mesityl group attached to the diagonally opposite N atom. Interestingly, the central N atom on the ligand is in the same plane as N-B(S,Se)-N plane, with one of the P atom located above and the other P atom below this plane. The metric parameters observed in **2.1** and **2.2** are not unusual. The B(1)-S(1) bond length in compound **2.1** (1.752(8) Å) and B(1)-Se(1) distance in **2.2** (1.871(5) Å) are in agreement to that seen in the only known examples of this type, $[HC\{(CMe)(2,6\text{-}Me_2C_6H_3N)\}_2]BE$ (1.741(2) Å, E = S; 1.896(4) Å, E = Se).[9] The B-N distances among compound **2.1** and **2.2** are comparable and lie in the range (1.494(5)-1.498(6) Å) and agree with the reported values.[9] The delocalization of the negative charge on the ligand backbone is rather non-uniform as reflected in the two types of P-N bond lengths in both **2.1** and **2.2**. In compound **2.2** the terminal P-N distances 1.667(3) and 1.659(3) Å are slightly longer than the P(2)-N(2) and P(1)-N(2) bond length (1.578(3) and 1.577(3) Å) suggesting that the negative charge largely resides on the remote P-N-P moiety. The trigonal planar N_2BS and N_2BSe moieties in **2.1** and **2.2** respectively, exhibit the N-B-N bite angle of 117.10(2)° and 117.80(3)°. These angles are wider than the corresponding angle in **2.1** (110.60(2)º). This wider bite angle would certainly have its effect in bringing the two thiol (or selenol) groups in the intermediate $\mathbf{L_1}B(EH)_2$ close enough to facilitate intramolecular evolution of H_2E (*vide supra*). The N-B-N angle of **2.1** and **2.2** is also wider than that in $[HC\{(CMe)(2,6\text{-}Me_2C_6H_3N)\}_2]BS$ (111.52°) and $[HC\{(CMe)(2,6\text{-}Me_2C_6H_3N)\}_2]BSe$ (112.6°),[9] respectively.

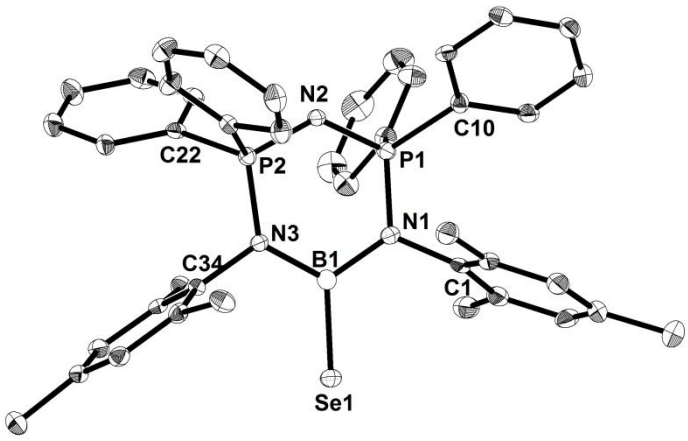

Figure 2. Single crystal X-ray structure of $\mathbf{L_1}$B=Se (**2.2**). All hydrogen atoms have been deleted for clarity. Thermal ellipsoids have been drawn at 30% probability. Selected bond lengths [Å] and bond angles [°]: B(1)–Se(1) 1.871(5), B(1)–N(1) 1.498(6), B(1)–N(3) 1.495(6), N(1)–P(1) 1.659(3), N(2)–P(1) 1.577(3), N(2)–P(2) 1.578(3), N(3)–P(2) 1.667(3), C(1)–N(1) 1.462(5), C(16)–P(1) 1.800(4), C(28)–P(2) 1.799(4), C(10)–P(1) 1.794(4), C(22)–P(2) 1.794(4), N(3)–C(34) 1.458(5), N(1)–B(1)–N(3) 117.82(3), N(1)–B(1)–Se(1) 121.34(3), N(3)–B(1)–Se(1) 120.83(3), N(2)–P(2)–N(3) 109.34(2), N(2)–P(1)–N(1) 109.67(2), P(2)–N(2)–P(1) 128.71(2), C(22)–P(2)–C(28) 107.82(2), C(22)–P(2)–N(3) 110.16(2), N(3)–P(2)–C(28) 113.81(2), N(2)–P(2)–C(22) 109.50(2), N(2)–P(2)–C(28) 106.08(2), C(10)–P(1)–C(16) 107.30(4), C(10)–P(1)–N(2) 111.41(2), C(16)–P(1)–N(2) 110.84(2), N(1)–P(1)–C(10) 110.41(2), N(1)–P(1)–C(16) 111.88(2), C(1)–N(1)–B(1) 119.35(3), C(1)–N(1)–P(1) 117.27(3), B(1)–N(1)–P(1) 123.22(3), C(34)–N(3)–P(2) 116.83(2), C(34)–N(3)–B(1) 116.91(3).

In order to understand the geometric features of X-ray structures, we have performed a geometry optimization of compound **2.1** at B3LYP/cc-pVDZ level of theory. The optimized structure correctly reproduces the experimental crystal structure (within 1-3 % for bond lengths and 0.5-1.5 % for bond-angles). The planarity of N_3BS unit, the extent of ring puckering and the relative orientations of phenyl groups and mesityl groups are also well reproduced. All attempts to obtain alternative structures by geometry optimization starting with different

orientations of phenyl and mesityl groups yielded the same optimized structure. This clearly shows that these geometrical features arise due to electronic factors.

To gain further insight into the nature of bonding in these complexes, we make use of the delocalized Kohn-Sham (KS) orbitals along with localized orbitals produced through the natural bond orbital (NBO) analysis. The frontier KS orbitals involving the BS unit and the ligand atoms of the ring are plotted in Figure. **3**. Clearly, the HOMO corresponds to sulfur lone pair, the HOMO-1 to the B-S π bond, and HOMO-8 to the B-S σ bond. The NBO calculation yields a σ orbital (1.976e) and a π orbital (1.966e) localized on B-S unit with strong polarization towards S. The NBO analysis shows a positive charge of +0.69e on B and a negative charge of -0.55e on S. Therefore, the B-S bond can be clearly considered as a polar double-bond. The NBOs corresponding to B-N bonds are in-plane nitrogen lone pairs (1.622e) with significant interaction with two boron-centered NBOs (0.438e, 0.474e) clearly confirming a B-N coordination bond.

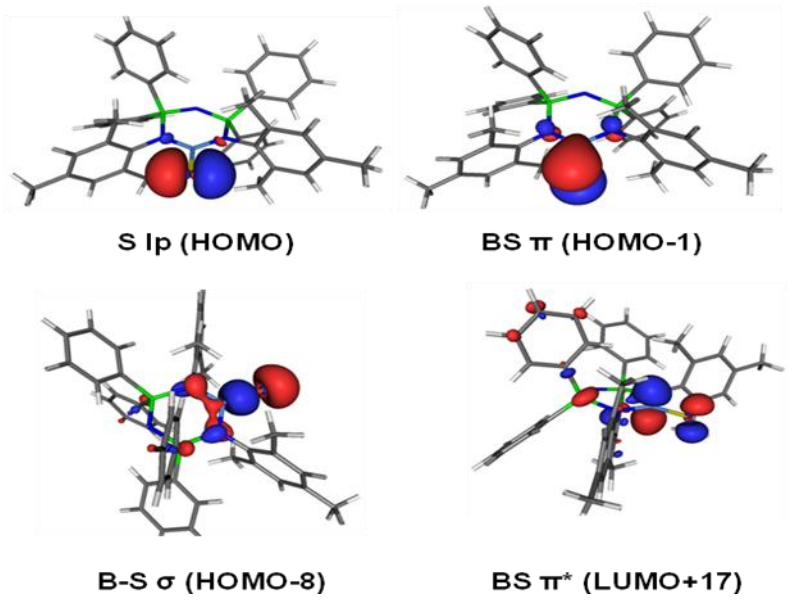

Figure 3. Frontier Kohn-Sham orbitals on B=S unit of compound **2.1**.

The three KS occupied π orbitals shown in Figure. **4** are mainly nitrogen centered with almost no contribution from phosphorus atoms. While two of these are centered on terminal nitrogen atoms with a partial delocalization over the B-S unit, the other one is

mainly centered on the central nitrogen. The corresponding NBOs are found to be mainly nitrogen centered lone pairs. This indicates the absence of significant resonant delocalization of π electrons. A NICS value of [1.0 ppm] computed at the ring center also confirms the absence of aromaticity. The central and terminal nitrogens carry negative charge of -1.44e and -1.1e respectively, in contrast to positive charge of +2.04e carried by each phosphorus atom. An additional in-plane σ orbital mainly centered on the central nitrogen atom supports the view that this atom carries maximum negative charge.

Based on X-ray data and results of geometry optimization and calculation of NBO charges several Lewis structures can be drawn for compound **2.1** (Scheme 5). Form **I** corresponds to a doubly iminophosphorane-stablized species with a formal negative charge at a B atom. Positive charges at P atom (phoshonium) and a negative charge at the central N atom maintain the electrical neutrality. Form **III** is similar to form **I** in a manner that it also

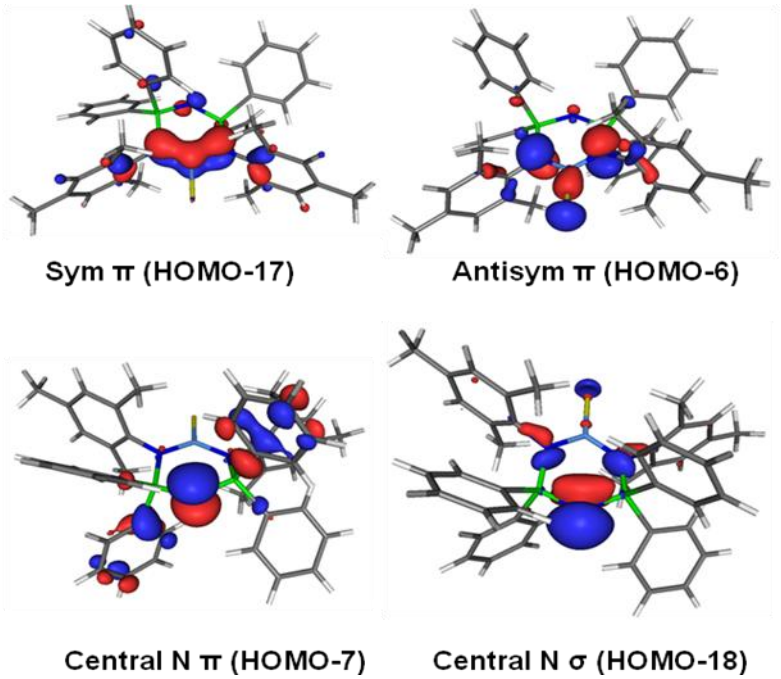

Figure 4. π orbitals of the N_3P_2B ring and σ orbitals of the central N of compound **2.1**.

represents an iminophosphorane-stablized thioxoborane species with the negatively charged B atom and a formal positive charge at one of the P atoms, whereas it differs from form **I** with respect to the central N–P–N portion of the ligand with the other P atom forming a P=N with

the central N atom. The short central P–N distances (1.575(3) Å) compared to terminal P–N distances (1.661(3) Å) as observed in X-ray are supportive of it. Form **II** being the donor stabilized B=S fragment (thioxoborenium) possesses a formal positive charge at the B atom and a negative charge at the central N atom representing a zwitterionic structure of **2.1**. Form **IV** represents a neutral structure with the terminal nitrogens forming a N→B donor and a N–B covalent bond and maintains the P–N distances in the ligand backbone between single (1.78 Å) and double (1.56 Å) PN bonds. Overall, a strong electron transfer from the two terminal N atoms to the $[B{=}S]^+$ fragment in compound **2.1** is indicated to result in a stable thioxoborane.

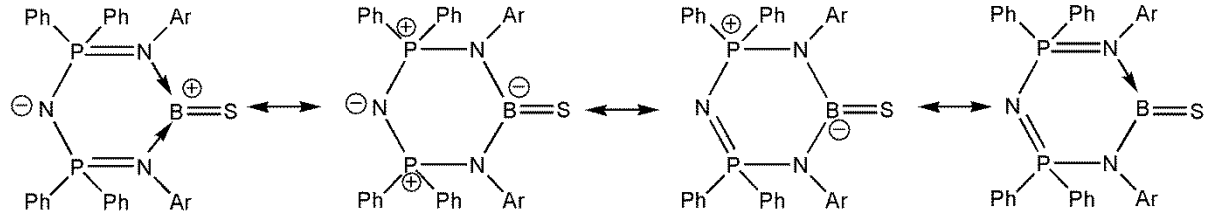

Ar = 2,4,6-$Me_3C_6H_2$

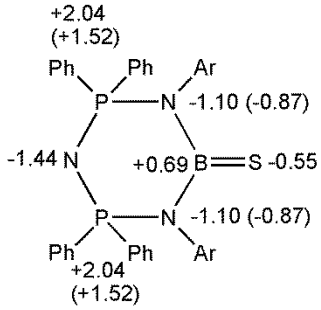

Scheme 5. Resonance structures for thioxoborane, LB=S (**3**), forms **$\overline{\text{III}}$** and **$\overline{\text{IV}}$** represent symmetrical resonance structure for half of **III** and **IV** respectively, and NBO charges. Numbers in the parentheses denote consolidated NBO charges whereas other numbers are bare NBO charges.

2.3 Conclusions

In conclusion, we have demonstrated a facile and rational synthetic strategy for the preparation of terminal doubly bonded boron chalcogen compounds. We think that the resulting compounds **L$_1$**B=E (E = S or Se) are novel precursors to attempt interesting reaction chemistry. From theoretical calculations performed on **L$_1$**B=S, we can conclude that most of the negative charge in the ligand backbone is located on the terminal and remote nitrogen atoms and that the HOMO belongs to the S lone pair and can be easily donated to Lewis acids.

2.4 Experimental Section

2.4.1 Starting materials

All chemicals used in this work were purchased from commercial sources and were used without further purification.

2.4.2 General procedure

All syntheses were carried out under an inert atmosphere of dinitrogen in oven dried glassware using standard Schlenk techniques[20] or a glovebox where O_2 and H_2O levels were maintained usually below 0.1 ppm. All the glassware were dried at 150 °C in an oven for at least 12 h and assembled hot and cooled *in vacuo* prior to use. Solvents were purified by MBRAUN solvent purification system MB SPS-800. THF was dried over (Na/benzophenone ketyl) and distilled under nitrogen and degassed prior to use. $CDCl_3$ for NMR was dried over 4 Å molecular sieves.

2.4.3 Physical measurements

The ^{1}H, ^{13}C, $^{31}P\{^{1}H\}$ and ^{11}B NMR spectra were recorded with a Bruker 400 MHz spectrometer with TMS, H_3PO_4 (85 %) and $BF_3{\cdot}OEt_2$ respectively, as external references and chemical shifts were reported in ppm. Downfield shifts relative to the reference were quoted

positive while the upfield shifts were assigned negative values. High resolution mass spectra were recorded on a Waters SYNAPT G2−S instrument. IR spectra of the complexes were recorded in the range 4000–400 cm^{-1} using a Perkin Elmer Lambda 35-spectrophotometer over KBr plates. The absorptions of the characteristic functional groups were only assigned and other absorptions (moderate to very strong) were only listed. Melting points were obtained in sealed capillaries on a Büchi B–540 melting point instrument.

Single crystal X-ray diffraction data for **2.1** were collected on a Bruker AXS KAPPA APEX-II CCD diffractometer (Monochromatic MoKα radiation) equipped with Oxford cryosystem 700 plus at 100 K. Data collection and unit cell refinement for the data sets were done using the Bruker APPEX-II suite, data reduction and integration were performed using SAINTV 7.685A (Bruker AXS, 2009) and absorption corrections and scaling were done using SADABSV2008/1 (Bruker AXS, 2009). Single crystal X-ray diffraction data for **2.2** were collected using a Rigaku XtaLAB mini diffractometer equipped with Mercury375M CCD detector. The data were collected with graphite monochromatic MoKα radiation (λ = 0.71073 Å) at 100.0(2) K using scans. During the data collection, the detector distance was maintained at 50 mm (constant) and the detector was placed at 2θ = 29.85° (fixed) for all the data sets. The data collection and data reduction were done using Crystal Clear suite.[21] The crystal structures were solved by using either OLEX2[22] or WINGX package using SHELXS-97 and the structure were refined using SHELXL-97 2008.[23] All non hydrogen atoms were refined anisotropically. A disordered THF molecule found in the asymmetric unit of **2.1** could not be treated using standard commands available in SHELXL. The squeeze method was used to remove the contribution of this disordered molecule from the original *hkl* file. The resulting squeezed *hkl* file was used for further refinement.

2.4.4 Theoretical calculations

DFT calculations for geometry optimization of compound **2.1** were carried out at B3LYP/cc-pVDZ level of theory with Gaussian 09 package.[24] NBO charge analysis has been done at DFT optimized geometry.[25]

2.4.5 Synthetic procedure

Synthesis of [{N(Ph$_2$PN(2,4,6-Me$_3$C$_6$H$_2$))$_2$} B=S] (2.1): To a solution of **L$_1$**BH$_2$ (**1.11**) (1.98 g, 3.0 mmol) in toluene (50 mL) at 0 °C was added S_8 (192 mg, 6 mmol in 40 mL toluene). The initial clear solution became turbid and eventually yielded a precipitate over a period of 24 hours of stirring at room temperature. This precipitate was isolated by filtration and washed with cold toluene on the filter stick to afford a white solid. This was crystallized from THF at -10 ºC. Yield: (1.35 g, 65 %). M.p. 187-190 ºC. IR (ν cm^{-1}, KBr): 3046, 2929, 2875, 1479, 1436, 1261, 1216, 1202, 1151, 1112, 1096 (s, B=S), 1050, 1001, 945, 850, 828, 748, 724, 688, 551, 526. ^{1}H NMR (400 MHz, $CDCl_3$, δ ppm): 1.86 (s, *o*-C*H*$_3$, 12 H), 2.23 (s, *p*-C*H*$_3$, 6 H), 6.68 (s, 2,4,6-Me$_3$C$_6$*H*$_2$, 4 H), 7.36-7.31 (m, Ph, 8 H), 7.58-7.52 (m, Ph, 12 H) ppm; ^{13}C NMR (100 MHz, $CDCl_3$, δ ppm): 20.4 (s, *o*-*C*H$_3$), 21.1 (s, *p*-*C*H$_3$), 127.9 (d, $J_{C\text{-}P}$ = 13.7 Hz, aromatic), 129.8 (dd, $J_{C\text{-}P}$ = 123.5 & 3.0 Hz, aromatic), 129.9 (s, aromatic), 132.5 (s, aromatic), 132.8 (d, $J_{C\text{-}P}$ = 11.2 Hz, aromatic), 135.9 (s, aromatic), 136.5 (s, aromatic), 138.2 (s, aromatic) ppm; ^{31}P{^{1}H} NMR (162 MHz, $CDCl_3$, δ ppm): 23.5 ppm; ^{11}B NMR (128.4 MHz, $CDCl_3$): δ = 41.0 ppm (br). Mass spectrum (+ve ion, EI), *m/z* = calculated (found): 693.2675 (693.2664) [M–H]$^+$.

Synthesis of [{N(Ph$_2$PN(2,4,6-Me$_3$C$_6$H$_2$))$_2$} B=Se] (2.2): Toluene (40 mL) was added to a flask containing **L$_1$**BH$_2$ **(1.11)** (1.326 g, 2.0 mmol) and elemental Se (0.32 g, 4.0 mmol) at room temperature. Heating at 80 ºC for 2 hours gave light greenish solution that was filtered while hot and pure **2.2** was collected as pale-green powder from this solution at room temperature. The mother liquor gave crystals of **2.2** at 4 ºC. Yield: (1.02 g, 69 %). M.p. 185-187 ºC. IR (ν cm^{-1}, KBr): 3050, 2919, 2861, 1479, 1437, 1262, 1214, 1201, 1152,

1112, 1076 (s, B=Se), 998, 851, 827, 747, 725, 695, 563, 520. ^{1}H NMR (400 MHz, $CDCl_3$, δ ppm): 1.85 (s, *o*-CH_3, 12 H), 2.23 (s, *p*-CH_3, 6 H), 6.69 (s, 2,4,6-$Me_3C_6H_2$, 4 H), 7.31-7.36 (m, Ph, 8 H), 7.53-7.58 (m, Ph, 12 H) ppm. ^{13}C NMR (100 MHz, $CDCl_3$ δ ppm): 20.6 (s, *o*-CH_3), 21.1 (s, *p*-CH_3), 128.0 (d, $J_{C\text{-}P}$ = 13.6 Hz, aromatic), 128.8 (d, $J_{C\text{-}P}$ = 2.8 Hz, aromatic), 130.0 (s, aromatic), 132.6 (s, aromatic), 132.9 (d, $J_{C\text{-}P}$ = 11.1 Hz, aromatic), 136.2 (s, aromatic), 136.9 (b, aromatic), 138.3(s, aromatic) ppm. ^{31}P{^{1}H} NMR (162 MHz, $CDCl_3$ δ ppm):21.6 ppm. ^{11}B NMR (128.4 MHz, $CDCl_3$ δ ppm): 45.2 (br) ppm. Mass spectrum (+ve ion, EI), *m/z* = calculated (found): 742.2201 (742.3522) [M^+].

2.5 Crystallographic Data

Table 1. Crystal data and structure refinement details for compounds 2.1 and 2.2.

Compound	**2.1**	**2.2**
Empirical Formula	$C_{42}H_{42}N_3P_2BS$	$C_{42}H_{42}N_3P_2BSe$
Formula mass	693.60	740.49
T (K)	100 (2)	100 (2)
Crystal system	Orthorhombic	Tetragonal
Space Group	*Pnc*2	$I4_1/a$
a (Å)	16.3428(2)	37.392(3)
b (Å)	15.9077(1)	37.392(3)
c (Å)	15.6847(1)	10.8529(1)
α (°)	90	90
β (°)	90	90
γ (°)	90	90
V (Å)	4077.7(4)	15174(3)
Z	4	16
D_{calc} (g cm^{-3})	1.13	1.297
M (MoKα) (mm^{-1})	0.189	1.108
F (000)	1464	6144
θ range (°)	2.25-25.36	3.08-25.35
Index range	$-19 \le h \le 19$	$-45 \le h \le 45$
	$-19 \le k \le 19$	$-42 \le k \le 45$
	$-18 \le l \le 18$	$-13 \le l \le 12$
Reflections collected	63447	46219
Independent reflections	7460	6935
Data/restraints/parameters	7460/0/450	6935/0/448
R1, wR2 [$I > 2\sigma(I)$][a]	0.0341,0.0884	0.0632,0.1326
R1, wR2 (all data)	0.0378,0.0901	0.0822,0.1459
GOF	1.058	1.102
$\Delta\rho_{max, min}$/ e $Å^{-3}$	0.17,-0.17	0.60,-0.59

[a] $R1 = \Sigma||Fo| - |Fc||/\Sigma|Fo|$. $wR2 = [\Sigma w(|Fo^2| - |Fc^2|)^2/\Sigma w|Fo^2|^2]^{1/2}$

2.6 References

1. (a) Leung, W.-P.; Kan, K.-W.; Chong, K.-H. *Coord. Chem. Rev.* **2007**, *251*, 2253. (b) Tokitoh, N.; Okazaki, R. *Coord. Chem. Rev.* **2000**, *210*, 251.

2. Neculai, D.; Roesky, H. W.; Neculai, A. M.; Magull, J.; Walfort, B.; Stalke, D. *Angew. Chem., Int. Ed*. **2002**, *41*, 4294.

3. Franz, D.; Szilvasi, T.; Irran, E.; Inoue, S. *Nature Commun.* DOI: 10.1038/ncomms10037.

4. Tokitoh, N.; Ito, M.; Okazaki, R. *Organometallics* **1996,** *37*, 5145.

5.Vidovic, D.; Moore, J. A.; Jones, J. N.; Cowley, A. H. *J. Am. Chem. Soc*. **2005,** *127*, 4566.

6. Wang, Y.; Hu, H.; Zhang, J.; Cui, C. *Angew. Chem., Int. Ed*. **2011,** *50*, 2816.

7. Loh, Y. K.; Chong, C. C.; Ganguly, R.; Li, Y.; Vidovic, D.; Kinjo, R. *Chem. Commun.* **2014,** *50*, 8561.

8. Braunschweig, H.; Radacki, K.; Schneider, A. *Science* **2010,** *328*, 345.

9. Wang, H.; Zhang, J.; Hu, H.; Cui, C. *J. Am. Chem. Soc*. **2010,** *132*, 10998.

10. Franz, D.; Irran, E.; Inoue, S. *Angew. Chem., Int. Ed*. **2014,** *53*, 14264.

11. Boronic Acids: Preparation and Applications in Organic Synthesis, Medicine and Materials, Second Edition. (Ed.: D. G. Hall), Wiley-VCH Verlag GmbH & Co. KGaA, **2011**.

12. Westcott, S. A. *Angew. Chem., Int. Ed*. **2010,** *49*, 9045.

13. Siebert, W.; Gast, E.; Riegel F.; Schmidt, M. *J. Organomet. Chem*. **1975,** *90*, 13.

14. Binder, H.; Ziegler, A.; Ahlrichs, R.; Schiffer, H. *Chem. Ber.* **1987,** *120*, 1545.

15. Tokitoh, N.; Ito, M.; Okazaki, R. *Organometallics* **1995,** *14*, 4460.

16. Köster, R.; Seidel, G.; Yalpani, M. *Chem. Ber*. **1989,** *122*, 1815.

17. Davidson, G. in *Elements of Group III*, Specialist Periodical Reports, Inorganic Chemistry of the Main Group Elements, Vol. 4, (Sr. Reporter: C. C. Addison), The Chemical Society, London, **1977**, pp. 99-101.

18. (a) Franz, D.; Inoue, S. *Chem. Eur. J*. **2014,** *20*, 10645. (b) Jancik,V.; Peng,Y.; Roesky, H. W.; Li, J.; Neculai, D.; Neculai, A. M.; Herbst-Irmer, R. *J. Am. Chem. Soc*. **2003,** *125*, 1452. (c) González-Gallardo, S.; Jancik, V.; Cea-Olivares, R.; Toscano, R. A.; Moya-Cabrera, M. *Angew. Chem., Int. Ed*. **2007,** *46*, 2895.

19. Jaiswal, K.; Prashanth, B.; Bawari, D.; Singh, S. *Eur. J. Inorg. Chem*. **2015,** 2565.

20. Shriver, D. F.; Drezdon, M. A. The Manipulation of Air–Sensitive Compounds, 2nd Ed. McGraw–Hill, New York, USA, 1969.

21. CrystalClear 2.0, Rigaku Corporation, Tokyo, Japan.

22. Dolomanov, O. V.; Bourhis, L. J.; Gildea, R. J.; Howard, J. A. K.; Puschmann, H. *J. Appl. Cryst.* **2009**, *42*, 339.

23. SHELXS-97, Program for Structure Solution: Sheldrick, G. M. *Acta Crystallogr. Sect. A.* **2008**, *64*, 112.

24. Gaussian 09, Revision D.01, Frisch, M. J.; Trucks,G. W.; Schlegel, H. B.; Scuseria,G. E.; Robb, M. A.; Cheeseman, J. R.; Scalmani, Barone, G.; V.; Mennucci, B.; Petersson, G. A.; Nakatsuji, H.; Caricato,M.; Li,X.; Hratchian, H. P.; Izmaylov, A. F.; Bloino, J.; Zheng, G.; Sonnenberg, J. L.; Hada, M.; Ehara, M.; Toyota, K.; Fukuda, R.; Hasegawa, J.; Ishida, M.; Nakajima, T.; Honda, Y.; Kitao, O.; Nakai, H.; Vreven, T.; Montgomery, J. A.; Peralta, Jr. J. E.; Ogliaro, F.; Bearpark,M.; Heyd,J. J.; Brothers, E.; Kudin, K. N.; Staroverov, V. N.; Kobayashi, R.; Normand,J.; Raghavachari, K.; Rendell, A.; Burant, J. C.; Iyengar, Tomasi, S. S.; Cossi, J. M.; Rega, N.; Millam, J. M.; Klene, M.; Knox, J. E.; Cross, J. B.; Bakken, V.; Adamo, C.; Jaramillo, J.; Gomperts, R.; Stratmann, R. E.; Yazyev,O.; Austin, A. J.; Cammi, R.; Pomelli, C.; Ochterski, J. W.; Martin, R. L.; Morokuma, K.; Zakrzewski, V. G.; Voth, G. A.; Salvador, P.; Dannenberg, J. J.; Dapprich, S.; Daniels, A. D.; Farkas, Ö.; Foresman, J. B.; Ortiz, J. V.; Cioslowski, J.; Fox, D. J.; Gaussian, Inc., Wallingford CT, **2009**.

25. NBO Version 3.1, Glendening, E. D.; Reed, A. E.; Carpenter, J. E.; Weinhold, F.

Synthesis and Structural Investigation of Hydro- and Chloro-borenium Complexes Supported by Bis(phosphinoimine)amide

Chapter 3

Abstract: The reaction of a dihydroboron species complexed with a bis(phosphinimino)amide, $\mathbf{L_1}BH_2$ (**1.11**), ($\mathbf{L_1}$ = $[N(Ph_2PN(2,4,6\text{-}Me_3C_6H_2))_2]^-$) with 3 equivalents of $BH_2Cl{\cdot}SMe_2$ or one equivalent of BCl_3 affords the first stable monohydroborenium ion, $[\mathbf{L_1}BH]^+[HBCl_3]^-$ (**3.1**) that is stable without a weakly coordinating bulky anion. Compound **3.1** can also be prepared directly by refluxing $\mathbf{L_1}H$ with 3 equivalents of $BH_2Cl{\cdot}SMe_2$. Complex $\mathbf{L_1}BH_2$ (**1.11**), with 3 equivalents of BCl_3 undergoes metathesis reaction to afford $\mathbf{L_1}BCl_2$ and subsequent abstraction of chlorine to afford the chloroborenium ion, $[\mathbf{L_1}BCl]^+[BCl_4]^-$ (**3.2**). Additionally, a facile synthesis of hydroborenium complexes $[\mathbf{L_1}BH]^+[HB(C_6F_5)_3]^-$ (**3.3**) and $[\mathbf{L_1}BH]^+[B(C_6F_5)_4]^-$ (**3.4**) *via* hydride abstraction, using Lewis acid ($B(C_6F_5)_3$) or weakly coordinating ion pair $[Ph_3C][B(C_6F_5)_4]$, from $\mathbf{L_1}BH_2$ (**1.11**) has been carried out. Complex **3.4** easily forms an adduct with 4-dimethylaminopyridine (DMAP) $[\mathbf{L_1}BH(DMAP)]^+[B(C_6F_5)_4]^-$ (**3.5**) exhibiting its Lewis acid behaviour. All the complexes reported in this work have been isolated in good yields. Solid state structures of **3.1** and **3.2** have been investigated by single crystal X-ray structural analysis.

Fine Tuning of Lewis Acidity: The case of borenium hydride complexes derived from bis(phosphinimino)amide boron precursors, Jaiswal, K.; Prashanth, B.; Singh, S. *Chem. –Eur.J.;* 2016, *Accepted manuscript.*

3.1 Introduction

The chemistry of cations from *p*-block elements is very rich and has been dominated by cations derived from the elements of group 13, 14 and 15.[1] These cations have been classified either on the basis of same number of valence electrons or their similar geometry. On the basis of number of valence electrons these cation have been classified as onium-, enium- and inium-cations with 8, 6 and 4 valance electron (ve). Our interest is centered on enium-cations (6ve) of group 13 in general and borenium cations in particular that are three coordinated 6ve species. A brief introductory remark about isoelectronic enium-cations of group 14 and 15 is presented below before a detailed account of borenium cations from group 13 is presented.

Three coordinated 6ve cations from group 14 as enium-cations have general formula $[R_3E]^+$ (E = C, Si, Ge, Sn, Pb). Representative examples of $[R_3E]^+$ cations are presented below in Chart 1. This area of group 14 enium-cations has been reviewed from time to time and a plethora of examples are known. The first structurally characterized carbenium was tert-butyl cation with $[Sb_2F_{11}]^-$ as the counter anion.[2a] Later, another similar tert-butyl cation was characterized with $[HCB_{11}Cl_{11}]^-$ anion.[2b] In 2000, the first fluorinated carbocation $[(CH_3)_2CF]^+[AsF_6]^-$ was structurally characterized and later on highly substituted [(*m*-$CF_3C_6H_4)(C_6F_5)CF]^+$ derivative, containing the less coordinating $[As_2F_{11}]^-$ anion have shown only weak interaction between the ions.[2C] Some more examples of carbocation have been depicted in (Chart 1).[2d-f] Apart from carbocations, silylium ions are most electrophilic cations known so far and show very high Lewis acidity. To stabilize tricordinate silylium ions without appreciable any anion coordination, a highly bulky ligand is required (Chart 1).[3a-b] Just like silicon, enium ions of Ge, Sn an Pb also need high steric demand in order to shield their cationic centre as shown below (Chart 1).[3c]

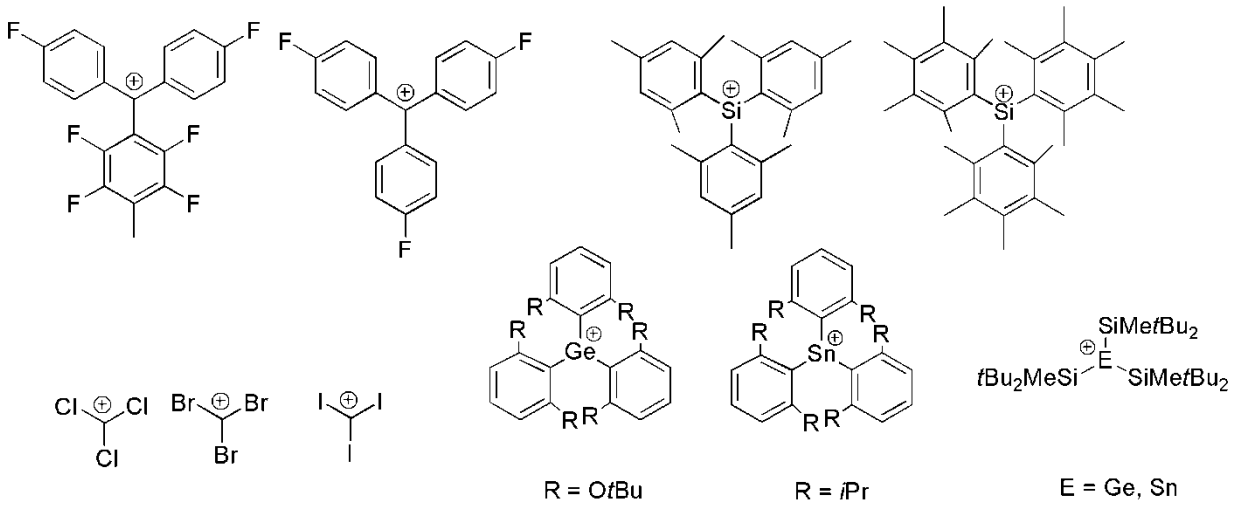

Chart 1. Representative examples of some structurally characterized enium-cations of group 14 elements.

Group 15 enium-cations have general formula $[R_2E]^+$ (E = P, As, Sb, Bi) where trivalent state of the central atom and a lone pair maintains an electron count of 6ve. In the past, the chemistry of highly reactive phosphenium ion $[P(R/Y)_2]$ was part of many studies. Stability of these phosphenium ions increases with the π–donor ability of the substituents and their Lewis acidity is enhanced by using substituents with a stronger electron withdrawing inductive effect for example in the series $[P(NH_2)_2]^+ < [PCl(NH_2)]^+ < [PCl_2]^+$.[4a] Similar to cations of other main group elements, use of weakly coordinating anions has been very instrumental in developing the chemistry of pnictogen cations as well.

Until 2012, there were no reports on structurally characterized phosphenium cations with at least one halogen and pseudohalogen substituent at the P center. The structures of $[PX(NR_2)]^+$ (R = TMS; X = Cl, N_3, NCO, NCS) and (R = *i*Pr; X = Cl, N_3)[4a] were determined by X-ray crystallography and $[GaCl_4]^-$ was the counter anion in all these cases. Some more examples of heavier pnictogen cations in +3 oxidation state have been shown below and these were typically synthesized through halide abstraction with Lewis acids (Chart 2).[4b-f]

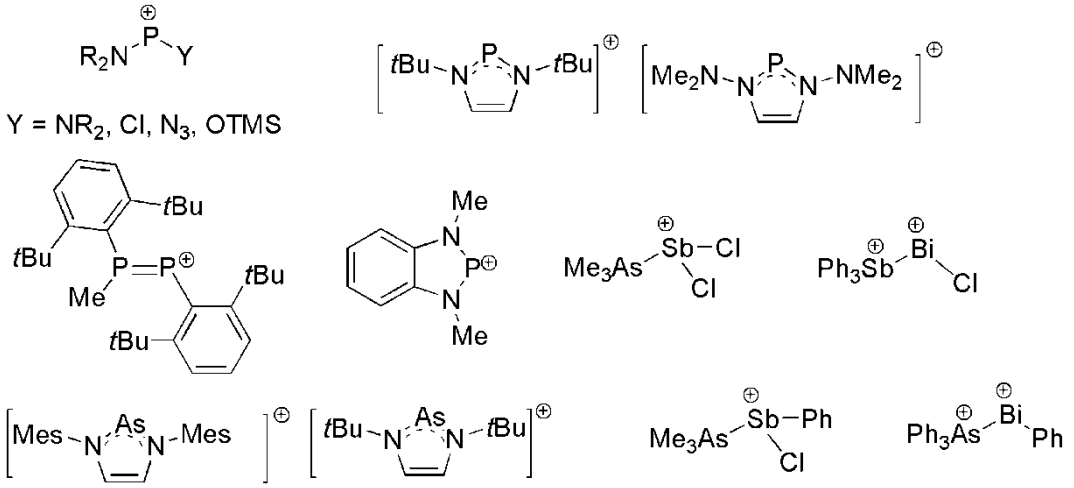

Chart 2. Representative examples of some pnictogen cations with formal oxidation state of +3.

The pnictonium cations (oxidation state +V) and the halopnictonium cations $[P_nX_4]^+$ with pnictogen atoms in oxidation state +V are not related to the present work and therefore have not been discussed.

Above discussion gives a brief account of 6 valence electron isoelectronic cations of the type $[R_3E]^+$ (E = group 14) and $[R_2E]^+$ (E = group 15 elements). The following section of the introduction will discuss another type of isoelectronic three coordinated cations $[R_2E{\leftarrow}L]^+$ from group 13 elements (Chart 3)[5a-h] with the focus on the lighter congener boron that forms borenium cations $[R_2B{\leftarrow}L]^+$.

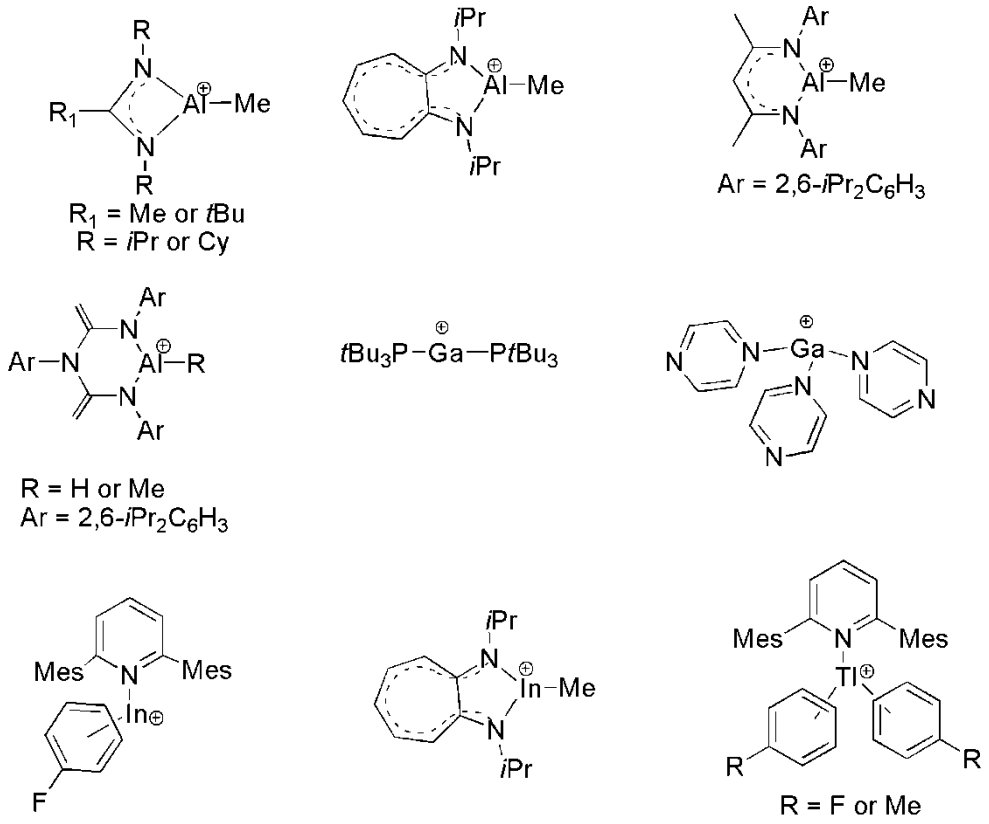

Chart 3. Representative examples of some heavier group 13 cations (based on Al, Ga, In and Tl).

Cationic species of boron are classified on the basis of the coordination number at the boron centre. The popular terms for two, three and four coordinate cationic boron centres

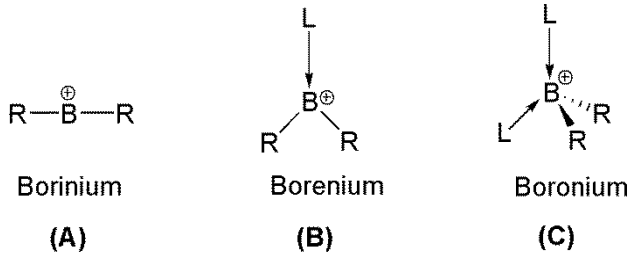

Chart 4. Types of cationic boron species.

are borinium, borenium and boronium cations, respectively. As shown in (Chart 4) borinium (A), borenium (B) and boronium cations (C) are two coordinated (with two σ bond), three coordinated (with two σ and one dative bond) and four coordinated (with two σ and two dative bonds) species, respectively. Our main focus lies in borenium cations however, borinium and boronium are also discussed briefly in this thesis. Despite a broader range of known related borenium species the discussion is restricted to hydro- and chloro-borenium species to make the contents simpler.

Borinium cations are (**A**, Chart 4) two coordinated and highly reactive species with extraordinary Lewis acidity due to the presence of two empty *p*-orbitals at boron. It is also notable that borinium cations are analogous to the 'two-coordinate carbon dications (R_2C^{2+})' but due to the high reactivity of these borinium cations (R_2B^+), only high vaccum mass spectrometry was speculated to be the best possible way to detect these cations in the gas phase by using low molecular weight boron species (R_3B; R = H, Me, Et, F, Cl, OR, SMe) (Scheme 1) until 1981.[6]

$$\overset{+}{G}H + BMe_3 \longrightarrow \overset{+}{B}Me_2 + CH_4 + G$$

$$G = CH_4,\ H_2S \text{ and } CH_2O$$

Scheme 1. Detection of short lived borinium species under vaccum using mass spectrometry.

The first attempt made by French and co-workers in 1958, revealed the detection of a borinium ion mixture by reacting diphenylchloroborane (Ph_2BCl) with $AlCl_3$ in nitrobenzene or phenyl ethyl ketone.[7a] However, later re-examination of the same reaction revealed the formation of borenium and boronium species instead of borinium.[7a,b] In 1982, Nöth and co-workers isolated the first structurally characterized borinium species *via* bromide abstraction from the amidoboron bromide (tmp)B(NMe_2)Br (tmp = 2,2,6,6-tetramethylpiperidino) by $AlBr_3$ to afford $[tmp{=}B{=}NMe_2]^+[AlBr_4]^-$, which showed the requirement of lone pair

donating substituents that can compensate for the electron deficiency on boron *via* dative π bond (**A,** Chart 5).[8] In 1986, Kölle and Nöth once again synthesized borinium species adapting the same strategy *via* abstraction of chloride using Lewis acid $AlCl_3$ (**B,** Chart 5).[9] Both the molecules were prepared by abstraction of halide from subsequent amidoboron halide and showed allene type arrangements with nearly linear geometry of the N–B–N moiety.

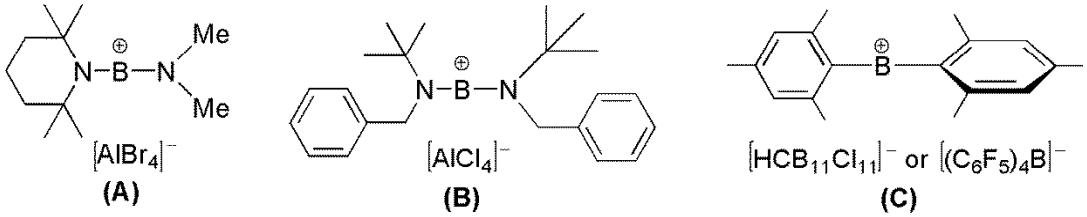

Chart 5. Some known examples of borinium species.

After a very long gap of activity in the area of synthetic cationic boron chemistry, in 2002 Stephan and co-workers reported the first borinium species bis(tri-tertbutylphosphinimide) $[(t\text{-}Bu_3PN)_2B]^+$ *via* hydride abstraction from $[(t\text{-}Bu_3PN)_2BH]$ using trityl salt $[Ph_3CB(C_6F_5)_4]$, which showed that the Lewis acidic boron centre, was sterically protected by the phosphinimide ligand and thus allowed the delocalization of positive charge over four adjacent pnictogen centres (Scheme 2).[10] Later in 2014, Fukushima and co-workers isolated another borinium species which was stabilized by the diarylated group instead of lone pair donating substituents (**C**, Chart 5).[11]

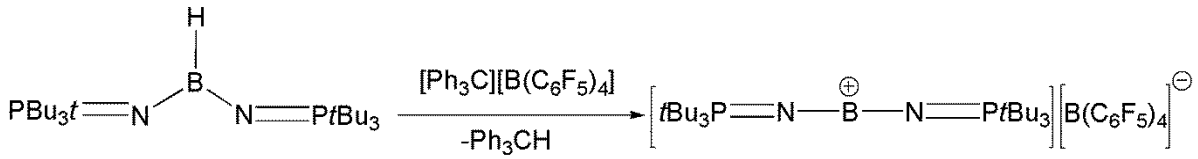

Scheme 2. Synthesis of bis(tri-*tert*-butylphosphinimide) borinium species.

Borenium species (**B**, chart 4) are three coordinated species having two σ and one dative bond (from a Lewis base) that occupy the third coordination site on boron, making them more stable than the borinium species. Lewis acidity of these borenium species are expected to be less in comparison to the borinium species but still better than its neutral form due to the combined effect of the net positive charge and empty *p*-orbital located at boron. Lewis acidity of borenium species spans a wide range, depending on the substituent attached to the boron atom. Lewis acidity of borenium species largely depends on the steric as well as the electronic availability of the vacant *p*-orbital on the boron atom. For example, highly substituted $[9\text{-BBN}\cdot NEt_3]^+[NTf_2]^-$ (**A,** Chart 6)[12] have additional hyperconjugative interaction with proximal σ-bonds compared to $[BH_2\cdot NMe_3]^+[I]^-$ (**B,** Chart 6),[13] however, the steric congestion in **A** discourage **A** form becoming an effective Lewis acid as compared to **B**. In this case the steric factor is dominating over the electronic factor. However, the relatively less hindered β-diketiminato derived borenium ion (**C,** Chart 6)[14] is unlikely to interfere sterically with an incoming nucleophile (such as a chloride ion) but still does not react to form tetra-coordinated boron adduct, because the boron *p*-orbital is strongly populated due to the involvement of the aromatic π-system, showing dominance of the electronic factors.

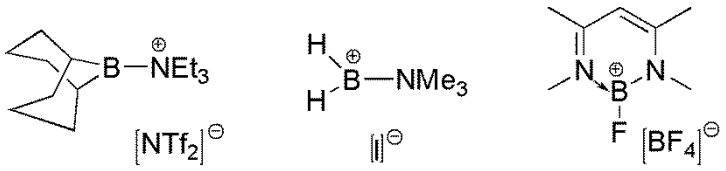

(A) **(B)** **(C)**

Chart 6. Evaluation of steric *vs* electronic factors in controlling Lewis acid of borenium species.

The three examples that were published prior to 1985 were discussed in a review by Nöth[15a] and a more detailed review published by Piers and co-worker showed an increase in

the number of reports on these cations,[15b] focusing mainly on the synthetic methods for borenium complexes. One of the two most common methods of borenium ion generation is Lewis acid mediated halide or hydride abstraction from four coordinated neutral boron complexes (Scheme 3).[16]

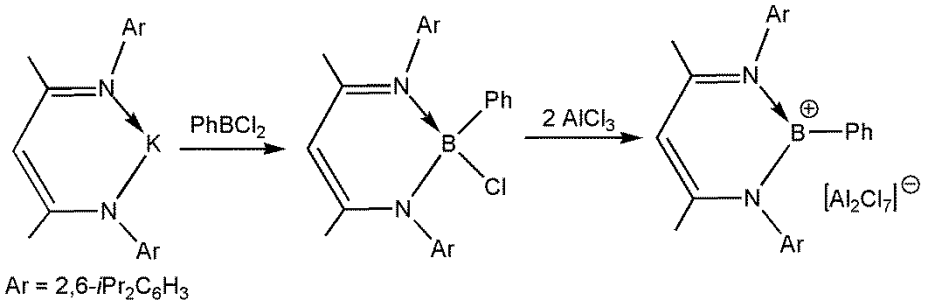

Scheme 3. Lewis acid mediated halide abstraction resulting in borenium species.

In 1987, Jutzi and co-workers reported borenium species (**A** and **B,** Chart 7)[17] from the reaction of dichloro(η^1–pentamethylcyclopentadienyl)borane with bulky nitrogen donor based acridine and phenanthridine. In 1991, Kuhn and co-workers also reported borenium species by the abstraction of a fluoride ion *via* Lewis acidic $BF_3{\cdot}OEt_2$, supported by a β–diketiminato ligand (**C,** Chart 7).[14] A few reported examples of borenium cations[17,14,32,23d] **A** to **F** have been shown below (Chart 7).

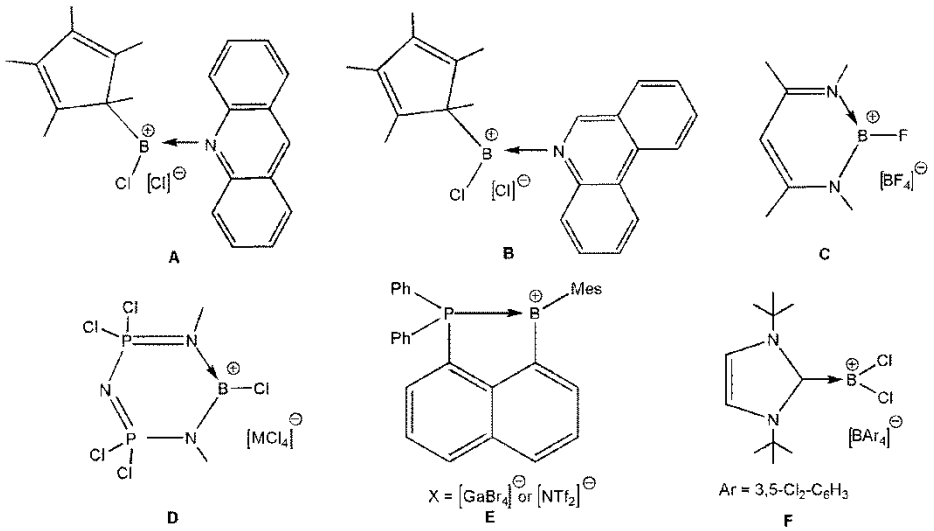

Chart 7. Examples of borenium cations.

Applying the same protocol in 2008, Piers and co-workers synthesized the monohydroborenium cation based on the dipyromethane ligand $[(BODIPY)BH]^+$ stabilized by a bulky weakly coordinating anion $[B(C_6F_5)_4]^-$ (Scheme 4).[18] In the same manner, Gabbaï and co-workers reported the dimesitylborenium cation $[Mes_2B{\cdot}DMAP]^+$ $[OTf]^-$ *via* reaction of dimesitylfluoroborane with trimethylsilyl triflate and DMAP.[19]

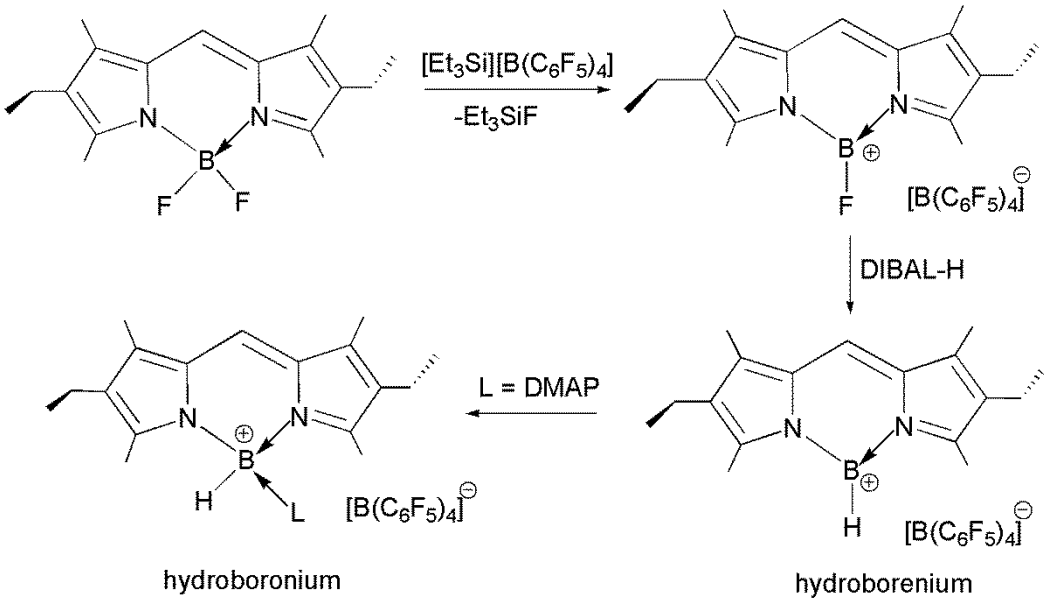

Scheme 4. Synthesis of monohydroborenium cation $[(BODIPY)BH]^+$, based on dipyromethane ligand.

In a similar process, Vedejs and co-workers prepared a reactive borenium ion based on 2,3-benzazaborolidine *via* hydride abstraction, using trityl salt $[Ph_3C][BF_4]$.[20] A variety of borenium species have been prepared in the last decade exploiting tertiary amines,[21] various pyridines[21g, 22] or N-heterocyclic carbenes (NHCs)[22a,23] for stabilization and have been used for hydrogenation,[23h] borylation,[21b-e,21c,24] hydrosilylation,[21g,25] haloborylation,[22d] hydroboration[21f,23g,26] and Diels-Alder transformation[27] of a diverse range of substituents. In this area Vedejs and co-worker demonstrated the ability of borenium species, derived from hindered amine borane complexes, to undergo intramolecular aliphatic C–H borylation.[28] In the same manner, Ingleson and co-workers demonstrated the ability of borenium ions to

direct arene borylation by using of catecholboron chloride as the starting material.[21c] The same group also demonstrated the ability of borenium ions, $[X_2BL]^+$ (X = halide, L = 2-DMAP) in haloboration of internal alkynes to generate tetrasubstituted alkenes.[22d] The same group also successfully demonstrated the hydride ion affinity of borenium cations to activate H_2 in frustrated Lewis pairs[29] and then usage of $[(acridine)BCl_2]^+$ as a strong boron- and carbon-based Lewis acid.[30] Recently, the same group once again showed the ability of borenium species for complete reductive cleavage of CO molecules using $[(H_2B(NEt_3))_2(\mu\text{–}H)]^+$.[31] Similarly, Stephan and co-workers showed the hydride ion affinity of borenium species derived from $[(I\textit{i}Pr_2)(BC_8H_{14})][B(C_6F_5)_4]$ [$I\textit{i}Pr_2 = C_3H_2(N\textit{i}Pr)_2$], to activate H_2 in the presence of $t\text{Bu}_3\text{P}$.[23h] The same borenium species also acts as a metal free catalyst for hydrogenation of imines and enamines at room temperature.

Boronium species (**C**, Chart 4) are four coordinate boron species having two σ and two dative bonds (**L**) offering them more stability, less reactivity and less Lewis acidic character than the borinium and boronium species. A few examples of boronium cations[17,22b,33,12] **A** to **E** are presented below (Chart 8).

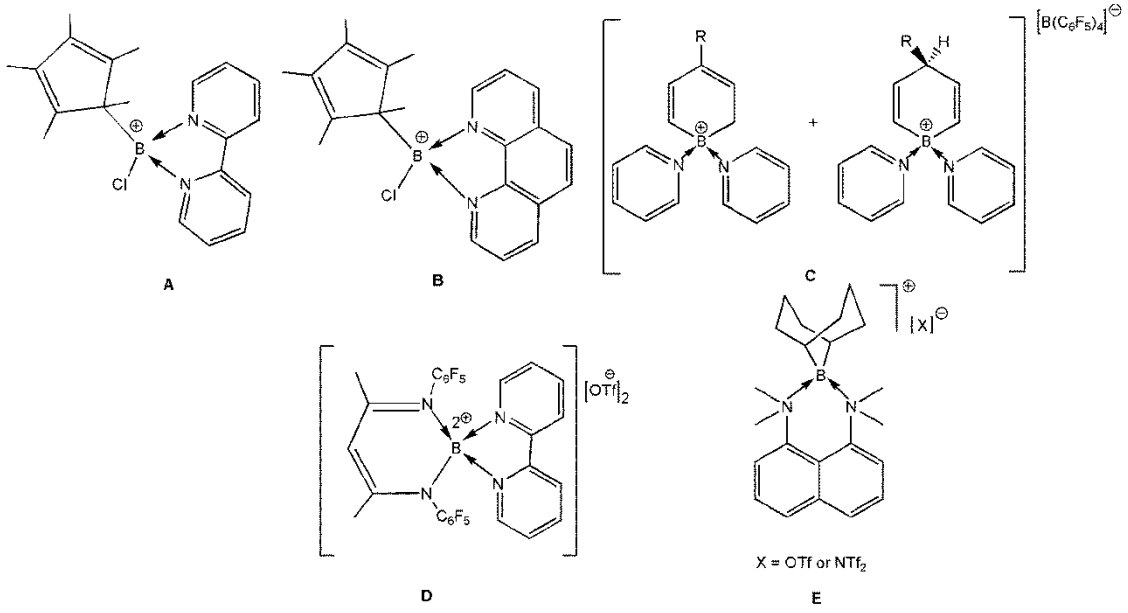

Chart 8. Examples of boronium cations.

Among all types of boron cation discussed above the four coordinate boron cations are more prevalent in literature in comparison to two coordinated and three coordinated boron cations. However, the chemistry of three coordinate boron species has attracted more attention due to a balance of ease of synthesis, stability, reactivity and Lewis acidity in comparison to difficult synthetic routes to be adopted for borinium ions due to their high reactivity whereas, the high coordination number of boronium form makes them easy to prepare but compromise their Lewis acidity.

Recently, our group reported on the synthesis and characterization of a dihydroboron species, $\mathbf{L_1}BH_2$ (**1.11**) complex with a bulky monoanionic bis(phosphinimino)amide ligand ($\mathbf{L_1}$ = $[N(Ph_2PN(2,4,6\text{-}Me_3C_6H_2))_2]^-$).[34] Here, we were interested in preparing a series of borenium species by using two different methods: (**I**) hydride-halide exchange followed by halide abstraction and (**II**) Lewis acid mediated hydride abstraction.

3.2 Results and Discussion

Reaction of $\mathbf{L_1}BH_2$ (**1.11**) with three equivalents of $BH_2Cl{\cdot}SMe_2$ in toluene at 60 °C (*Path 1*, Scheme 5) results in the formation of the hydroborenium species $[\mathbf{L_1}BH]^+[HBCl_3]^-$ (**3.1**). Compound **3.1** has also been conveniently prepared by other alternative routes as shown in Scheme 5; *Path 2* involving the reaction of **1.11** with one equivalent of BCl_3 and *Path 3* by reacting $\mathbf{L_1}H$ with three equivalents of $BH_2Cl{\cdot}SMe_2$ at 110 °C. While the course of reaction is straight forward for *Path 2* the reaction through *Path 1* proceeds *via* hydride abstraction by the Lewis acid, BCl_3 formed *in-situ*, and BH_3 as the other possible product whereas *Path 3* involves hydrogen evolution to first give $\mathbf{L_1}BHCl$[35] which subsequently reacts with the second equivalent of $BH_2Cl{\cdot}SMe_2$ to generate $BH_2Cl_2^-$ that undergoes metathesis with the third equivalent of $BH_2Cl{\cdot}SMe_2$ to generate BH_3 and $BHCl_3^-$ counter anion. To the best of our knowledge, compound **3.1** is the first example of a stable hydroborenium ion, containing a simple anion $[BHCl_3]^-$, that does not require a bulky weakly coordinating anion for

stability.[15,10,11,15,36] The only hydroborenium cation reported in the literature is dipyrromethene

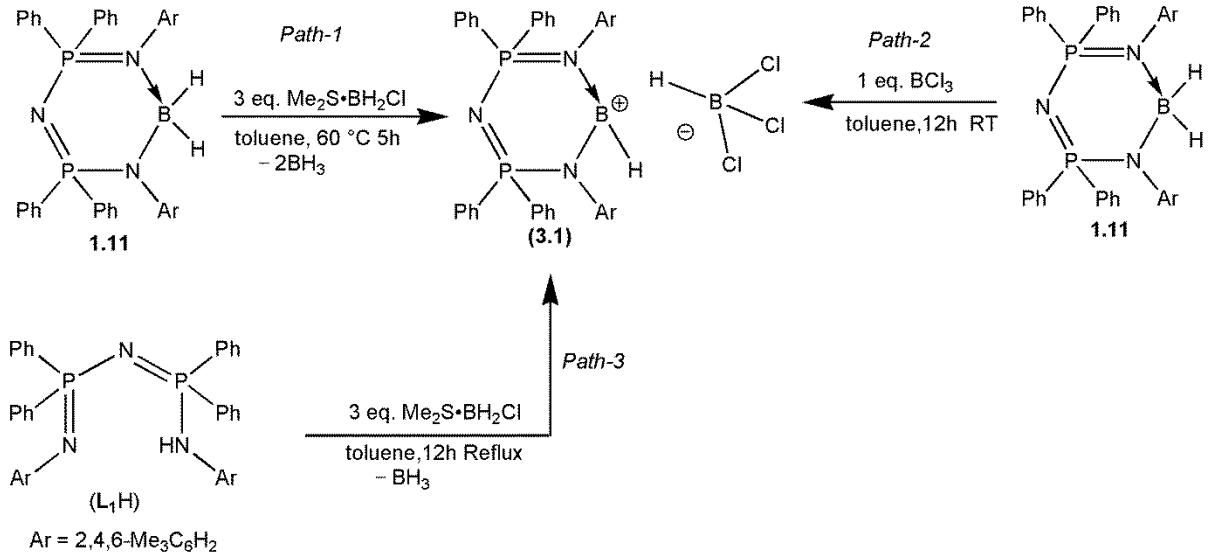

Scheme 5: Synthesis of a hydroborenium cation, $[\mathbf{L_1}BH]^+[HBCl_3]^-$ (**3.1**).

complexed with a substituted boron atom, $[(BODIPY)BH]^+$ that is stabilized by a bulky weakly coordinating anion, $[B(C_6F_5)_4]^-$.[17] Other notable hydrido boron cations include the hexaphenylcarbodiphosphorane stabilized dihydrido borenium cation, $[(Ph_3P)_2CBH_2]^+[HB(C_6F_5)_3]^-$ reported by Alcarazo and coworkers[37] and the work of Chen et al. on three coordinate $[BH_4]^-$, $[I]^-$, and $[OTf]^-$ salts of dicationic hydrido boron complexes stabilized by carbodicarbene.[38] Compound **3.1** was characterized by spectroscopic, spectrometric, and single crystal X-ray techniques. The HRMS investigations under +ve ion mode of **3.1** revealed the signal at *m/z* = 662.3032 (calculated *m/z* = 662.3043) as the base peak corresponding to the cationic moiety $[M\text{-}BHCl_3]^+$. The IR spectrum of **3.1** showed the B–H stretch at 2545 and 2470 cm^{-1}.[34] In the ^1H NMR spectrum of complex **3.1** the B*H* resonance appeared as a broad signal around 4.27 ppm and *o*-C*H*$_3$ and *p*-C*H*$_3$ were observed at 1.67 and 2.29 ppm, respectively. A downfield shift in the $^{31}P\{^1H\}$ NMR spectrum of **3.1** (22.7 ppm) was observed when compared to $\mathbf{L_1}BH_2$ (19.2 ppm).[34] The ^{11}B NMR spectrum of **3.1** showed a

sharp doublet at 3.30 ppm with $^{1}J_{B\text{-}H}$ of 164.3 Hz, this signal can be attributed to the anionic moiety of **3.1**.[39] The signal for B atom of the cationic moiety is not detected perhaps due to the low local symmetry around this boron atom.

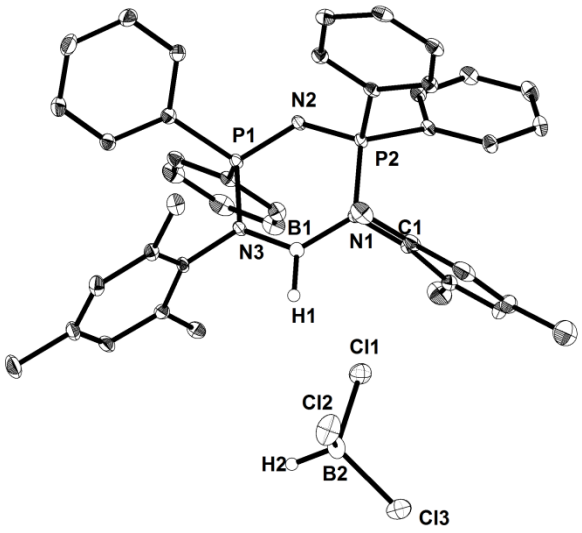

Figure. 1 Solid state structure of $[\mathbf{L_1}BH]^{+}$ **[**$BHCl_3]^{-}$ (**3.1**). All hydrogen atoms except on boron atoms have been deleted for clarity. Thermal ellipsoids have been drawn at 30% probability. Selected bond lengths [Å] and bond angles [°]: B(1)–H(1) 1.110(2), B(1)–N(1) 1.432(5), B(1)–N(3) 1.437(1), N(1)–P(2) 1.680(2), N(2)–P(1) 1.580(5), N(2)–P(2) 1.579(1), N(3)–P(1) 1.679(4), P(2)–C(1) 1.797(2), P(2)–C(16) 1.796(2), P(1)–C(22) 1.798(2), P(1)–C(28) 1.788(2), N(3)–C(34) 1.460(2), N(1)–C(1) 1.457(2), B(2)–H(2) 1.070(3), B(2)–Cl(1) 1.866(2), B(2)–Cl(2) 1.839(3), B(2)–Cl(3) 1.866(2), N(1)–B(1)–N(3) 125.8(1), N(1)–B(1)–H(1) 118.5(1), N(3)–B(1)–H(1) 115.6(1), N(2)–P(2)–N(1) 107.8(1), N(2)–P(1)–N(3) 108.3(1), C(1)–N(1)–B(1) 116.68(1), C(1)–N(1)–P(2) 120.26(1), C(12)–P(2)–C(16) 105.87(1), C(12)–P(2)–N(1) 112.33(1), C(16)–P(2)–N(1) 109.95(1), C(33)–N(3)–B(1) 116.61(1), C(33)–N(3)–P(1) 121.13(1), C(27)–P(1)–C(22) 107.52(1), C(22)–P(1)–N(3) 104.94(1), C(27)–P(1)–N(3) 110.15(1), C(22)–P(1)–N(2) 110.66(1), C(27)–P(1)–N(2) 110.76(1), H(2)–B(2)–Cl(1) 111.4(1), H(2)–B(2)–Cl(2) 107.5(1), H(2)–B(2)–Cl(3) 110.8(1), Cl(1)–B(2)–Cl(2) 109.1(1), Cl(1)–B(2)–Cl(3) 109.2(1), Cl(2)–B(2)–Cl(3) 108.7(1).

Single crystals of **3.1** suitable for X-ray structural analysis were grown from toluene. Compound **3.1** crystallizes in the monoclinic crystal system with $P2_1/n$ space group (Figure 1). In the solid state ion pairs of a molecule of **3.1** are well separated, probably due to the bulky nature of the cationic moiety, and the molecules of **3.1** are also discrete showing no intermolecular interactions. The coordination environment around cationic boron is distorted trigonal planar whereas the anionic part exhibits a distorted tetrahedral geometry. The central N_3P_2B ring in **3.1** slightly deviates from planarity. The B-H bond length (1.110(2) Å) in the cationic part of **1** is longer than the B-H distance in its counter anion (1.070(3) Å) and that reported in the BODIPY derived borenium ion (0.950 Å).[17] The B-N distances in **3.1** (1.432(5) and 1.437(1) Å) are slightly shorter than that in its precursor $\mathbf{L_1}BH_2$ (1.588(5) and 1.615(5) Å). The N(1)-B(1)-N(3) bond angle in **3.1** (125.75(1)°) is wider than the N-B-N bond angle in its precursor $\mathbf{L_1}BH_2$ (110.60(2)°).[34]

To investigate the reaction chemistry of the newly synthesized hydroborenium species, $[\mathbf{L_1}BH]^+ [BHCl_3]^-$ (**3.1**) oxidative addition of sulfur into the B-H bonds was attempted with an anticipation to isolate the cationic mercaptoborane compound, $[\mathbf{L_1}BSH]^+ [BHCl_3]^-$. The reaction of sulfur with compound **3.1** does not progress at room temperature however, under reflux conditions in toluene the insertion of sulfur presumably occurs converting the hydride into a thiol function which due to the presence of $HBCl_3^-$ anion releases HCl and formation of $[\mathbf{L_1}H_2]^+Cl^-$ as the only isolable soluble product. Use of Et_3N or lutidine as bases in the reaction lead to the isolation a mixture of ammonium salts and $[\mathbf{L_1}H_2]^+Cl^-$. In the ^1H NMR spectrum of complex $[\mathbf{L_1}H_2]^+Cl^-$ the N*H* resonance appeared as a broad signal around 8.66 ppm and *o*-CH_3 and *p*-CH_3 were observed at 2.03 and 2.07 ppm, respectively. A downfield shift in the $^{31}P\{^1H\}$ NMR spectrum of $[\mathbf{L_1}H_2]^+Cl^-$ (16.0 ppm) was observed when compared to $\mathbf{L_1}H$ (2.3).

The reaction of $\mathbf{L_1}BH_2$ with 3 equivalent of BCl_3 in toluene (Scheme 6) under reflux gave a chloroborenium species, $[\mathbf{L_1}BCl]^+[BCl_4]^-$ (**3.2**). The synthetic approach to prepare **3.2** is quite

unique in the sense that it involves the exchange of hydrides with chlorides and subsequent abstraction of one of the chloride by BCl_3 to afford the chloroborenium ion. Generation of the borenium cation by halide or hydride abstraction is known[15] but metathesis of B-H to B-Cl and subsequent abstraction of chlorine in a single reaction/in situ is reported /tested for the first time. The overall course of the reaction is metathesis of $\mathbf{L_1}BH_2$ to $\mathbf{L_1}BCl_2$ and abstraction of chloride from $\mathbf{L_1}BCl_2$ by the third equivalent of BCl_3 leading to the formation of $[\mathbf{L_1}BCl]^+$ $[BCl_4]^-$ ion pair. Lewis acidity of BCl_3 has been estimated to be comparable to that of $B(C_6F_5)_3$ however, the later has also been exploited as a precursor to weakly coordinating anion $[XB(C_6F_5)_3]^-$ formed as a consequence of hydride abstraction by it (X = H or C_6F_5). In the present case we believe that the strong donor characteristic of the bis(phosphinimino)amide ligand offers necessary stability to the resulting boron cation and at the same time enables/encourages BCl_3 to abstract the chloride from $\mathbf{L_1}BCl_2$ to form the $[BCl_4]^-$ counter ion. This methodology in principle eliminates the necessity of a weakly coordinating anions however, as expected this ligand also supports the borenium cations generated using $B(C_6F_5)_3$ or weakly coordinating anion $[B(C_6F_5)_4]^-$.

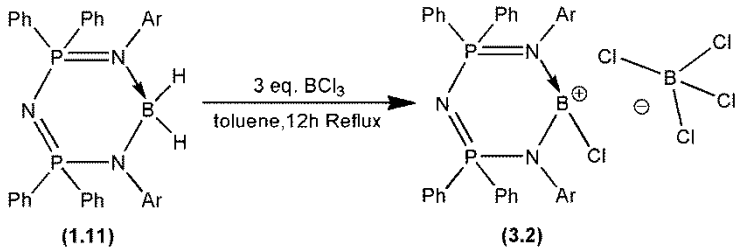

Scheme 6. Synthesis of chloroborenium complex, $[\mathbf{L_1}BCl]^+[BCl_4]^-$ (**3.2**).

Compound **3.2** was characterized by spectroscopic, spectrometric and single crystal X-ray techniques. The HRMS investigations under +ve ion mode of **3.2** revealed the signal at *m/z* 696.2628 (calculated *m/z* = 696.2643) that can be assigned to the cation $[\mathbf{L_1}BCl]^+$ or $[M\text{-}BCl_4]^+$.

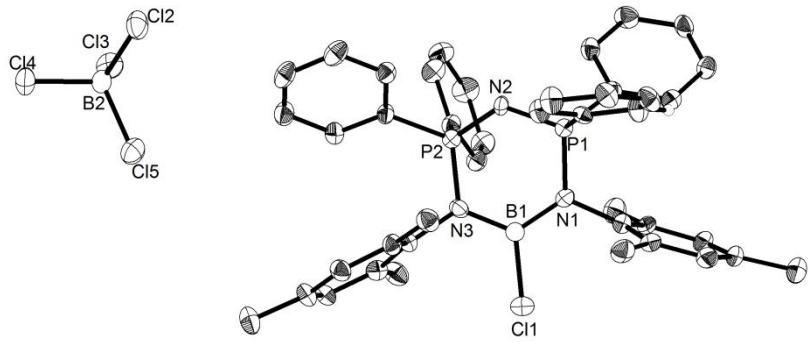

Figure 2. Solid state structure of $[LBCl]^{+}[BCl_4]^{-}$ (**3.2**). All hydrogen atoms have been deleted for clarity. Thermal ellipsoids have been drawn at 30% probability. Selected bond lengths (Å) and bond angles (°): B(1)–Cl(1) 1.782(1), B(1)–N(1) 1.462(1), B(1)–N(3) 1.453(1), N(1)–P(1) 1.701(2), N(2)–P(1) 1.613(7), N(2)–P(2) 1.611(6), N(3)–P(2) 1.717(8), P(2)–C(22) 1.830(1), P(2)–C(28) 1.834(1), P(1)–C(10) 1.814(9), P(1)–C(16) 1.826(8), N(3)–C(34) 1.519(9), N(1)–C(1) 1.503(1), B(2)–Cl(2) 1.876(1), B(2)–Cl(3) 1.884(1), B(2)–Cl(4) 1.887(1), B(2)–Cl(5) 1.870(2), N(1)–B(1)–N(3) 124.01(7), N(1)–B(1)–Cl(1) 118.14(6), N(3)–B(1)–Cl(1) 117.86(6), N(2)–P(1)–N(1) 109.48(3), N(2)–P(2)–N(3) 108.22(3), C(22)–P(2)–C(28) 108.67(3), C(28)–P(2)–N(2) 106.91(3), C(22)–P(2)–N(2) 111.78(3), C(34)–N(3)–B(1) 121.30(6), C(34)–N(3)–P(2) 115.13(4), C(10)–P(1)–C(16) 107.84(3), C(10)–P(1)–N(2) 108.20(3), C(16)–P(1)–N(2) 111.02(3), C(16)–P(1)–N(1) 109.60(3), C(10)–P(1)–N(1) 110.67(3), C(1)–N(1)–B(1) 121.06(6), C(1)–N(1)–P(1) 119.24(4), Cl(2)–B(2)–Cl(3) 109.04(5), Cl(2)–B(2)–Cl(4) 108.64(5), Cl(2)–B(2)–Cl(5) 110.35(5), Cl(3)–B(2)–Cl(4) 108.94(5).

The ^{1}H NMR spectrum of complex **3.2** showed *o*-CH_3 and *p*-CH_3 at 1.68 and 2.34 ppm, respectively and other peaks are consistent with the backbone. A downfield shift in the $^{31}P\{^{1}H\}$ NMR signal of **3.2** (26.26 ppm) was observed when compared to $\mathbf{L_1}BH_2$ (**1.11)** (19.2 ppm).[34] The ^{11}B NMR spectrum of **3.2** showed a sharp singlet at 7.14 ppm, the signal is most likely due to $[BCl_4]^{-}$. The cationic boron centre probably gives a signal too broad to be observed.

Single crystals of **3.2** suitable for X-ray structural analysis were grown from THF. Compound **3.2** crystallizes in the monoclinic crystal system with $P2_1/n$ space group (Figure 2). The coordination environment around boron is distorted trigonal planar whereas the anion $[BCl_4]^-$ as expected exhibits a distorted tetrahedral geometry. The central N_3P_2B ring in **3.2** slightly deviates from planarity. The B-Cl bond length (1.782(2) Å) in the cationic part of **3.2** is shorter than the B-Cl distance in its counter anion (1.876(1) Å) and comparable to that reported in β-diketiminato derived borenium ion $[(HC(CMe_2)_2(NC_6F_5)_2)BCl]^+[AlCl_4]^-$[40] and boratophosphazene derived borenium ion $[(N(PCl_2)_2(NCH_3)_2)BCl]^+[AlCl_4]^-$[32a] (1.740 and 1.752 Å), respectively. The B-N distances in **3.2** (1.445(2) and 1.432(3) Å) are slightly shorter than that in its precursor (1.588(5) and 1.615(5) Å). The N-B-N bond angle in **3.2** (123.9(3)°) is comparable to that reported in boratophosphazene derived borenium ion $[(N(PCl_2)_2(NCH_3)_2)BCl]^+[AlCl_4]^-$ (124.0°) and wider than the N-B-N bond angle in β-diketiminato derived borenium ion $[(HC(CMe_2)_2(NC_6F_5)_2)BCl]^+[AlCl_4]^-$ (117.2°).

The reaction of $\mathbf{L_1}BH_2$ (**1.11**) with the Lewis acids $B(C_6F_5)_3$ or $[Ph_3C][B(C_6F_5)_4]$ in toluene (Scheme 7) proceed under hydride abstraction to yield the corresponding hydroborenium species $[\mathbf{L_1}BH]^+[A]^-$ [A = $HB(C_6F_5)_3$ (**3.3**), $B(C_6F_5)_4$ (**3.4**)].

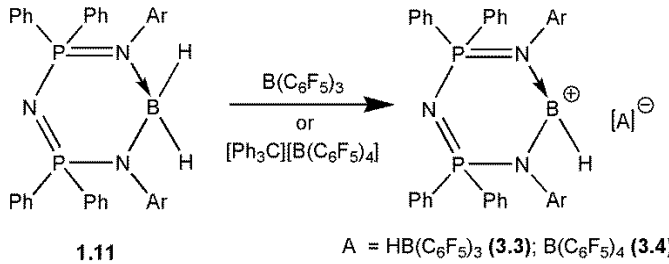

Scheme 7. Synthesis of hydroborenium complexes $[\mathbf{L_1}BH]^+[HB(C_6F_5)_3]^-$ (**3.3**) and $[\mathbf{L_1}BH]^+[B(C_6F_5)_4]^-$ (**3.4**).

Compounds **3.3** and **3.4** showed good solubility in polar solvents and separated as liquid clathrate from benzene and toluene, addition of *n*-hexane to these clathrates afforded off-white

solids. Compounds **3.3** and **3.4** were characterized by spectroscopic and spectrometric techniques. Due to clathrate nature of these molecules, single crystals could not be grown and limited their characterization by X-ray technique. The ^{1}H NMR spectrum of the hydroborenium species **3.3** and **3.4** showed a broad peak at 4.38 ppm for hydride and showed downfield shift as compared to its precursor **1.11**(19.2 ppm). The ^{1}H NMR resonance signals for *o*-CH_3 and *p*-CH_3 groups on mesityl substituents of the ligand for **3.3** (1.75 and 1.72 ppm) and for **3.4** (2.33 and 2.32 ppm) were in accordance with the ligand backbone and composition of these molecules. The ^{31}P{^{1}H} spectra of **3.3** and **3.4** showed sharp single resonances at 22.7 and 22.6 ppm respectively, which were downfield shifted as compared to their precursor **1.11** (19.2 ppm).[34] The ^{11}B NMR spectrum of **3.3** showed a sharp doublet at -24.4 ppm with $^{1}J_{B\text{-}H}$ of 88 Hz, this signal can be attributed to the anionic moiety $[HB(C_6F_5)_3]^-$ of **3.3**.[41] The ^{11}B NMR spectrum of **3.4** showed a sharp singlet at -16.6, this signal can be attributed to the anionic moiety $[B(C_6F_5)_4]^-$ of **3.4**.[42] The signal for B atom of the cationic moiety in both compounds was not detected perhaps due to the low local symmetry around the cationic boron centre. The ^{19}F NMR spectrum of **3.3** showed a doublet at −132.2 ppm with $^{3}J_{F\text{-}F}$ = 18.8 Hz, a triplet at −164.4 ppm with $^{3}J_{F\text{-}F}$ = 20.3 Hz, and a multiplet at −166.9 ppm as expected for perfluorinated phenyl rings. The ^{19}F NMR spectrum of **3.4** showed a broad peak at −132.2 ppm, a triplet at −162.2 ppm with $^{3}J_{F\text{-}F}$ = 20.7 Hz, and a multiplet at −166.8 ppm as expected for perfluorinated phenyl rings. The ^{1}H NMR, aliphatic region of ^{13}C NMR and ^{31}P{^{1}H} spectrum of **3.4** were identical to that of **3.3**. These counter ions independent chemical shifts for the cationic parts of **3.3** and **3.4**, with same cation, suggested well separated counter ions for these molecules. Moreover, the ^{19}F and ^{11}B NMR features of **3.4** correlated well with that of $[Ph_3C][B(C_6F_5)_4]$[42] again emphasizing the presence of well separated counter ions in **3.3** and **3.4**. The EI mass spectrum (+ve ion) of **3.3** and **3.4** showed the cationic fragment, $[M\text{-}HB(C_6F_5)_3]^+$ and $[M\text{-}B(C_6F_5)_4]^+$ as the base peak at *m/z* = 662.3025 and 662.3021, respectively. The IR spectrum of

3.3 showed the B-H stretching bands at 2558 and 2254 cm^{-1} for the cationic and anionic moieties. Similarly, the IR spectrum of **3.4** revealed the B-H stretch for the cationic moiety at 2549 cm^{-1}.

The reaction of $[\mathbf{L_1}BH]^+[B(C_6F_5)_4]^-$ (**3.4**) with DMAP in toluene (Scheme 8) formed the expected adduct, yielding the corresponding hydroboronium species $[\mathbf{L_1}BH{\cdot}DMAP]^+[B(C_6F_5)_4]^-$.

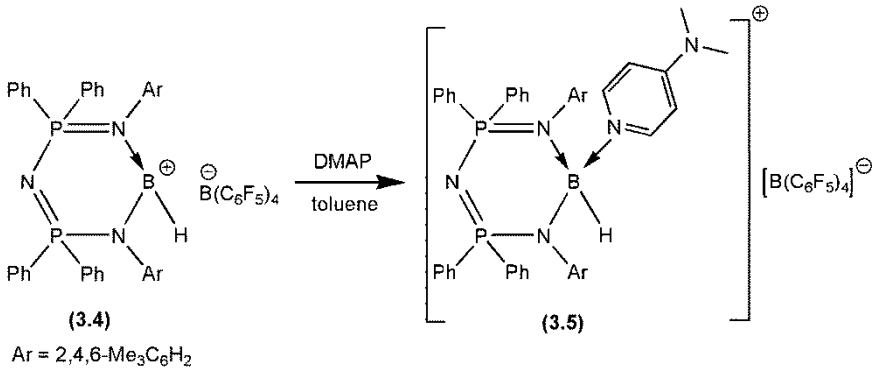

Scheme 8. Synthesis of a hydroboronium complex $[\mathbf{L_1}BH{\cdot}DMAP]^+[B(C_6F_5)_4]^-$ (**3.5**).

The ^1H NMR spectrum of the hydroboronium species **3.5** showed a broad peak at 4.07 ppm for hydride and showed upfield shift (of about 0.3 ppm) as compared to its precursor **3.4**. The ^1H NMR resonance signals for **3.5** showed two *o*-CH_3 peaks, the one at 1.99 ppm for (3H) and the second appeared as broad singlet from 1.39-1.92 ppm (9H) and the corrosponding *p*-CH_3 were seen at 2.22 ppm respectively, and the rest of the signals were in accordance with the ligand backbone and composition. The ^1H NMR resonance signals for DMAP in **3.5** appeared at 2.97 ppm. The $^{31}P\{^1H\}$ spectrum of **3.5** showed up as a sharp single resonance at 21.9, which is upfield shifted as compared to its precursor **3.4** (22.6 ppm).[23] The ^{11}B NMR spectrum of **3.5** showed a sharp singlet at -16.6, this signal can be attributed to the anionic moiety $[B(C_6F_5)_4]^-$ of **3.5**.[42] The signal for B atom of the cationic moiety in **3.5** was not detected. The ^{19}F NMR spectrum of **3.5** showed a broad peak at −132.5 ppm, a triplet at −163.1 ppm with $^3J_{F\text{-}F}$ = 20.7 Hz, and a multiplet at −166.8 ppm as expected for perfluorinated phenyl rings. The EI mass spectrum (+ve ion) of **3.5** showed the cationic

fragment, $[M+H -B(C_6F_5)_4]^+$ as the base peak at *m/z* = 785.3979. The IR spectrum of **3.5** showed the B-H strectching bands at 2430 cm^{-1}. From the above data i.e NMR and IR, we can clearly confirm that the hydroborenium species in **3.4** is Lewis acidic in nature to coordinate with DMAP to form a hydroboronium compound.

3.3 Conclusion

In conclusion we have demonstrated the synthesis of hydroborenium and chloroborenium species with or without bulky anion supported by bis(phosphinimino)amide ligand. Hydroborenium species showed good Lewis acidity with the reaction of DMAP. Further studies of the Lewis acidity of these borenium species is underway.

3.4 Experimental Section

3.4.1 General procedure

All the syntheses were carried out under an inert atmosphere of dinitrogen in oven dried glassware using standard Schlenk techniques[43] or a glovebox where O_2 and H_2O levels were maintained usually below 0.1 ppm. All the glassware were dried at 150 °C in an oven for at least 12 h and assembled hot and cooled *in vacuo* prior to use. Solvents were purified by MBRAUN solvent purification system MB SPS-800. THF was dried over (Na/benzophenone ketyl) and distilled under nitrogen and degassed prior to use. $CDCl_3$ for NMR was dried over 4 Å molecular sieves.

3.4.2 Starting materials

All the chemicals used in this work were purchased from commercial sources and were used without further purification. $[Ph_3C][B(C_6F_5)_4]$[42] was synthesized as per the procedure mentioned in the literature.

3.4.3 Physical measurements

The ^{1}H, ^{13}C, $^{31}P\{^{1}H\}$ and ^{11}B NMR spectra were recorded with a Bruker 400 MHz spectrometer with TMS, H_3PO_4 (85 %) and $BF_3{\cdot}OEt_2$ respectively, as external references and chemical shifts were reported in ppm. Downfield shifts relative to the reference were quoted positive while the upfield shifts were assigned negative values. High resolution mass spectra were recorded on a Waters SYNAPT G2−S instrument. IR spectra of the complexes were recorded in the range 4000–400 cm^{-1} using a Perkin Elmer Lambda 35-spectrophotometer over KBr plates. The absorptions of the characteristic functional groups were only assigned and other absorptions (moderate to very strong) were only listed. Melting points were obtained in sealed capillaries on a Büchi B–540 melting point instrument.

Single crystal X-ray diffraction data for **3.1** and **3.2** were collected using a Rigaku XtaLAB mini diffractometer equipped with Mercury375M CCD detector. The data were collected with graphite monochromatic MoKα radiation (λ = 0.71073 Å) at 100.0(2) K using scans. During the data collection, the detector distance was maintained at 50 mm (constant) and the detector was placed at 2θ = 29.85° (fixed) for all the data sets. The data collection and data reduction were done using Crystal Clear suite.[44] The crystal structures were solved by using either OLEX2[45] or WINGX package using SHELXS-97 and the structure were refined using SHELXL-97 2008.[46] All non hydrogen atoms were refined anisotropically.

3.4.4 Synthetic procedure

Synthesis of $[\{N(Ph_2PN(2,4,6\text{-}Me_3C_6H_2))_2\}BH]^{+}BHCl_3^{-}$ (3.1): To a solution of $\mathbf{L_1}H$ (2.60 g, 4.0 mmol) in toluene (50 mL) at - 30 °C was added $BH_2Cl{\cdot}Me_2S$ (1.20 mL, 12 mmol, 10 M in Me_2S). The reaction mixture was brought to room temperature and was stirred for 2 hours followed by reflux for 12 hours. Evaporation of all volatiless under vacuum afforded a white solid that was washed with (2 x 20 mL) hexane and dried under vacuum. This material obtained was crystallized from toluene at room temperature. Yield: (2.81 g, 89.6 %). M.p.

175-177 ºC. IR (ν cm^{-1}, KBr): = 3051, 2962, 2923, 2545, 2470 (B-H stretch), 1587, 1438, 1328, 1296, 1191, 1116, 1023,726. ^{1}H NMR (400 MHz, $CDCl_3$, δ ppm): 1.67 (s, *o*-CH_3, 12 H), 2.29 (s, *p*-CH_3, 6 H), 4.27 (broad, B*H*), 6.85 (s, 2,4,6-$Me_3C_6H_2$, 4 H), 7.65-7.54 (m, Ph, 16 H), 7.82-7.78 (m, Ph, 4 H). ^{13}C NMR (100 MHz, $CDCl_3$, δ ppm): 19.3 (s, *o*-CH_3), 20.9 (s, *p*-CH_3), 125.1 (d, $J_{C\text{-}P}$ = 2.0 Hz, aromatic), 126.4 (d, $J_{C\text{-}P}$ = 2.0 Hz, aromatic), 129.4 (m not resolved, due to $J_{C\text{-}P}$ & $J_{C\text{-}B}$, aromatic), 130.6 (s, aromatic), 132.5 (m not resolved, due to $J_{C\text{-}P}$ & $J_{C\text{-}B}$, aromatic), 134.2 (s, aromatic), 134.9 (s, aromatic), 136.4 (s, aromatic), 139.0 (s, aromatic). ^{31}P{^{1}H} NMR (162 MHz, $CDCl_3$, δ ppm): 22.7. ^{11}B NMR (128.4 MHz, $CDCl_3$, δ ppm): 3.3 (d, $^{1}J_{B\text{-}H}$ = 164.3 Hz). Mass spectrum (+ve ion, EI), *m/z* = calculated (found): 662.3032 (662.3043) $[M\text{-}BHCl_3]^+$.

Alternative synthesis for (3.1): (a) To a solution of **L_1BH_2** (**1.11**) (2.65 g, 4.0 mmol) in toluene (40 mL) at - 30 °C was added $BH_2Cl{\cdot}Me_2S$ (1.2 mL, 10 M in Me_2S, 12 mmol). The reaction mixture was brought to room temperature and was further heated at 60 ºC for 5 hours. Evaporation of all volatiless under vacuum afforded white sticky solid. This sticky solid was washed with (2 x 20 mL) hexane to give white solid. Yield: (2.62 g, 84 %).

(b) To a solution of **L_1BH_2** (**1.11**) (2.65 g, 4.0 mmol) in toluene (40 mL) at - 30 °C was added BCl_3 (4 mL, 1 M in toluene, 4 mmol). The reaction mixture was brought to room temperature and was further stirred for 12 hours. Evaporation of all volatiles under vacuum afforded white solid. Yield: (2.9 g, 93 %).

Synthesis of $[\{N(Ph_2PN(2,4,6\text{-}Me_3C_6H_2))_2\}H_2]^+ Cl^-$: To a mixture of **$[L_1BH]^+BHCl_3^-$ (3.1)** (1.56 g, 2.0 mmol) and sulfur (0.064 g, 2.0 mmol) at - 30 °C was added (40 mL) toluene. In the same solution was added Et_3N (0.28 mL, 2 mmol). The reaction mixture was brought to room temperature and was further heated at 110 ºC for 12 hours. Evaporation of all volatiless under vacuum afforded white solid. ^{1}H NMR (400 MHz, $CDCl_3$, δ ppm): 2.03 (s, *o*-CH_3, 12 H), 2.07 (s, *p*-CH_3, 6 H), 6.53 (s, 2,4,6-$Me_3C_6H_2$, 4 H), 7.19 (m, Ph, 8 H), 7.35 (m, Ph, 4 H),

7.65 (m, Ph, 6 H), 7.76 (m, Ph, 2 H), 8.66 (broad, N*H*). $^{31}P\{^{1}H\}$ NMR (162 MHz, $CDCl_3$, δ ppm): 16.0.

Synthesis of $[\{N(Ph_2PN(2,4,6\text{-}Me_3C_6H_2))_2\}BCl]^+BCl_4^-$ (3.2): To a solution of $\mathbf{L_1}BH_2$ (**1.11**) (2.65 g, 4.0 mmol) in toluene (40 mL) at - 70 °C was added BCl_3 (12 mL, 1 M in toluene, 12 mmol). The reaction mixture was brought to room temperature and was further stirred for 12 hours. The reaction mixture was refluxed for 12 hours. Evaporation of all volatiles under vacuum afforded a white solid. This was crystallized from THF at room temperature. Yield: (3.05 g, 90 %). M.p. 152-154 ºC. IR (ν cm^{-1}, KBr): 2923, 1588, 1476, 1438, 1288, 1225, 1114, 695. ^{1}H NMR (400 MHz, $CDCl_3$, δ ppm): 1.68 (s, *o*-CH_3, 12 H), 2.34 (s, *p*-CH_3, 6 H), 6.88 (s, 2,4,6-$Me_3C_6H_2$, 4 H), 7.63-7.55 (m, Ph, 16 H), 7.84-7.80 (m, Ph, 4 H). ^{13}C NMR (100 MHz, $CDCl_3$, δ ppm): 19.2 (s, *o*-CH_3), 21.0 (s, *p*-CH_3), 124.4 (d, $J_{C\text{-}P}$ = 2.0 Hz, aromatic), 125.7 (d, $J_{C\text{-}P}$ = 2.0 Hz, aromatic), 129.4 (m not resolved, due to $J_{C\text{-}P}$ & $J_{C\text{-}B}$, aromatic), 130.8 (s, aromatic), 132.2 (s, aromatic), 132.9 (m not resolved, due to $J_{C\text{-}P}$ & $J_{C\text{-}B}$, aromatic), 135.1 (s, aromatic), 136.9 (s, aromatic), 139.4 (s, aromatic).$^{31}P\{^{1}H\}$ NMR (162 MHz, $CDCl_3$, δ ppm): 26.3. ^{11}B NMR (128.4 MHz, $CDCl_3$, ppm): δ 7.1. Mass spectrum (+ve ion, EI), *m/z* = calculated (found): 696.2643 (696.2628) $[M]^+$.

Synthesis of $[\{N(Ph_2PN(2,4,6\text{-}Me_3C_6H_2))_2\}BH]^+[HB(C_6F_5)_3]^-$ (3.3):

A toluene solution (10 mL) of $B(C_6F_5)_3$ (0.52 g, 1.0 mmol) was added dropwise at room temperature to a solution of complex $\mathbf{L_1}BH_2$ (**1.11**) (0.66 g, 1.0 mmol) in toluene (10 mL). The mixture was stirred for 0.5 h during which transparent oily compound formed. After removal of all volatiles under vacuum the oil was washed with hexane (30 mL) gave an off white solid.Yield : (1.05 g, 90 %). M.p: 106-108 °C. IR (ν cm^{-1}, nujol): 2962, 2927, 2861, 2558 (B-H stretch), 1646, 1508, 1465, 1380, 1329, 1301, 1117, 970, 909,735, 650, 538. ^{1}H NMR (400 MHz, $CDCl_3$, δ ppm): 1.75 (s, 12 H, *o-Me*), 2.33 (s, 6 H, *p-Me*), 4.38 (broad, 1 H, B−*H*), 6.91 (s, 2,4,6-$Me_3C_6H_2$, 4 H), 7.61−7.56 (m, 8 H, Ph), 7.75−7.69 (m, 8 H, Ph),

7.82−7.78 (m, 4H, Ph). ^{13}C NMR (100 MHz, $CDCl_3$, δ ppm): 19.1 (s, *o*-*C*H_3), 20.7 (s, *p*-*C*H_3), 125.3 (d not resolved, due to $J_{C\text{-}P}$ & $J_{C\text{-}B}$, aromatic), 126.5 (d not resolved, due to $J_{C\text{-}P}$ & $J_{C\text{-}B}$, aromatic), 129.2 (m not resolved, due to $J_{C\text{-}P}$ & $J_{C\text{-}B}$, aromatic), 130.6 (s, aromatic), 132.6 (m not resolved, due to $J_{C\text{-}P}$ & $J_{C\text{-}B}$, aromatic), 134.2 (s, aromatic), 134.7 (s, aromatic), 135.4 (m not resolved, due to $J_{C\text{-}F}$ & $J_{C\text{-}B}$, aromatic) 136.5 (s, aromatic), 137.7 (m not resolved, due to $J_{C\text{-}F}$ & $J_{C\text{-}B}$, aromatic), 139.1 (s, aromatic), 147.2 (m not resolved, due to $J_{C\text{-}F}$ & $J_{C\text{-}B}$, aromatic), 149.5 (m not resolved, due to $J_{C\text{-}F}$ & $J_{C\text{-}B}$, aromatic). ^{31}P{^{1}H} NMR (162 MHz, $CDCl_3$, δ ppm): 22.7. ^{19}F NMR (376 MHz, $CDCl_3$, δ ppm): –133.12 (d, $^3J_{F\text{-}F}$ = 18.8 Hz, 6F, *o*-C_6F_5), –164.15 (t, $^3J_{F\text{-}F}$ = 20.3 Hz, 3F, *p*-C_6F_5), –166.9 (m, 6F, *m*-C_6F_5). ^{11}B NMR (128 MHz, $CDCl_3$, δ ppm): −24.4 (d, $J_{B\text{-}H}$ = 88.0 Hz). Mass spectrum (+ve ion, EI), *m/z* = calculated (found): 662.3032 (662.3025) $[M\text{-}HB(C_6F_5)_3]^+$.

Synthesis of $[\{N(Ph_2PN(2,4,6\text{-}Me_3C_6H_2))_2\}BH]^+[B(C_6F_5)_4]^-$ (3.4):

A toluene (10 mL) solution of $[Ph_3C][B(C_6F_5)_4]$ (0.93 g, 1.0 mmol) was added dropwise at room temperature to a solution of complex $\mathbf{L_1}BH_2$ (**1.11**) (0.66 g, 1.0 mmol) in toluene (10 mL). The mixture was stirred for 0.5 h during which yellow oil droplets developed. After removal of all volatiles under vacuum, the oil was washed with hexane (30 mL) that gave a white solid.Yield: (1.12 g, 85 %). M.p: 110-112 °C. IR (ν cm^{-1}, nujol): 2931, 2857, 2549 (B-H stretch), 1644, 1454, 1058, 969, 853, 829, 722, 586. ^{1}H NMR (400 MHz, $CDCl_3$, δ ppm): 1.72 (s, 12 H, *o-Me*), 2.32 (s, 6 H, *p-Me*), 4.38 (broad, 1 H, B−*H*), 6.89 (s, 2,4,6-$Me_3C_6H_2$, 4 H), 7.58−7.53 (m, 8 H, Ph), 7.71−7.66 (m, 8 H, Ph), 7.79−7.76 (m, 4H, Ph). ^{13}C NMR (100 MHz, $CDCl_3$, δ ppm): 19.1 (s, *o*-*C*H_3), 20.7 (s, *p*-*C*H_3), 124.3 (d not resolved, due to $J_{C\text{-}P}$ & $J_{C\text{-}B}$, aromatic), 125.5 (d not resolved, due to $J_{C\text{-}P}$ & $J_{C\text{-}B}$, aromatic), 129.2 (m not resolved, due to $J_{C\text{-}P}$ & $J_{C\text{-}B}$, aromatic), 130.6 (s, aromatic), 132.6 (m not resolved, due to $J_{C\text{-}P}$ & $J_{C\text{-}B}$, aromatic), 134.2 (s, aromatic), 134.7 (s, aromatic), 135.4 (m not resolved, due to $J_{C\text{-}F}$ & $J_{C\text{-}B}$, aromatic) 136.5 (s, aromatic), 137.7 (m not resolved, due to $J_{C\text{-}F}$ & $J_{C\text{-}B}$, aromatic), 139.1 (s,

aromatic), 147.2 (m not resolved, due to $J_{C\text{-}F}$ & $J_{C\text{-}B}$, aromatic), 149.5 (m not resolved, due to $J_{C\text{-}F}$ & $J_{C\text{-}B}$, aromatic). $^{31}P\{^{1}H\}$ NMR (162 MHz, $CDCl_3$, δ ppm): 22.6. ^{19}F NMR (376 MHz, $CDCl_3$, δ ppm): –132.5 (b, 8F, *o*-C_6F_5), –162.2 (t, $^{3}J_{F\text{-}F}$ = 20.7 Hz, 4F, *p*-C_6F_5), –166.8 (m, 8F, *m*-C_6F_5). ^{11}B NMR (128 MHz, $CDCl_3$, δ ppm): −16.6. Mass spectrum (+ve ion, EI), *m/z* = calculated (found): 662.3032 (662.3021) $[M\text{-}B(C_6F_5)_4]^+$.

Synthesis of $[\{N(Ph_2PN(2,4,6\text{-}Me_3C_6H_2))_2\}BH\cdot DMAP]^+[B(C_6F_5)_4]^-$ (3.5):

A toluene solution (10 mL) of DMAP (61 mg, 0.5 mmol) was added dropwise at room temperature to a solution of complex $[\mathbf{L_1}BH]^+[B(C_6F_5)_4]^-$ (0.67 g, 0.5 mmol) in toluene (10 mL). The mixture was stirred for 2 h during which oily nature of the compound disappeared. After removal of all volatiles under vacuum and washing the residue with hexane (30 mL) gave a off white solid. Yield : (0.66 g, 90 %). M.p: 83-85 °C. IR (ν cm^{-1}, nujol): 2958, 2924, 2861, 2430 (B-H stretch), 1627, 1458, 1259, 1079, 976, 820, 689, 575. ^{1}H NMR (400 MHz, $CDCl_3$, δ ppm): 1.39–1.92 (b, 9 H, *o-Me*), 1.99 (s, 3 H, *o-Me*), 2.22 (s, 6 H, *p-Me*), 2.97 (s, 6 H, N*Me*$_2$), 4.07 (broad, 1 H, B−*H*), 6.25 (b, 2 H, Ph), 6.73 (s, 2,4,6-$Me_3C_6H_2$, 4 H), 7.24−7.17 (m, 5 H, Ph), 7.35−7.30 (m, 3 H, Ph), 7.47 (b, 6 H, Ph), 7.65−7.61 (m, 3H, Ph), 7.79 (b, 5 H, Ph). ^{13}C NMR (100 MHz, $CDCl_3$, δ ppm): 20.1(*p*-*C*H_3), 20.6 (m, *o*-*C*H_3)*, 39.2, 105.8 (m, aromatic), 126.3 (s, aromatic), 128.3 (s, aromatic), 128.5 (d not resolved, due to $J_{C\text{-}P}$ & $J_{C\text{-}B}$, aromatic), 129.3 (s, aromatic), 129.5(s, aromatic), 130.4 (m, aromatic), 131.6 (m, aromatic), 131.9 (m, aromatic), 132.2 (d not resolved, due to $J_{C\text{-}P}$ & $J_{C\text{-}B}$, aromatic), 132.8 (m, aromatic), 135.1 (m, aromatic), 135.6 (s, aromatic), 137.0 (m, aromatic), 137.6 (m, aromatic), 143.9, 147.0 ((m, aromatic), 149.4 (m, aromatic). $^{31}P\{^{1}H\}$ NMR (162 MHz, $CDCl_3$, δ ppm): 21.9. ^{19}F NMR (376 MHz, $CDCl_3$, δ ppm): –132.5 (b, 8F, *o*-C_6F_5), –163.10 (t, $^{3}J_{F\text{-}F}$ = 20.7 Hz, 4F, *p*-C_6F_5), –166.78 (m, 8F, *m*-C_6F_5). ^{11}B NMR (128 MHz, $CDCl_3$, δ ppm): −16.6. Mass spectrum (+ve ion, EI), *m/z* = calculated (found): 785.3956 (785.3979) $[M+H]^+$.

(m)* = ^{1}H NMR showed two different type of *o*-CH_3 which also reflected in ^{13}C NMR to giving a multiplet of two different type of carbons.

3.5 Crystallographic Data

Table 1. Crystal data and structure refinement details for compounds 3.1 and 3.2.

Compound	**3.1**	**3.2**
Chemical formula	$C_{42}H_{44}N_3P_2B_2Cl_3$	$C_{42}H_{42}N_3P_2B_2Cl_5$
Molar mass	780.80	849.68
Crystal system	Monoclinic	Monoclinic
Space group	$P2_1/n$	$P2_1/c$
T (K)	100 (2)	100 (2)
a (Å)	10.3449(2)	13.917(4)
b (Å)	24.2326(4)	18.051(6)
c (Å)	16.1667(3)	17.021(6)
α (°)	90.00	90
β (°)	92.304(7)	100.71(2)
γ (°)	90.00	90
V (Å^3)	4049.5(1)	4201(2)
Z	4	4
D(calcd.) [g·cm^{-3}]	1.28	1.343
μ(Mo-K_α) [mm^{-1}]	0.339	0.456
Index range	$-12 \leq h \leq 12$	$-16 \leq h \leq 16$
	$-29 \leq k \leq 29$	$-21 \leq k \leq 21$
	$-19 \leq l \leq 19$	$-20 \leq l \leq 20$
Reflections collected	28454	38515
Independent reflections	7400	7709
Data/restraints/parameters	7400/0/489	7709/0/493
$R1$, $wR2$ [$I>2\sigma(I)$][a]	0.0442, 0.1194	0.075/0.1653
$R1$, $wR2$ (all data)[a]	0.0476, 0.1231	0.1936,0.2344
GOF	1.026	0.9786

[a] $R1 = \Sigma||Fo| - |Fc||/\Sigma|Fo|$. $wR2 = [\Sigma w(|Fo^2| - |Fc^2|)^2/\Sigma w|Fo^2|^2]^{1/2}$

3.6 References

1. Engesser, T. A.; Lichtenthaler, M. R.; Schleep, M.; Krossing, I. *Chem. Soc. Rev.* **2016,** *45,* 789.
2. (a) Hollenstein, S.; Laube, T. *J. Am. Chem. Soc.* **1993,** *115,* 7240. (b) Stoyanov, E. S.; Stoyanova, I. V.; Tham, F. S.; Reed, C. A. *Angew. Chem., Int. Ed,* **2012,** *51,* 9149. (c) Christe, K. O.; Zhang, X.; Bau, R.; Hegge, J.; Olah, G. A.; Prakash, G. K. S.; Sheehy, J. A. *J. Am. Chem. Soc.* **2000,** *122,* 481. (d) Douvris, C.; Stoyanov, E. S.; Tham, F. S.; Reed, C. A. *Chem. Commun.* **2007,** 1145. (e) Krossing, I.; Bihlmeier, A.; Raabe, I.; Trapp, N. *Angew. Chem. Int. Ed.* **2003,** *42,* 1531. (f) Mercier, H. P. A.; Moran, M. D.; Schrobilgen, G. J.; Steinberg, C.; Suontamo, R. J. *J. Am. Chem. Soc.* **2004,** *126,* 5533.
3. (a) Kim, K.-C.; Reed, C. A.; Elliott, D. W.; Mueller, L. J.; Tham, F.; Lin, L.; Lambert, J. B. *Science* **2002,** *297,* 825. (b) Schäfer, A.; Reißmann, M.; Jung, Schäfer, A.; Saak, W.; Brendler, E.; Müller, T. *Organometallics* **2013,** *32,* 4713. (c) Schäfer, A.; Saak, W.; Haase, D.; Müller, T. *J. Am. Chem. Soc.* **2011,** *133,* 14562.
4. (a) Beck, J.; Hilbert, T. *Eur. J. Inorg. Chem.* **2004,** 2019. (b) Gudat, D.; Haghverdi, A.; Hupfer, H.; Nieger, M. Chem. – Eur. J. 2000, 6, 3414. (c) Burford, N.; Losier, P.; Macdonald, C.; Kyrimis, V.; Bakshi, P. K.; Cameron, T. S. *Inorg. Chem.* **1994,** *33,* 1434. (d) Slattery, J. M.; Hussein, S. *Dalton Trans.* **2012,** *41,* 1808. (e) Reeske, G.; Cowley, A. H. *Chem. Commun.* **2006,** 1784. (f) Carmalt, C. J.; Lomeli, V. *Chem. Commun.* **1997,** 2095.
5. (a) Coles, M. P.; Jordan, R. F. *J. Am. Chem. Soc.* **1997,** *119,* 8125. (b) Ihara, E.; Young, V. G., Jr.; Jordan, R. F. *J. Am. Chem. Soc.* **1998,** *120,* 8277. (c) Radzewich, C. E.; Guzei, I. A. Jordan, R. F. *J. Am. Chem. Soc.* **1999,** *121,* 8673. (d) Masuda, J. D.; Stephan, D. W. *Dalton Trans. 2006,* 2089. (e) Higelin, A.; Sachs, U.; Keller, S.; Krossing, I. *Chem. –Eur. J.* **2012,** *18,* 10029. (f) Lichtenthaler, M. R.; Stahl, F.;

Kratzert, D.; Benkmil, B.; Wegner, H. A.; Krossing, I. *Eur. J. Inorg. Chem.* **2014,** 4335. (g) Mansaray, H. B.; Tang, C. Y.; Vidovic, D.; Thompson, A. L.; Aldridge, S. *Inorg. Chem.* **2012,** *51*, 13017. (h) Delpech, F.; Guzei, I. A.; Jordan, R. F. *Organometallics* **2002,** *21*, 1167.

6. Zheng, X.; Tao, W. A.; Cooks, R. G. *J. Am. Soc. Mass Spect.* **2001,** *12*, 948.
7. (a) Davidson, J. M.; French, C. M. *J. Chem. Soc.* **1958,** 114. (b) Moodie, R. B.; Ellul, B.; Connor, T. M. *Chem. Ind.* **1966,** 767. (c) Uddin, M. K.; Fujiyama, R.; Kiyooka, S.; Fujio, M.; Tsuno, Y. *Tetrahedron Lett*. **2004,** *45*, 3913.
8. Nöth, H.; Staudigl, R.; Wanger, H-.U. *Inorg. Chem.* **1982,** *21*, 706.
9. Kölle, P.; Nöth, H. *Chem. Ber.* **1986,** *119*, 313.
10. Cortenay, S.; Mutus, J. Y.; Schurko, R. W.; Stephan, D. W. *Angew. Chem., Int. Ed.* **2002,** *41*, 498.
11. Shoji, Y.; Tanaka, N.; Mikami, K.; Uchiyama, M.; Fukushima, T. *Nat. Chem.* **2014,** *6*, 498.
12. Prokofjevs, A.; Kampf, J. W.; Vedejs, E. *Angew. Chem., Int. Ed.* **2011,** *50*, 2098.
13. Bratt, P. J.; Brown, M. P.; Seddon, K. R. *J. Chem. Soc., Dalton Trans.* **1976,** 353.
14. Kuhn, N.; Kuhn, A.; Lewandowski, J.; Speis, M. *Chem. Ber*. **1991,** *124*, 2197.
15. (a) Kölle, P.; Nöth, H. *Chem. Rev.* **1985,** *85*, 399. (b) Piers, W. E.; Bourke, S. C.; Conroy, K. D. *Angew. Chem., Int. Ed.* **2005,** *44*, 5016.
16. Cowley, A. H.; Lu, Z.; Jones, J. N.; Moore, J. A. *J. Organomet. Chem.* **2004,** *689*, 2562.
17. Jutzi, P.; Krato, B.; Hursthouse, M.; Howes, A. J. *Chem. Ber*. **1987,** *120*, 1091.
18. Bonnier, C.; Piers, W. E.; Parvez, M.; Sorensen, T. S. *Chem. Commun.* **2008,** 4593.
19. Chiu, C-. W.; Gabbaï, F. P. *Organometallics* **2008,** *27*, 1657.

20. Vedejs, E.; Nguyen, T.; Powell, D. R.; Schrimpf, M. R. *Chem. Commun.* **1996,** 2721.(a) Prokofjevs, A.; Kampf, J. W.; Solovyev, A.; Curran, D. P.; Vedejs, E. *J. Am. Chem. Soc.* **2013,** *135*, 15686. (b) De Vries, T. S.; Prokofjevs,A.; Harvey, J. N.; Vedejs, E. *J. Am. Chem. Soc.* **2009,** *131*, 14679. (c) DelGrosso, A.; Singleton, P. J.; Muryn, C. A.; Ingleson, M. J. *Angew. Chem., Int. Ed.* **2011,** *50*, 2102. (d) Solomon, S. A.; Del Grosso, A.; Clark, E. R.; Bagutski, V.; McDouall, J. J. W.; Ingleson, M. J.; *Organometallics* **2012,** *31*, 1908. (e) Bagutski, V.; Del Grosso, A.; Carrillo, J. A.; Cade, I. A.; Helm, M. D.; Lawson, J. R.; Singleton, P. J.; Solomon, S. A.; Marcelli, T.; Ingleson, M. J. *J. Am. Chem.Soc.* **2013,** *135*, 474. (f) Eisenberger, P.; Bailey, A. M.; Crudden, C. M. *J. Am. Chem. Soc.* **2012,** *134*, 17384. (g) Denmark, S. E.; Ueki, Y. *Organometallics* **2013,** *32*, 6631.

21. (a) Mansaray, H. B.; Rowe, A. D. L.; Phillips, N.; Niemeyer, J.; Kelly, M.; Addy, D. A.; Bates, J. I.; Aldridge, S. *Chem. Commun.* **2011,** *47*, 12295. (b) Ghesner, I.; Piers, W. E.; Parvez, M.; McDonald, R. *Chem. Commun.* **2005,** 2480. (c) Del Grosso, A.; Helm, M. D.; Solomon, S. A.; Caras-Quintero, D.; Ingleson, M. J. *Chem. Commun.* **2011,** *47*, 12459. (d) Lawson, J. R.; Clark, E. R.; Cade, I. A.; Solomon, S. A.; Ingleson, M. J. *Angew. Chem., Int. Ed.* **2013,** *52*, 7518.

22. (a) Matsumoto, T.; Gabbaï, F. P. *Organometallics* **2009,** *28*, 4252. (b) McArthur, D.; Butts, C. P.; Lindsay, D. M. *Chem. Commun.* **2011,** *47*, 6650. (c) Solovyev, A.; Geib, S. J.; Lacôte, E.; Curran, D. P. *Organometallics* **2012,** *31*, 54. (d) Muthaiah, S.; Do, D. C. H.; Ganguly, R.; Vidović, D. *Organometallics* **2013,** *32*, 6718. (e) Wang, Y.; Abraham, M. Y.; Gilliard, R. J.; Sexton, D. R.; Wei, P.; Robinson, G. H. *Organometallics* **2013,** *32*, 6639. (f) Do, D. C. H.; Muthaiah, S.; Ganguly, R.; Vidović, D. *Organometallics* **2014,** *33*, 4165. (g) Prokofjevs, A.; Boussonnière, A.; Li, L.; Bonin, H.; Lacôte, E.; Curran, D. P.; Vedejs, E. *J. Am. Chem. Soc.* **2012,** *134*,

12281. (h) Farrell, J. M.; Hatnean, J. A.; Stephan, D. W. *J. Am. Chem. Soc.* **2012,** *134*, 15728.

23. (a) Del Grosso, A.; Pritchard, R. G.; Muryn, C. A.; Ingleson, M. J. *Organometallics* **2010,** *29*, 241. (g) Ingelson, M. J. *Synlett*, **2012,** 1411. (h) Stahl, T.; Müther, K.; Ohki, Y.; Tatsumi, K.; Oestreich, M. *J. Am. Chem. Soc.* **2013,** *135*, 10978.
24. Chen,J.; Lalancette, R. A.; Jaekle, F. *Chem. Commun.* **2013,** *49*, 4893.
25. Bentivegna, B.; Mariani, C. I.; Smith, J. R.; Ma, S.; Rheingold, A. L.; Brunker, T. J. *Organometallics* **2014,***33*, 2820.
26. Hu, Q.-Y.; Zhou, G.; Corey, E. J. *J. Am. Chem. Soc.* **2004,** *126*,13708.
27. Prokofjevs, A.; Vedejs, E. *J. Am. Chem. Soc.* **2011,** *133*, 20056.
28. Clark, E. R.; Del Grosso, A.; Ingleson, M. J. *Chem. -Eur. J.* **2013,** *19*, 2462.
29. Clark, E. R.; Ingleson, M. J. *Organometallics* **2013,** *32*, 6712.
30. Curless, L. D.; Clark, E. R.; Cid, J.; Del Grosso, A.; Ingleson, M. J. *Chem. commun.* **2015,** 10903.
31. (a) Gates, D. P.; McWilliams, A. R.; Ziembinski, R.; Liablesands, L. M.; Guzei, I. A.; Yap, G. P. A.; Rheingold, A. L.; Manners, I. *Chem.-Eur. J.* **1998,** *4*, 1489. (b) Devillard, M.; Brousses, R.; Miqueu, K.; Bouhadir, G.; Bourissou, D. *Angew. Chem., Int. Ed.* **2015,** *54*, 5722.
32. Vidovic, D.; Findlater, M.; Cowley, A. H. *J. Am. Chem. Soc.* **2007,** *129*, 8436.
33. Jaiswal, K.; Prashanth, B.; Bawari, D.; Singh, S. *Eur. J. Inorg. Chem*. **2015,** 2565.
34. Jaiswal, K.; Prashanth, B.; Singh, S. *unpublished results.*
35. (a) Hudnall, T. W.; Gabbaï, F. P. *Chem. Commun.* **2008,** 4596. (b) Kinjo, R.; Donnadieu, B.; Celik, M. A.; Frenking, G.; Bertrand, G. *Science* **2011,** *333*, 610.
36. Inés, B.; Patil, M.; Carreras, J.; Goddard, R.; Thiel, W.; Alcarazo,M. *Angew. Chem., Int. Ed.* **2011,** *50*, 8400.

37. Chen, C. W.-C.; Lee, C.-Y.; Lin, B.-C.; Hsu, Y.-C.; Shen, J.-S.; Hsu, C.-P.; Yap, G. P. A.; Ong, T.-G. *J. Am. Chem. Soc.* **2014,** *136*, 914.

38. Eaton, G. R. *J. Chem. Edu.* **1969,** *46*, 547.

39. Vidovic, D.; Reeske, G.; Findlater, M.; Cowley, A. H. *Dalton Trans* **2008,** 2293.

40. Masuda, J. D.; Walsh, D. M.; Wei, P.; Stephan, D. W. *Organometallics* **2004,** *23*, 1819.

41. Ihara, E.; Young, V. G., Jr.; Jordan, R. F. *J. Am. Chem. Soc.* **1998,** *120,* 8277.

42. Shriver, D. F.; Drezdon, M. A. The Manipulation of Air–Sensitive Compounds, 2nd Ed. McGraw–Hill, New York, USA, **1969**.

43. CrystalClear 2.0, Rigaku Corporation, Tokyo, Japan.

44. Dolomanov, O. V.; Bourhis, L. J.; Gildea, R. J.; Howard, J. A. K.; Puschmann, H. *J. Appl. Cryst.* **2009**, *42*, 339.

45. SHELXS-97, Program for Structure Solution: Sheldrick, G. M. *Acta Crystallogr. Sect. A.* **2008**, *64*, 112.

Chapter 4

4.1 Summary

Looking back in the recent past, the chemistry of *p*-block elements have received a lot of attention not just to study fundamental aspects including structure and bonding in the molecules but also to explore their applications as Lewis acids to catalysts and catalyst promoters. The work presented in the thesis delineates synthesis and characterization of [N, N'] chelate complexes of group 13 elements and their reaction chemistry. The work mainly poised around boron and its cationic complexes which can be interesting candidates for potential applications from catalysis to molecular transformations. In recent years, in the field of main group chemistry Group 13 cationic complexes especially boron cations have gained more attention and have been used for organic transformation reactions.

Owing to less development in the area of cationic boron complexes and complexes of boron with chalcogens, the central theme of our work is to explore synthetic methods to prepare such derivatives. The ligands based on P=N moieties have been chosen due to their strong donor capability as compare to the ligands with C=N moieties. The advantage of facile donation of electrons, to the central atom, by P=N moieties made us interested to work with *bis*(phosphinimino)amide ligand with N_3P_2 backbone. Therefore, donor properties of these ligands have been compared with the known systems with the (C_3N_2) backbone of *β*-diketiminato and (CP_2N_2) of *bis*(phosphinimino)methanide ligands. Selection of central atom and metal ions and synthesis of their complexes with the chosen ligands were undertaken with the following objectives:

(i) Stable and soluble heteroleptic complexes of group 13 element to explore their reaction chemistry.

(ii) Synthesis of thioxo– and selenoxo–borane complexes *via* reaction of borondihydride complex as a precursor with heavier chalcogens (S or Se).

(iii) Application of borondihydride complex for the synthesis of stable three coordinated cationic borenium complexes.

A chapter wise summary of the results obtained is presented below:

Summary of Chapter 1

In the present work monoanionic [N,N'] chelating ligands based on N_3P_2 skeleton were used. Based on the substitution on N, these ligands were named as [HN($Ph_2PN(2,4,6\text{-}Me_3C_6H_2)$)$_2$] (**L$_1$**H) and [HN($Ph_2PN(2,6\text{-}i Pr_2C_6H_3)$)$_2$] (**L$_2$**H). These ligands have been prepared by reactions of tetraphenyldiphosphazane $(Ph_2P)_2NH$ with mesitylazide 2,4,6-$Me_3C_6H_2N_3$ and a bulky azide 2,6-$iPr_2C_6H_3N_3$. The ligands can be easily deprotonated using *n*BuLi or Li[N($SiMe_3$)$_2$] in Et_2O to yield [{N($Ph_2PN(2,4,6\text{-}Me_3C_6H_2)$)$_2$}Li·$OEt_2$] **L$_1$**Li·$OEt_2$ (**1.1**) and [{N($Ph_2PN(2,6\text{-}iPr_2C_6H_3)$)$_2$}Li·$OEt_2$] **L$_2$**Li·$OEt_2$ (**1.2**), respectively. These derivatives were useful as the alternating source of the ligands to prepare the metal complexes under salt metathesis reactions with metal halide sources.

The reactions of **1.1** with the trihalides, MX_3 of group 13 elements afforded the corresponding dihalide complexes, [{N($Ph_2PN(2,4,6\text{-}Me_3C_6H_2)$)$_2$}$MX_2$] **L$_1$**$MX_2$ (M = B, X = F (**1.3**); M = Al, X = Cl (**1.4**); M = Ga, X = Cl (**1.5**); M = In, X = Br (**1.6**). The reactions of **L$_1$**H and **L$_2$**H with $BH_2Cl·SMe_2$ gave the corresponding mononuclear complexes [{N($Ph_2PN(2,4,6\text{-}Me_3C_6H_2)$)$_2$}BHCl] (**L$_1$**BHCl (**1.7**)) and [{N($Ph_2PN(2,6\text{-}iPr_2C_6H_3)$)$_2$}BHCl] (**L$_2$**BHCl (**1.8**)) respectively, as rare examples of monochloroborane complexes. Similarly, the reactions of **L$_1$**H with $AlMe_3$, $AlH_3·NMe_2Et$ and $BH_3·SMe_2$ respectively, gave the corresponding mononuclear complexes, [{N($Ph_2PN(2,4,6\text{-}Me_3C_6H_2)$)$_2$}$AlMe_2$] (**L$_1$**$AlMe_2$ (**1.9**)), [{N($Ph_2PN(2,4,6\text{-}Me_3C_6H_2)$)$_2$}$AlH_2$] (**L$_1$**$AlH_2$ (**1.10**)), and a rare borondihydride [{N($Ph_2PN(2,4,6\text{-}Me_3C_6H_2)$)$_2$}$BH_2$] (**L$_1$**$BH_2$ (**1.11**)). These complexes are six-membered [N,N'] chelates of the monoanionic N_3P_2 ligand backbone. The molecular unit of complexes showed a distorted tetrahedral geometry around central atom. All the complexes reported in

Chapter 1 have been isolated in good yields and would serve as useful synthons to elaborate their reaction chemistry.

Especially the complex $\mathbf{L_1}BH_2$ (**1.11**) turned out to be a good synthon to elaborate its reaction chemistry which has been further discussed in the same chapter showing that the treatment of borondihydride complex $\mathbf{L_1}BH_2$ **(1.11)** with 2 equivalent of HCl gave the borondichloride complex $\mathbf{L_1}BCl_2$ **(1.12)**. In contrast, the hydridebromide complex $\mathbf{L_1}BHBr$ **(1.13)** and hydrideiodide complexes $\mathbf{L_1}BHI$ **(1.14)** were prepared by reacting $\mathbf{L_1}BH_2$ **(1.11)** with excess of C_2H_5Br and CH_3I, respectively. The hydride triflate complex $\mathbf{L_1}BH(OSO_2CF_3)$ **(1.15)** was prepared by reacting $\mathbf{L_1}BH_2$ **(1.11)** of 2 equivalent of TfOH at room temperature. Use of $\mathbf{L_1}BH_2$ **(1.11)** as a synthon has been further discussed in Chapters 2 and 3.

Summary of Chapter 2

The unusual reactivity of borondihydride complex $\mathbf{L_1}BH_2$ (**1.11**) with elemental sulfur and selenium had been investigated. The reactions involved oxidative insertion of S and Se into B-H bonds with subsequent release of H_2S (or H_2Se) from the intermediate species ($\mathbf{L_1}B(SH)_2$ or $\mathbf{L_1}B(SeH)_2$) resulting in the formation of stable compounds with terminal boron-chalcogen double bonds $\mathbf{L_1}B{=}S$ (**2.1**) and $\mathbf{L_1}B{=}Se$ (**2.2**). The electronic structures of $\mathbf{L_1}B{=}S$ and $\mathbf{L_1}B{=}Se$ were elucidated by multi-nuclear NMR and single crystal X-ray diffraction methods which showed B atom to be present in a trigonal planar arrangement. The mesityl substituents on the terminal N atoms of the ligand are oriented perpendicular to the N-B(S, Se)-N plane and provide necessary steric protection. Ab initio calculations on $\mathbf{L_1}B{=}S$ (**2.1**) are in excellent agreement with its experimental structure and clearly support the existence of boron-sulfur double bond.

Summary of Chapter 3

The last chapter of the thesis described our interest to further explore the reactivity of $\mathbf{L_1}BH_2$ **(1.11)** to synthesize the cationic boron complexes and studies on their Lewis acid character.

The reaction of a borondihydride species $\mathbf{L_1}BH_2$ (**1.11**) with 3 equivalents of $BH_2Cl{\cdot}SMe_2$ or one equivalent of BCl_3 afforded the first stable monohydroborenium ion, $[\mathbf{L_1}BH]^+[HBCl_3]^-$ (**3.1**) that is stable without a weakly coordinating bulky anion. Compound **3.1** can also be prepared directly by refluxing $\mathbf{L_1}H$ with 3 equivalents of $BH_2Cl{\cdot}SMe_2$.

Complex $\mathbf{L_1}BH_2$ (**1.11**) on reaction with 3 equivalents of BCl_3 undergoes metathesis reaction to afford $\mathbf{L_1}BCl_2$ and subsequent abstraction of chlorine with the third equivalent of BCl_3 gave the chloroborenium ion, $[\mathbf{L_1}BCl]^+[BCl_4]^-$ (**3.2**). Solid state structure of complexes **3.1** and **3.2** revealed that the ion pairs in both the molecules are well separated. Moreover, no interaction between the boron cation and the anions ($[HBCl_3]^-$ and $[BCl_4]^-$), was detected. Additionally, a facile synthesis of hydroborenium complexes $[\mathbf{L_1}BH]^+[HB(C_6F_5)_3]^-$ (**3.3**) and $[\mathbf{L_1}BH]^+[B(C_6F_5)_4]^-$ (**3.4**) *via* hydride abstraction, using Lewis acid ($B(C_6F_5)_3$) or weakly coordinating ion pair $[Ph_3C][B(C_6F_5)_4]$, from $\mathbf{L_1}BH_2$ (**1.11**) had been carried out. The counter ion independent chemical shifts for the cationic parts of **3.1**, **3.2** and **3.4** with different anions, suggested well separated ions for these molecules. Complex **3.4** easily forms an adduct with 4-dimethylaminopyridine (DMAP) $[\mathbf{L_1}BH(DMAP)]^+[B(C_6F_5)_4]^-$ (**3.5**) exhibiting its Lewis acid behaviour.

4.2 Future directions

The dihalides, aluminumdihydride, borondihydride and aluminumdimethyl complexes synthesized in this work are good synthons for further reaction chemistry. Borondihydride and aluminumdihydride complexes represent an interesting class of compounds due to their ability to deliver hydride ions and usefulness in hydroboration and hydroalumination reaction. In the future outlook, these borondihydride species could prove to be useful precursors to synthesize the unknown dithiol/diselenol derivatives of boron.

Based on the facts mentioned above the following could be the future prospect of this chemistry:

(i) Synthesis of cationic organoaluminum complexes from the dimethylaluminum complex with a variety of counter anions can be undertaken and their application in Lewis acid catalytic processes can be tested.

(ii) Variation in the steric bulk of the bis(phosphinimino)amide ligand the possibility to stabilize the dithiol/diselenol derivatives of boron can be explored. In order to achieve this goal substituents bulkier than mesityl group on the terminal N atoms of the ligand can be utilized with the anticipation that the steric bulk will provide kinetic stability to dithiol/diselenol derivatives.

(iii) The tendency of $\mathbf{L_1}$B=S (or $\mathbf{L_1}$B=Se) as Lewis bases can be explored to form adducts with Lewis acids. The Lewis basic tendency of $\mathbf{L_1}$B=S is supported by theoretical calculations that showed the HOMO to be predominantly S lone pair.

(iv) The borondihydride complex, $\mathbf{L_1}BH_2$ prepared in this work could be utilized in the reduction of CO_2 as well as a source of hydride in organic transformations.

(v) The hydridoborenium cations can easily form adducts with N or P based Lewis bases and can be further developed into a new type of frustrated Lewis pairs with the aim to apply them in as imine reduction, hydrogenation, small molecule activation and CO_2 reduction etc.

List of publications

1. Bis(phosphinimino)amide supported borondihydride compound and heteroleptic dihalo compounds of group 13, **Kuldeep Jaiswal**, Billa Prashanth, Deependra Bawari, Sanjay Singh, *Eur. J. Inorg. Chem*., **2015**, 2565-2573.
2. Reactivity of a dihydroboron species: Synthesis of a hydroborenium complex and an expedient entry into stable thioxo- and selenoxo-boranes, **Kuldeep Jaiswal**, Billa Prashanth, Satyam Ravi, K. R. Shamasundar and Sanjay Singh, *Dalton Trans*., **2015**, *44*, 15779-15785.
3. Fine Tuning of Lewis Acidity: The case of borenium hydride complexes derived from bis(phosphinimino)amide boron precursors, **Kuldeep Jaiswal**, Billa Prashanth and Sanjay Singh, *Chem. –Eur.J .;* **2016,** *Accepted manuscript.*

Supporting Information: Heteronuclear NMR Spectra of New Compounds

Contents

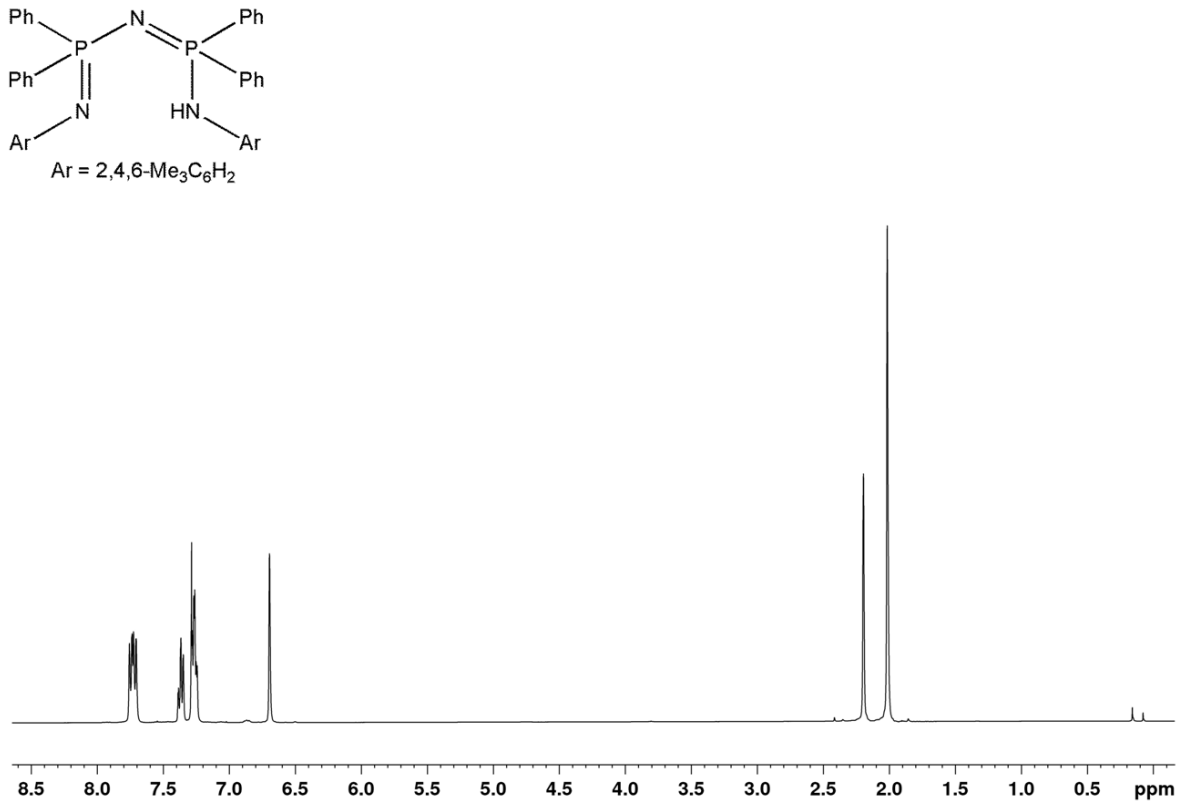

Fig. S1 ^{1}H NMR (400 MHz, $CDCl_3$) spectrum of [HN($Ph_2PN(2,4,6\text{-}Me_3C_6H_2N)$)$_2$] (**L$_1$**H).

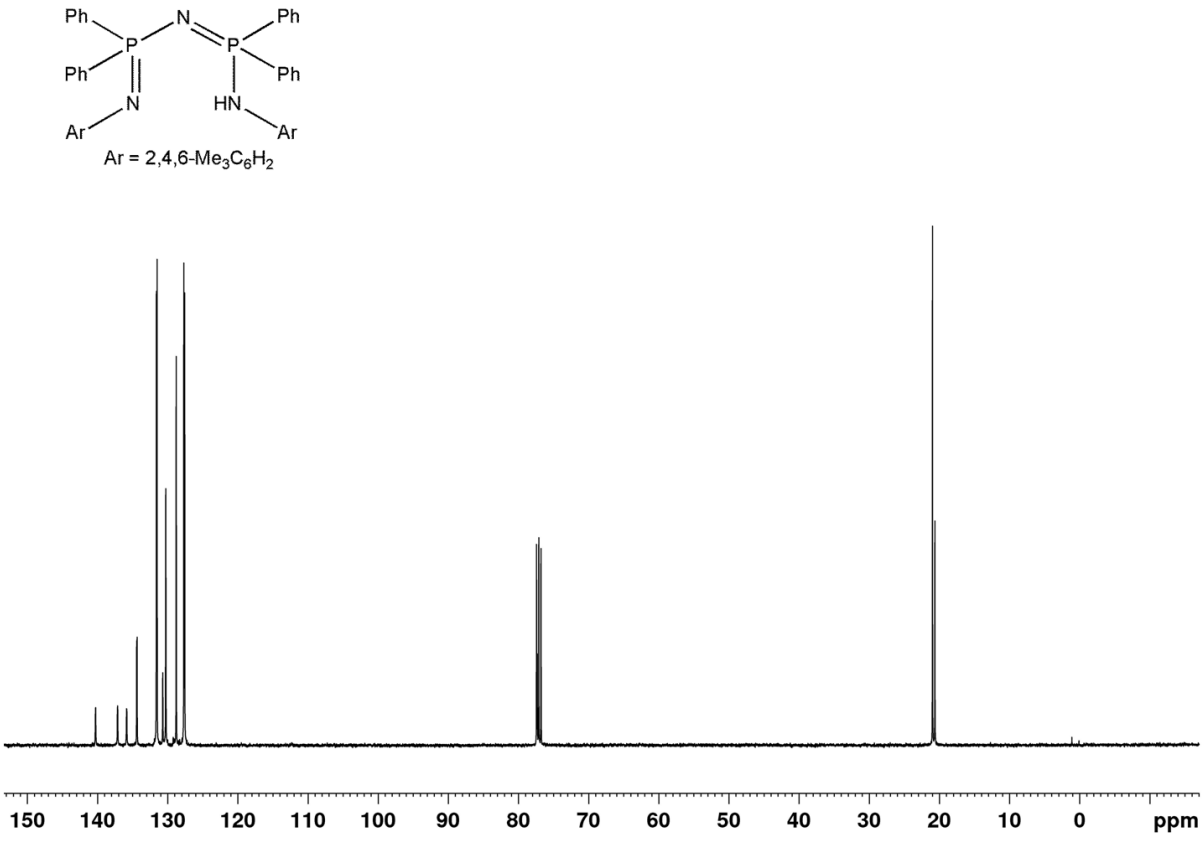

Fig. S2 ^{13}C NMR (100 MHz, $CDCl_3$) spectrum of [HN($Ph_2PN(2,4,6\text{-}Me_3C_6H_2N)$)$_2$] (**L$_1$**H).

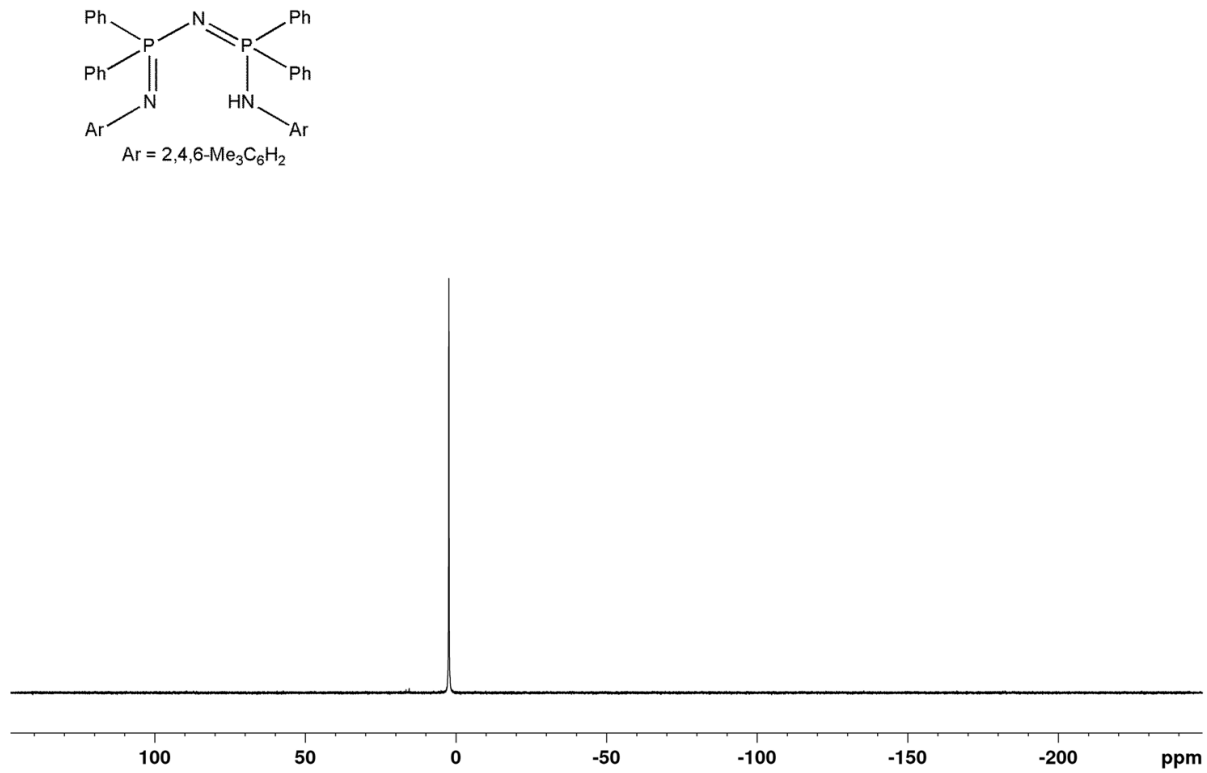

Fig. S3 $^{31}P\{^{1}H\}$ NMR (162 MHz, $CDCl_3$) spectrum of $[HN(Ph_2PN(2,4,6\text{-}Me_3C_6H_2N))_2]$ (**L_1H**).

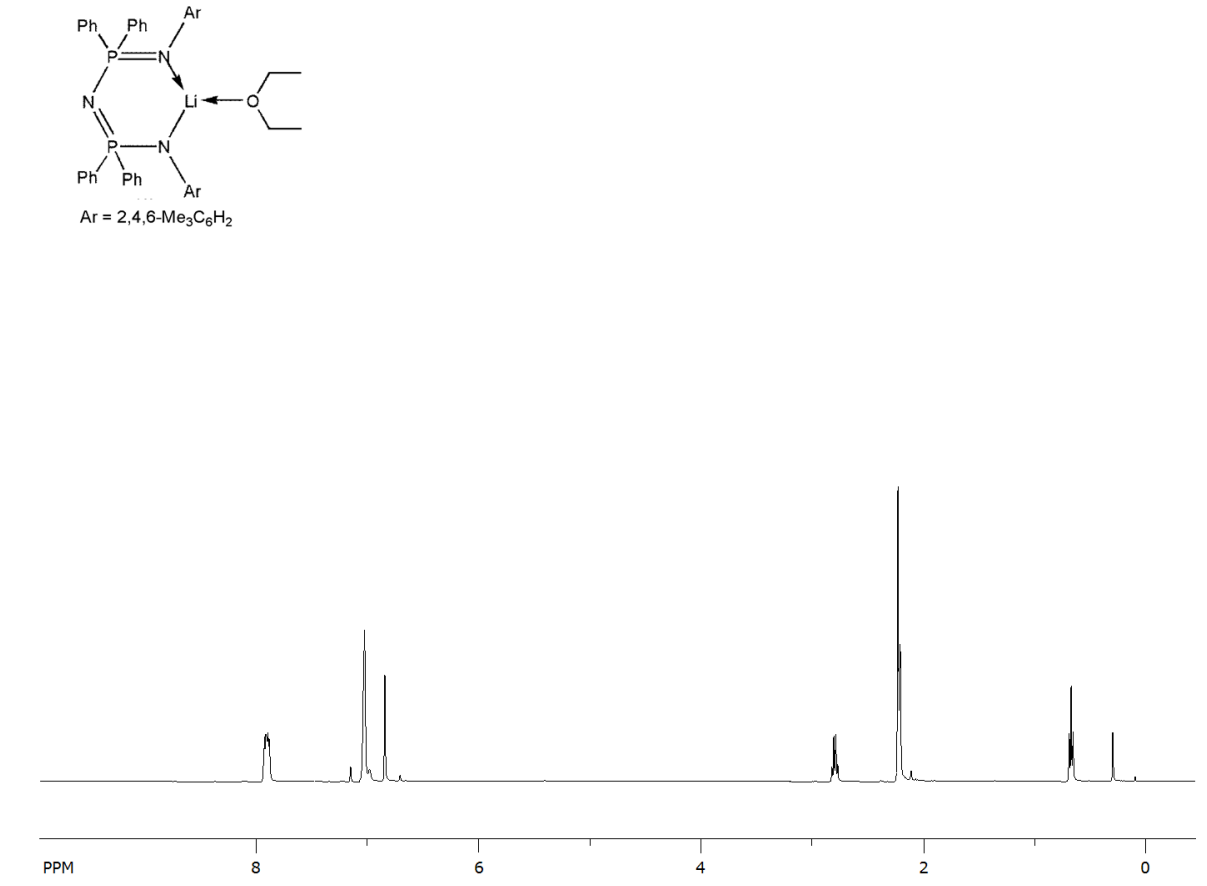

Fig. S4 ^{1}H NMR (400 MHz, C_6D_6) spectrum of $[\{N(Ph_2PN(2,4,6\text{-}Me_3C_6H_2N))_2\}Li{\cdot}OEt_2]$ (**1.1**).

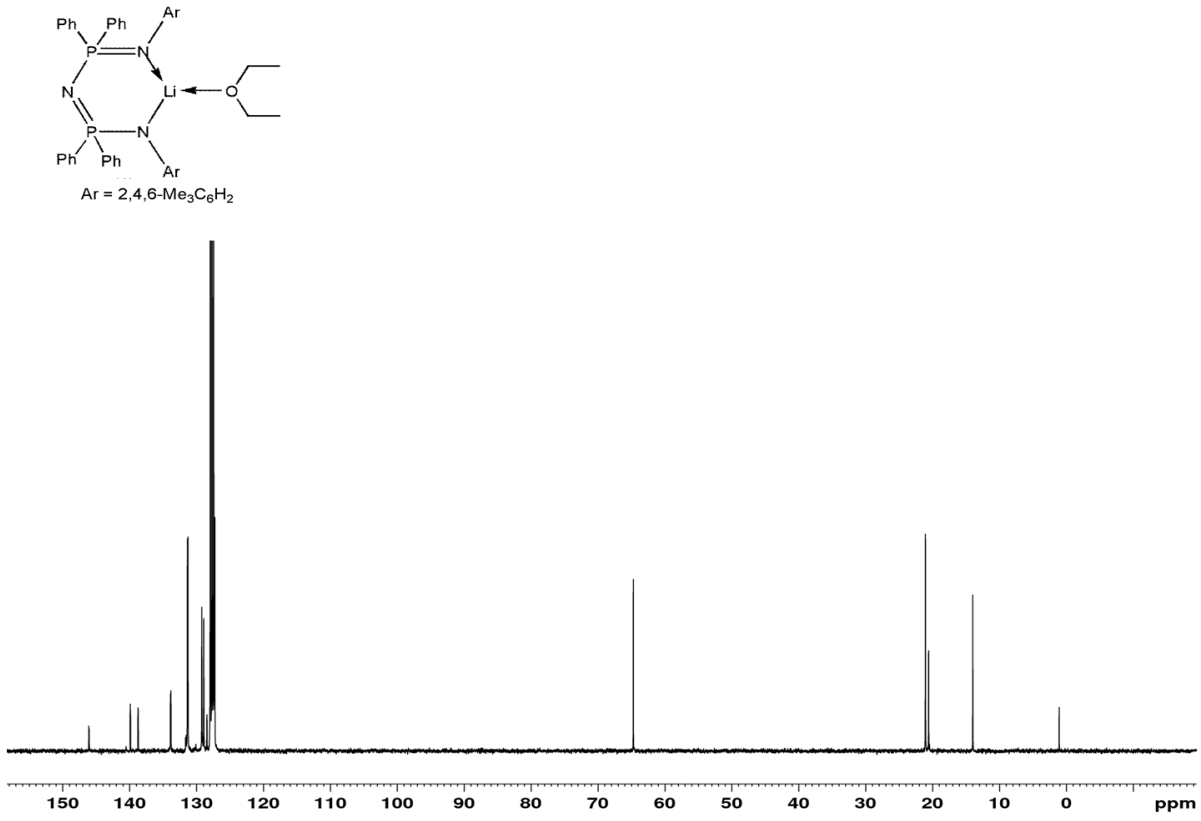

Fig. S5 ^{13}C NMR (100 MHz, C_6D_6) spectrum of [{N(Ph_2PN(2,4,6-$Me_3C_6H_2N$))$_2$}Li·OEt_2] (**1.1**).

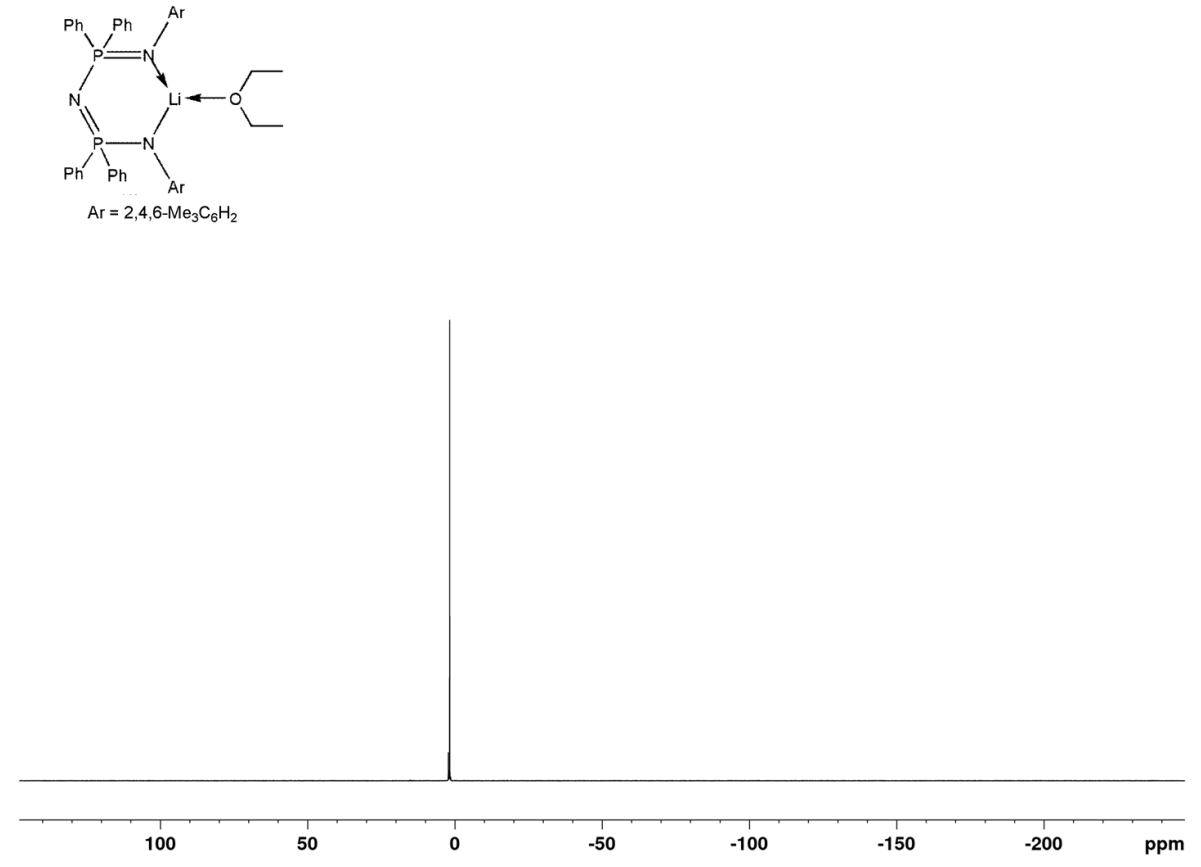

Fig. S6 $^{31}P\{^1H\}$ NMR (162 MHz, C_6D_6) spectrum of [{N(Ph_2PN(2,4,6-$Me_3C_6H_2N$))$_2$}Li·OEt_2] (**1.1**).

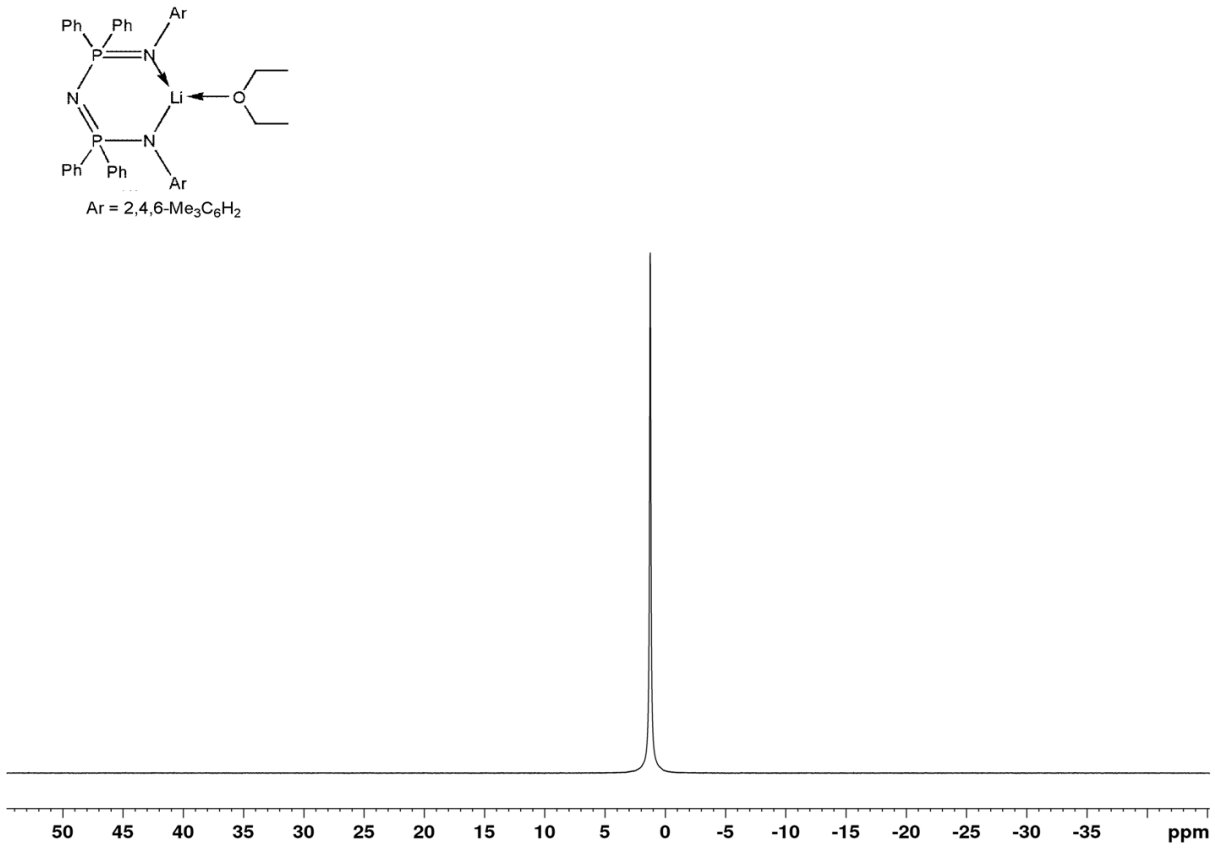

Fig. S7 ^{7}Li NMR (155 MHz, C_6D_6) spectrum of [{N(Ph_2PN(2,4,6-$Me_3C_6H_2N$))$_2$}Li·OEt_2] (**1.1**).

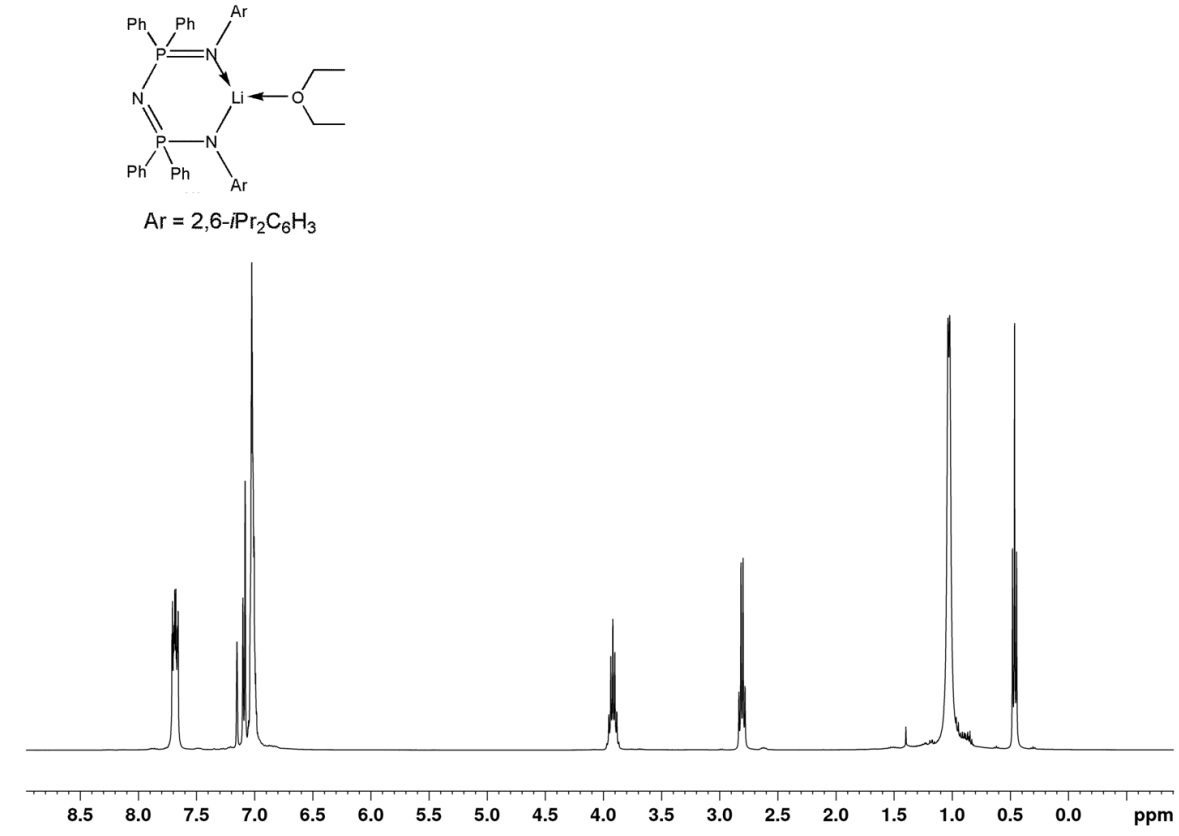

Fig. S8 ^{1}H NMR (400 MHz, C_6D_6) spectrum of [{N(Ph_2PN(2,6-$iPr_2C_6H_3N$))$_2$}Li·OEt_2] (**1.2**).

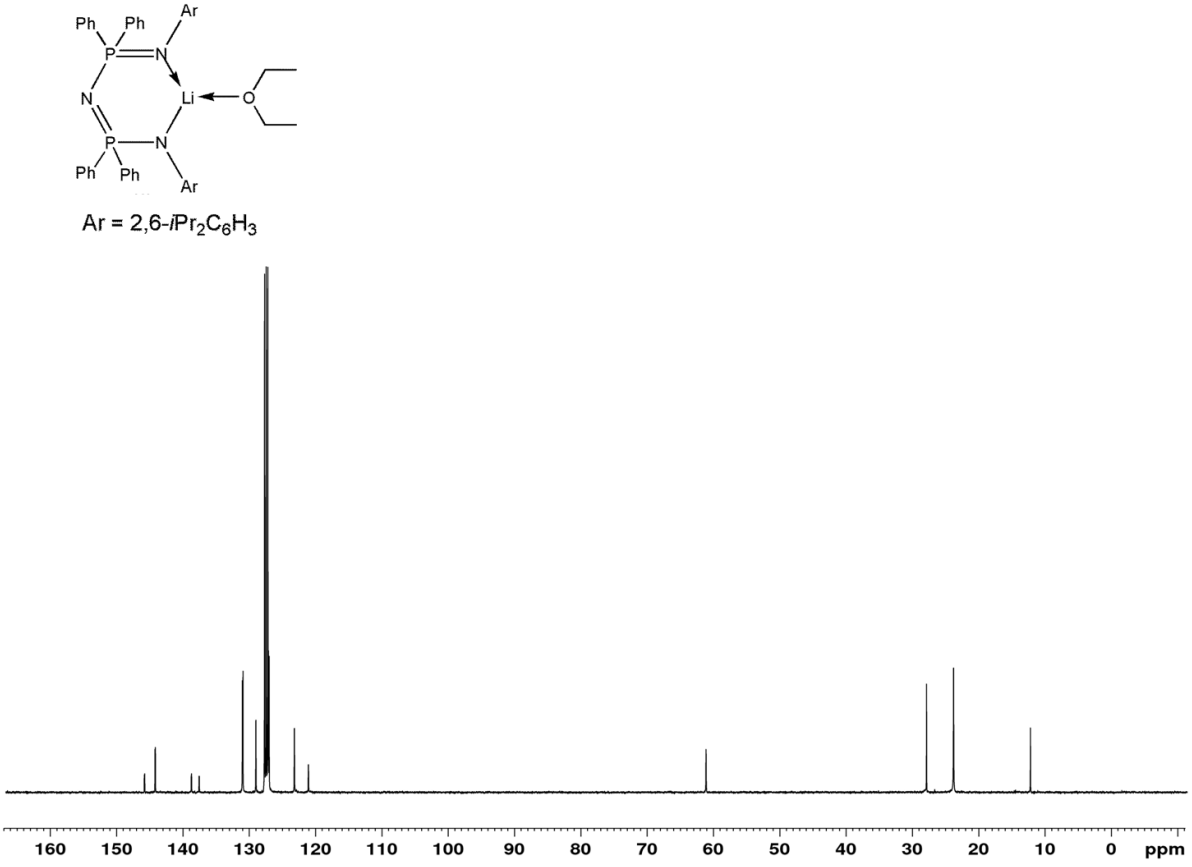

Fig. S9 ^{13}C NMR (100 MHz, C_6D_6) spectrum of [{N(Ph$_2$PN(2,6-*i*Pr$_2$C$_6$H$_3$N))$_2$}Li·OEt$_2$] (**1.2**).

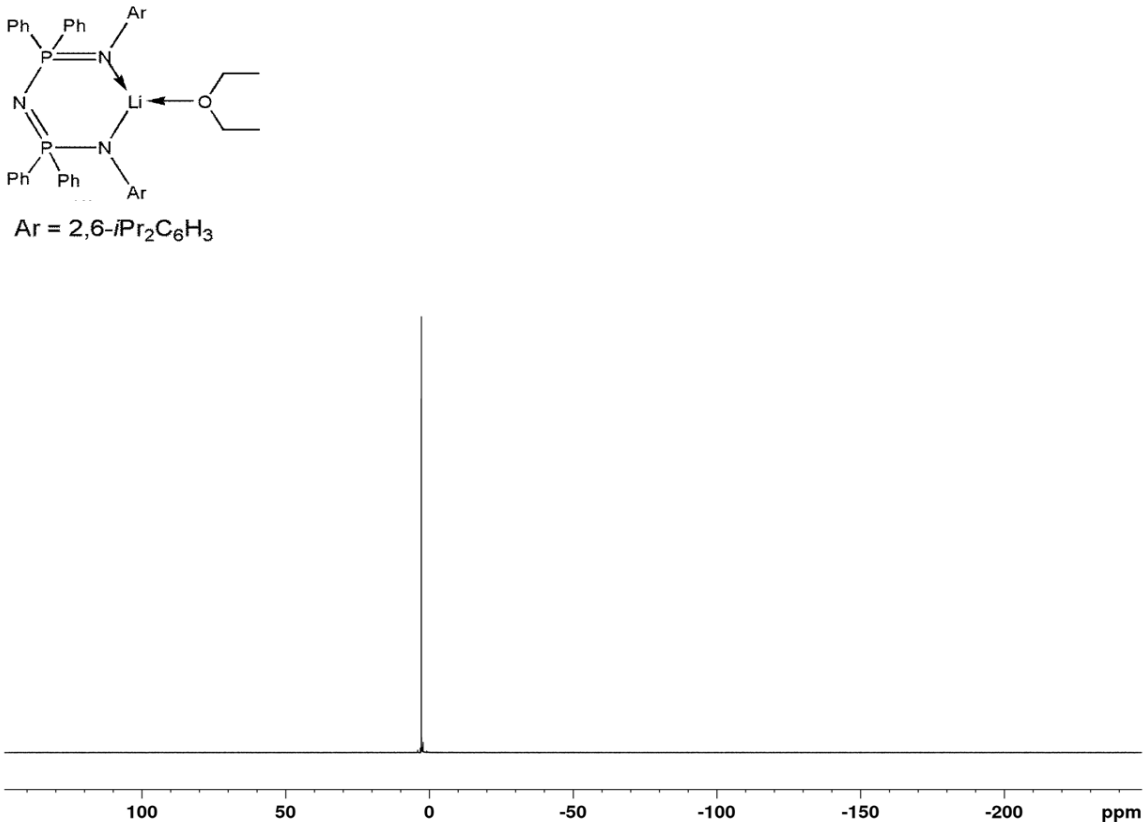

Fig. S10 ^{31}P{^{1}H} NMR (162 MHz, C_6D_6) spectrum of [{N(Ph$_2$PN(2,6-*i*Pr$_2$C$_6$H$_3$N))$_2$}Li·OEt$_2$] (**1.2**).

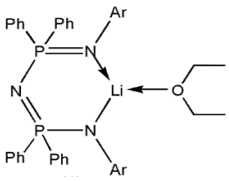

Ar = 2,6-*i*Pr$_2$C$_6$H$_3$

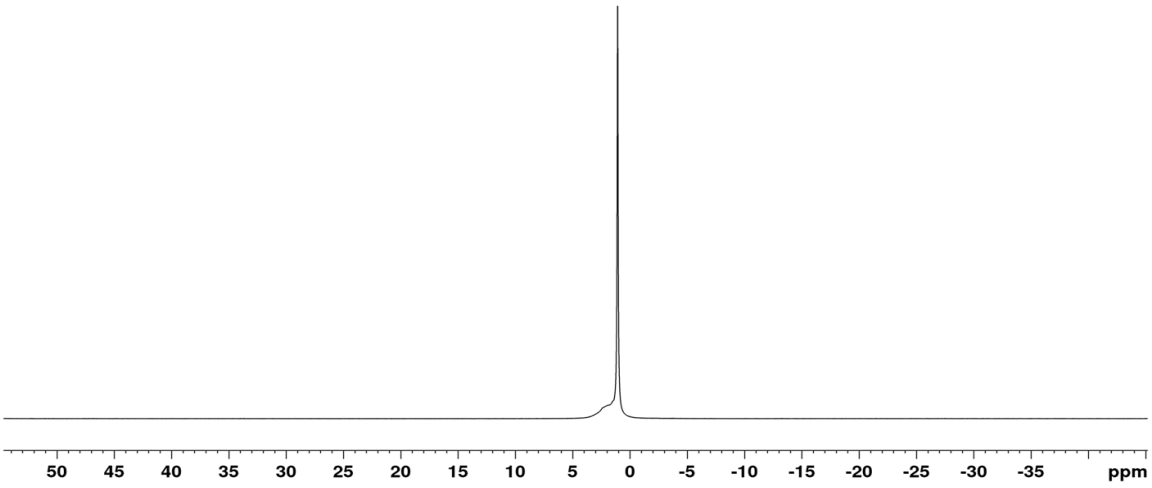

Fig. S11 ^{7}Li NMR (155 MHz, C_6D_6) spectrum of [{N(Ph$_2$PN(2,6-*i*Pr$_2$C$_6$H$_3$N))$_2$}Li·OEt2] (**1.2**).

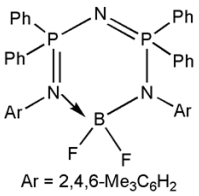

Ar = 2,4,6-Me$_3$C$_6$H$_2$

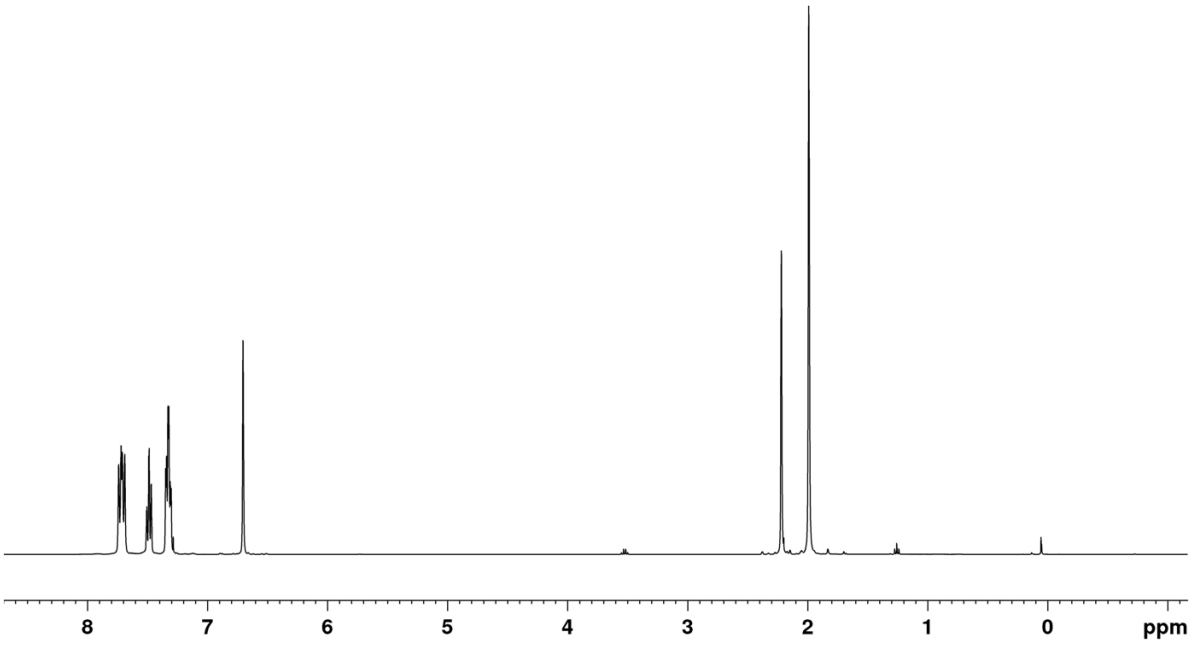

Fig. S12 ^{1}H NMR (400 MHz, $CDCl_3$) spectrum of [{N(Ph$_2$PN(2,4,6-Me$_3$C$_6$H$_2$N))$_2$}BF$_2$] (**1.3**).

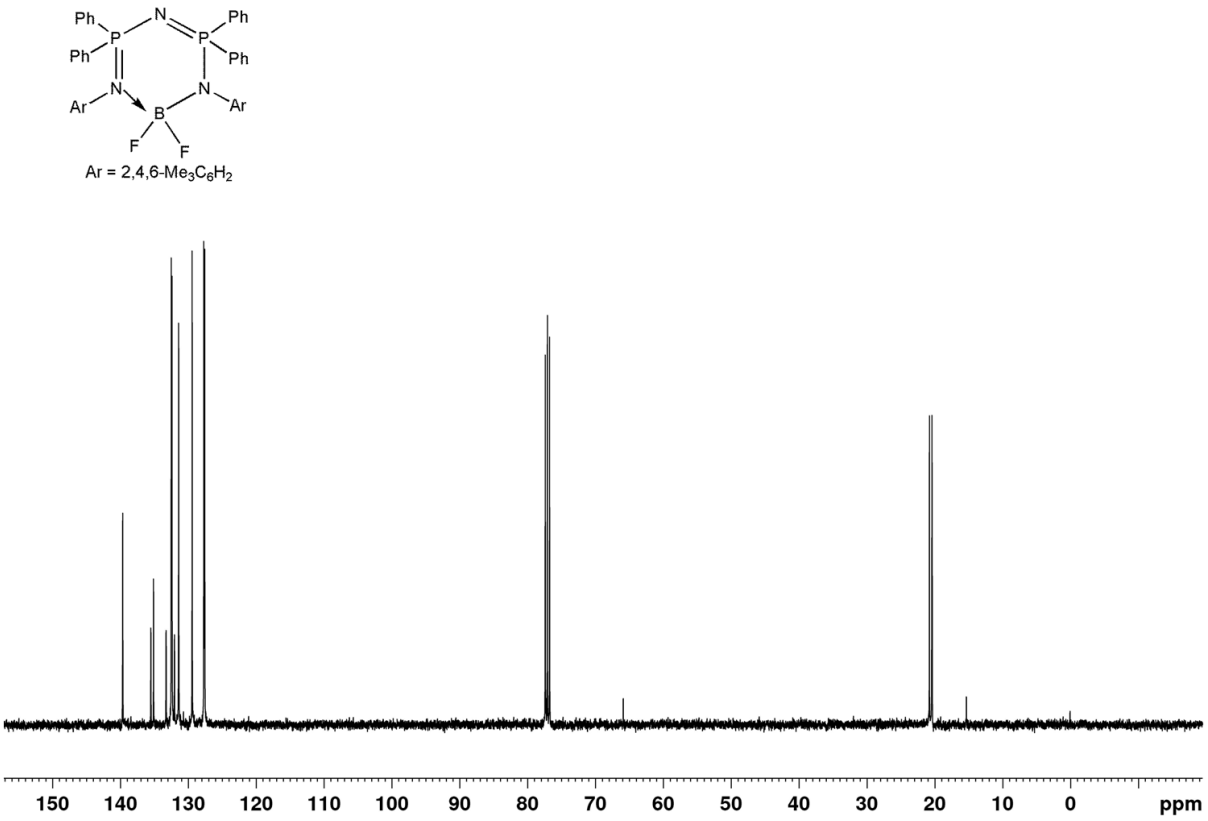

Fig. S13 ^{13}C NMR (100 MHz, $CDCl_3$) spectrum of [{N(Ph_2PN(2,4,6-$Me_3C_6H_2N$))$_2$}BF_2] (**1.3**).

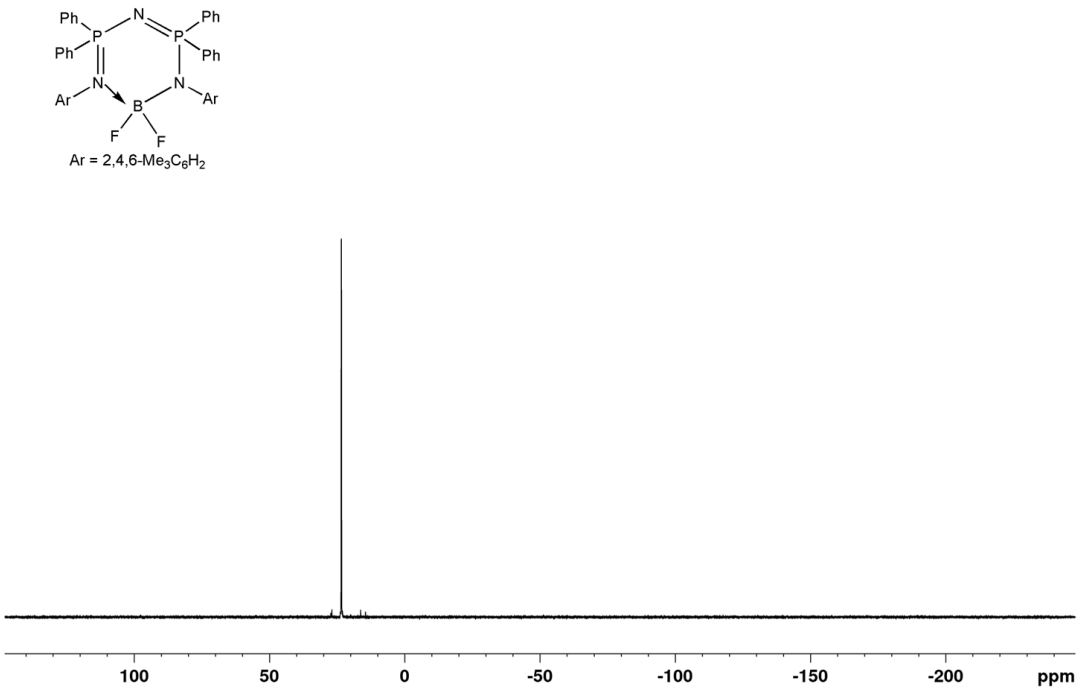

Fig. S14 $^{31}P\{^1H\}$ NMR (162 MHz, $CDCl_3$) spectrum of [{N(Ph_2PN(2,4,6-$Me_3C_6H_2N$))$_2$}BF_2] (**1.3**).

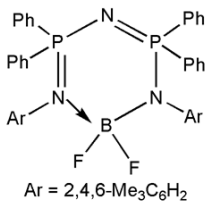

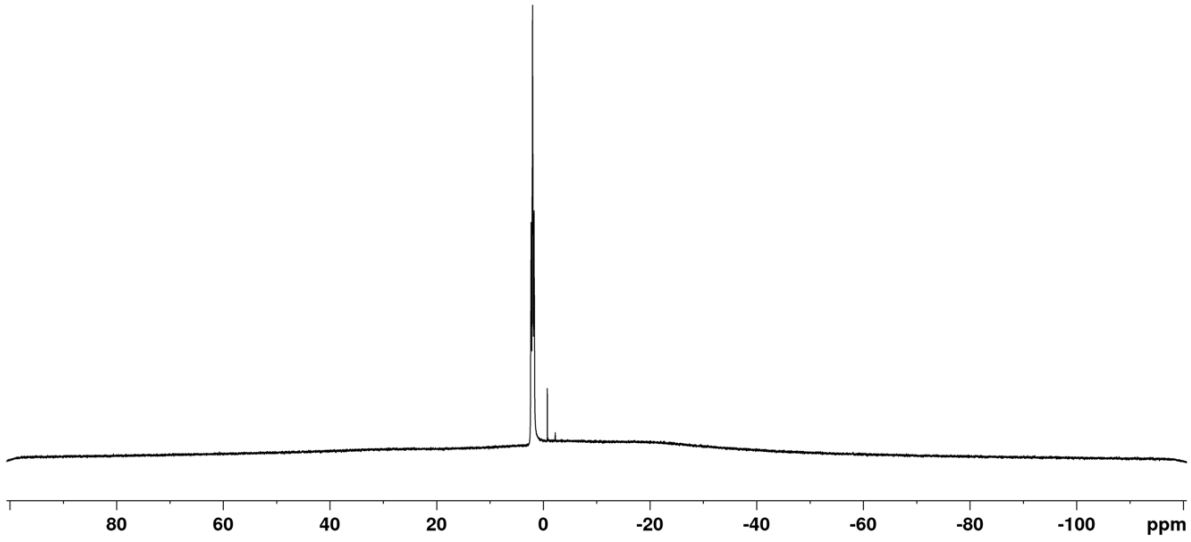

Fig. S15 ^{11}B NMR (128 MHz, $CDCl_3$) spectrum of [{N(Ph_2PN(2,4,6-$Me_3C_6H_2N$))$_2$}BF_2] (**1.3**).

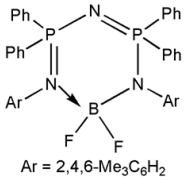

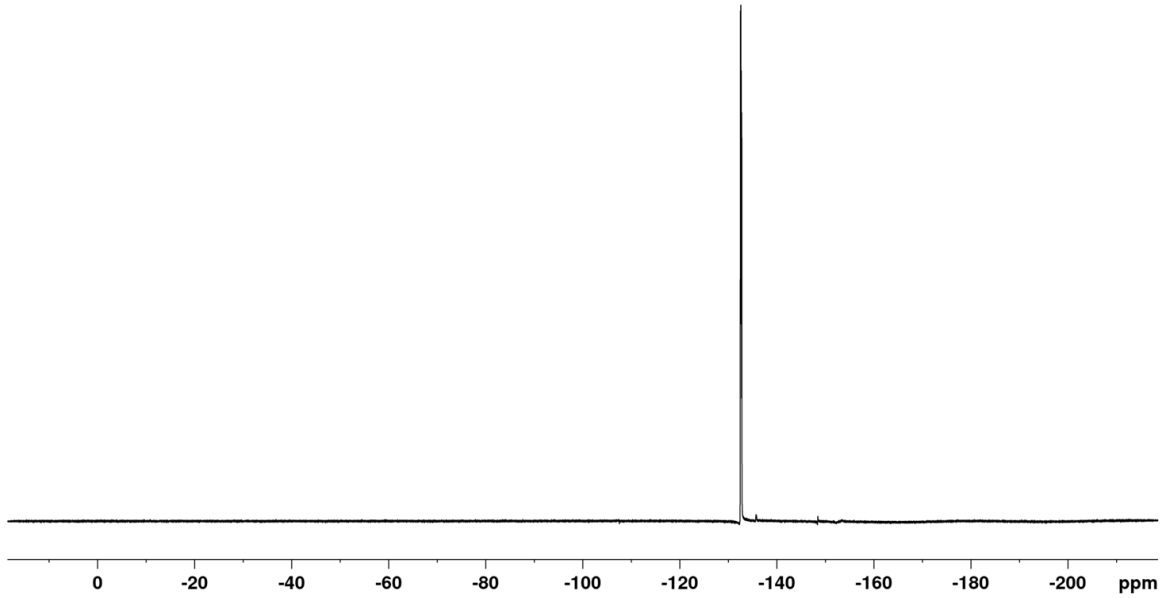

Fig. S16 ^{19}F NMR (376 MHz, $CDCl_3$) spectrum of [{N(Ph_2PN(2,4,6-$Me_3C_6H_2N$))$_2$}BF_2] (**1.3**).

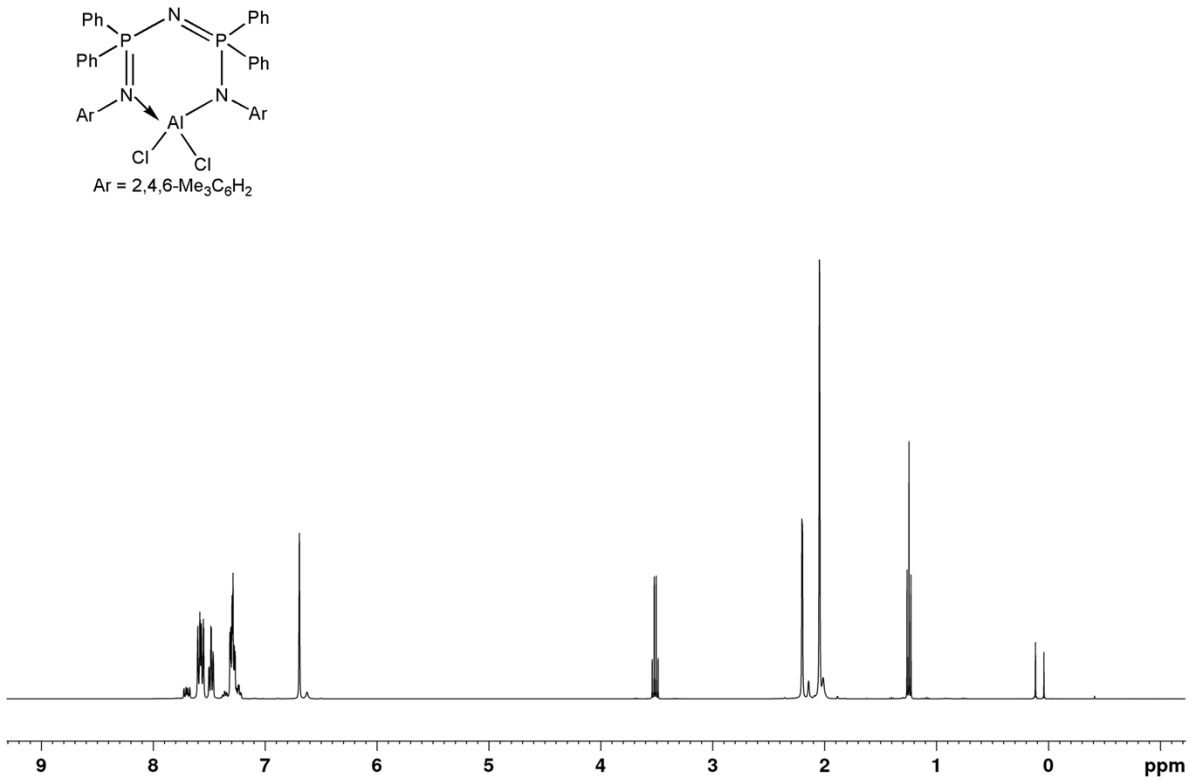

Fig. S17 ^{1}H NMR (400 MHz, $CDCl_3$) spectrum of [{N(Ph_2PN(2,4,6-$Me_3C_6H_2N$))$_2$}$AlCl_2$] (**1.4**).

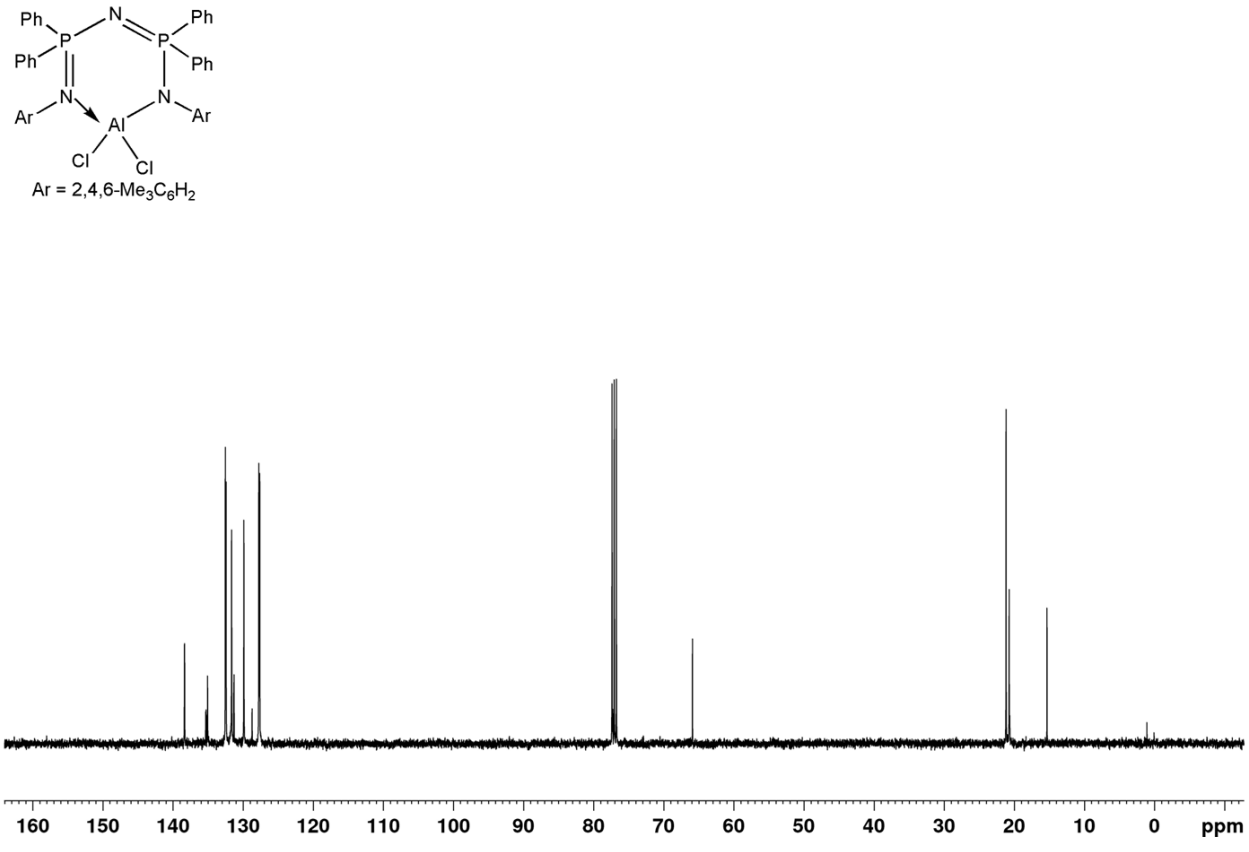

Fig. S18 ^{13}C NMR (100 MHz, $CDCl_3$) spectrum of [{N(Ph_2PN(2,4,6-$Me_3C_6H_2N$))$_2$}$AlCl_2$] (**1.4**).

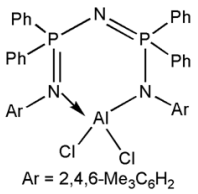

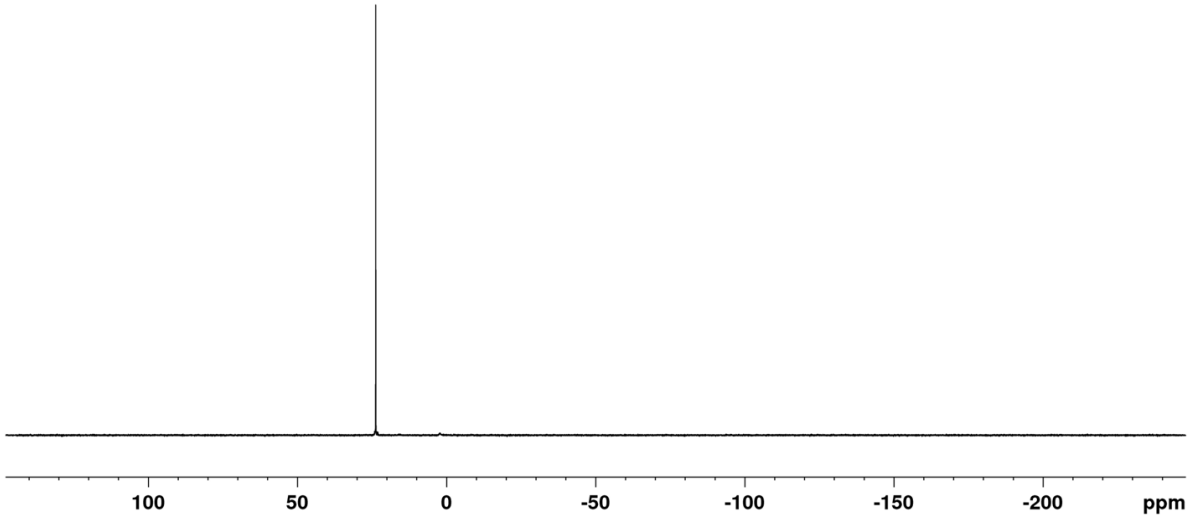

Fig. S19 $^{31}P\{^{1}H\}$ NMR (162 MHz, $CDCl_3$) spectrum of $[\{N(Ph_2PN(2,4,6\text{-}Me_3C_6H_2N))_2\}AlCl_2]$ (**1.4**).

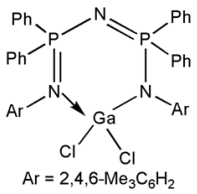

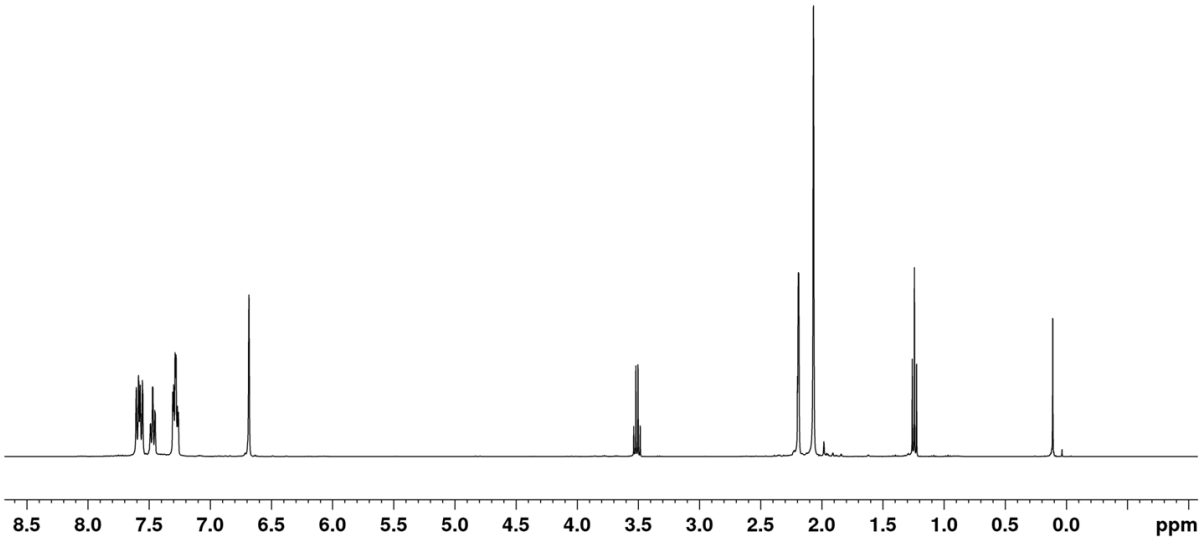

Fig. S20 ^{1}H NMR (400 MHz, $CDCl_3$) spectrum of $[\{N(Ph_2PN(2,4,6\text{-}Me_3C_6H_2N))_2\}GaCl_2]$ (**1.5**).

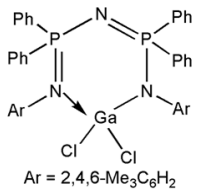

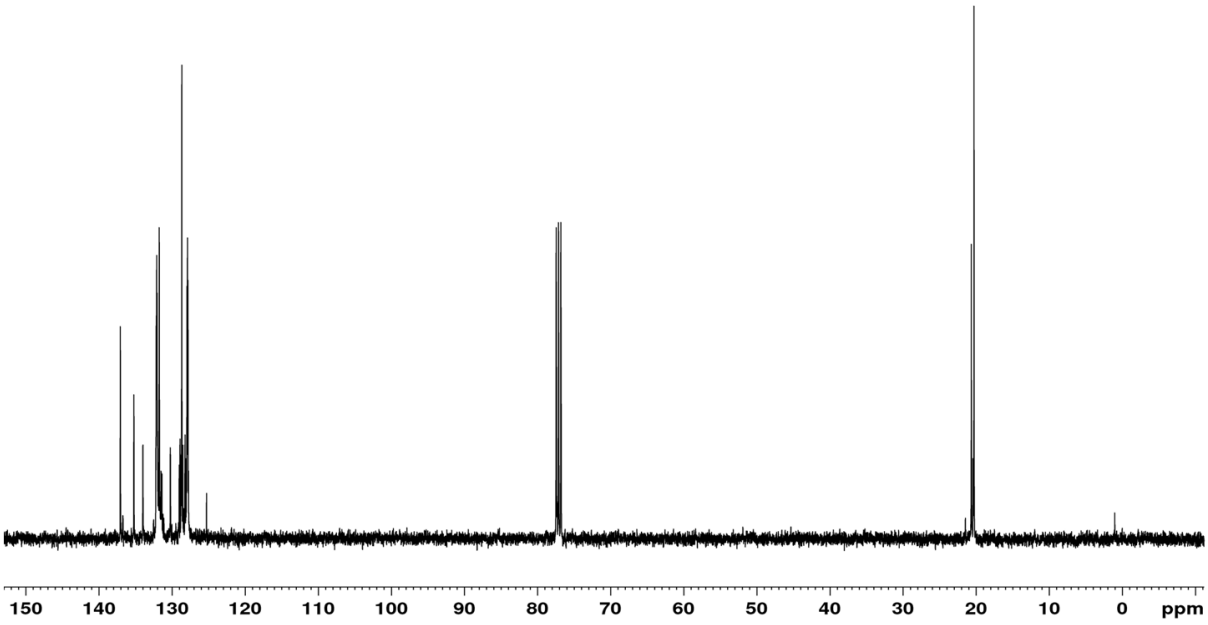

Fig. S21 ^{13}C NMR (100 MHz, $CDCl_3$) spectrum of [{N(Ph_2PN(2,4,6-$Me_3C_6H_2N$))$_2$}$GaCl_2$] (**1.5**).

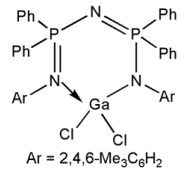

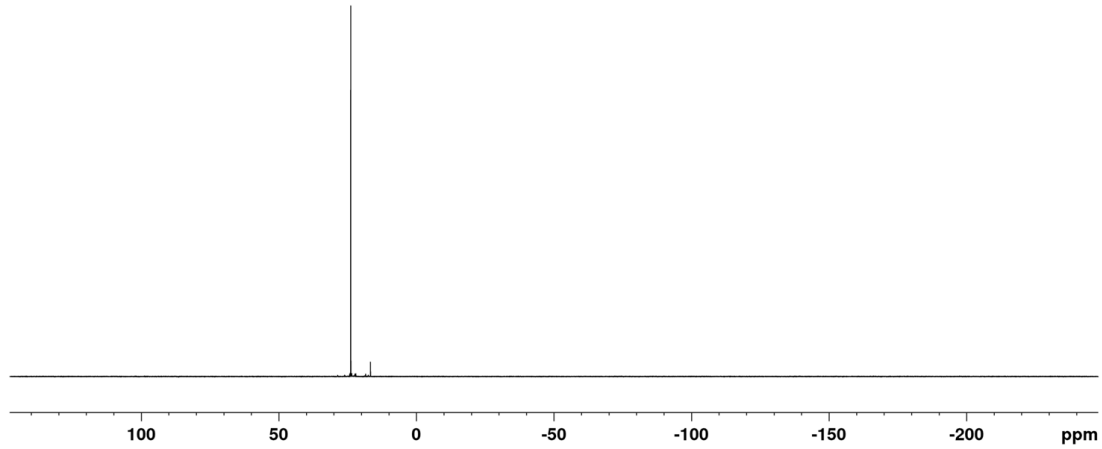

Fig. S22 $^{31}P\{^1H\}$ NMR (162 MHz, $CDCl_3$) spectrum of [{N(Ph_2PN(2,4,6-$Me_3C_6H_2N$))$_2$}$GaCl_2$] (**1.5**).

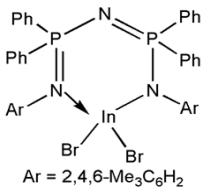

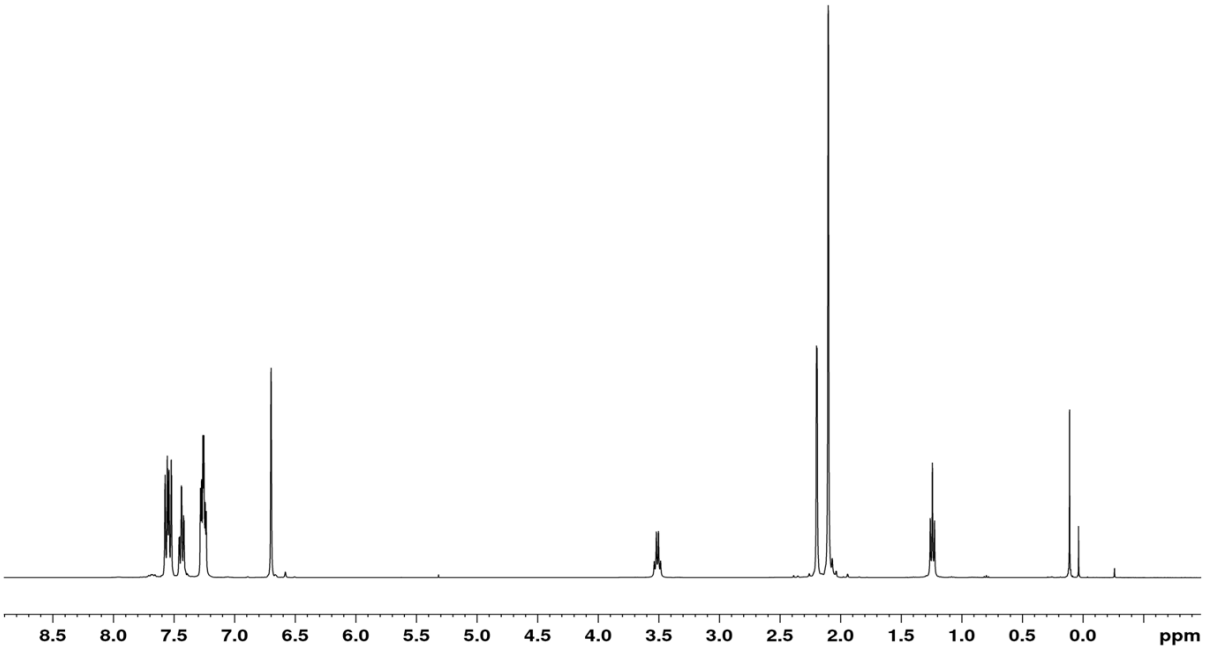

Fig. S23 ^{1}H NMR (400 MHz, $CDCl_3$) spectrum of [{N(Ph_2PN(2,4,6-$Me_3C_6H_2N$))$_2$}$InBr_2$] (**1.6**).

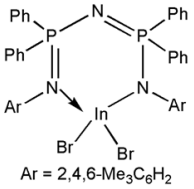

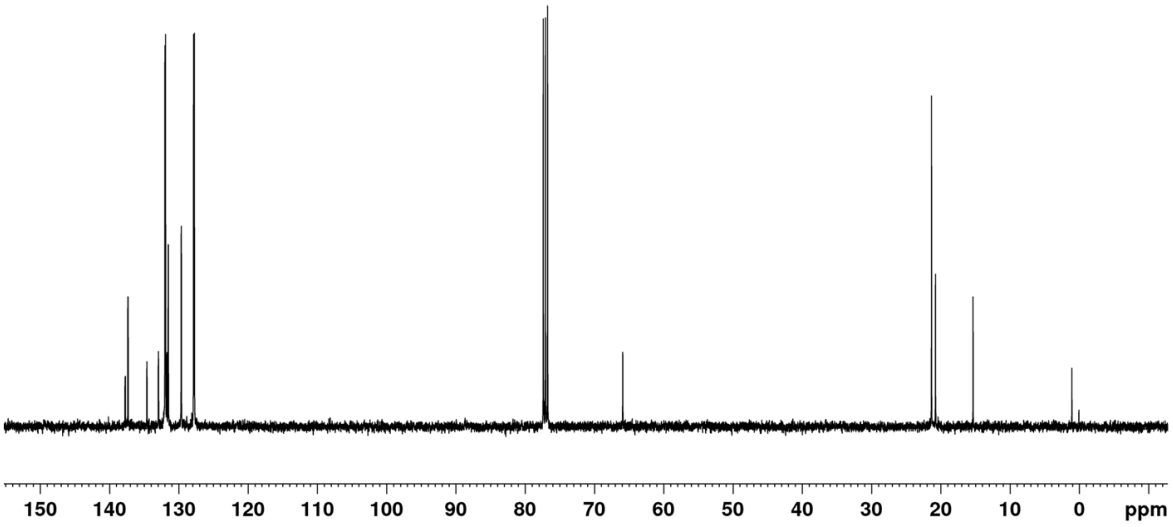

Fig. S24 ^{13}C NMR (100 MHz, $CDCl_3$) spectrum of [{N(Ph_2PN(2,4,6-$Me_3C_6H_2N$))$_2$}$InBr_2$] (**1.6**).

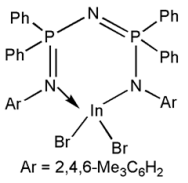

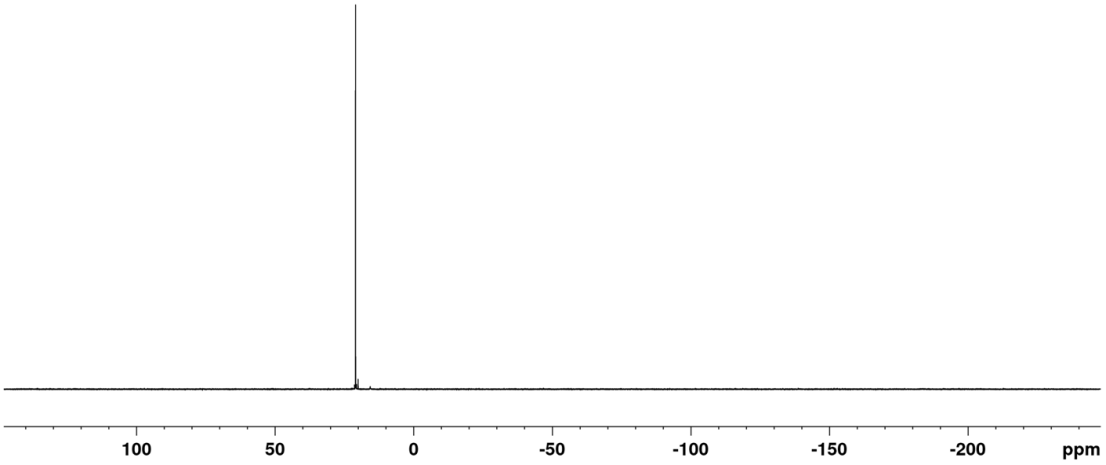

Fig. S25 $^{31}P\{^{1}H\}$ NMR (162 MHz, $CDCl_3$) spectrum of [{N($Ph_2PN(2,4,6\text{-}Me_3C_6H_2N)$)$_2$}$InBr_2$] (**1.6**).

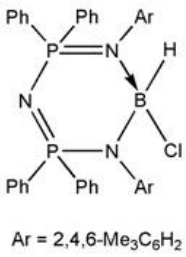

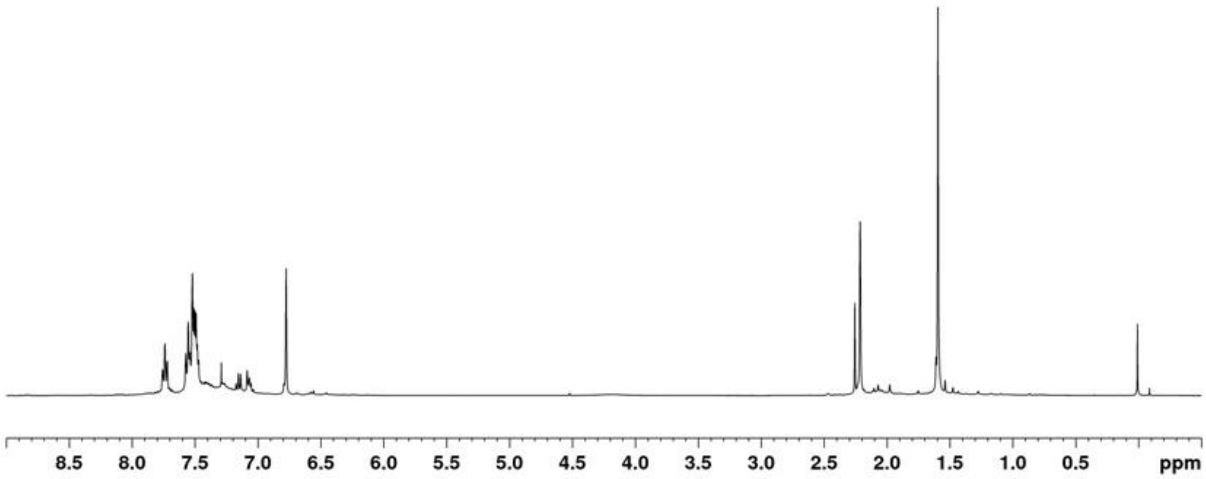

Fig. S26 ^{1}H NMR (400 MHz, $CDCl_3$) spectrum of [{N($Ph_2PN(2,4,6\text{-}Me_3C_6H_2N)$)$_2$}BHCl] (**1.7**).

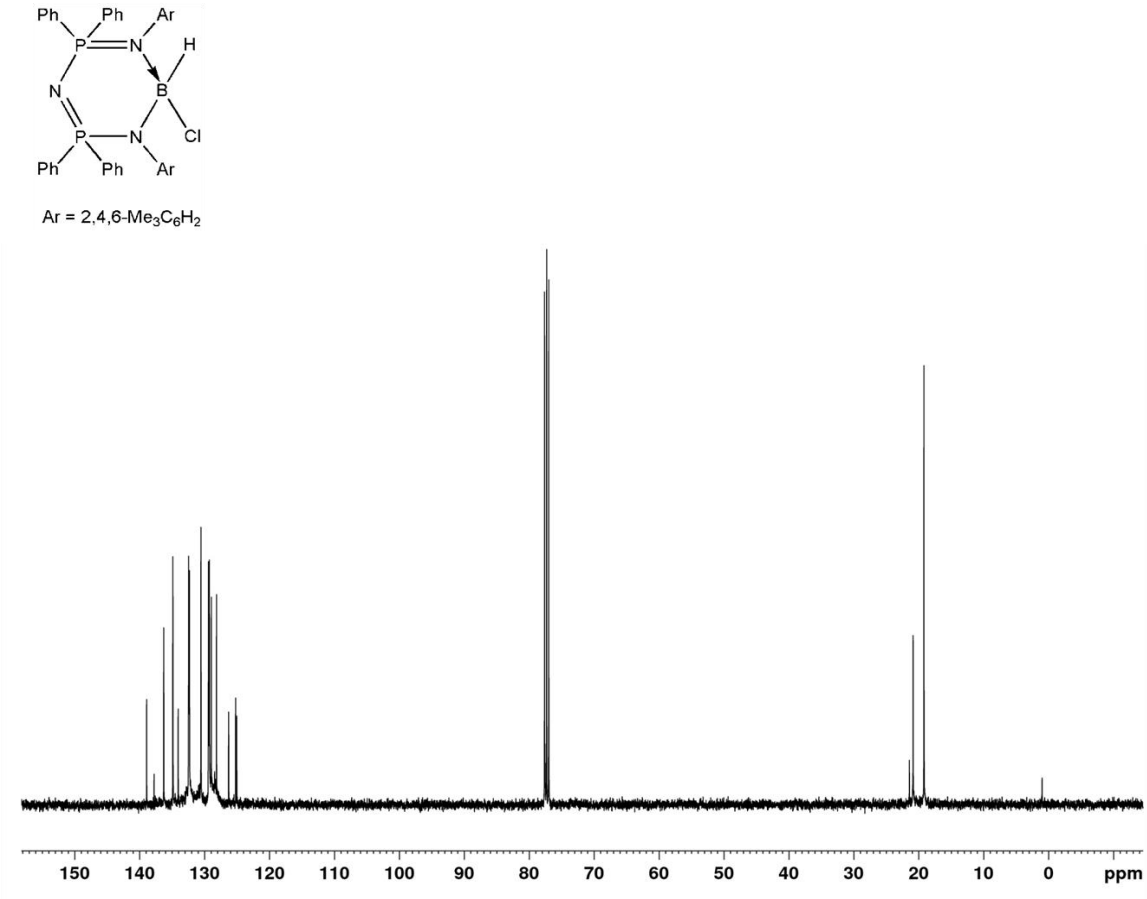

Fig. S27 ^{13}C NMR (100 MHz, $CDCl_3$) spectrum of [{N(Ph_2PN(2,4,6-$Me_3C_6H_2N$))$_2$}BHCl] (**1.7**).

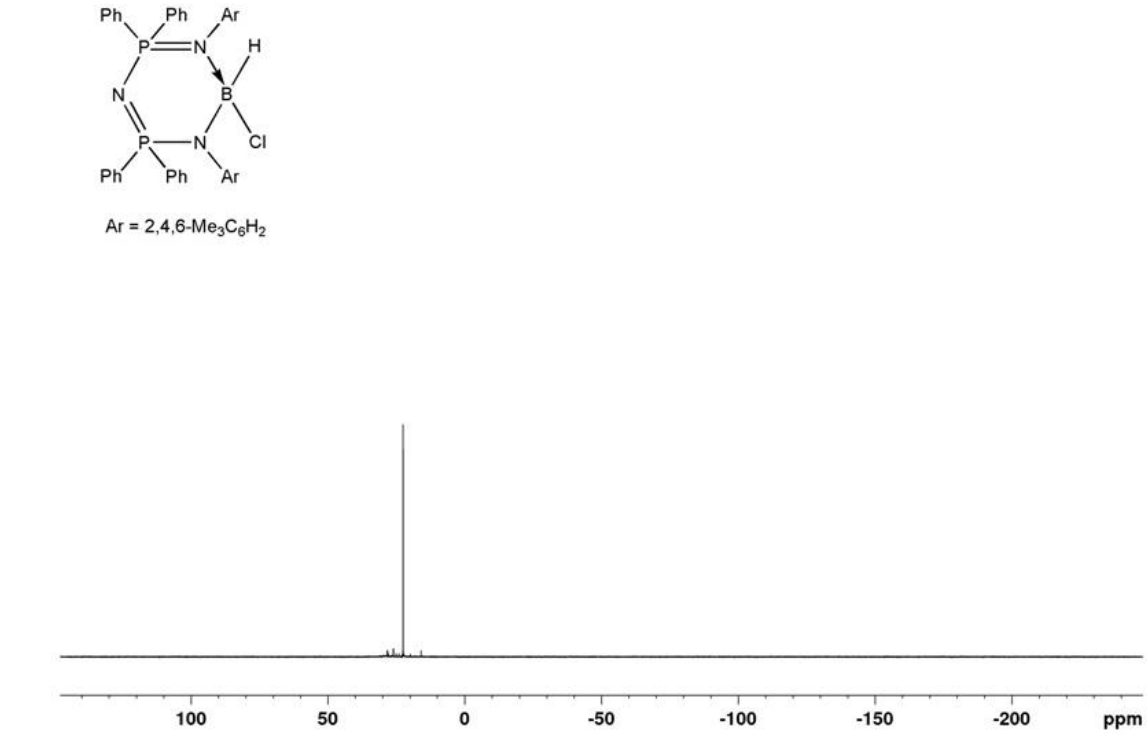

Fig. S28 $^{31}P\{^1H\}$ NMR (162 MHz, $CDCl_3$) spectrum of [{N(Ph_2PN(2,4,6-$Me_3C_6H_2N$))$_2$}BHCl] (**1.7**).

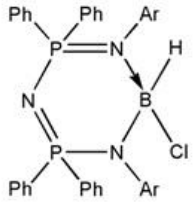

Ar = 2,4,6-$Me_3C_6H_2$

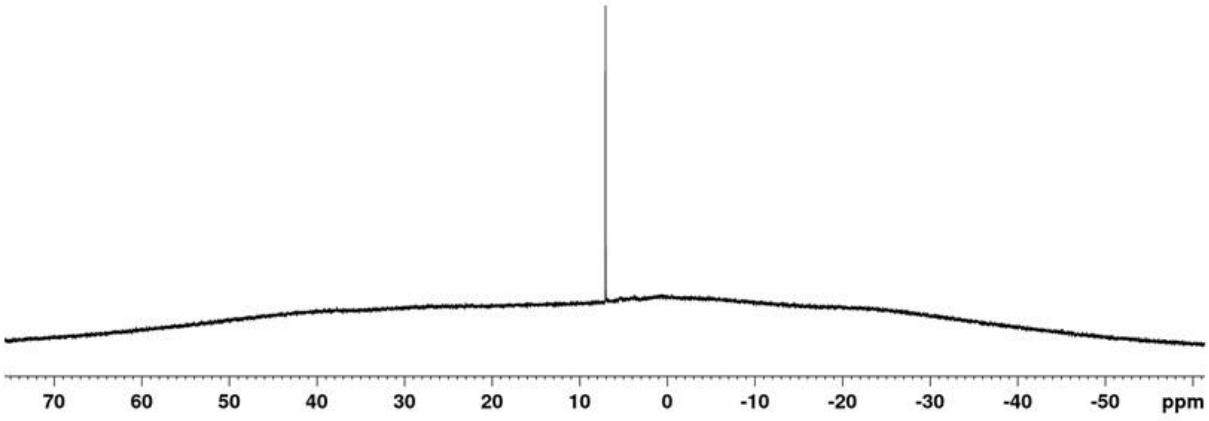

Fig. S29 ^{11}B NMR (128 MHz, $CDCl_3$) spectrum of [{$N(Ph_2PN(2,4,6\text{-}Me_3C_6H_2N))_2$}BHCl] (**1.7**).

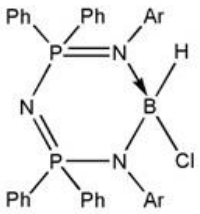

Ar = 2,6-*i*$Pr_2C_6H_3$

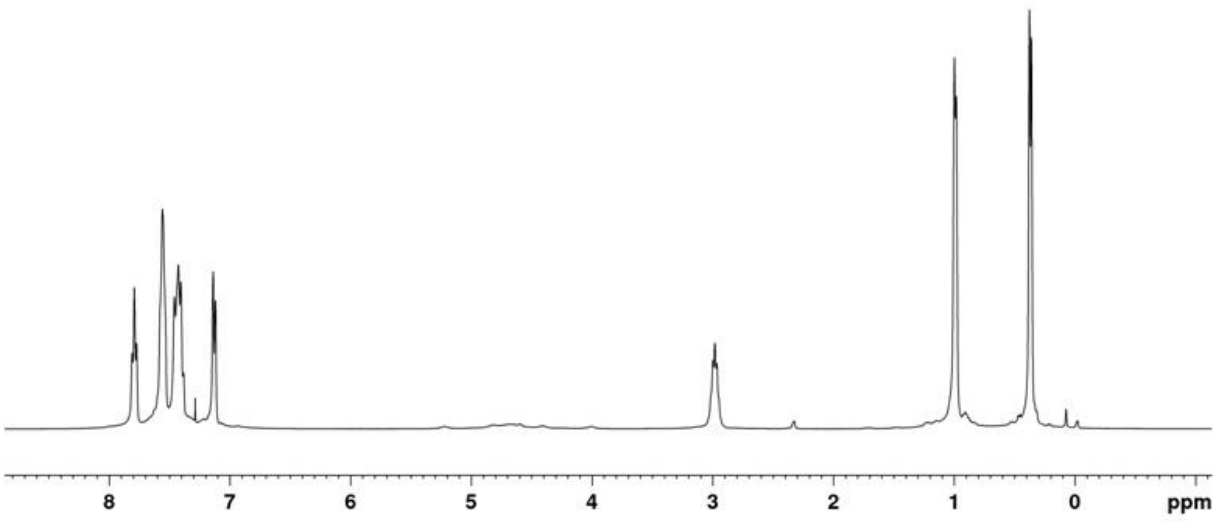

Fig. S30 ^{1}H NMR (400 MHz, $CDCl_3$) spectrum of [{$N(Ph_2PN(2,6\text{-}iPr_2C_6H_3N))_2$}BHCl] (**1.8**).

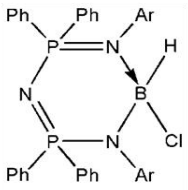

Ar = 2,4,6-$Me_3C_6H_2$

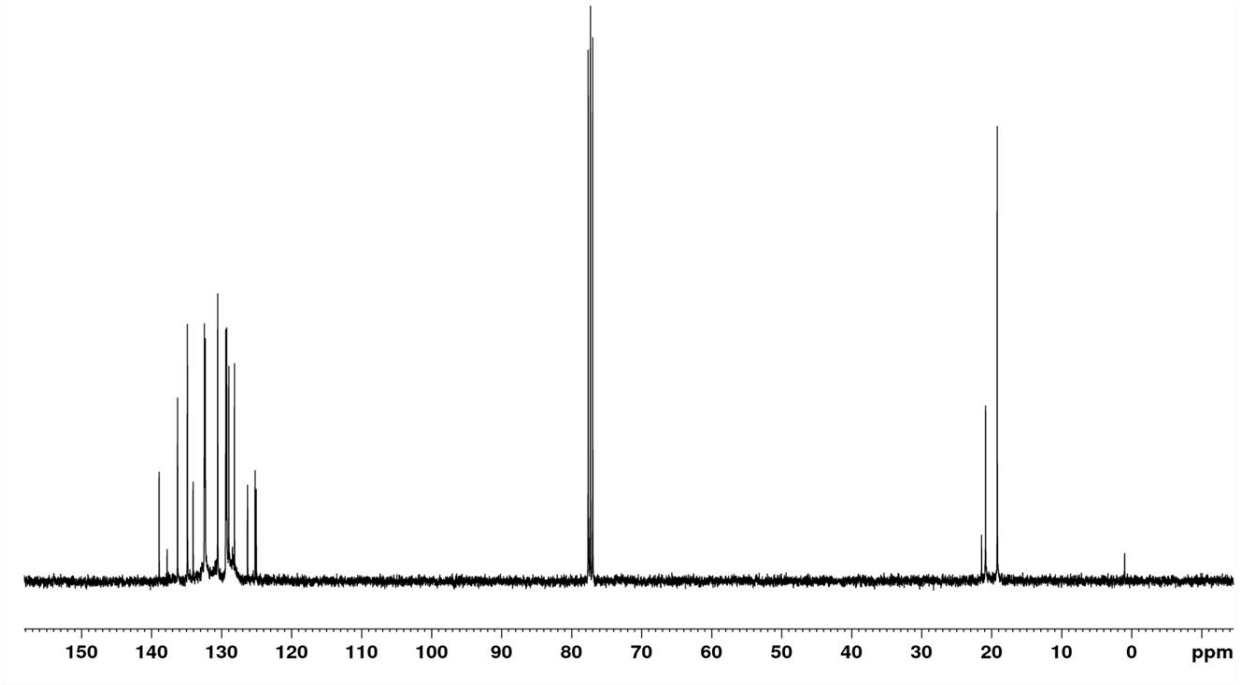

Fig. S31 ^{13}C NMR (100 MHz, $CDCl_3$) spectrum of [{N(Ph_2PN(2,6-*i*$Pr_2C_6H_3N$))$_2$}BHCl] (**1.8**).

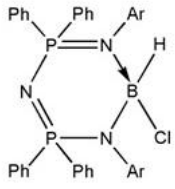

Ar = 2,6-*i*$Pr_2C_6H_3$

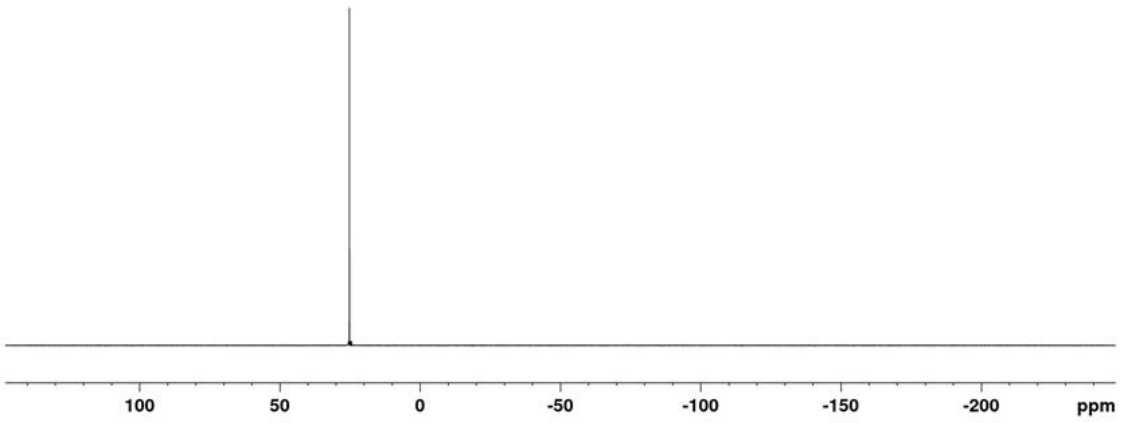

Fig. S32 $^{31}P\{^1H\}$ NMR (162 MHz, $CDCl_3$) spectrum of [{N(Ph_2PN(2,6-*i*$Pr_2C_6H_3N$))$_2$}BHCl] (**1.8**).

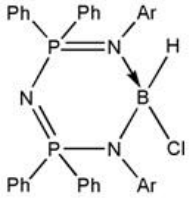

Ar = 2,6-*i*Pr$_2$C$_6$H$_3$

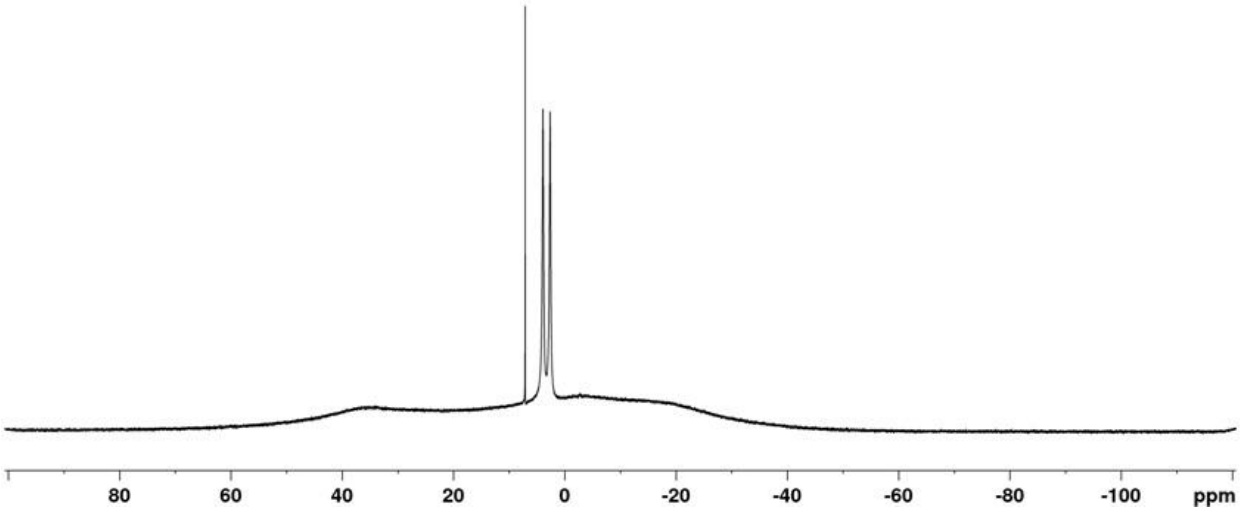

Fig. S33 ^{11}B NMR (128 MHz, $CDCl_3$) spectrum of [{N(Ph$_2$PN(2,6-*i*Pr$_2$C$_6$H$_3$N))$_2$}BHCl] **1.8**).

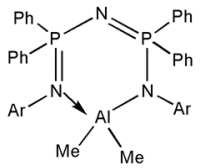

Ar = 2,4,6-Me$_3$C$_6$H$_2$

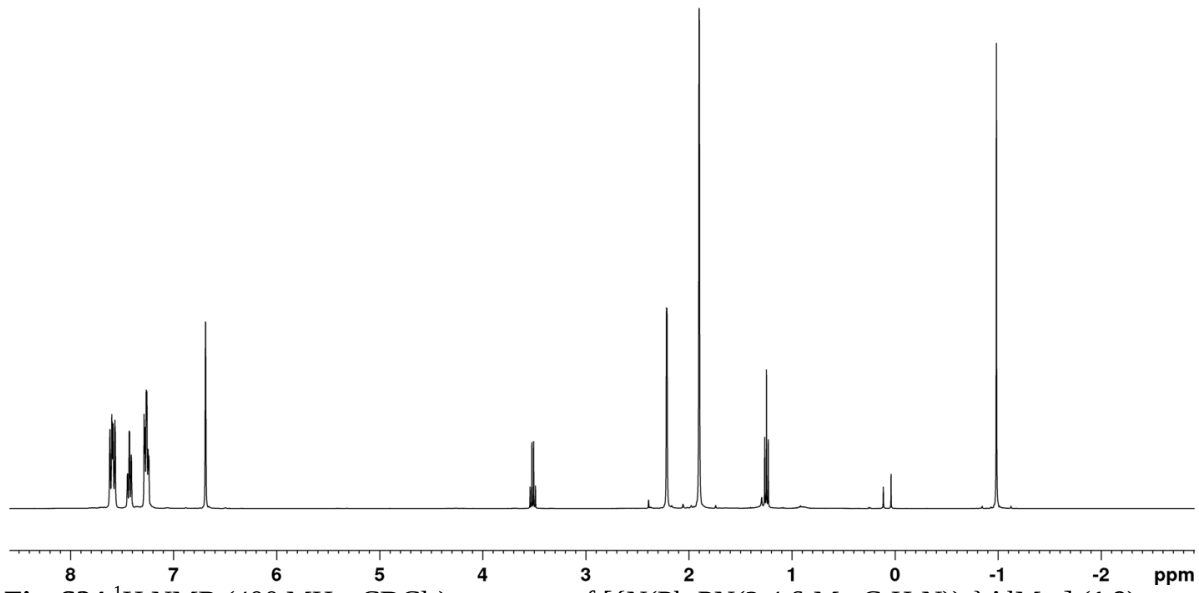

Fig. S34 ^{1}H NMR (400 MHz, $CDCl_3$) spectrum of [{N(Ph$_2$PN(2,4,6-Me$_3$C$_6$H$_2$N))$_2$}AlMe$_2$] (**1.9**).

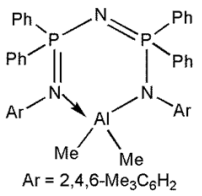

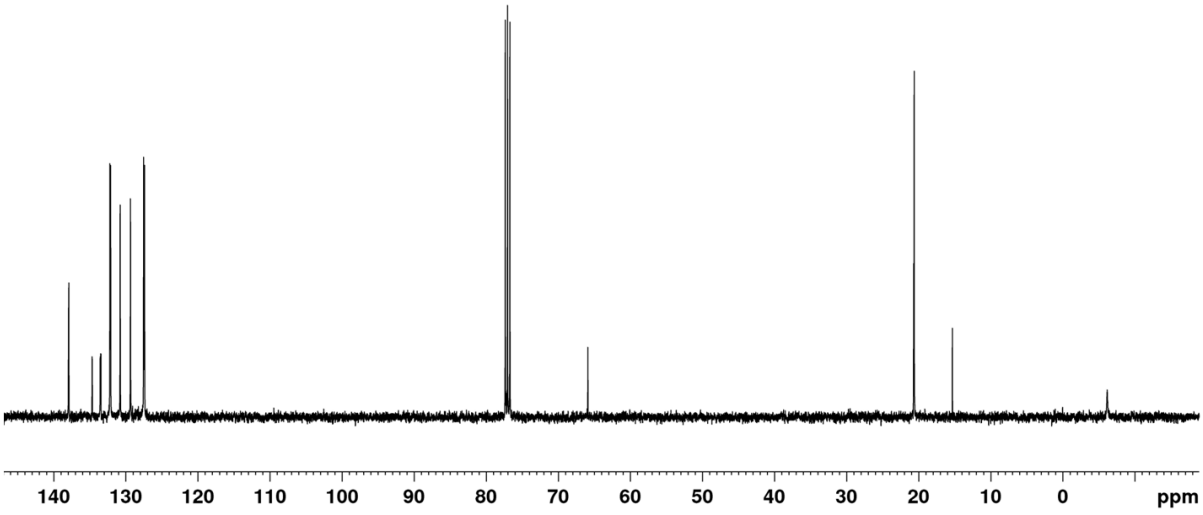

Fig. S35 ^{13}C NMR (100 MHz, $CDCl_3$) spectrum of [{N(Ph_2PN(2,4,6-$Me_3C_6H_2N$))$_2$}$AlMe_2$] (**1.9**).

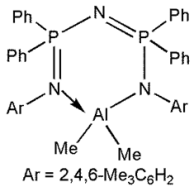

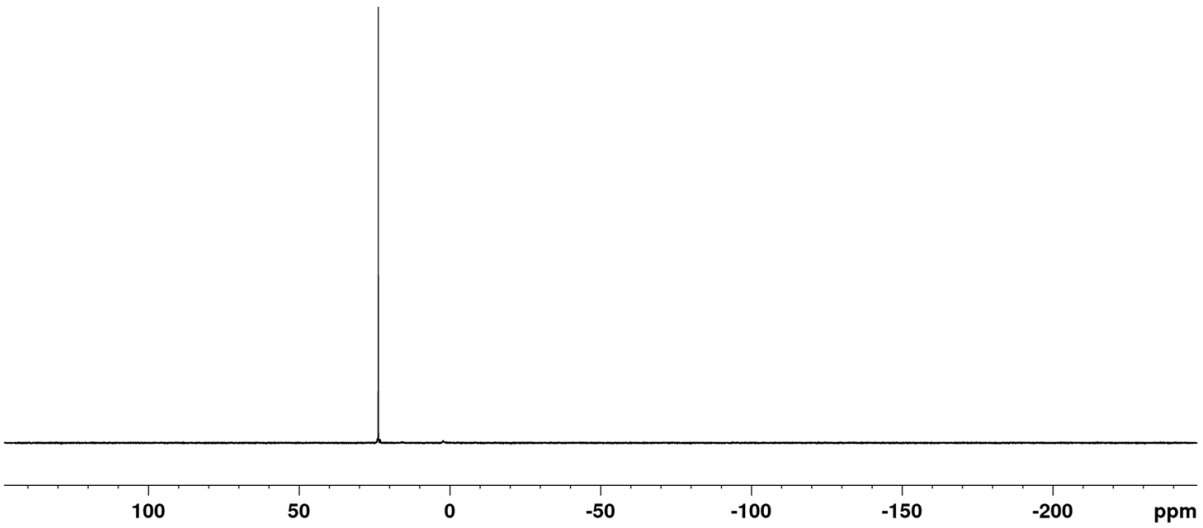

Fig. S36 $^{31}P\{^1H\}$ NMR (162 MHz, $CDCl_3$) spectrum of [{N(Ph_2PN(2,4,6-$Me_3C_6H_2N$))$_2$}$AlMe_2$] (**1.9**).

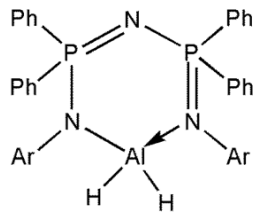

Ar = 2,4,6-$Me_3C_6H_2$

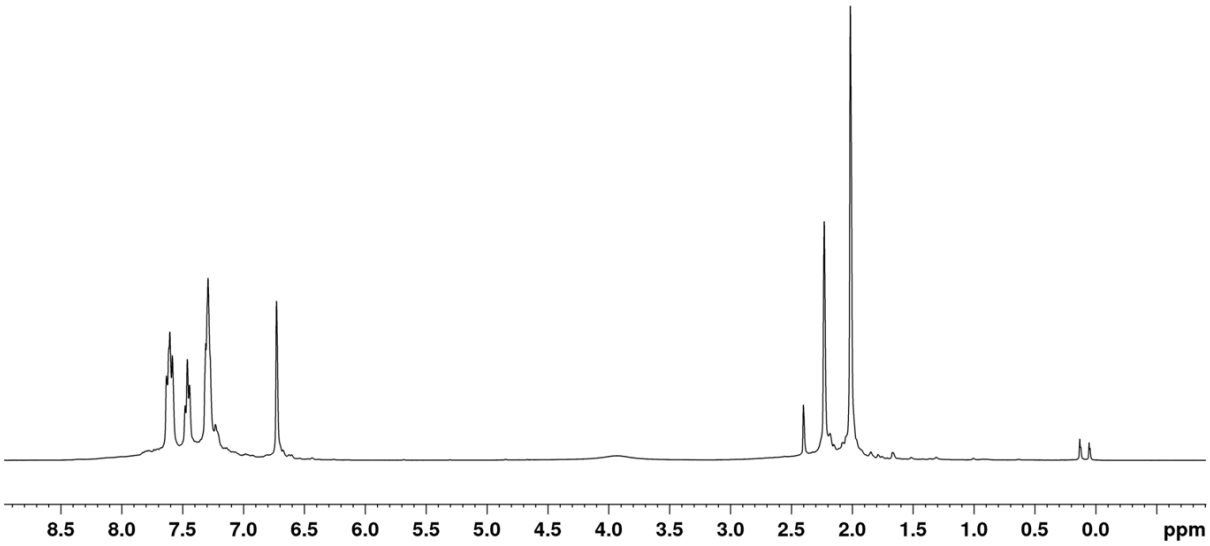

Fig. S37 ^{1}H NMR (400 MHz, $CDCl_3$) spectrum of [{N(Ph_2PN(2,4,6-$Me_3C_6H_2N$))$_2$}AlH_2] (**1.10**).

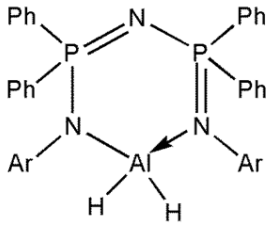

Ar = 2,4,6-$Me_3C_6H_2$

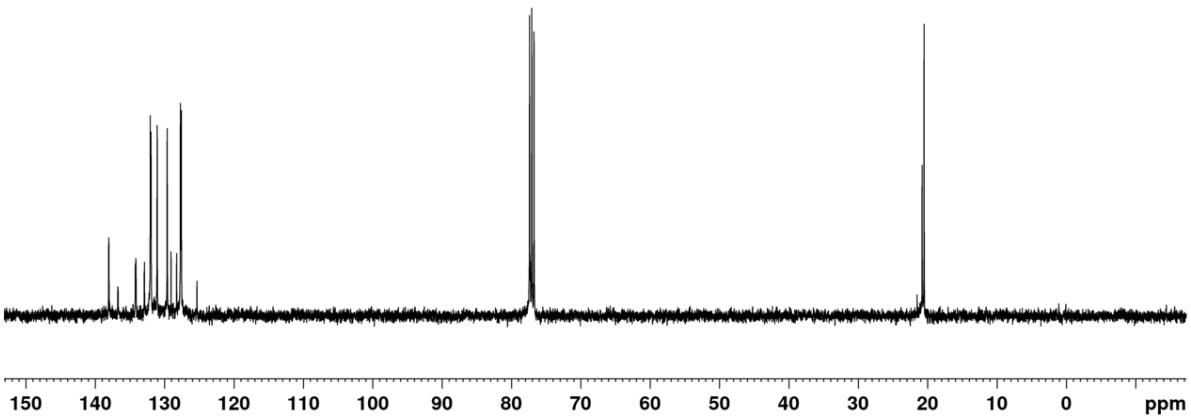

Fig. S38 ^{13}C NMR (100 MHz, $CDCl_3$) spectrum of [{N(Ph_2PN(2,4,6-$Me_3C_6H_2N$))$_2$}AlH_2] (**1.10**).

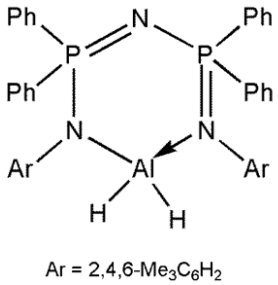

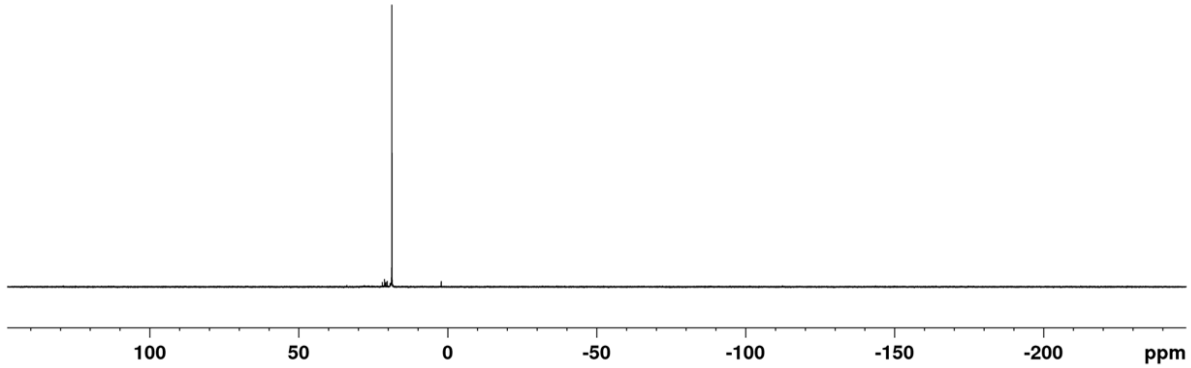

Fig. S39 $^{31}P\{^{1}H\}$ NMR (162 MHz, $CDCl_3$) spectrum of $[\{N(Ph_2PN(2,4,6\text{-}Me_3C_6H_2N))_2\}AlH_2]$ (**1.10**).

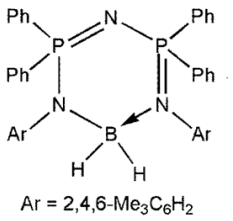

Fig. S40 ^{1}H NMR (400 MHz, $CDCl_3$) spectrum of $[\{N(Ph_2PN(2,4,6\text{-}Me_3C_6H_2N))_2\}BH_2]$ (**1.11**).

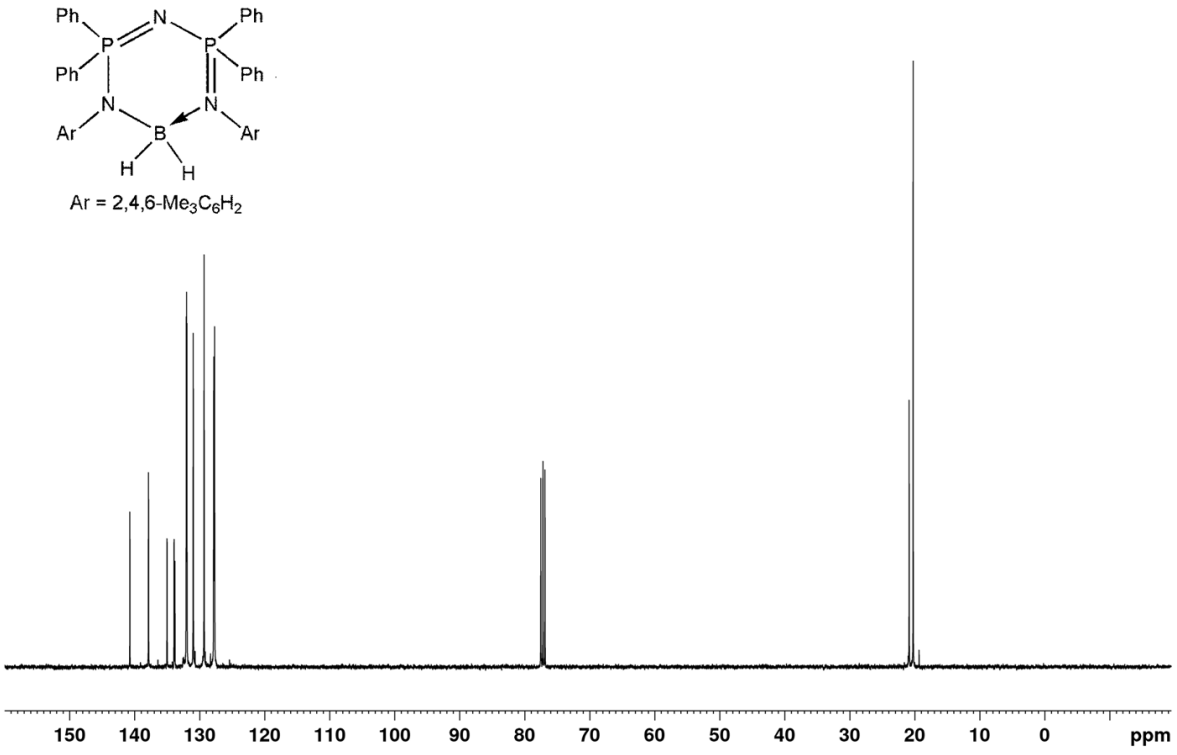

Fig. S41 ^{13}C NMR (100 MHz, $CDCl_3$) spectrum of [{N(Ph_2PN(2,4,6-$Me_3C_6H_2N$))$_2$}BH_2] (**1.11**).

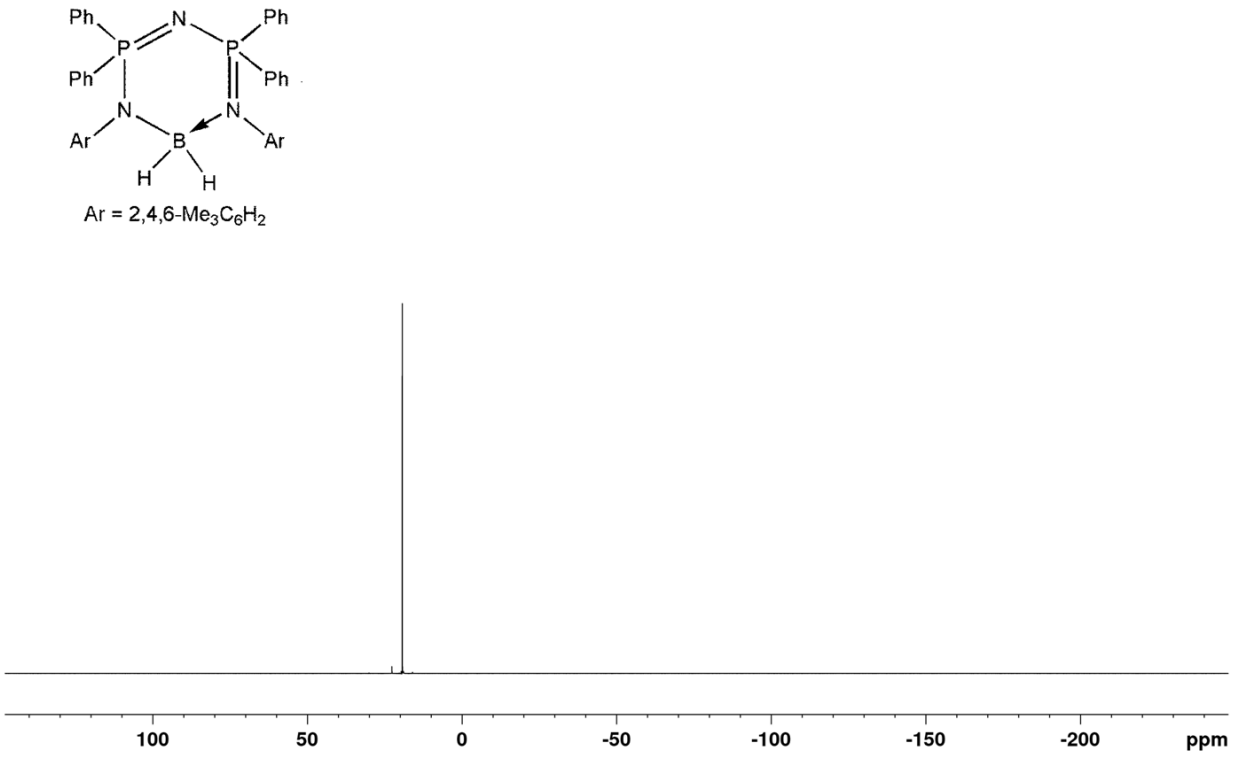

Fig. S42 $^{31}P\{^1H\}$ NMR (162 MHz, $CDCl_3$) spectrum of [{N(Ph_2PN(2,4,6-$Me_3C_6H_2N$))$_2$}BH_2] (**1.11**).

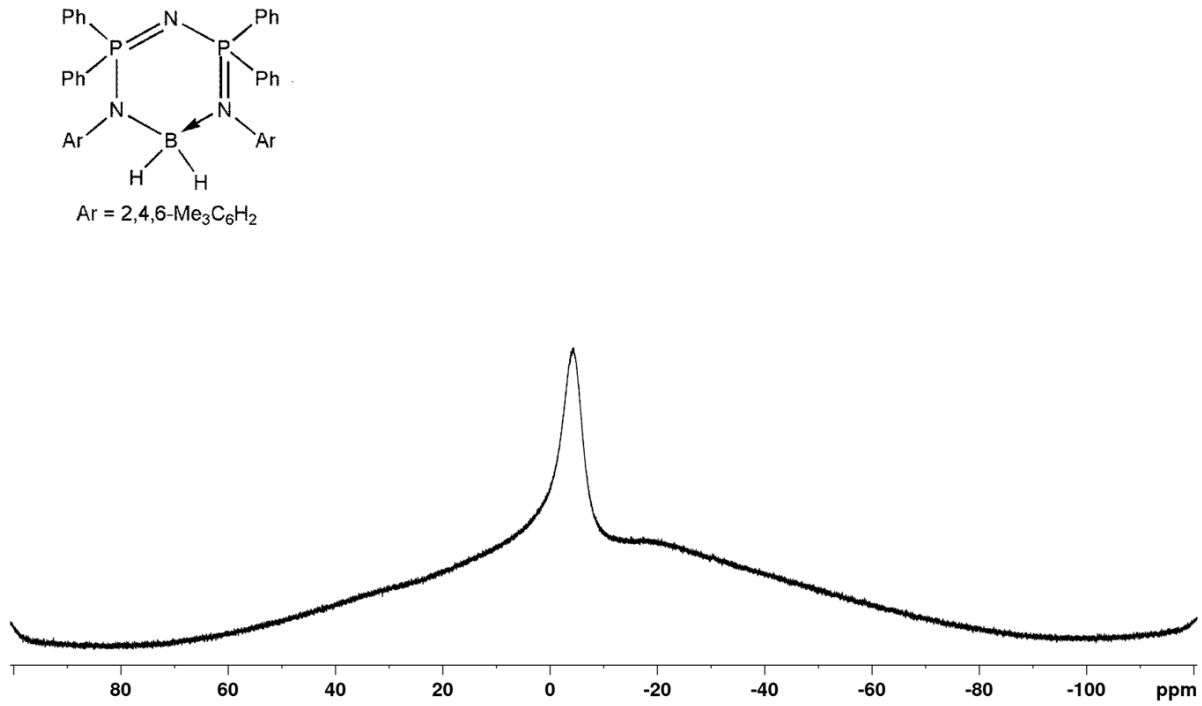

Fig. S43 ^{11}B NMR (128 MHz, $CDCl_3$) spectrum of [{N(Ph_2PN(2,4,6-$Me_3C_6H_2N$))$_2$}BH_2] (**1.11**).

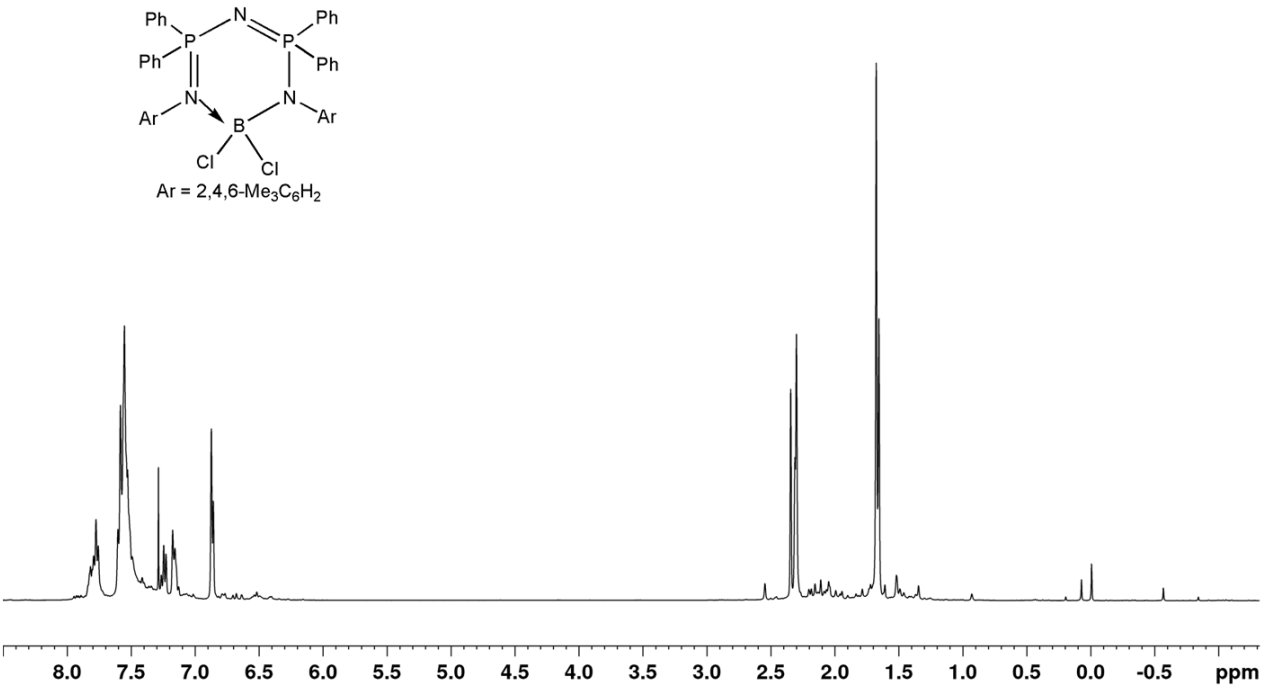

Fig. S44 ^{1}H NMR (400 MHz, $CDCl_3$) spectrum of [{N(Ph_2PN(2,4,6-$Me_3C_6H_2N$))$_2$}BCl_2] (**1.12**).

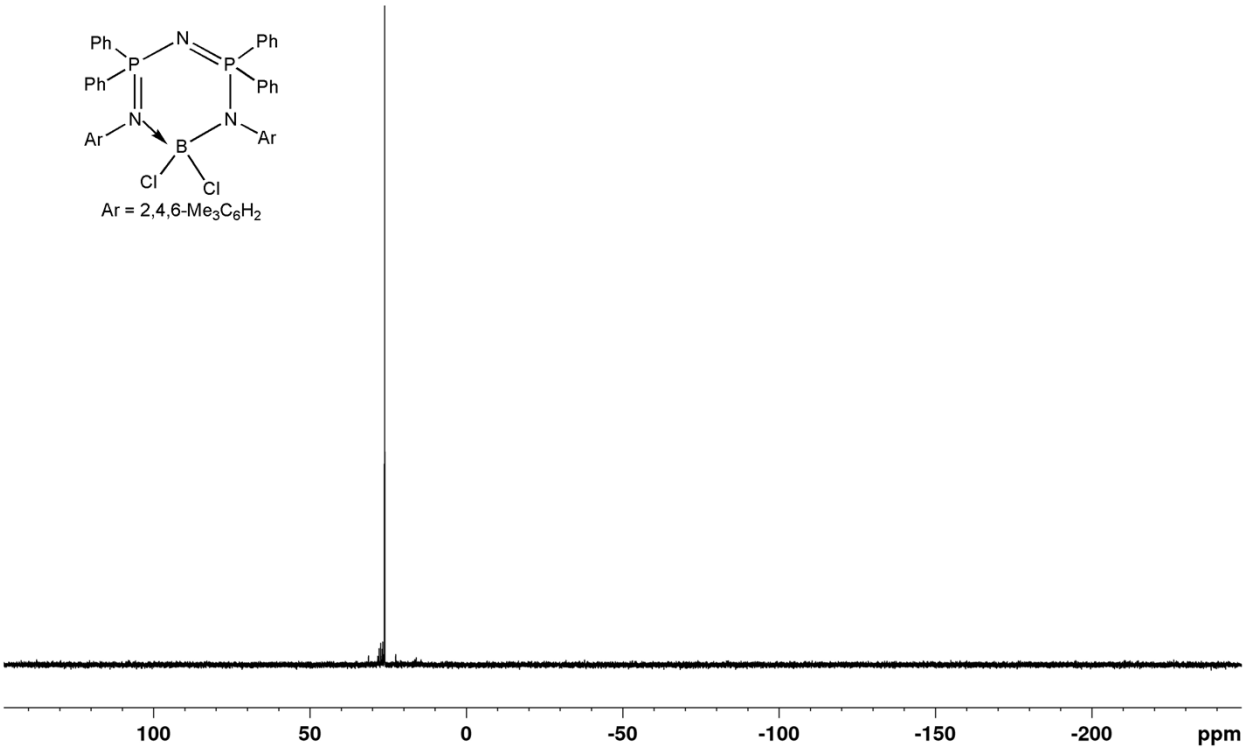

Fig. S45 $^{31}P\{^{1}H\}$ NMR (162 MHz, $CDCl_3$) spectrum of [{N(Ph_2PN(2,4,6-$Me_3C_6H_2N$))$_2$}BCl_2] (**1.12).**

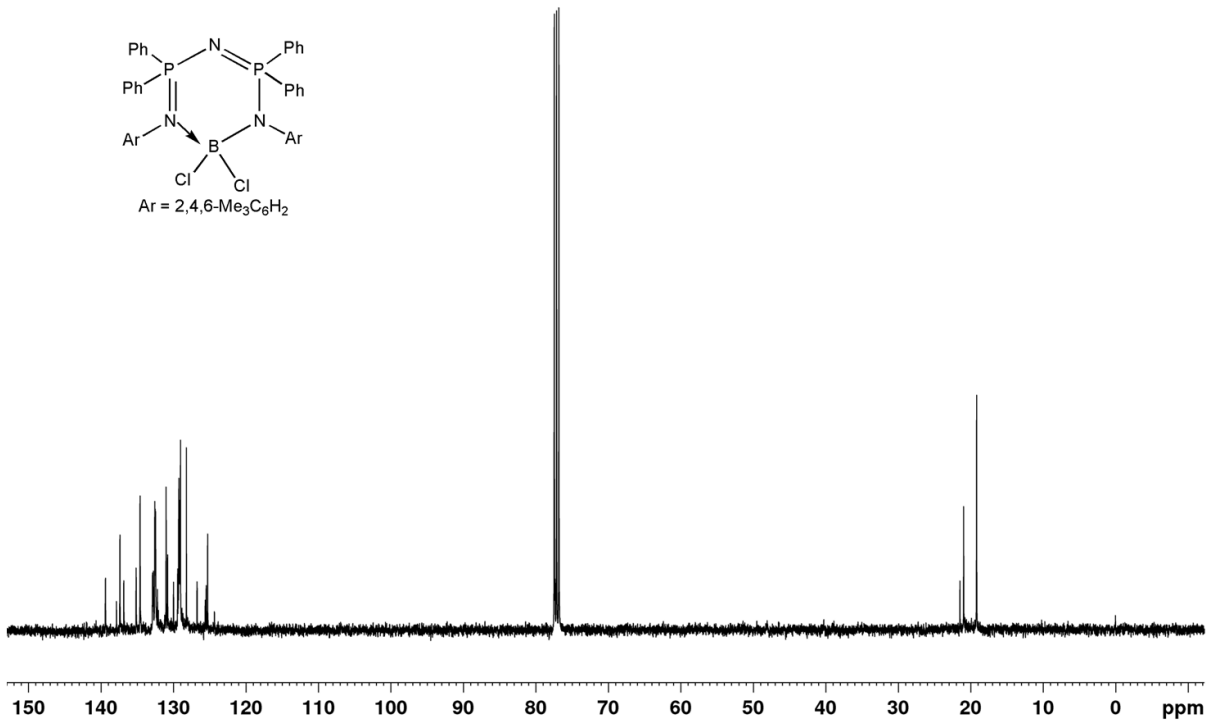

Fig. S46 ^{13}C NMR (100 MHz, $CDCl_3$) spectrum of [{N(Ph_2PN(2,4,6-$Me_3C_6H_2N$))$_2$}BCl_2] (**1.12**).

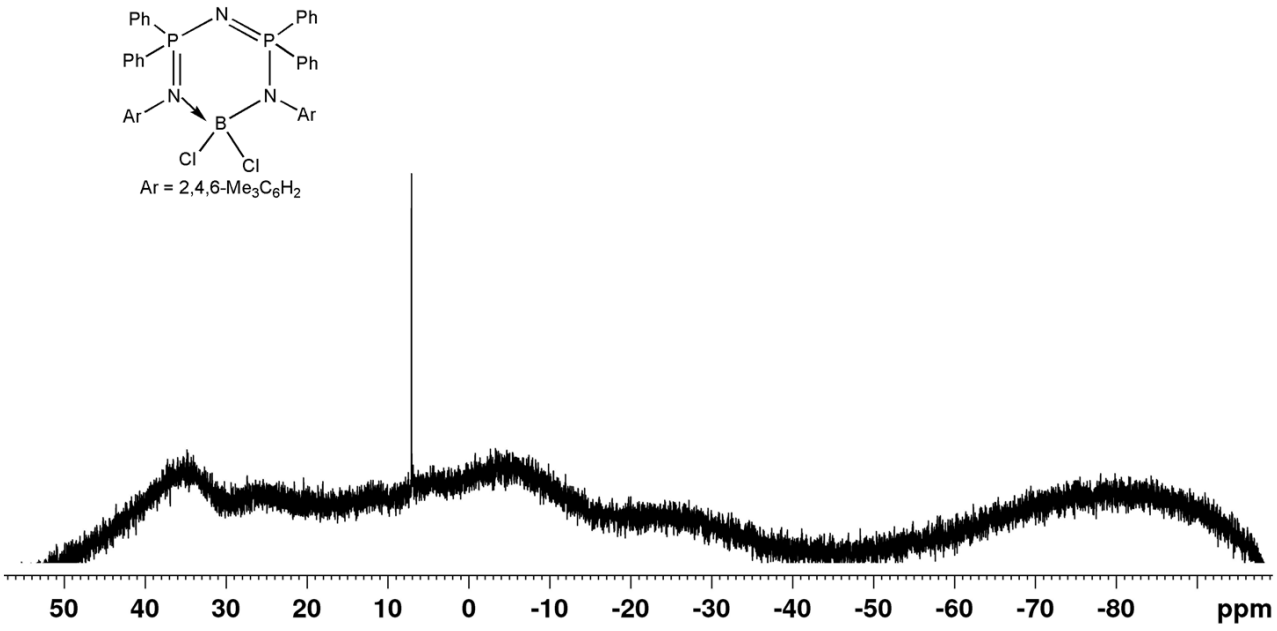

Fig. S47 ^{11}B NMR (128 MHz, $CDCl_3$) spectrum of [{N(Ph_2PN(2,4,6-$Me_3C_6H_2N$))$_2$}BCl_2] (**1.12**).

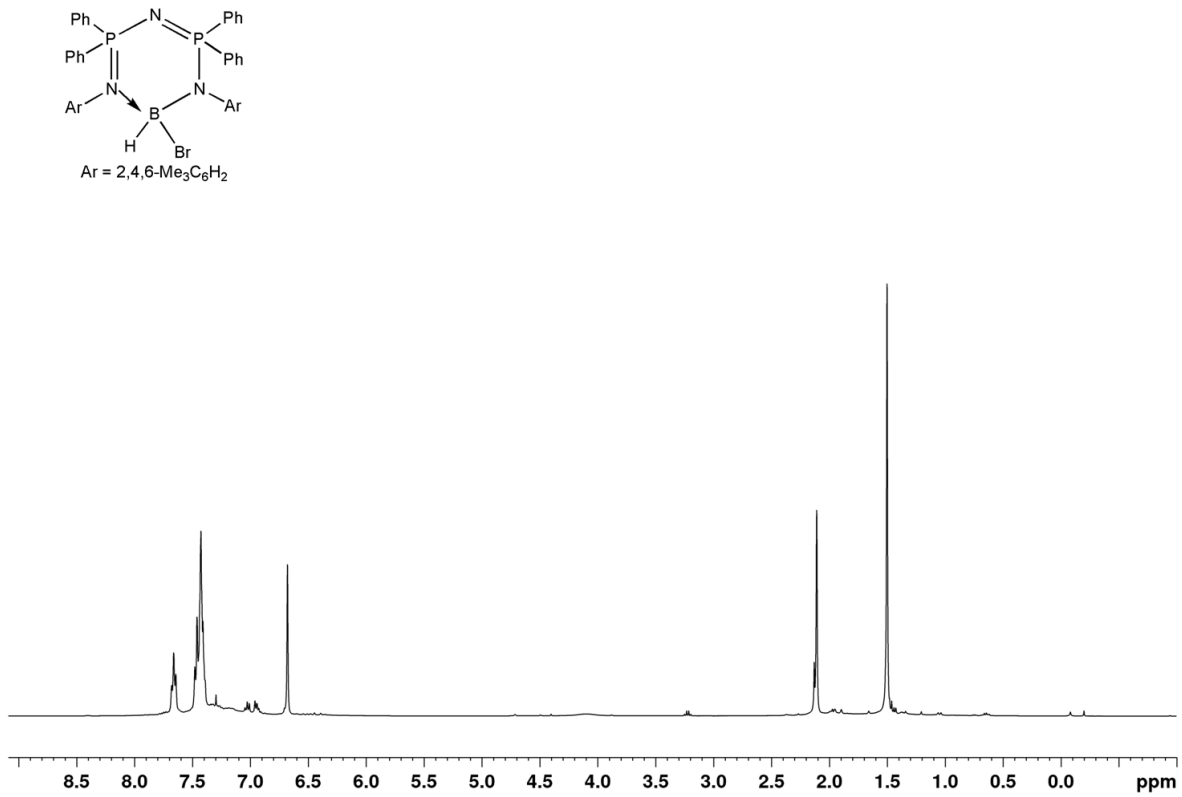

Fig. S48 ^{1}H NMR (400 MHz, $CDCl_3$) spectrum of [{N(Ph_2PN(2,4,6-$Me_3C_6H_2N$))$_2$}$BHBr$] (**1.13**).

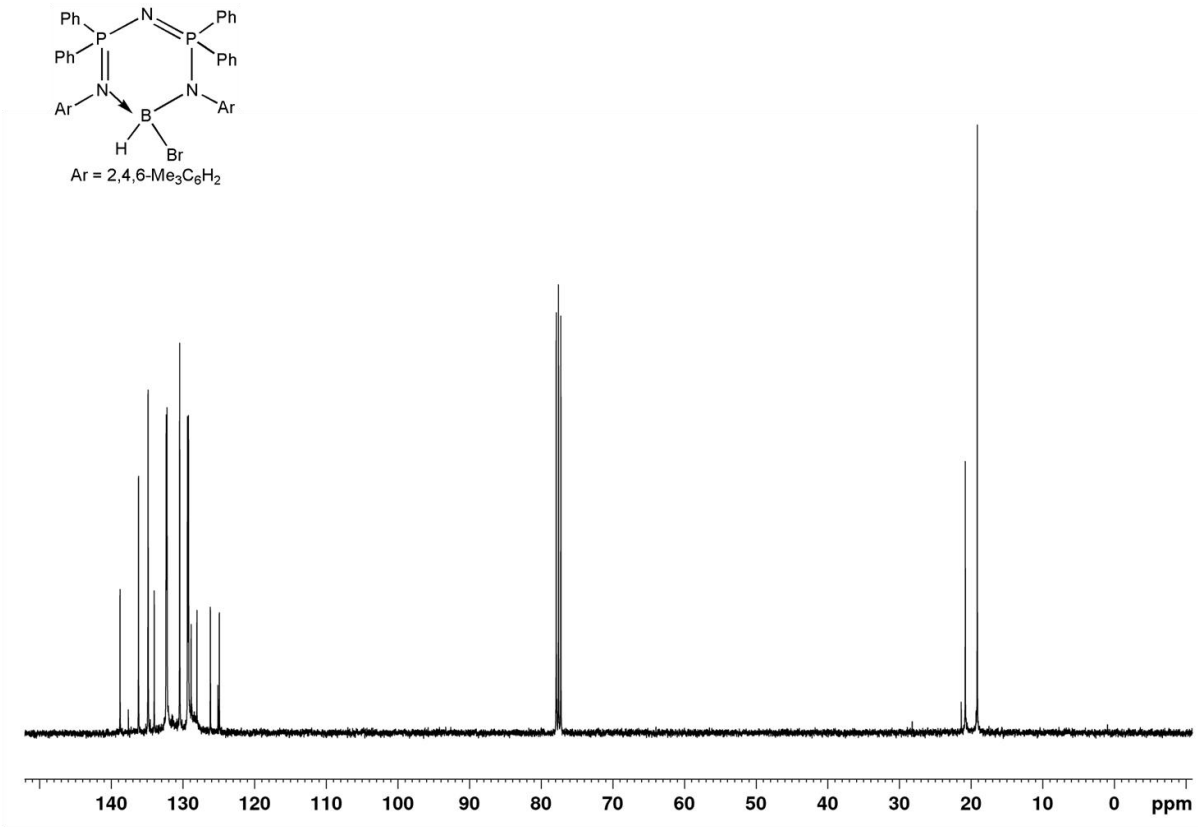

Fig. S49 ^{13}C NMR (100 MHz, $CDCl_3$) spectrum of [{N(Ph_2PN(2,4,6-$Me_3C_6H_2N$))$_2$}BHBr] (**1.13**).

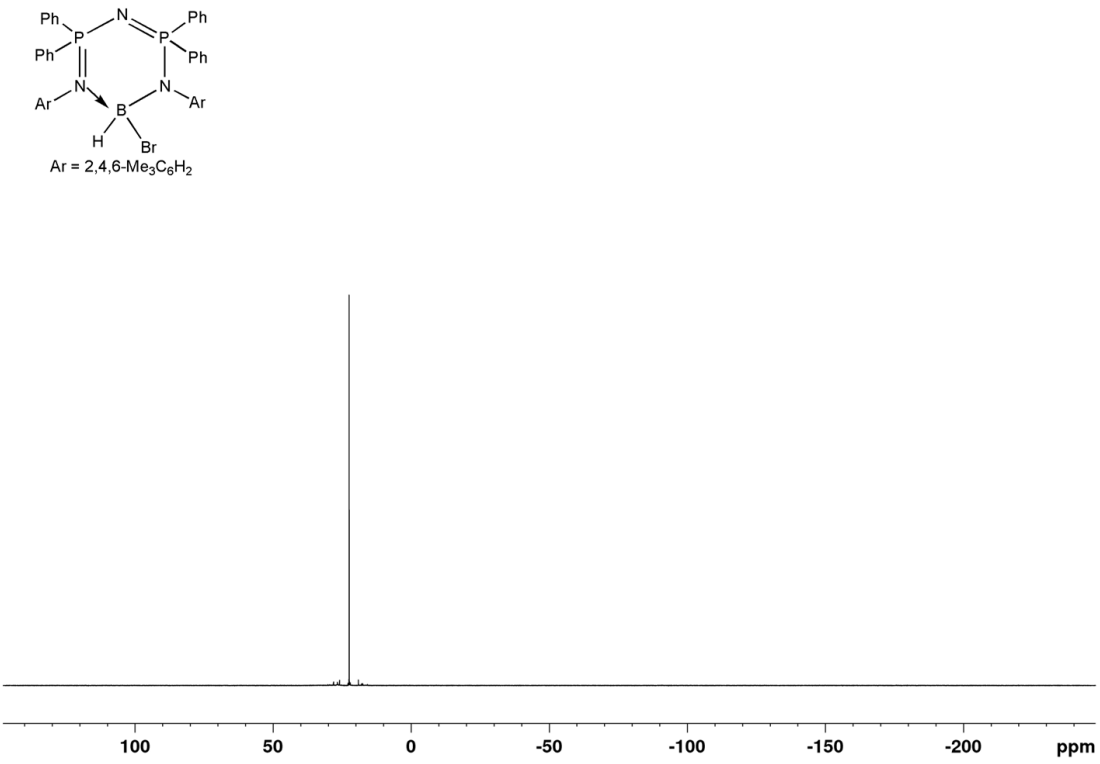

Fig. S50 $^{31}P\{^1H\}$ NMR (162 MHz, $CDCl_3$) spectrum of [{N(Ph_2PN(2,4,6-$Me_3C_6H_2N$))$_2$}BHBr] (**1.13**).

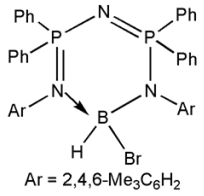

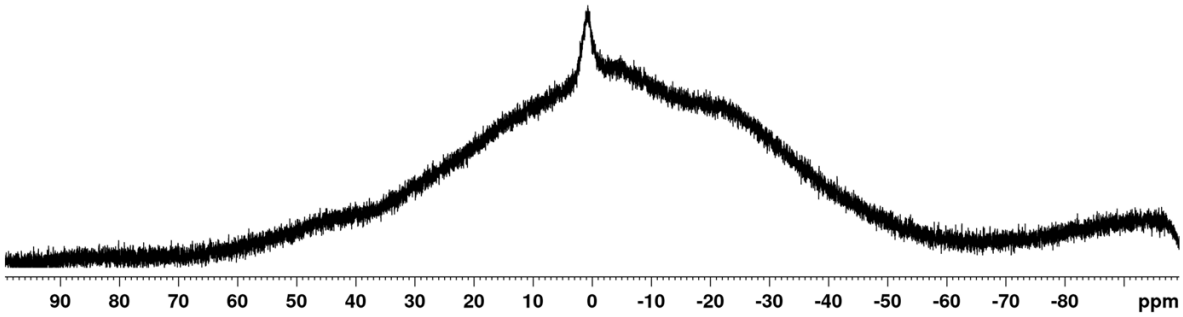

Fig. S51 ^{11}B NMR (128 MHz, $CDCl_3$) spectrum [{N(Ph_2PN(2,4,6-$Me_3C_6H_2N$))$_2$}BHBr] (**1.13**).

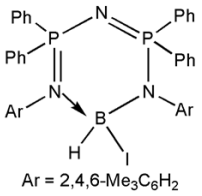

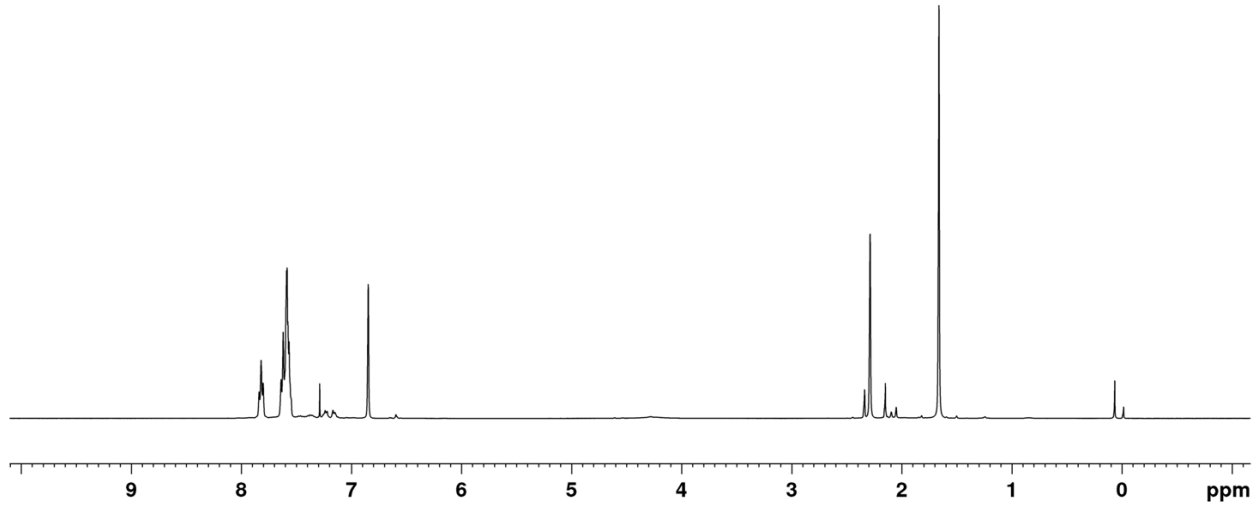

Fig. S52 ^{1}H NMR (400 MHz, $CDCl_3$) spectrum of [{N(Ph_2PN(2,4,6-$Me_3C_6H_2N$))$_2$}BHI] (**1.14**).

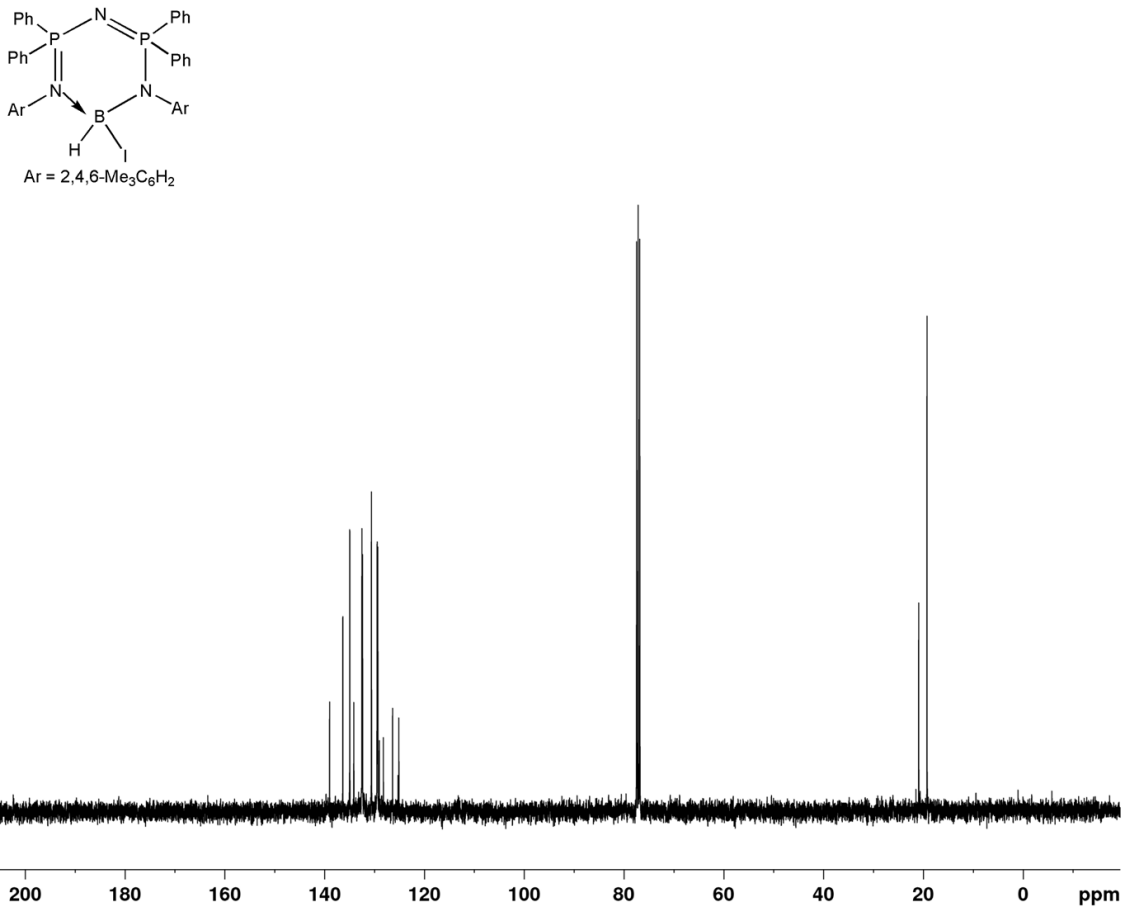

Fig. S53 ^{13}C NMR (100 MHz, $CDCl_3$) spectrum of [{N(Ph_2PN(2,4,6-$Me_3C_6H_2N$))$_2$}BHI] (**1.14**).

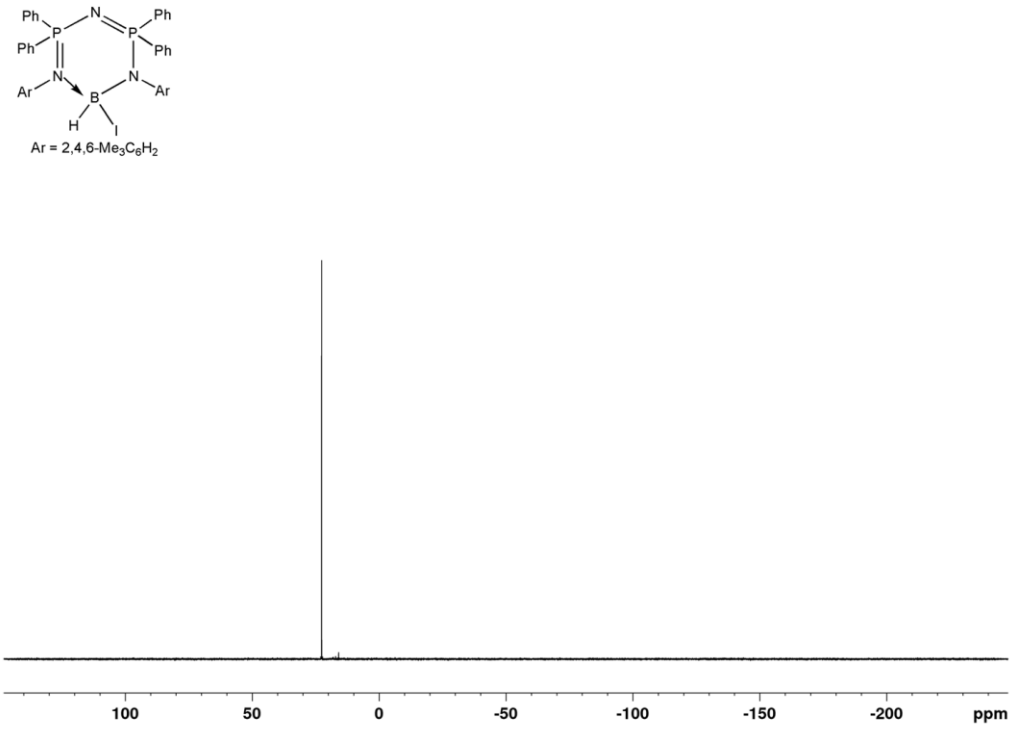

Fig. S54 $^{31}P\{^1H\}$ NMR (162 MHz, $CDCl_3$) spectrum of [{N(Ph_2PN(2,4,6-$Me_3C_6H_2N$))$_2$}BHI] (**1.14**).

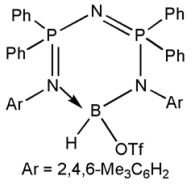

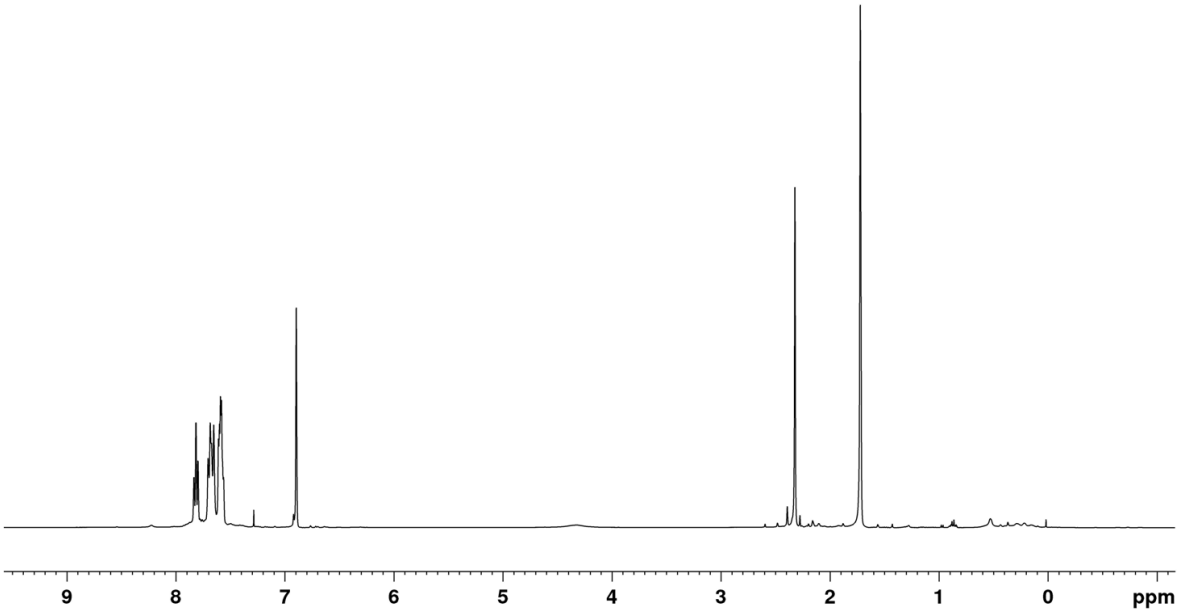

Fig. S55 ^{1}H NMR (400 MHz, $CDCl_3$) spectrum of [{N($Ph_2PN(2,4,6\text{-}Me_3C_6H_2N)$)$_2$}BHOTf] (**1.15**).

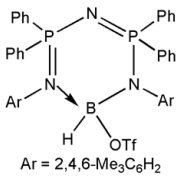

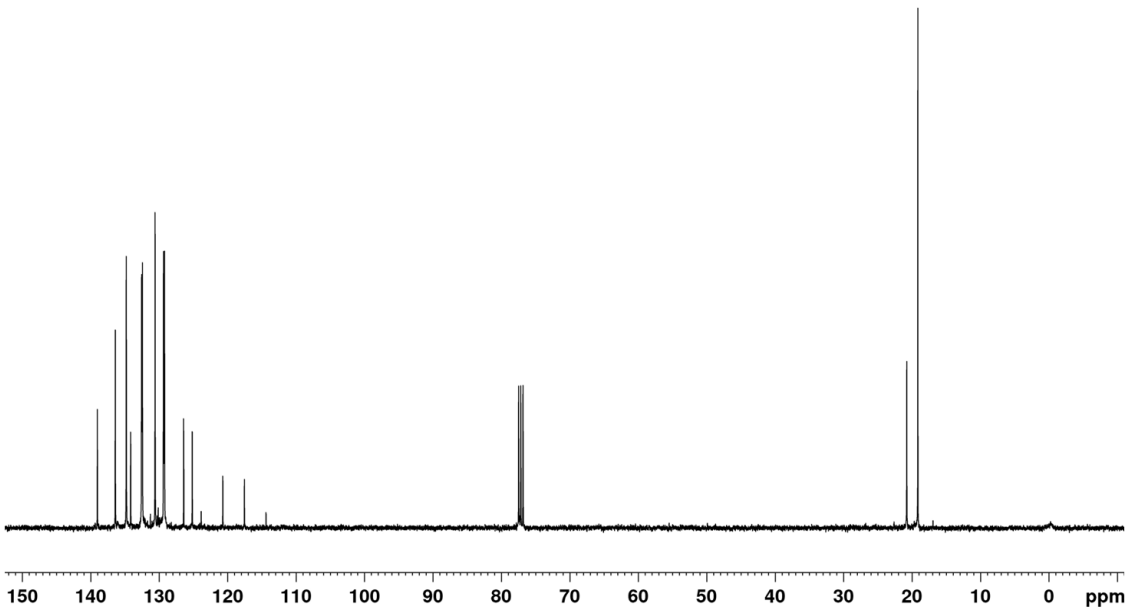

Fig. S56 ^{13}C NMR (100 MHz, $CDCl_3$) spectrum of [{N($Ph_2PN(2,4,6\text{-}Me_3C_6H_2N)$)$_2$}BHOTf] (**1.15**).

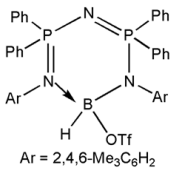

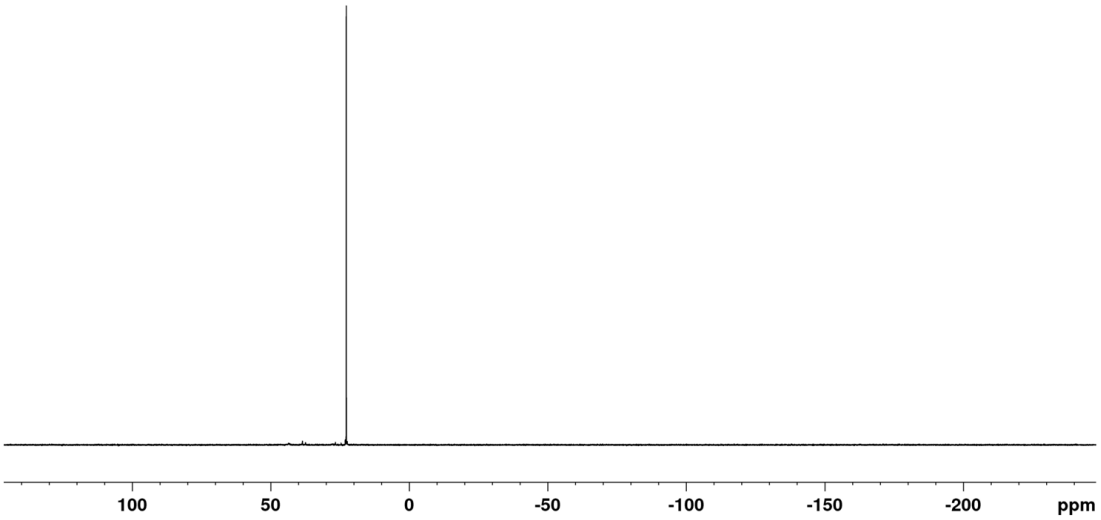

Fig. S57 $^{31}P\{^{1}H\}$ NMR (162 MHz, $CDCl_3$) spectrum of [{N($Ph_2PN(2,4,6\text{-}Me_3C_6H_2N)$)$_2$}BHOTf] (**1.15**).

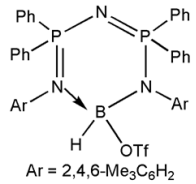

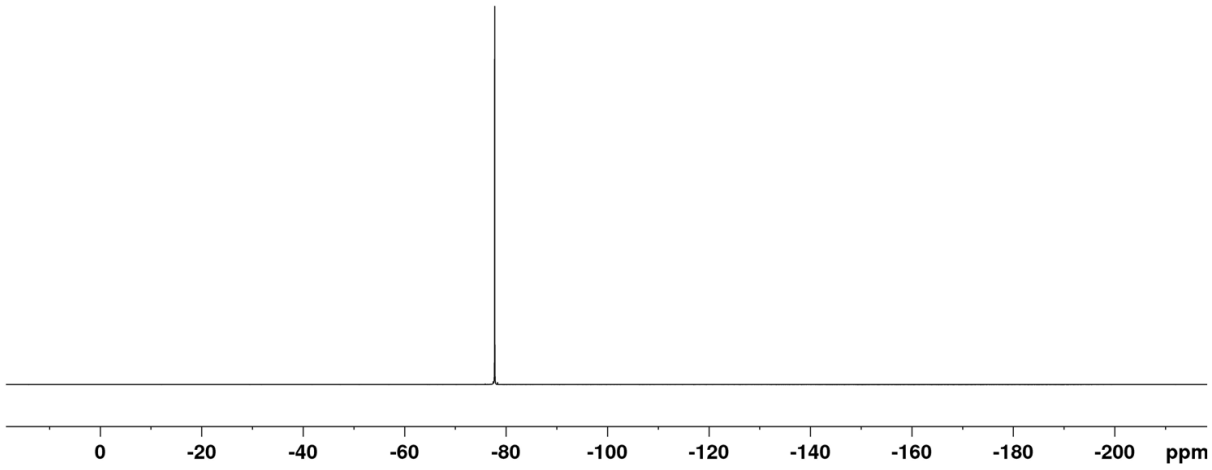

Fig. S58 ^{19}F NMR (376 MHz, $CDCl_3$)spectrum of [{N($Ph_2PN(2,4,6\text{-}Me_3C_6H_2N)$)$_2$}BHOTf] (**1.15**).

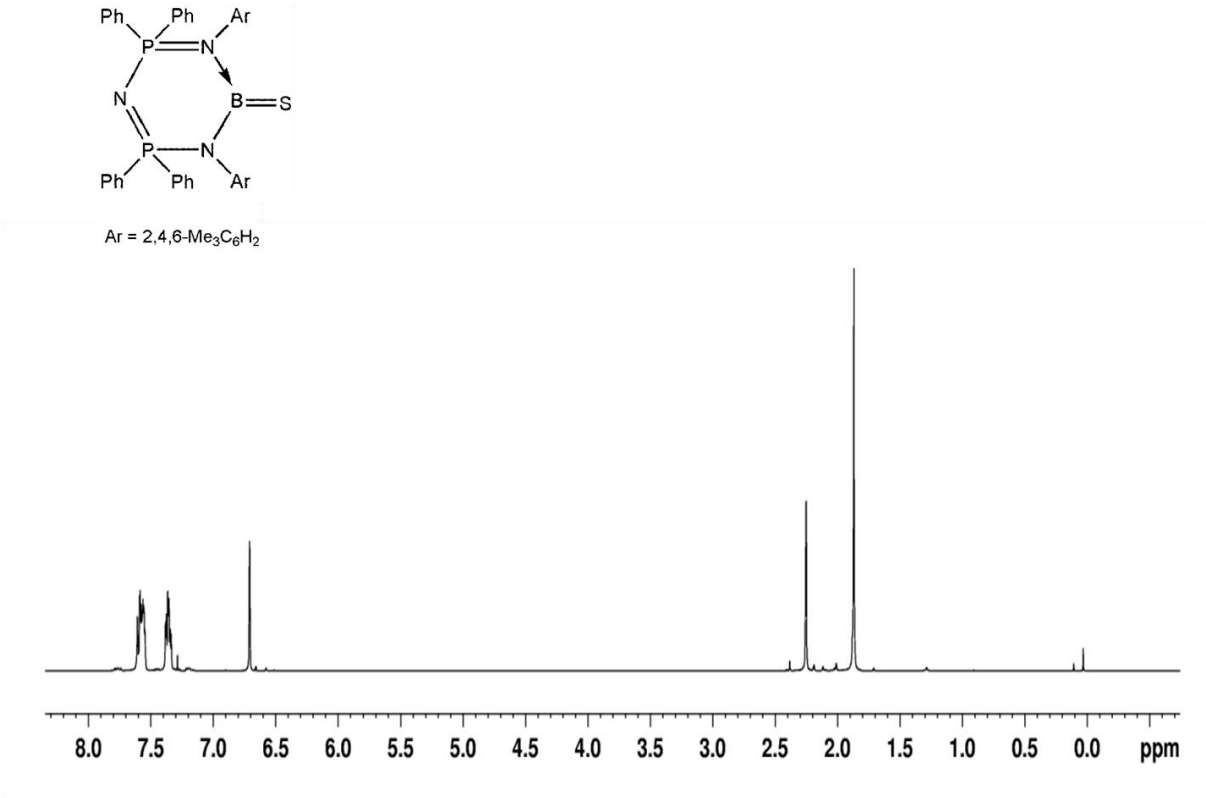

Fig. S59 ^{1}H NMR (400 MHz, $CDCl_3$) spectrum of [{N(Ph_2PN(2,4,6-$Me_3C_6H_2N$))$_2$}BS] (**2.1**).

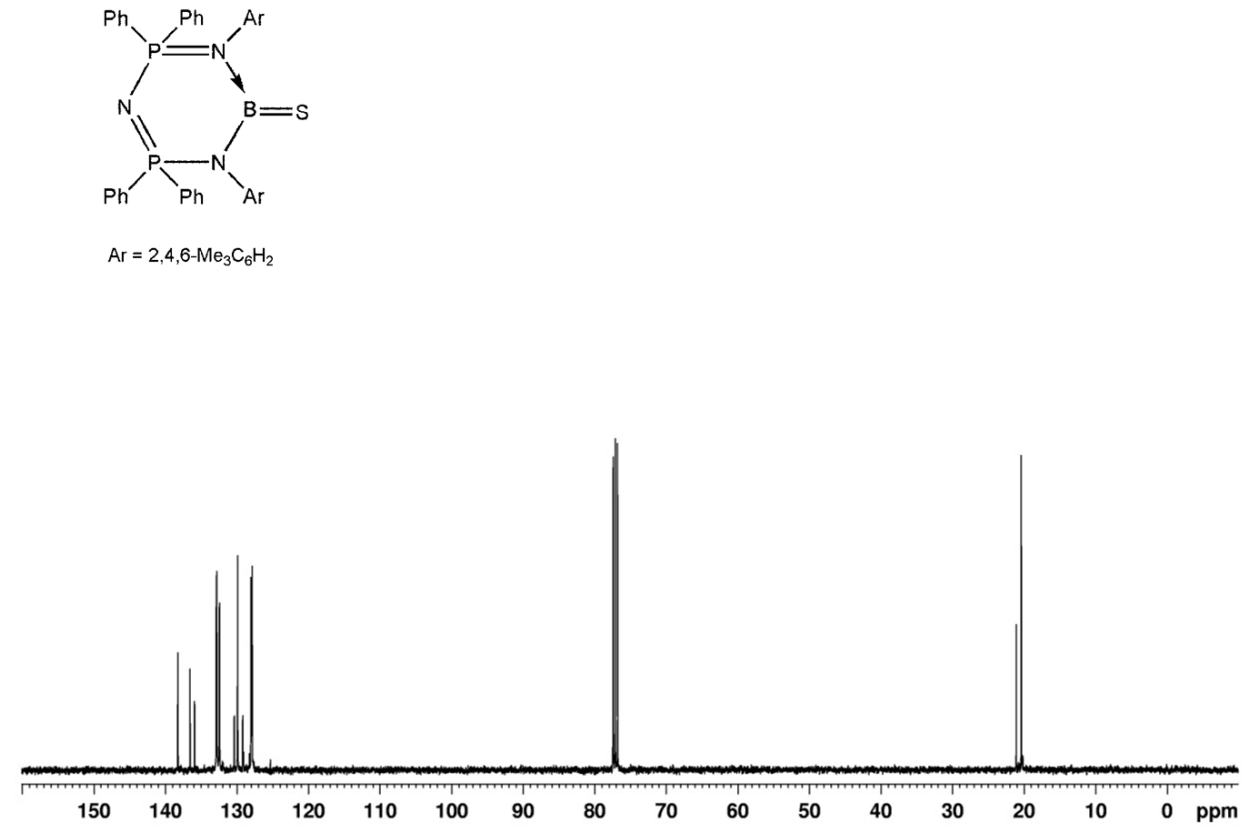

Fig. S60 ^{13}C NMR (100 MHz, $CDCl_3$) spectrum of [{N(Ph_2PN(2,4,6-$Me_3C_6H_2N$))$_2$}BS] (**2.1**).

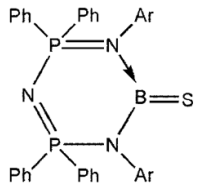

Ar = 2,4,6-$Me_3C_6H_2$

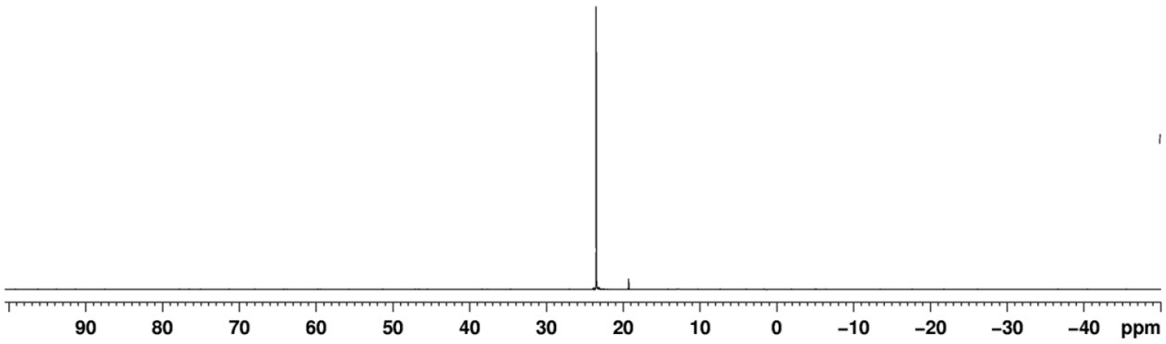

Fig. S61 $^{31}P\{^{1}H\}$ NMR (162 MHz, $CDCl_3$) spectrum of [{$N(Ph_2PN(2,4,6\text{-}Me_3C_6H_2N))_2$}BS] (**2.1**).

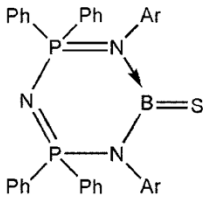

Ar = 2,4,6-$Me_3C_6H_2$

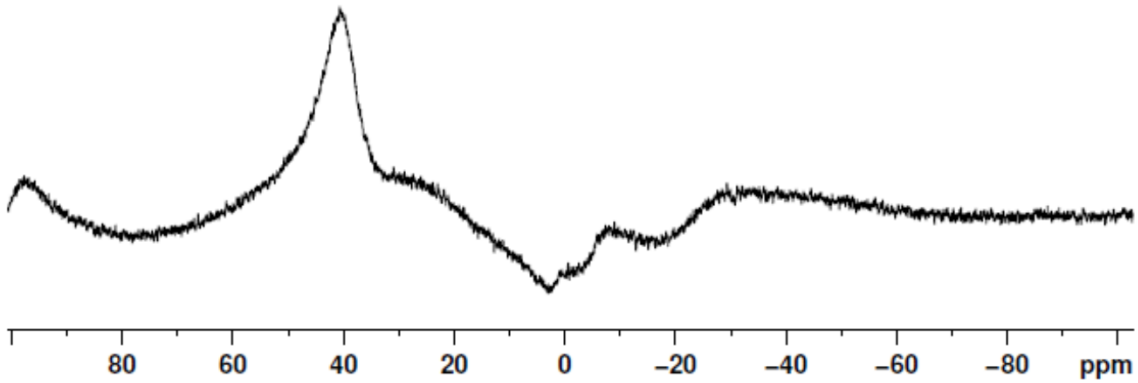

Fig. S62 ^{11}B NMR (128 MHz, $CDCl_3$) spectrum of [{$N(Ph_2PN(2,4,6\text{-}Me_3C_6H_2N))_2$}BS] (**2.1**).

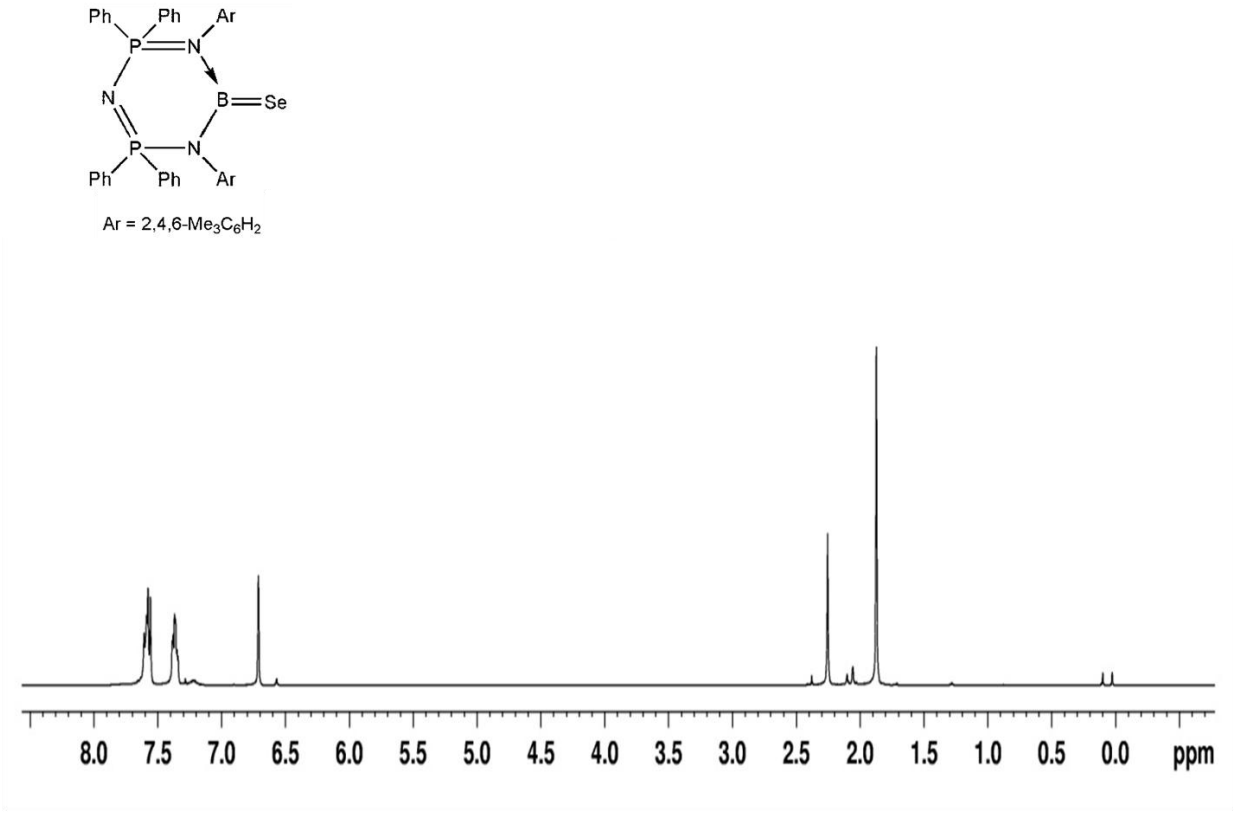

Fig. S63 ^{1}H NMR (400 MHz, $CDCl_3$) spectrum of [{N(Ph_2PN(2,4,6-$Me_3C_6H_2N$))$_2$}BSe] (**2.2**).

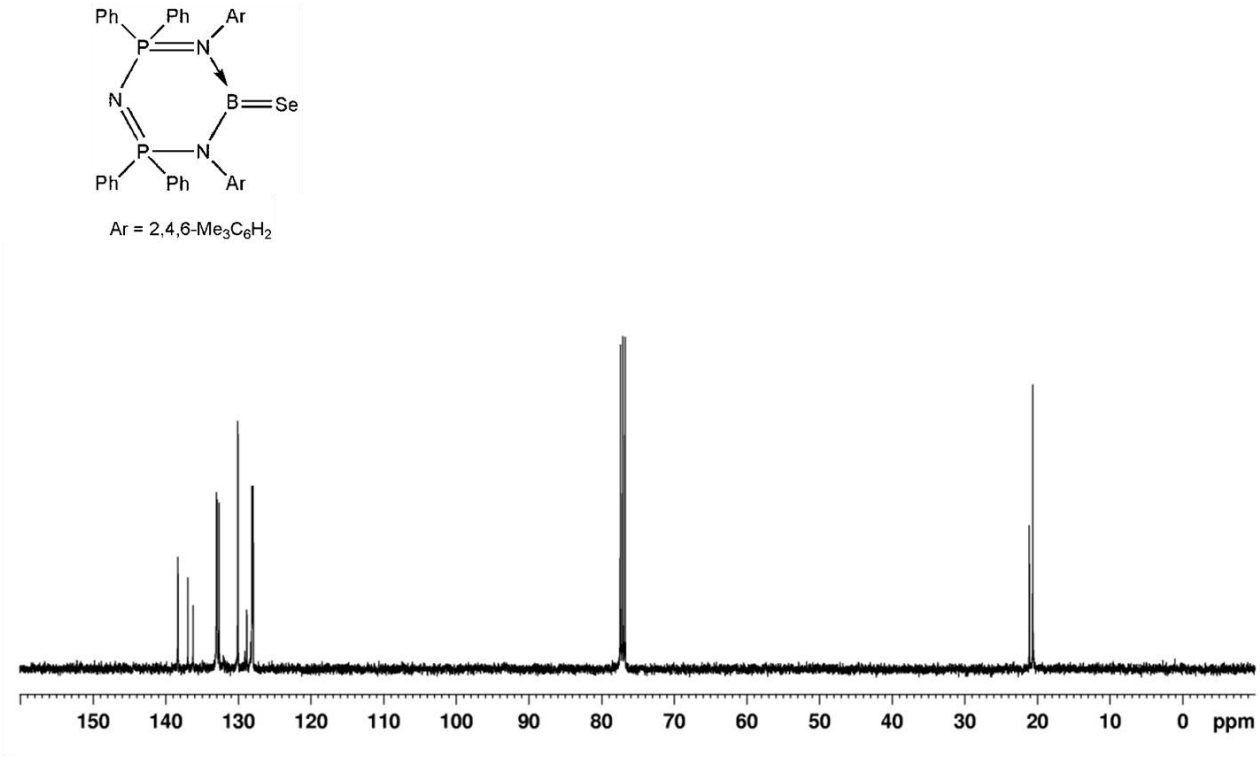

Fig. S64 ^{13}C NMR (100 MHz, $CDCl_3$) spectrum of [{N(Ph_2PN(2,4,6-$Me_3C_6H_2N$))$_2$}BSe] (**2.2**).

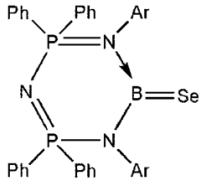

Ar = 2,4,6-$Me_3C_6H_2$

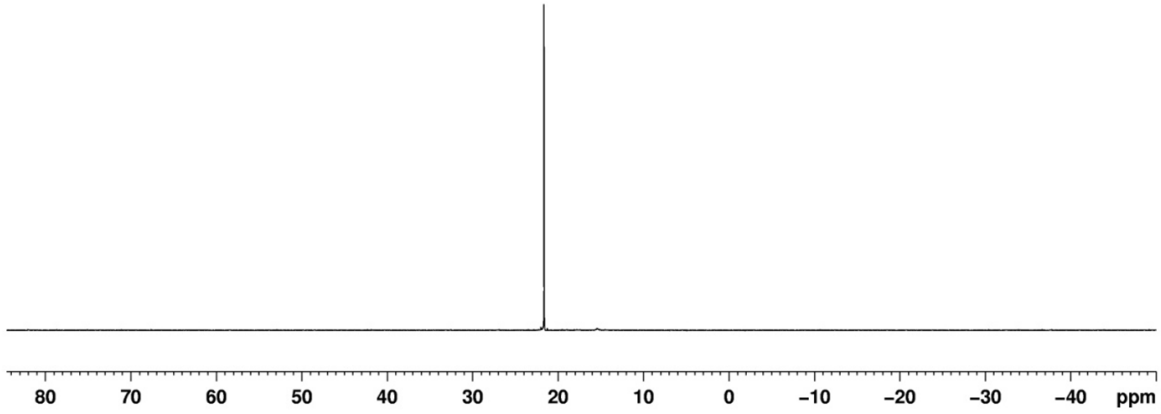

Fig. S65 $^{31}P\{^{1}H\}$ NMR (162 MHz, $CDCl_3$) spectrum of [{$N(Ph_2PN(2,4,6\text{-}Me_3C_6H_2N))_2$}BSe] (**2.2**).

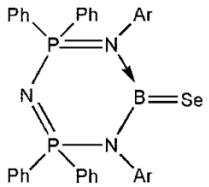

Ar = 2,4,6-$Me_3C_6H_2$

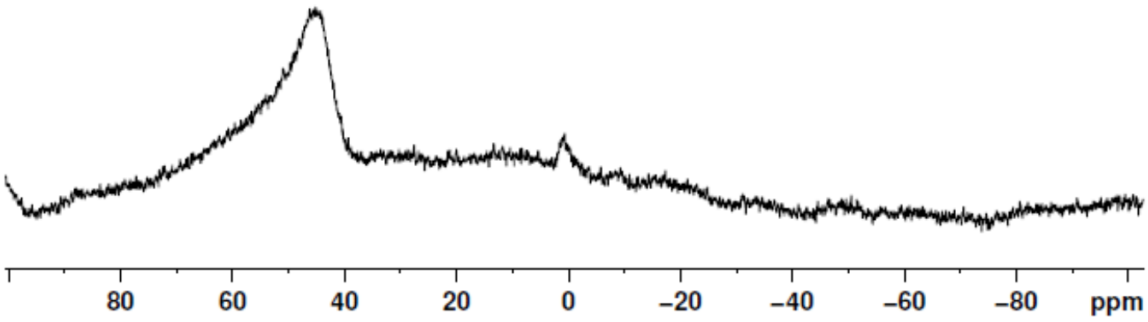

Fig. S66 ^{11}B NMR (128 MHz, $CDCl_3$) spectrum of [{$N(Ph_2PN(2,4,6\text{-}Me_3C_6H_2N))_2$}BSe] (**2.2**).

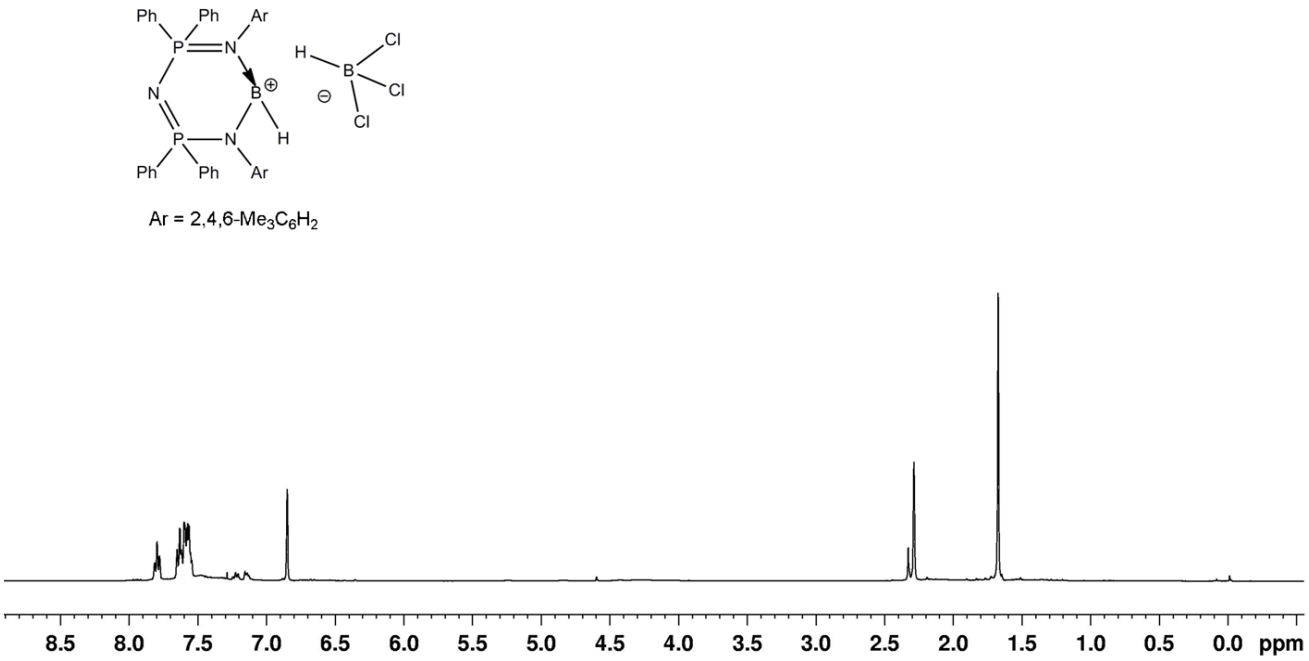

Fig. S67 ^{1}H NMR (400 MHz, $CDCl_3$) spectrum of $[\{N(Ph_2PN(2,4,6\text{-}Me_3C_6H_2N))_2\}BH]^+[BHCl_3]^-$ (**3.1**).

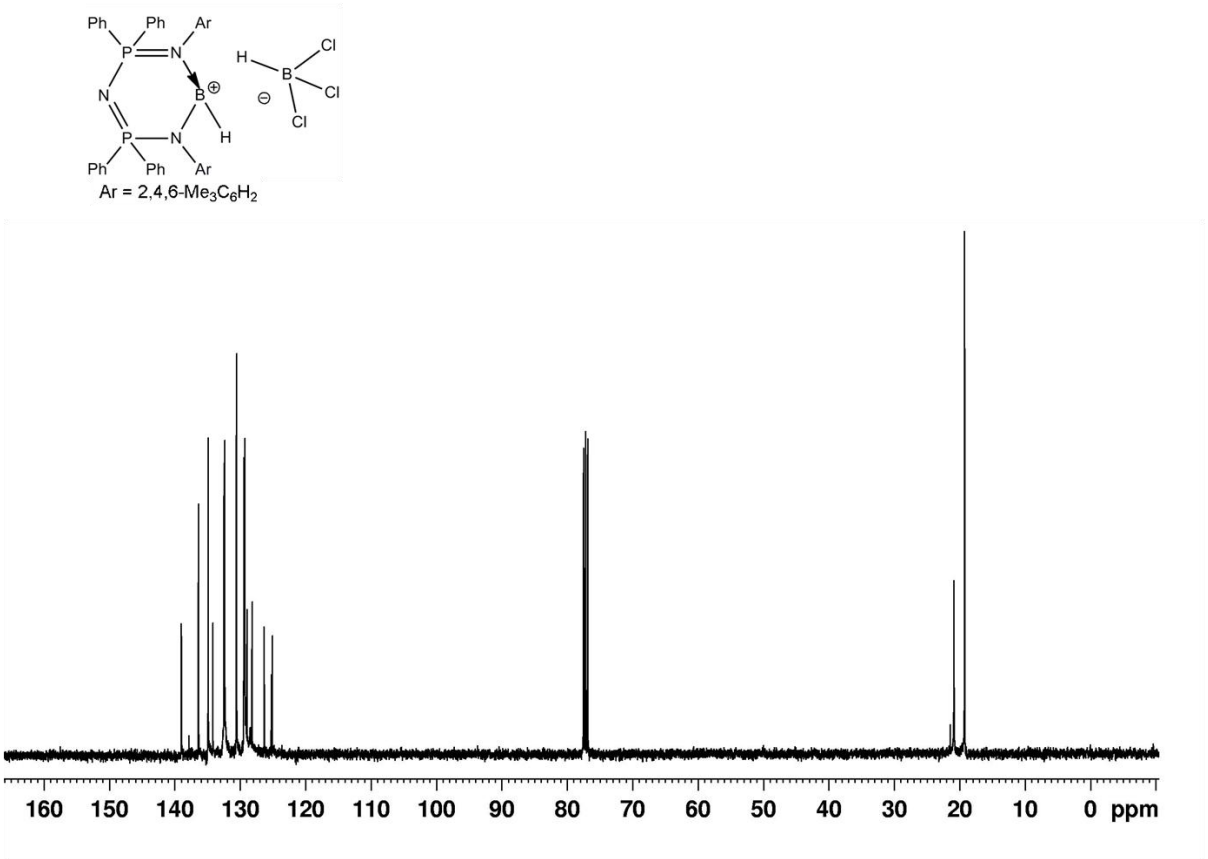

Fig. S68 ^{13}C NMR (100 MHz, $CDCl_3$) spectrum of $[\{N(Ph_2PN(2,4,6\text{-}Me_3C_6H_2N))_2\}BH]^+[BHCl_3]^-$ (**3.1**).

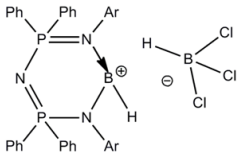

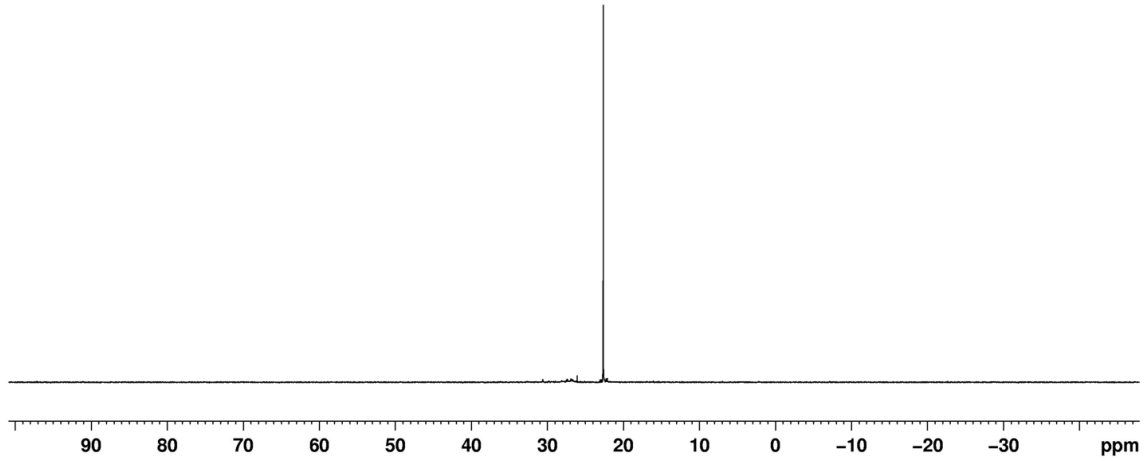

Fig. S69 $^{31}P\{^{1}H\}$ NMR (162 MHz, $CDCl_3$) spectrum of $[\{N(Ph_2PN(2,4,6\text{-}Me_3C_6H_2N))_2\}BH]^+[BHCl_3]^-$ (**3.1**).

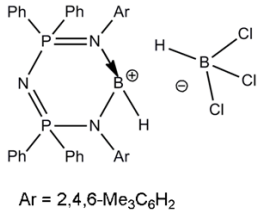

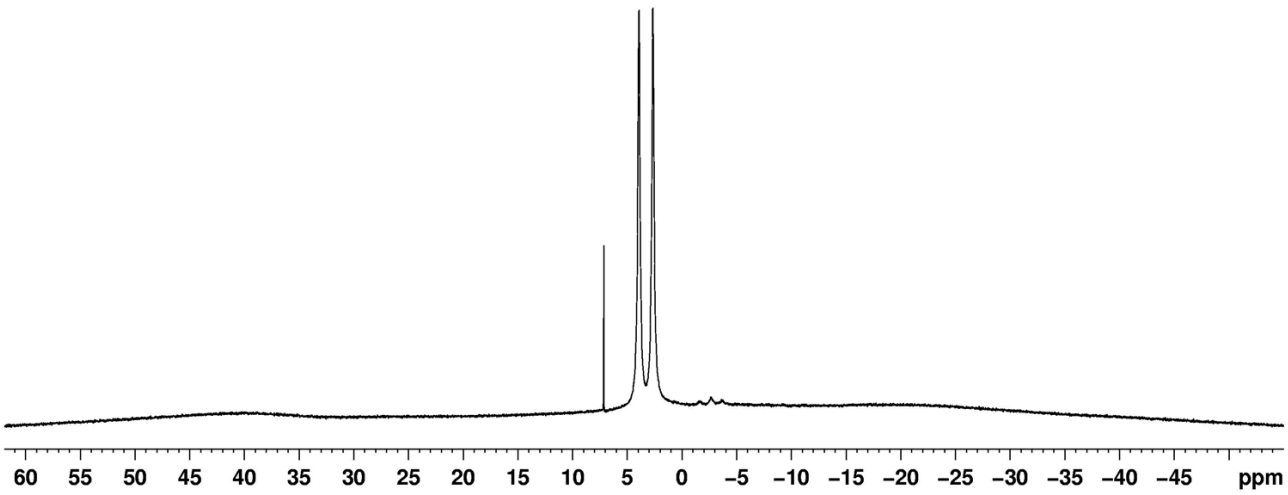

Fig. S70 ^{11}B NMR (128 MHz, $CDCl_3$) spectrum of $[\{N(Ph_2PN(2,4,6\text{-}Me_3C_6H_2N))_2\}BH]^+[BHCl_3]^-$ (**3.1**).

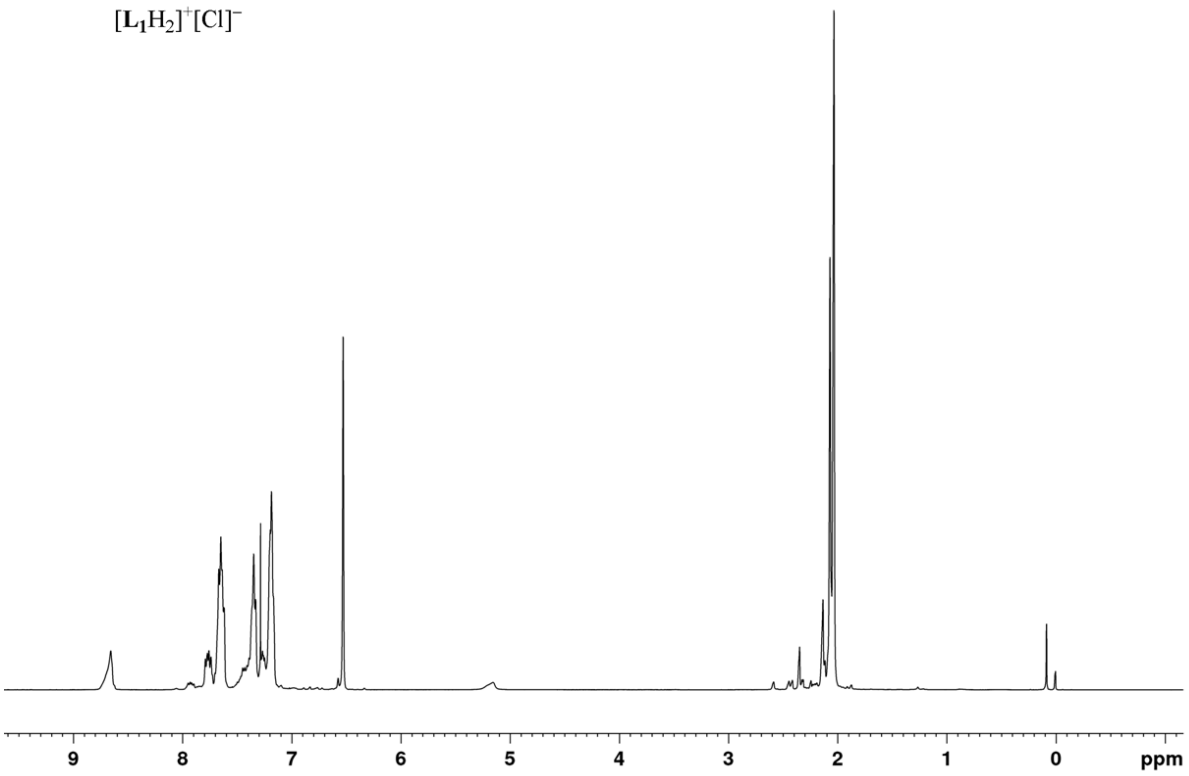

Fig. S71 ^{1}H NMR (400 MHz, $CDCl_3$) spectrum of $[\{N(Ph_2PN(2,4,6\text{-}Me_3C_6H_2N))_2\}H_2]^+[Cl]^-$.

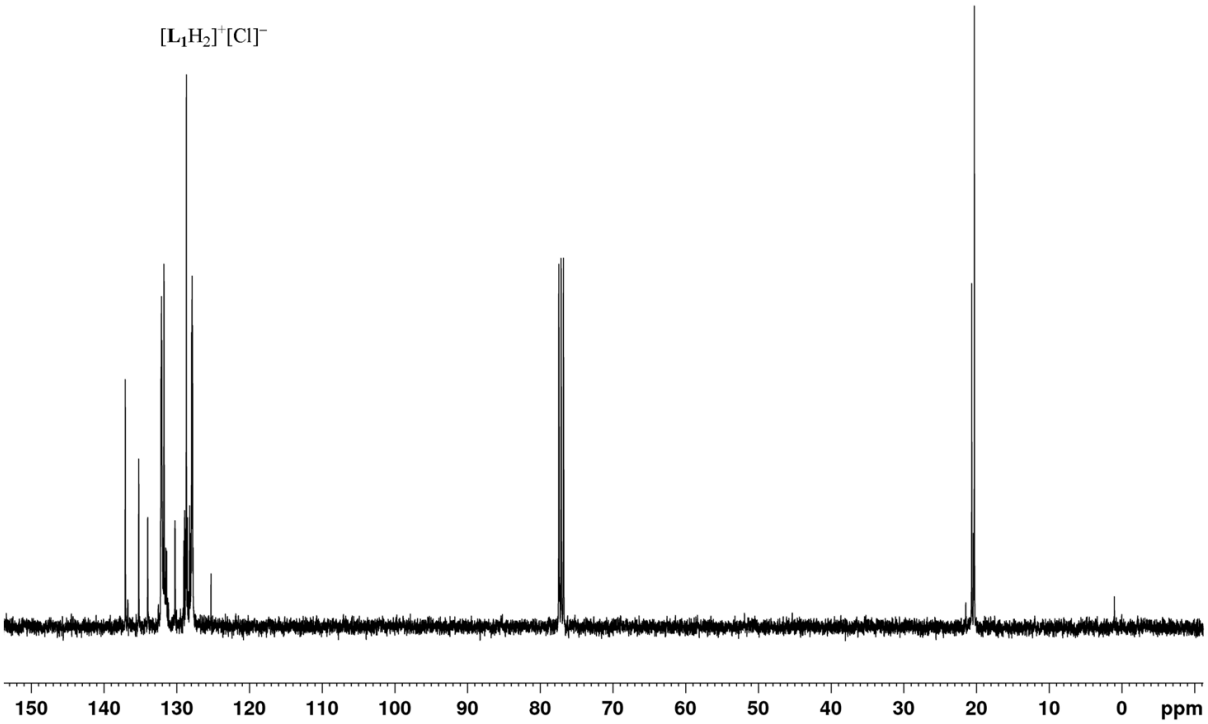

Fig. S72 ^{13}C NMR (100 MHz, $CDCl_3$) spectrum of $[\{N(Ph_2PN(2,4,6\text{-}Me_3C_6H_2N))_2\}H_2]^+[Cl]^-$.

$[\mathbf{L_1}H_2]^+[Cl]^-$

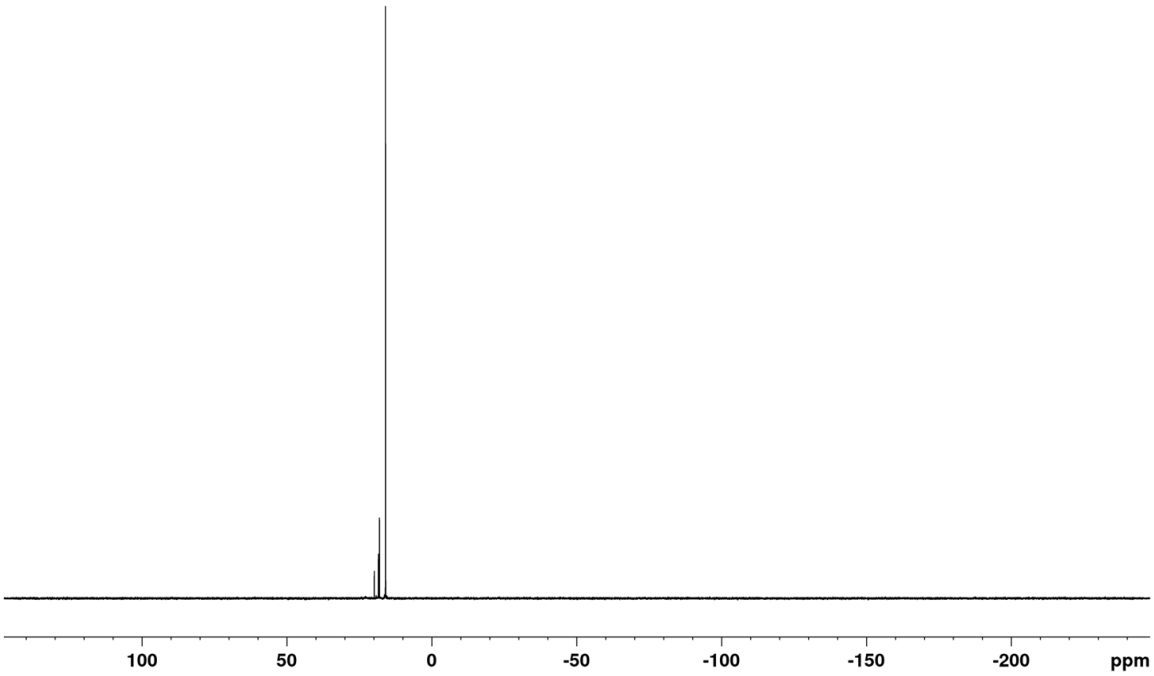

Fig. S73 $^{31}P\{^1H\}$ NMR (162 MHz, $CDCl_3$) spectrum of $[\{N(Ph_2PN(2,4,6\text{-}Me_3C_6H_2N))_2\}H_2]^+[Cl]^-$.

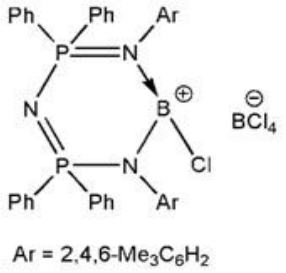

Ar = 2,4,6-$Me_3C_6H_2$

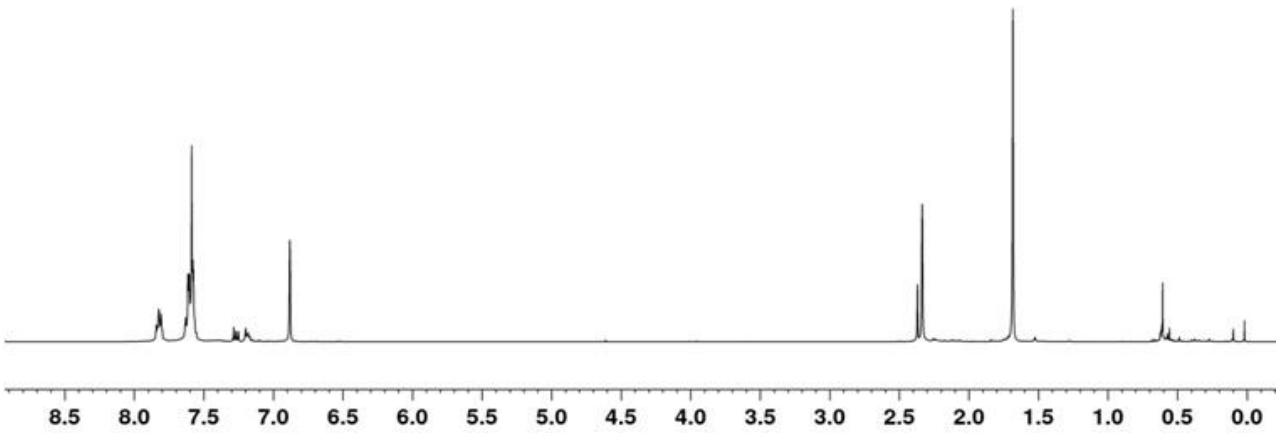

Fig. S74 ^1H NMR (400 MHz, $CDCl_3$) spectrum of $[\{N(Ph_2PN(2,4,6\text{-}Me_3C_6H_2N))_2\}BH]^+[BCl_4]^-$ (**3.2**).

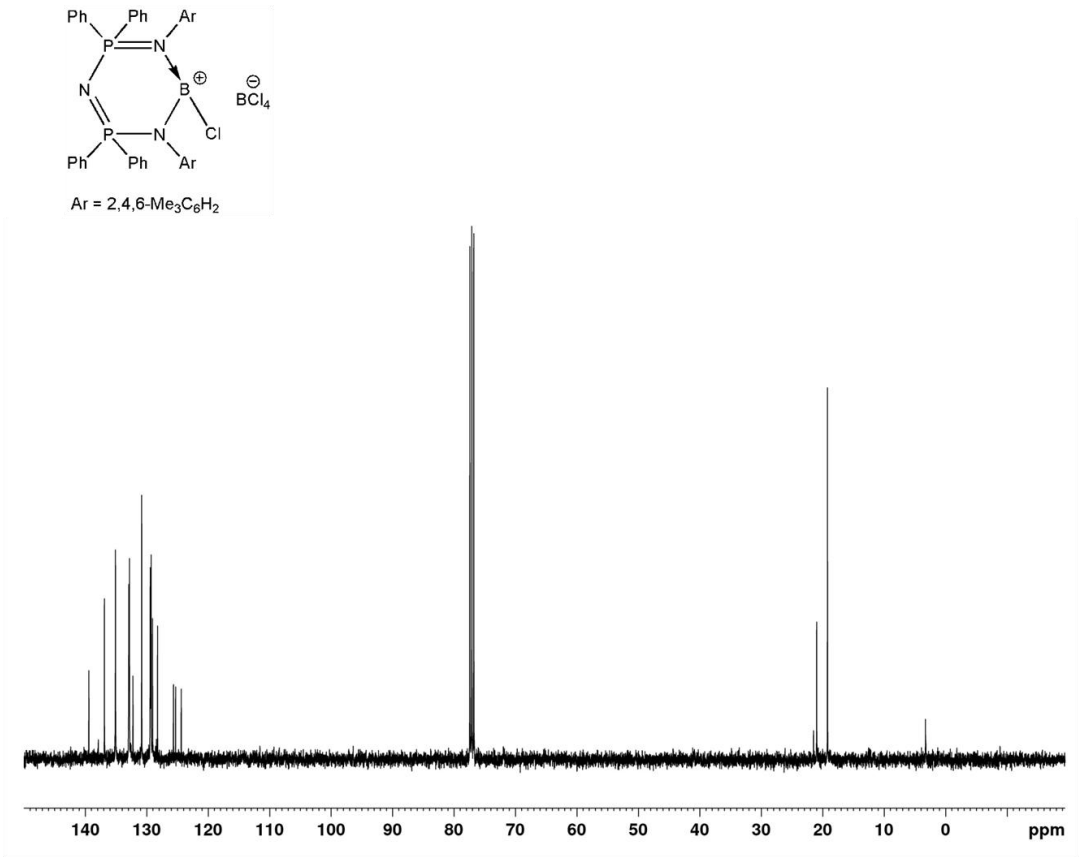

Fig. S75 ^{13}C NMR (100 MHz, $CDCl_3$) spectrum of $[\{N(Ph_2PN(2,4,6\text{-}Me_3C_6H_2N))_2\}BH]^+[BCl_4]^-$ (**3.2**).

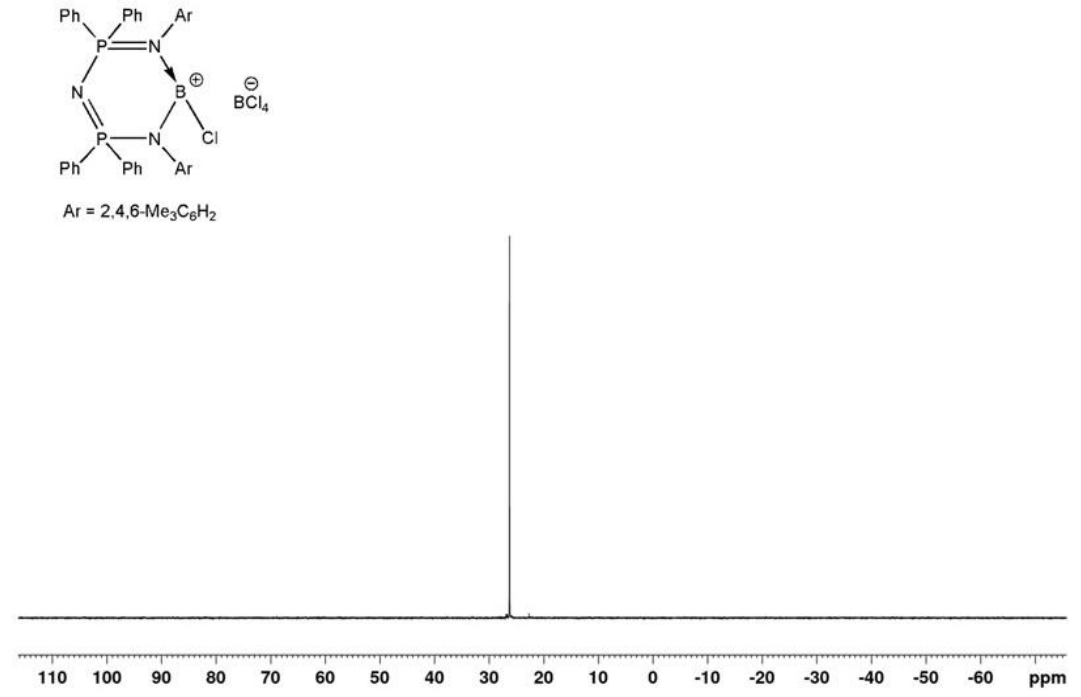

Fig. S76 $^{31}P\{^1H\}$ NMR (162 MHz, $CDCl_3$) spectrum of $[\{N(Ph_2PN(2,4,6\text{-}Me_3C_6H_2N))_2\}BH]^+[BCl_4]^-$ (**3.2**).

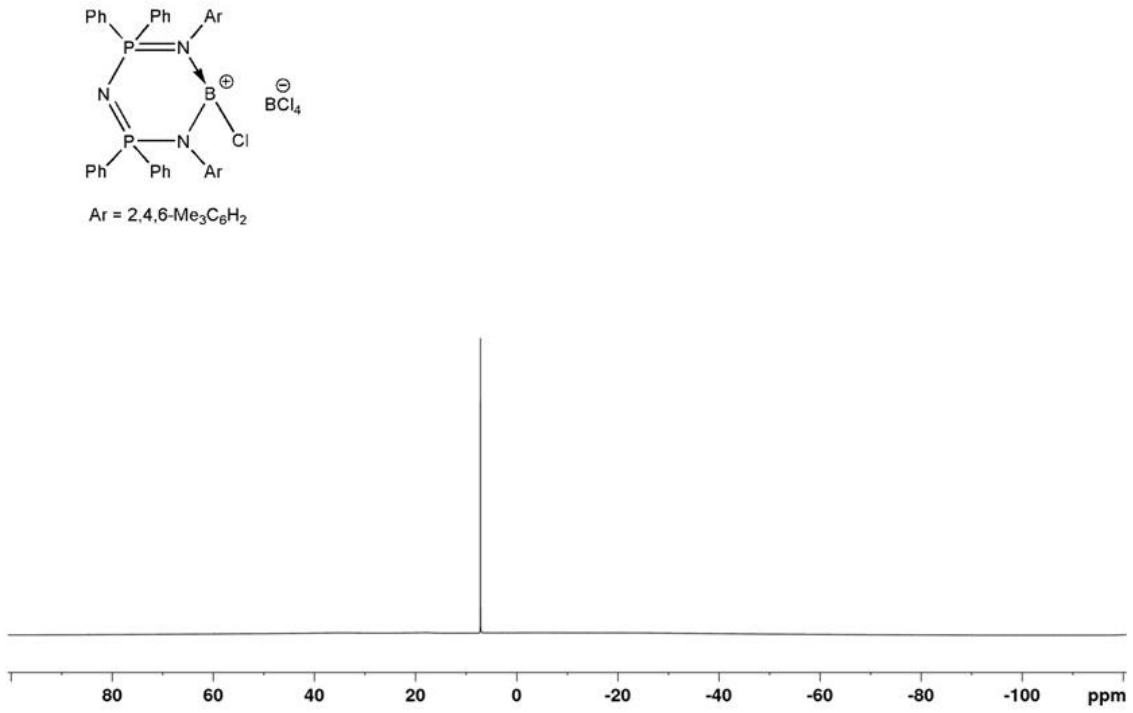

Fig. S77 ^{11}B NMR (128 MHz, $CDCl_3$) spectrum of $[\{N(Ph_2PN(2,4,6\text{-}Me_3C_6H_2N))_2\}BH]^+[BCl_4]^-$ (**3.2**).

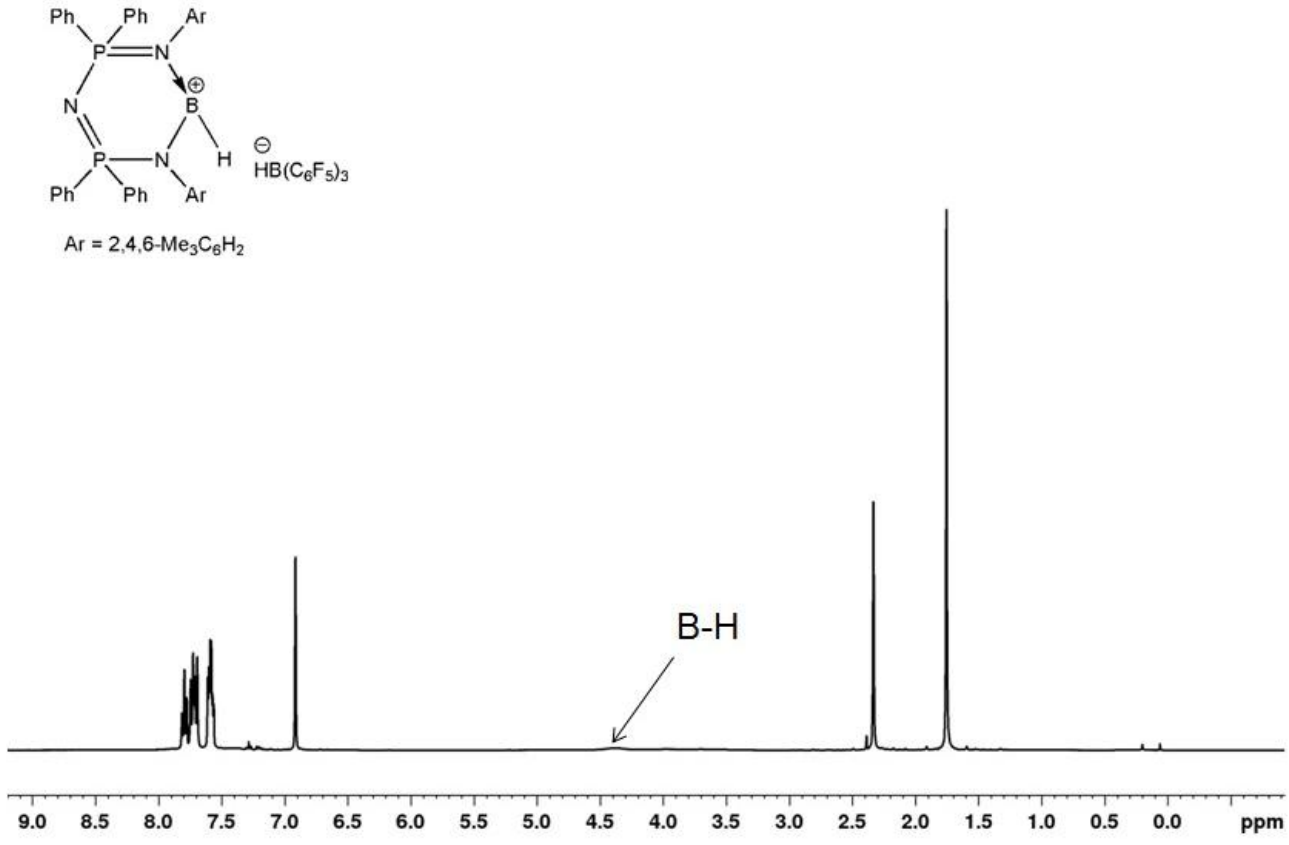

Fig. S78 ^{1}H NMR (400 MHz, $CDCl_3$) spectrum of $[\{N(Ph_2PN(2,4,6\text{-}Me_3C_6H_2N))_2\}BH]^+[HB(C_6F_5)_3]^-$ (**3.3**).

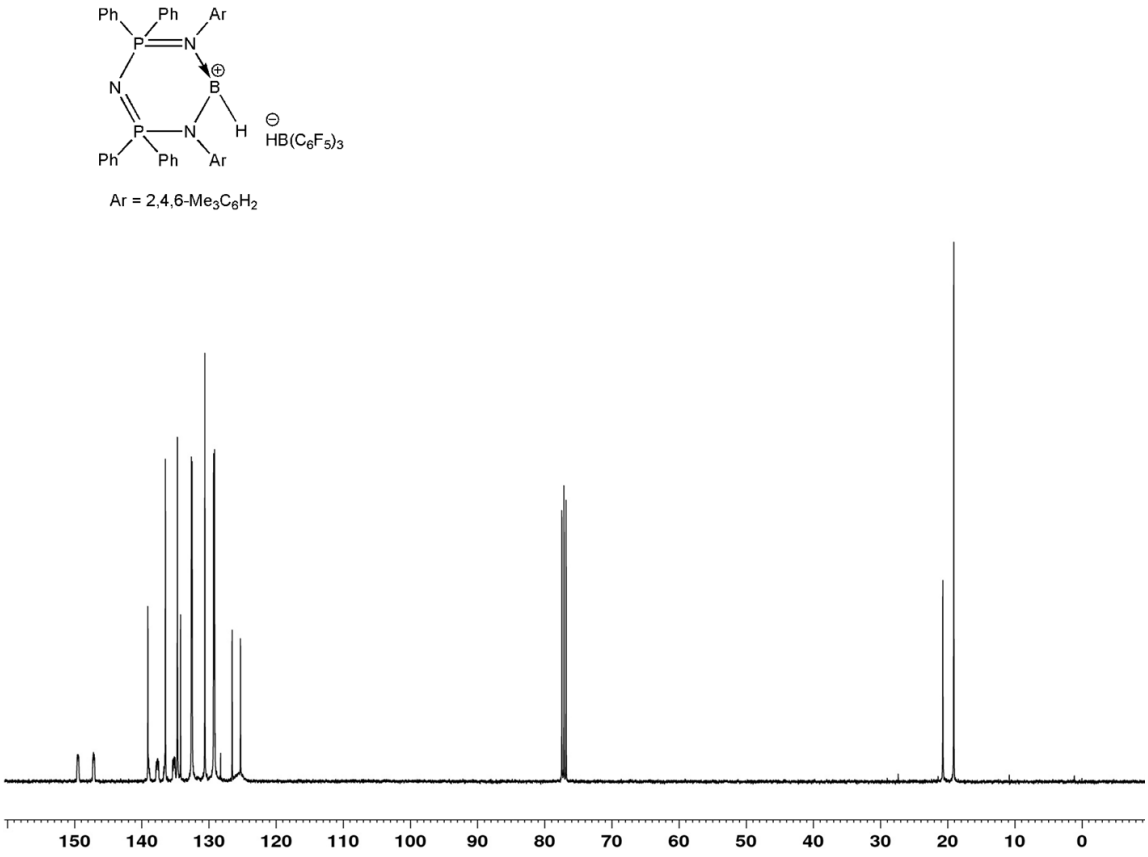

Fig. S79 ^{13}C NMR (100 MHz, $CDCl_3$) spectrum of $[\{N(Ph_2PN(2,4,6\text{-}Me_3C_6H_2N))_2\}BH]^+[HB(C_6F_5)_3]^-$ (**3.3**).

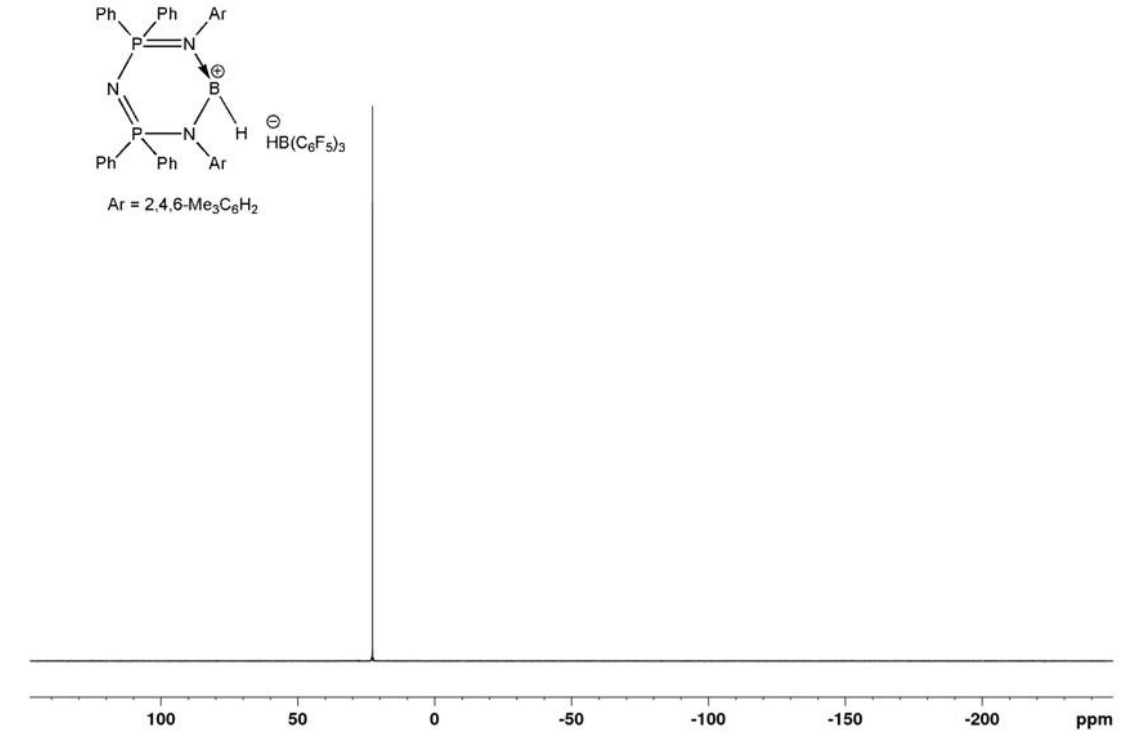

Fig. S80 $^{31}P\{^1H\}$ NMR (162 MHz, $CDCl_3$) spectrum of $[\{N(Ph_2PN(2,4,6\text{-}Me_3C_6H_2N))_2\}BH]^+[HB(C_6F_5)_3]^-$ (**3.3**).

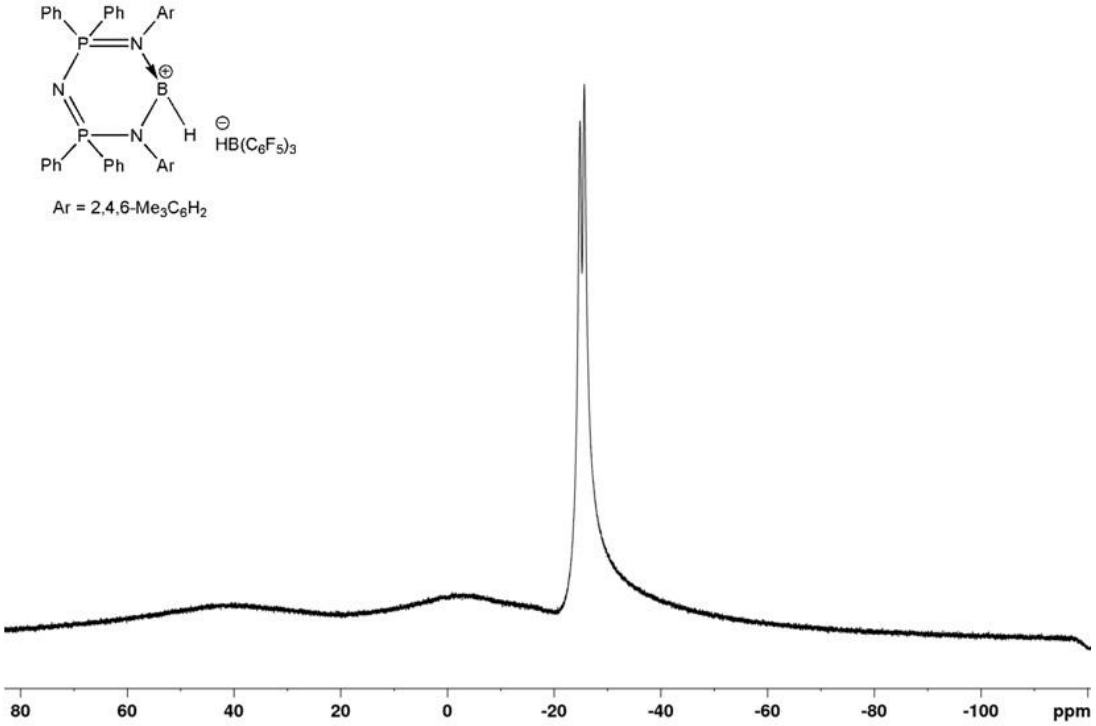

Fig. S81 ^{11}B NMR (128 MHz, $CDCl_3$) spectrum of $[\{N(Ph_2PN(2,4,6\text{-}Me_3C_6H_2N))_2\}BH]^+[HB(C_6F_5)_3]^-$ (**3.3**).

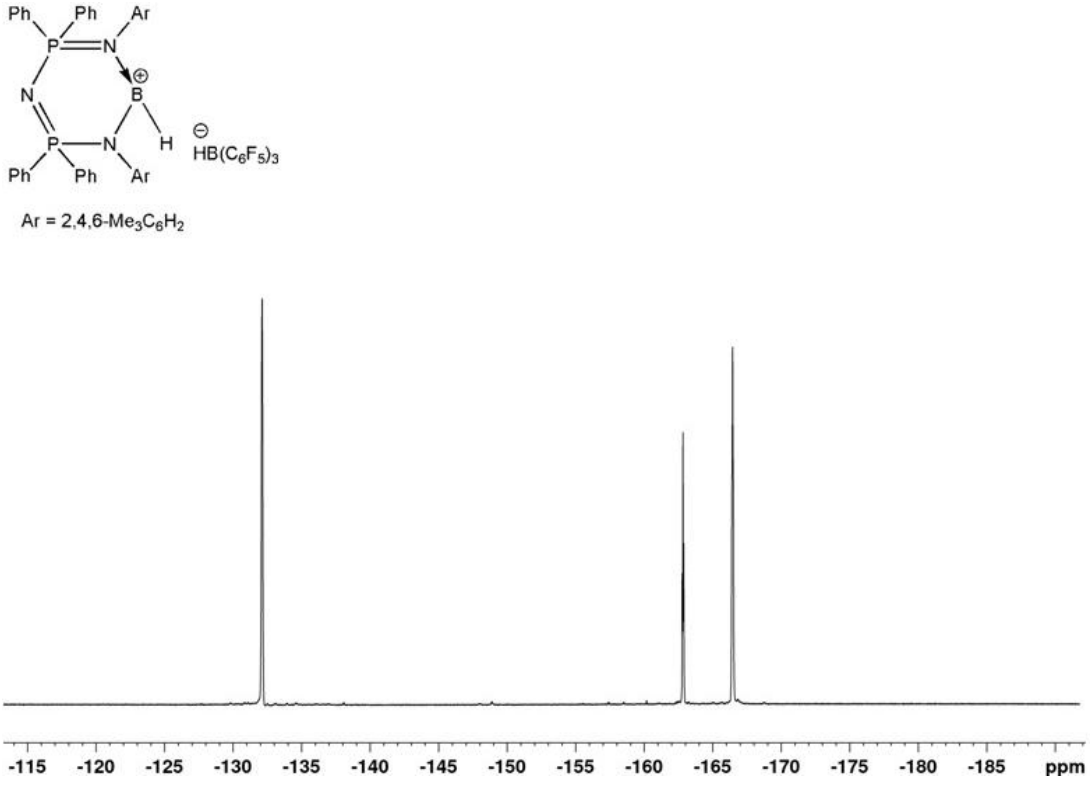

Fig. S82 ^{19}F NMR (376 MHz, $CDCl_3$) spectrum of $[\{N(Ph_2PN(2,4,6\text{-}Me_3C_6H_2N))_2\}BH]^+[HB(C_6F_5)_3]^-$ (**3.3**).

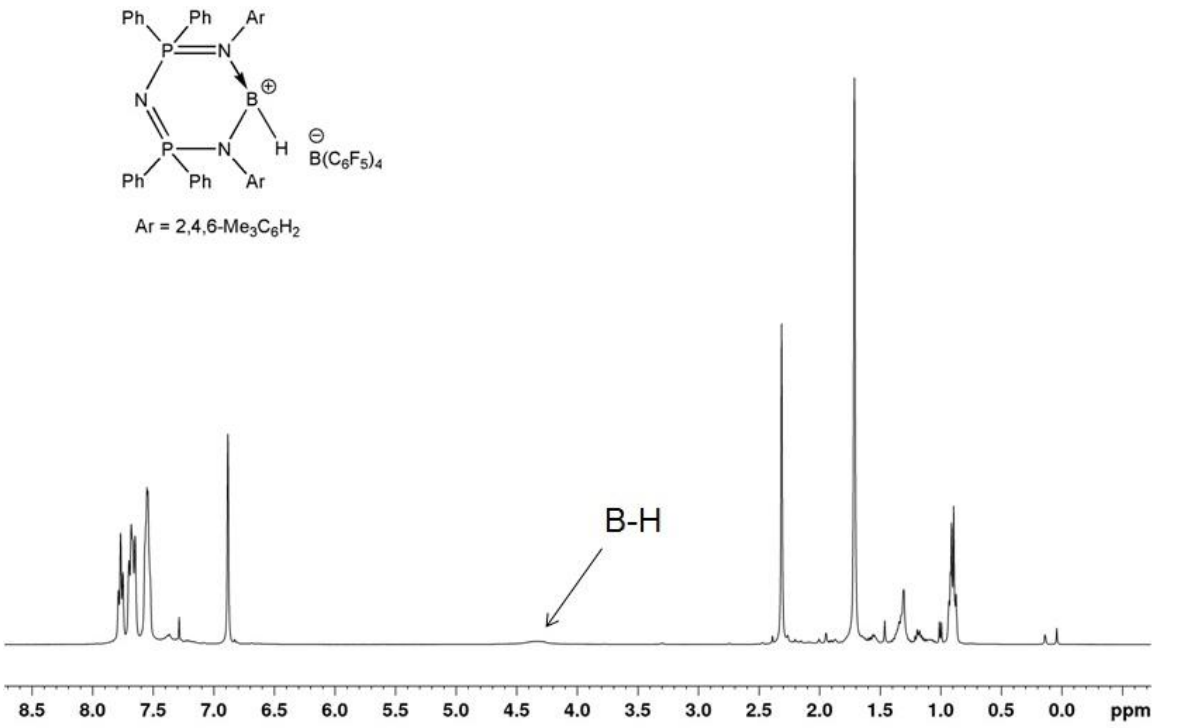

Fig. S83 ^{1}H NMR (400 MHz, $CDCl_3$) spectrum of $[\{N(Ph_2PN(2,4,6\text{-}Me_3C_6H_2N))_2\}BH]^+[B(C_6F_5)_4]^-$ (**3.4**).

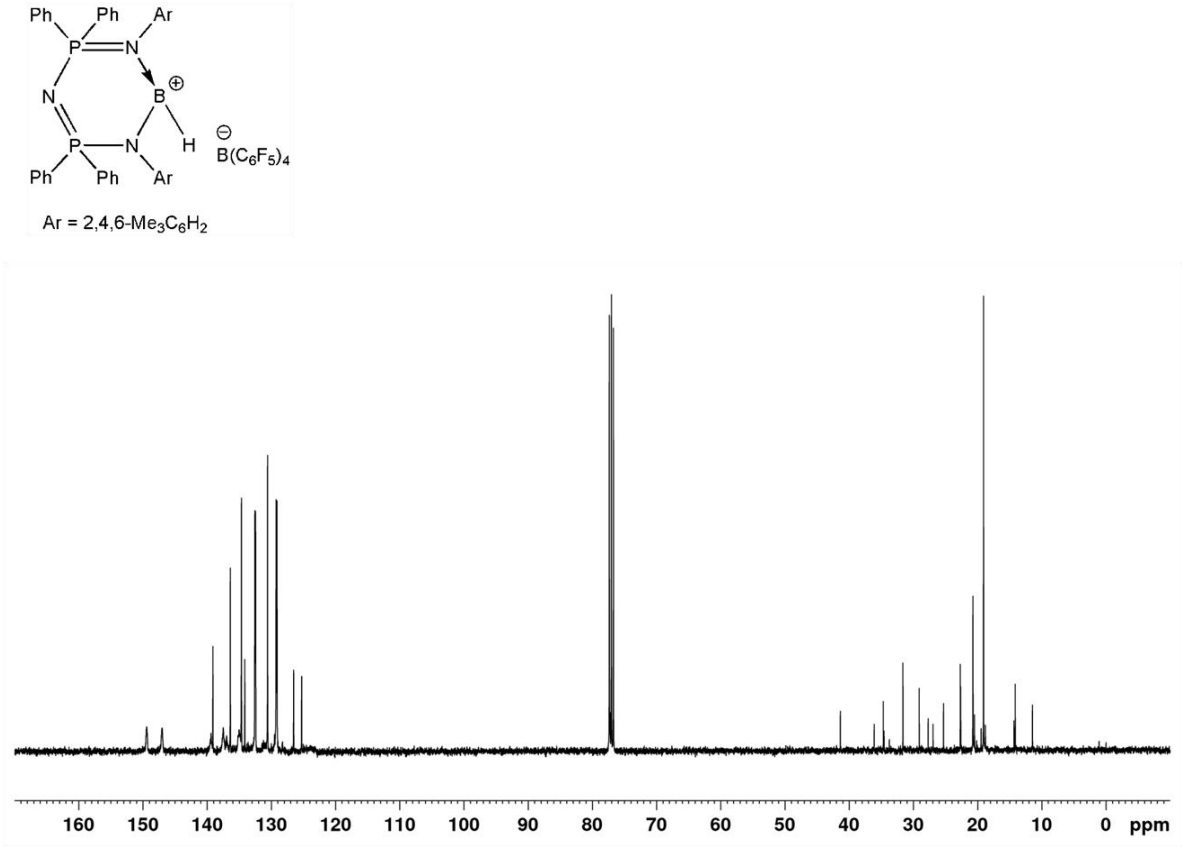

Fig. S84 ^{13}C NMR (100 MHz, $CDCl_3$) spectrum of $[\{N(Ph_2PN(2,4,6\text{-}Me_3C_6H_2N))_2\}BH]^+[B(C_6F_5)_4]^-$ (**3.4**).

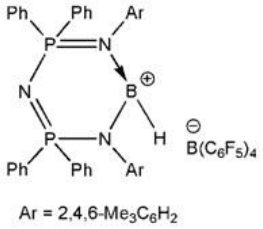

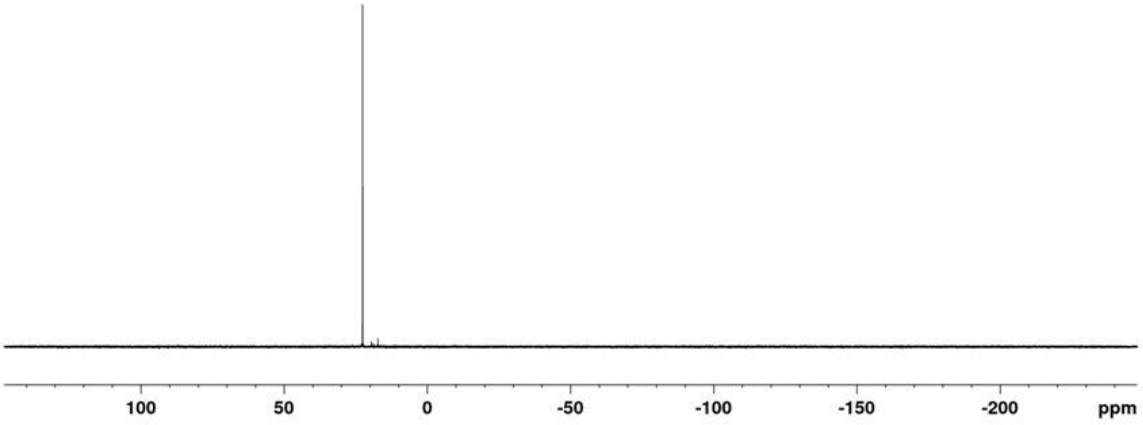

Fig. S85 $^{31}P\{^{1}H\}$ NMR (162 MHz, $CDCl_3$) spectrum of $[\{N(Ph_2PN(2,4,6\text{-}Me_3C_6H_2N))_2\}BH]^+[B(C_6F_5)_4]^-$ (**3.4**).

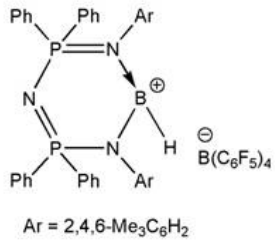

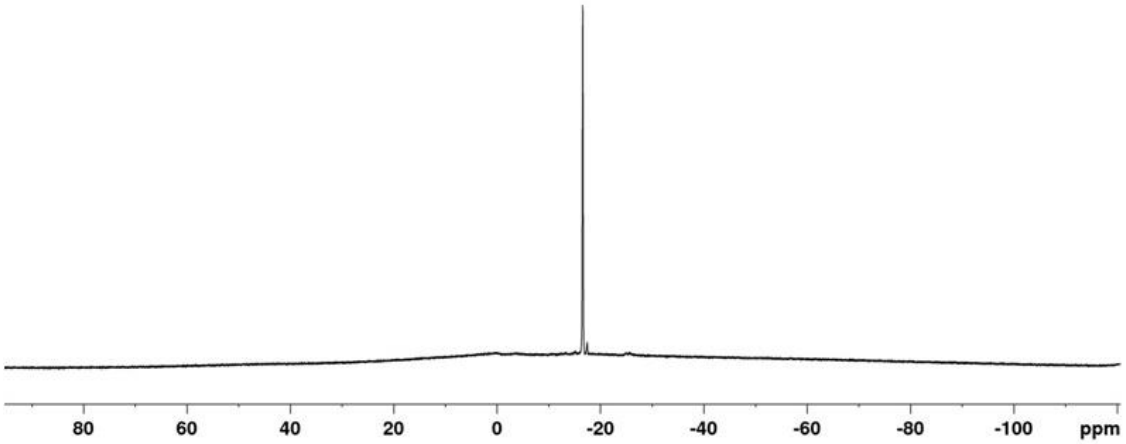

Fig. S86 ^{11}B NMR (128 MHz, $CDCl_3$) spectrum of $[\{N(Ph_2PN(2,4,6\text{-}Me_3C_6H_2N))_2\}BH]^+[B(C_6F_5)_4]^-$ (**3.4**)

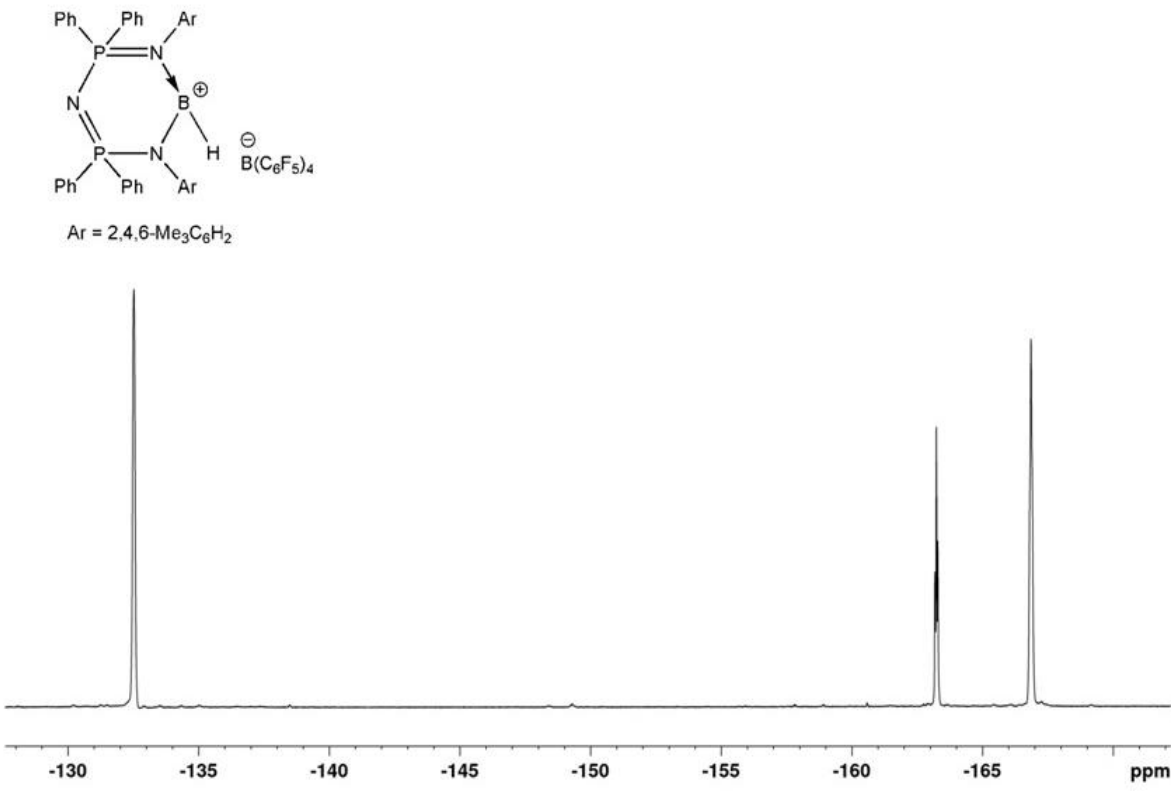

Fig. S87 ^{19}F NMR (376 MHz, $CDCl_3$) spectrum of $[\{N(Ph_2PN(2,4,6\text{-}Me_3C_6H_2N))_2\}BH]^+[B(C_6F_5)_4]^-$ (**3.4**).

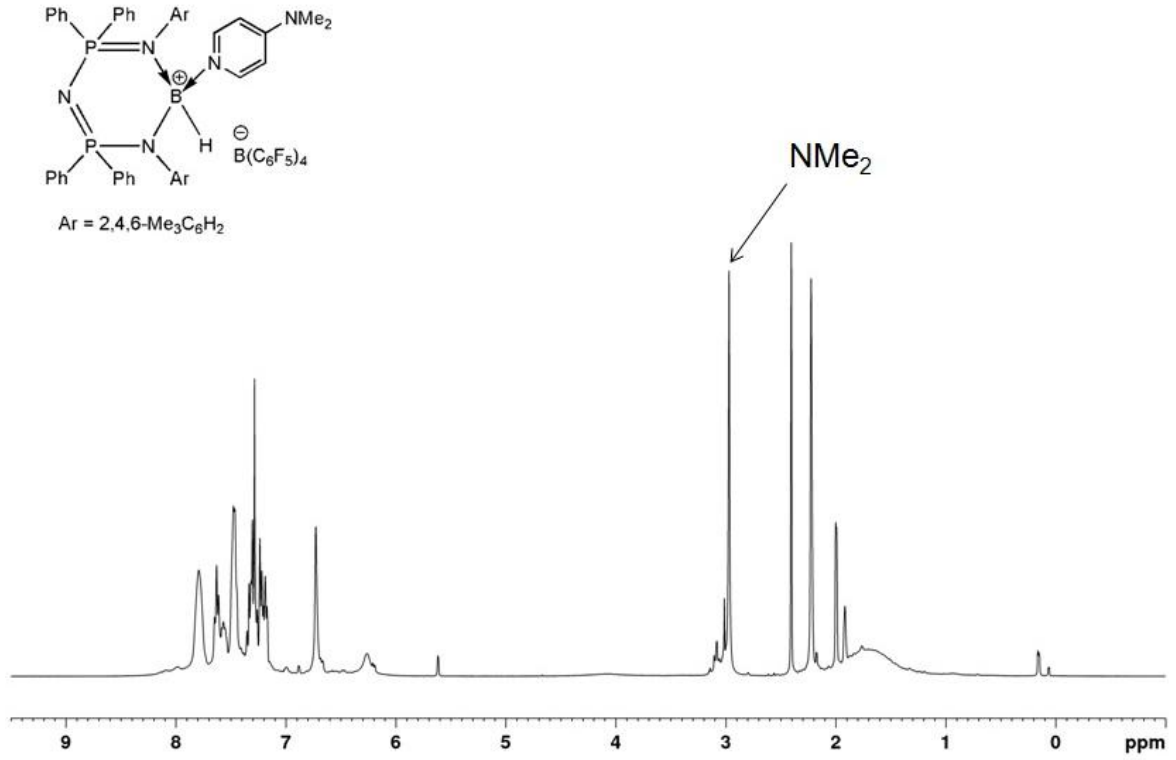

Fig. S88 ^1H NMR (400 MHz, $CDCl_3$) spectrum of $[\{N(Ph_2PN(2,4,6\text{-}Me_3C_6H_2N))_2\}BH\cdot DMAP]^+[B(C_6F_5)_4]^-$ (**3.5**).

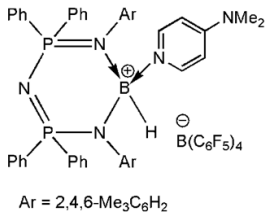

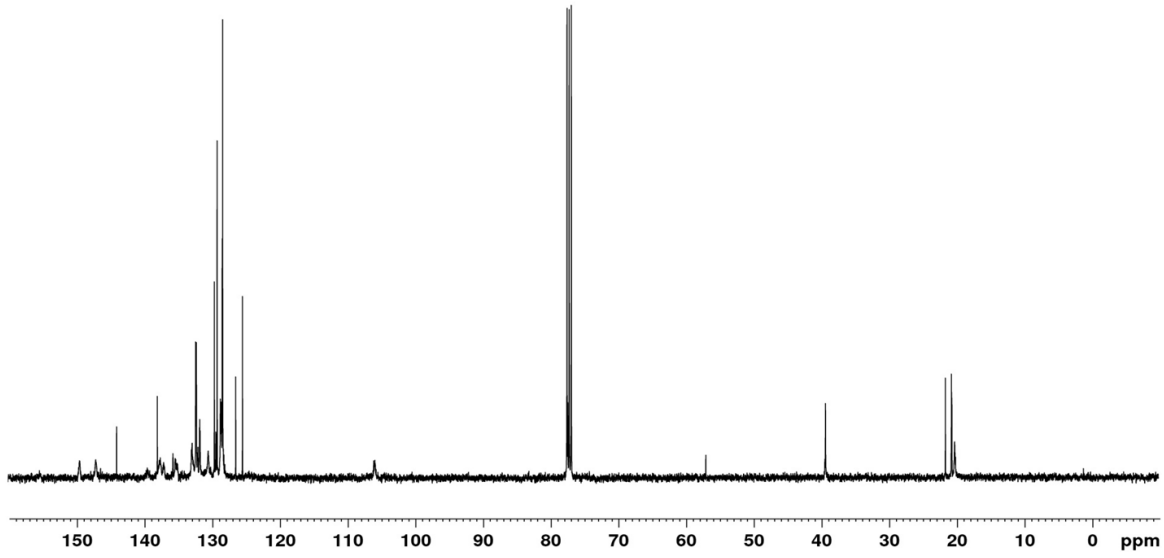

Fig. S89 ^{13}C NMR (100 MHz, $CDCl_3$) spectrum of [{N(Ph_2PN(2,4,6-$Me_3C_6H_2N$))$_2$}BH·DMAP]$^+$[$B(C_6F_5)_4$]$^-$ (**3.5**).

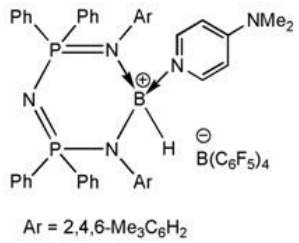

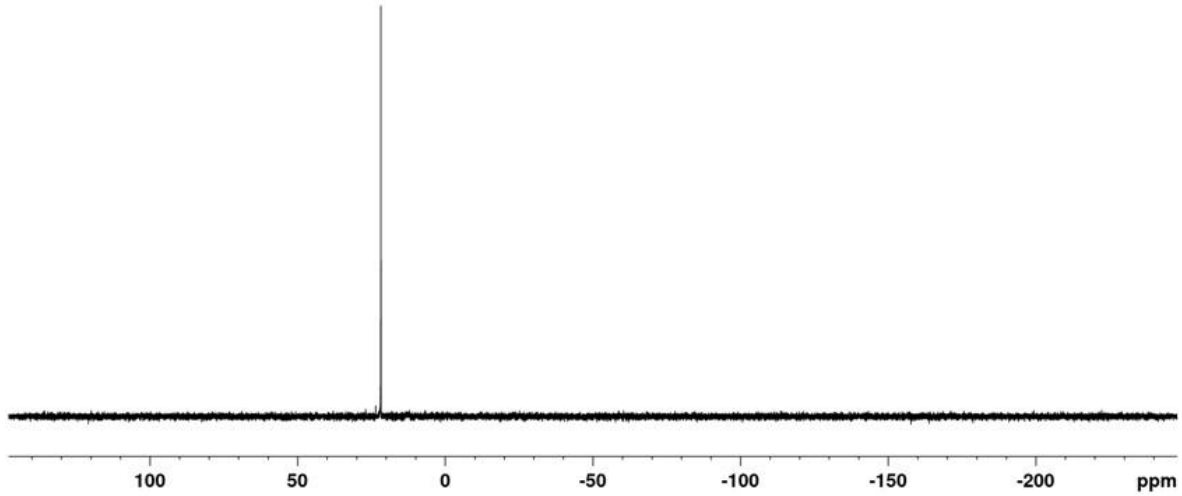

Fig. S90 $^{31}P\{^1H\}$ NMR (162 MHz, $CDCl_3$) spectrum of [{N(Ph_2PN(2,4,6-$Me_3C_6H_2N$))$_2$}BH·DMAP]$^+$[$B(C_6F_5)_4$]$^-$ (**3.5**).

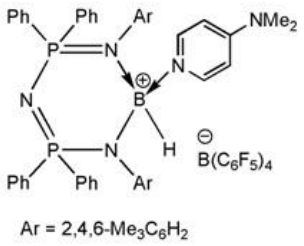

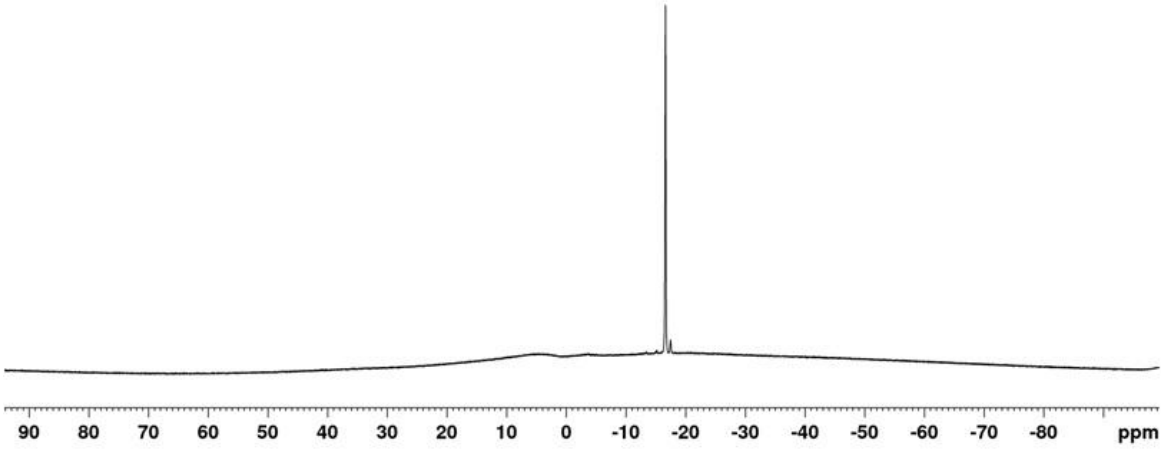

Fig. S91 ^{11}B NMR (128 MHz, $CDCl_3$) spectrum of [{N(Ph_2PN(2,4,6-$Me_3C_6H_2N$))$_2$}BH·DMAP]$^+$[$B(C_6F_5)_4$]$^-$ (**3.5**).

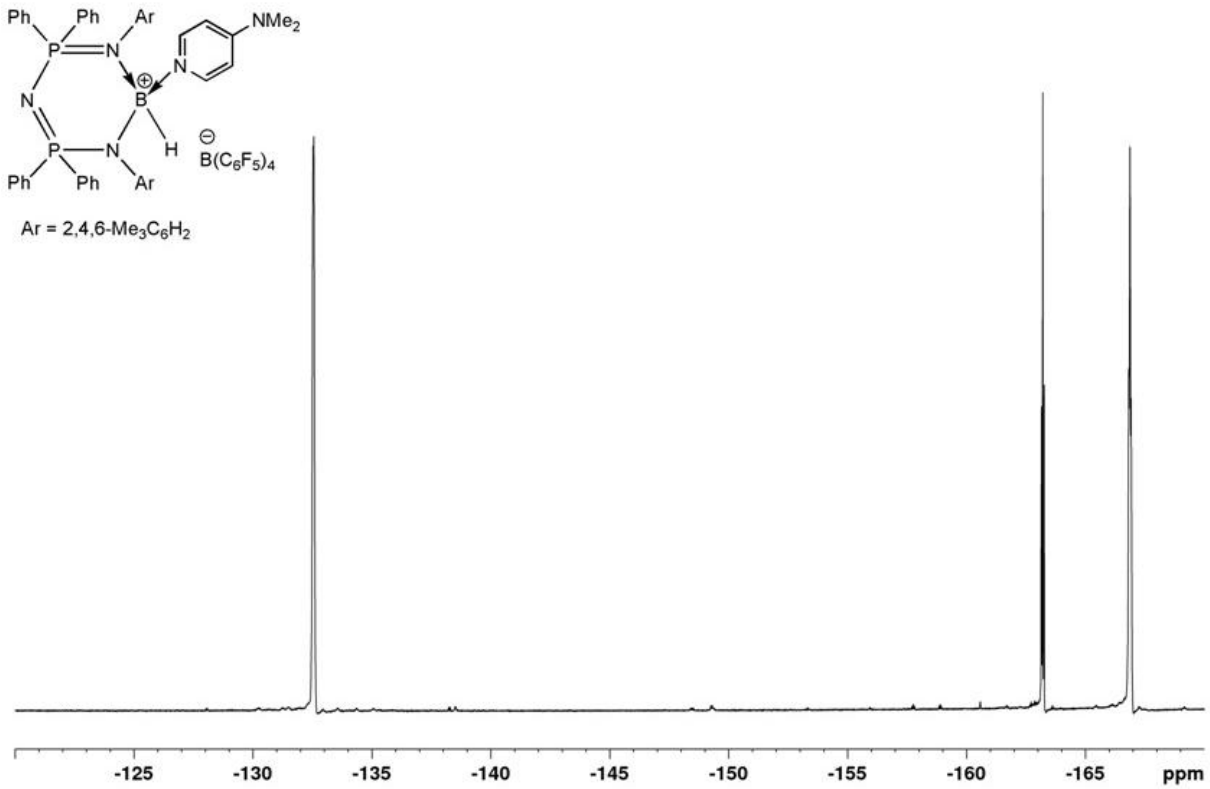

Fig. S92 ^{19}F NMR (376 MHz, $CDCl_3$) spectrum of [{N(Ph_2PN(2,4,6-$Me_3C_6H_2N$))$_2$}BH·DMAP]$^+$[$B(C_6F_5)_4$]$^-$ (**3.5**).